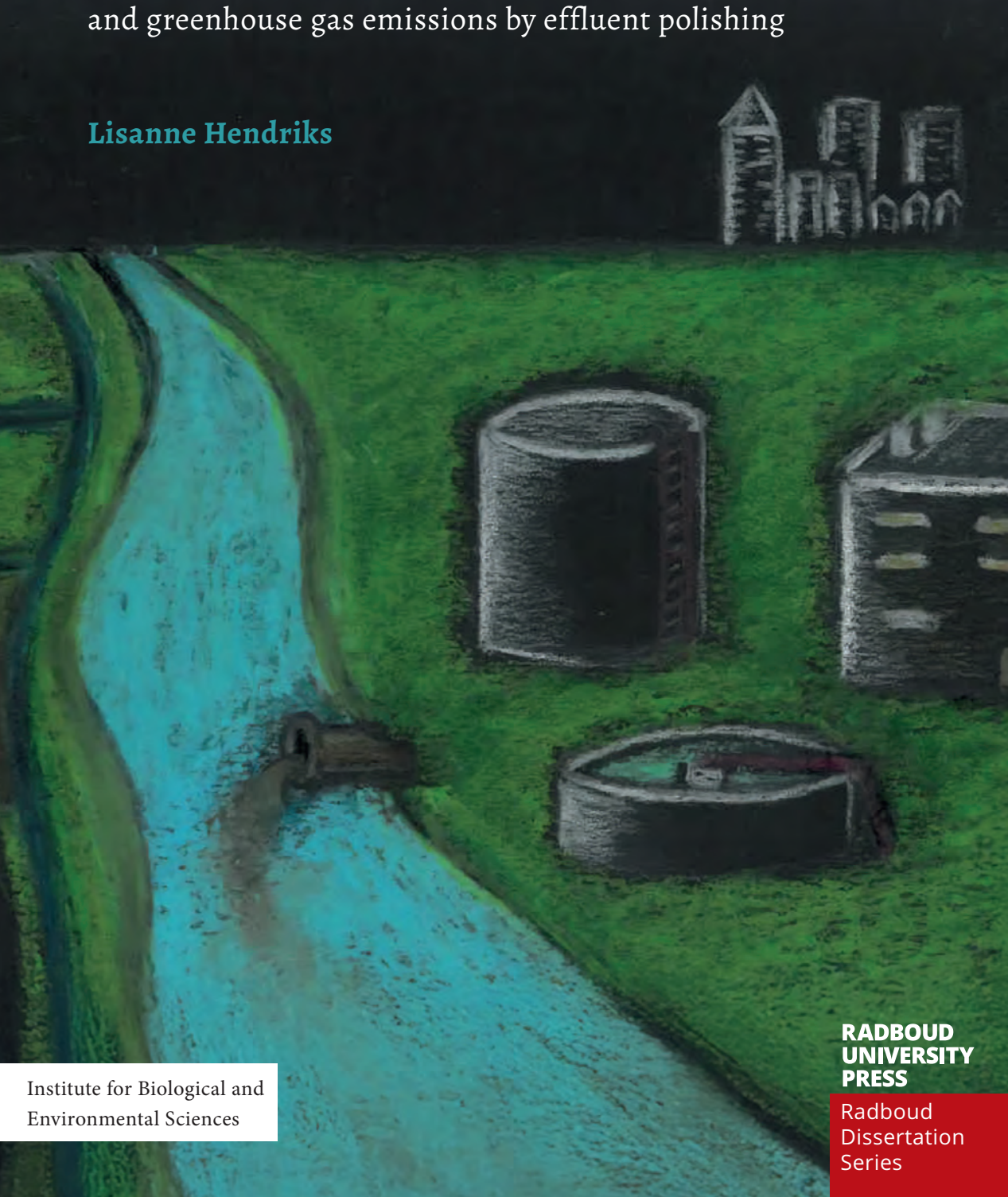


Macrophytes have the potential to counteract eutrophication and greenhouse gas emissions by effluent polishing



The future of wastewater treatment plants?

Macrophytes have the potential to counteract eutrophication and greenhouse gas emission by effluent polishing

Lisanne Hendriks

This publication has been made possible by 'Hoogheemraadschap de Stichtse Rijnlanden', 'Hoogheemraadschap Hollands Noorderkwartier' and 'Waterschap Rivierenland'.

Author: Lisanne Hendriks

Title: The future of wastewater treatment *plants*? Macrophytes have the potential to counteract eutrophication and greenhouse gas emissions by effluent polishing

Radboud Dissertations Series

ISSN: 2950-2772 (Online); 2950-2780 (Print)

Published by RADBOUD UNIVERSITY PRESS Postbus 9100, 6500 HA Nijmegen, The Netherlands www.radbouduniversitypress.nl

Design: Proefschrift AIO | Annelies Lips

Cover image: Angeline Hendriks Printing: DPN Rikken/Pumbo

ISBN: 9789465150284

DOI: 10.54195/9789465150284

Free download at: www.boekenbestellen.nl/radboud-university-press/dissertations

© 2025 Lisanne Hendriks

RADBOUD UNIVERSITY PRESS

This is an Open Access book published under the terms of Creative Commons Attribution-Noncommercial-NoDerivatives International license (CC BY-NC-ND 4.0). This license allows reusers to copy and distribute the material in any medium or format in unadapted form only, for noncommercial purposes only, and only so long as attribution is given to the creator, see http://creativecommons.org/licenses/by-nc-nd/4.0/.

The future of wastewater treatment plants?

Macrophytes have the potential to counteract eutrophication and greenhouse gas emissions by effluent polishing

Proefschrift ter verkrijging van de graad van doctor
aan de Radboud Universiteit Nijmegen
op gezag van de rector magnificus prof. dr. J.M. Sanders,
volgens besluit van het college voor promoties
in het openbaar te verdedigen op
vrijdag 17 januari 2025
om 10.30 uur precies

door

Lisanne Hendriks

geboren op 24 juni 1995 te Haarlem

Promotoren:

Prof. dr. L.P.M. Lamers Prof. dr. A.J.P. Smolders

Copromotor:

Dr. A.J. Veraart

Manuscriptcommissie:

Prof. dr. M.A.J. Huijbregts

Prof. dr. T. Vasconcelos Fernandes (IHE Delft, Wageningen University & Research)

Dr. P. Bodelier (NIOO-KNAW)

TABLE OF CONTENTS

Chapter 1	General introduction	9					
Chapter 2	Drainage ditches are year-round greenhouse gas hotlines in temperate peat landscapes						
Chapter 3	Effects of wastewater effluent discharge on river greenhouse gas emissions and microbial communities						
Chapter 4	Polishing wastewater effluent using plants: floating plants perform better than submerged plants in both nutrient removal and reduction of greenhouse gas emission	87					
Chapter 5	Combining different floating plants for optimal wastewater effluent polishing and carbon-capture	107					
Chapter 6	Sludge degradation, nutrient removal and reduced greenhouse gas emission by a Chironomus-Azolla wastewater treatment cascade	127					
Chapter 7	Combination of Azolla Filiculoides and duckweed for municipal wastewater effluent polishing in a year-round pilot at a wastewater treatment plant	161					
Chapter 8	Synthesis	189					
Appendices	References Data management Summary	204 229 231					
	Samenvatting	237					
	Dankwoord	245					
	About the author	251					
	Scientific outreach	252					



Chapter 1 General introduction

1.1 CLIMATE WARMING AND THE WATER CRISIS

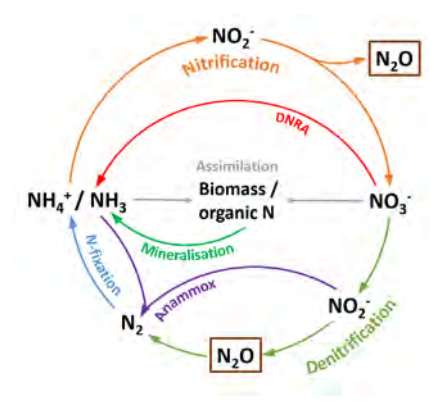
Since the industrial revolution, concentrations of greenhouse gases (GHGs) in the atmosphere have risen drastically, which most likely is the most important cause of climate warming (IPCC, 2023). GHG emissions have continued to increase due to global activity in industry, energy supply, transport, buildings and agriculture (IPCC, 2023). Widespread global changes also increased changes in extreme events, highly related to the world's water cycle: heatwaves, heavy precipitation, droughts and tropical cyclones (IPCC, 2023). Changes in these processes reduce human food and water security, by a disbalance between shortage and excess of freshwater. Furthermore, climate warming, and with that also water warming, and changes in extreme events affect freshwater quality. Poor quality of catchment soils and underwater sediments, and high input of dissolved organic carbon, pathogens, pesticides and especially nutrients impacts human health, ecosystems, and water system reliability (IPCC, 2023).

1.2 EUTROPHICATION IMPACTS WATER QUALITY AND FUELS GREENHOUSE GAS PRODUCTION

High nutrient input into freshwater systems, called eutrophication, is the leading form of pollution in these systems, which also enhances GHG production and emission (Li et al., 2021). Under normal circumstances, elements such as nitrogen (N), phosphorus (P) and carbon (C) are necessary for plant growth and microbial processes, and thus for productivity within a system. In eutrophicated freshwater systems, input of these elements is too high, resulting in a shift from systems having a macrophyte dominated state to having an alternative, phytoplankton dominated, stable state (Scheffer et al., 1993; Hilton et al., 2006). This results in low biodiversity, oxygen concentrations and light availability, and consequently, plant and animal death (Hilton et al., 2006). Limiting input of N, P and C into freshwater systems is therefore crucial for their water quality and functioning. Furthermore, tackling these elements in the aquatic systems themselves can limit their negative effects, whereby the elements are being used in different ways by organisms and show differential ways of cycling within aquatic systems.

1.2.1 Nitrogen

Inorganic nitrogen (N) can be present in the water system in various forms, with the most common ones being ammonium (NH,+) and nitrate (NO,-). Within the system, N acts as a substrate for various processes (Fig. 1.1). Atmospheric N enters the water column through N-fixation by diazotrophic bacteria (Zehr et al., 2003). Decomposition of organic matter results in the production of NH, called mineralisation or ammonification. In the presence of oxygen, nitrification takes place, whereby NH, is converted to NO.. Under anoxic circumstances, and when organic carbon (OC) or other electron donors, such as HS-, are sufficiently available, NO3 is converted into gaseous N (N2) through denitrification, or into NH4 through dissimilatory nitrate reduction to NH, (DNRA) by chemoorganoheterotrophic microbes. In addition, anammox bacteria oxidize NH, under anoxic circumstances, by using NO, as electron acceptor and thereby producing N, gas, a process called anammox (Strous et al., 1999). Primary producers, plants and algae, take up N compounds from the water through assimilation. When these organisms die, incorporated N is released in the organic form and converted to NH,+ through mineralisation or ammonification. Within the N cycle, nitrous oxide (N2O) can be formed. NO is a very potent greenhouse gas that has a global warming potential (GWP) of 273, meaning it contributes 273 times more to global warming than carbon dioxide (CO₂) on a 100-year timescale (IPCC, 2023). N₂O can be formed biologically by two processes: through incomplete denitrification or as a by-product of nitrification. Incomplete denitrification can occur when the availability of N is considerably higher than the availability of organic C (Firestone & Davidson, 1989), or when trace amounts of oxygen are present, inhibiting denitrification enzymes (Betlach & Tiedje, 1981). N₂O is formed as by-product of nitrification, and especially when oxygen is present but in low concentrations, N₂O may accumulate due to an increased N₂O/NO₂ ratio (Ji et al., 2015). Similarly, with low oxygen concentrations, NO, may accumulate due to a disbalance between NH₄ + oxidation and NO₂ oxidation, which can be used in a process called nitrifier denitrification and in that way produce N2O (Wrage-Mönnig et al., 2018). Microorganisms involved in N₂O production are NH₄ oxidizing bacteria and archaea, denitrifying bacteria, NH, oxidizing methanotrophs, nitrate ammonifiers (DNRA) and anammox bacteria (Francis et al., 2007; Yoshinari, 1985; Smith, 1982; Kartal et al., 2007). Yet, N₂O could also be consumed through denitrification, in the case of low concentrations of oxygen and alternative electron acceptors (Conthe et al., 2019).



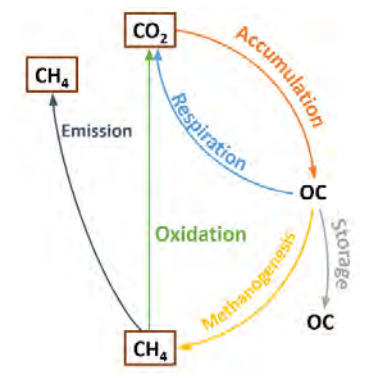


FIGURE 1.1 Nitrogen cycle.

FIGURE 1.2 Carbon cycle.

1.2.2 Phosphorus

Naturally, phosphorus (P) is naturally being released by physical and chemical weathering from rocks as phosphate (PO $_4^{3-}$) ions or deposited from the atmosphere, and in this way enters the sediment and water column (Newman, 1995; Hartmann et al., 2014). This inorganic PO₃- is taken up by plants and algae, and incorporated in their biomass. During plant an algal decay, P is released to the sediment in the organic form (Birch, 1961), where it is not directly available for plant uptake, however organic P can be made available through bacterial mineralisation (Richardson & Simpson, 2011). Furthermore, P availability is regulated by iron (Fe), aluminium (Al) and calcium (Ca). It is not directly available when it is adsorbed to Fe-, Al-(hydr)oxides or other particles, such as clay, or when it is immobilised in the form of Al, Fe and Ca minerals (Golterman, 2004; Tammeorg et al., 2020). Those processes are strongly influenced by pH and redox potential. At a very high or low pH, P can be liberated from Fe- and Al-bound P due to the competition between H+ or OH- (Boström et al., 1988; Zhou et al., 2005). At a high pH, calcium carbonate precipitates, and P may be co-precipitated or adsorbed to this precipitate (Boström et al., 1988; Diaz et al., 1995). Additionally, reduction of ferric iron (Fe(III)) to ferrous iron (Fe(II)), with input of labile organic matter at low redox potentials, can lead to the mobilization of P from the sediment to the water column, as Fe(II) has a lower efficiency of P-binding than Fe(III) (Boström et al., 1988; Smolders et al., 2001; Emsens et al., 2016). Consequently, the mobilization of P is also regulated by organic matter content and quality (Zhou et al., 2005; Harter, 1969).

1.2.3 Carbon

Carbon (C) can enter freshwater systems in its inorganic form (CO_2 or bicarbonate (HCO_3)), which is then used for photosynthesis by primary producers and accumulates within their biomass. Being taken up by primary producers, the carbon is converted to organic C (OC). Terrestrial derived organic C, produced from primary

1

production on the land, can also enter the water system through lateral flow from the land (Ward et al., 2017). The organic C can be stored in the aquatic sediment, but it can also be converted back to inorganic carbon through respiration. This process can occur under oxic circumstances, where plants, animals and many microorganisms use oxygen as electron acceptor, as well as under anoxic circumstances in the sediment, using alternative electron acceptors such as NO3, ferric iron and sulphate (SO 2-) (Kelly et al., 2001). The last step of decomposition of organic matter is methanogenesis, performed by methanogenic archaea. They use acetate or hydrogen and $CO_{,}$ as substrate to produce methane $(CH_{_{4}})$ (Madigan et al., 2018). $CH_{_{4}}$ is, next to N_2O a very potent greenhouse gas, with a GWP of 27 (IPCC, 2023). Although until recently CH₄ production was considered a strictly anaerobic process, new evidence shows the existence of oxic CH₄-producing pathways in freshwater ecosystems, which can have a considerable contribution to the total CH, production (Günthel et al., 2019; Hilt et al., 2022; Thottathil et al., 2022). Methanogenesis can take place when a sufficient amount of organic matter is present, which is mostly the case in the subsurface of eutrophic aquatic sediments. Labile organic carbon promotes CH production as it is easily broken down, and therefore not only the amount but also the quality of organic matter determines CH, production (Duc et al., 2010; Grasset et al., 2018; Nijman, 2023). Furthermore, higher temperatures result in higher CH, production, since anaerobic decomposition of organic matter increases with increasing temperature (Duc et al., 2010; Rodriguez et al., 2018). The produced CH, can either be emitted via diffusion from water column to atmosphere, or via ebullition. The latter process involves bubbles that are formed in the sediment and are directly released, also by disturbance of the sediment. During diffusion, CH, can be oxidized to CO2, which occurs under oxic, using oxygen, or under anoxic, using alternative electron acceptors, conditions (Strous & Jetten, 2004; Trotsenko & Murell, 2008; Martinez-Cruz et al., 2018). CH, oxidation increases with higher temperatures and more substrate availability, including higher nitrogen concentrations (Bodelier & Laanbroek, 2004; Lofton et al., 2014; Nijman et al., 2021). As CH4 bubbles are rising to the surface fast, they leave no time for oxidation thereby causing direct and considerable CH₄ emission to the atmosphere.

1.3 MAIN SOURCES OF NITROGEN, PHOSPHORUS AND CARBON

Around 70% of the global water withdrawal is used by agriculture (FAO & UN Water, 2021). The agricultural sector is also is the main contributor of N (75%) and P (38%) input to many surface waters worldwide as a non-point source (Mekonnen

& Hoekstra, 2015; Mekonnen & Hoekstra, 2017). Agricultural practice causes eutrophication of surface water, groundwater, and of receiving waters, by runoff of fertilizers and manure from the land to adjacent waters during rain or by lateral transport (Cherry et al., 2008; Pärn et al., 2012; Van Geest et al., 2021). Moreover, although not happening often, direct input of manure and fertilizer within the ditches draining the agricultural fields, results in extremely eutrophicated surface waters. Agricultural ditches discharge into other water systems such as rivers and lakes and may eutrophicate those waters as well. Next to agriculture, wastewater is an important (point) source of nutrients and harmful compounds, where it accounts for 23% and 54% of the global N and P load to freshwater systems (Mekonnen & Hoekstra, 2015; Mekonnen & Hoekstra, 2017). Worldwide, only half of produced wastewater is being treated (Jones et al., 2021). The untreated wastewater discharges high amounts of nutrients to receiving water bodies such as rivers, streams and lakes. However, also when being treated, which is the case in for example the Netherlands, nutrient concentrations of the treated wastewater, called effluent, excess the concentrations present in the receiving waters leading to eutrophication of (natural) waterbodies (Carey & Migliaccio, 2009; Preisner et al., 2020).

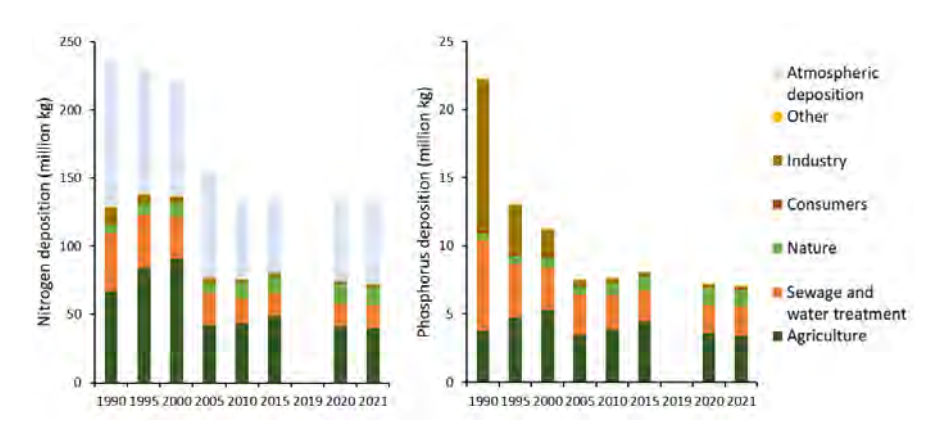


FIGURE 1.3 Sources of nitrogen and phosphorus input in Dutch surface waters. Source: Emissieregistratie.nl

Also focussing only on the Netherlands, the main sources for N and P loading within freshwater systems are agriculture (~58% N and ~48% P) and wastewater (~25% N and ~31% P), although natural areas, through runoff and water birds play a small role as well (Fig. 1.3). It is expected that also carbon enters the aquatic systems mostly through these ways, yet information on this is lacking. For sewage and water treatment, input of N, P and C could be due to overflow of untreated wastewater, however more than 80% comes from discharge of effluent into receiving waterbodies. These are all indirect sources, meaning N, P and C enter the surface water through

the sediment, groundwater, wastewater and air. Although the total input of N and P has lowered since the 1990's, it is stagnating since 2005 and still too high.

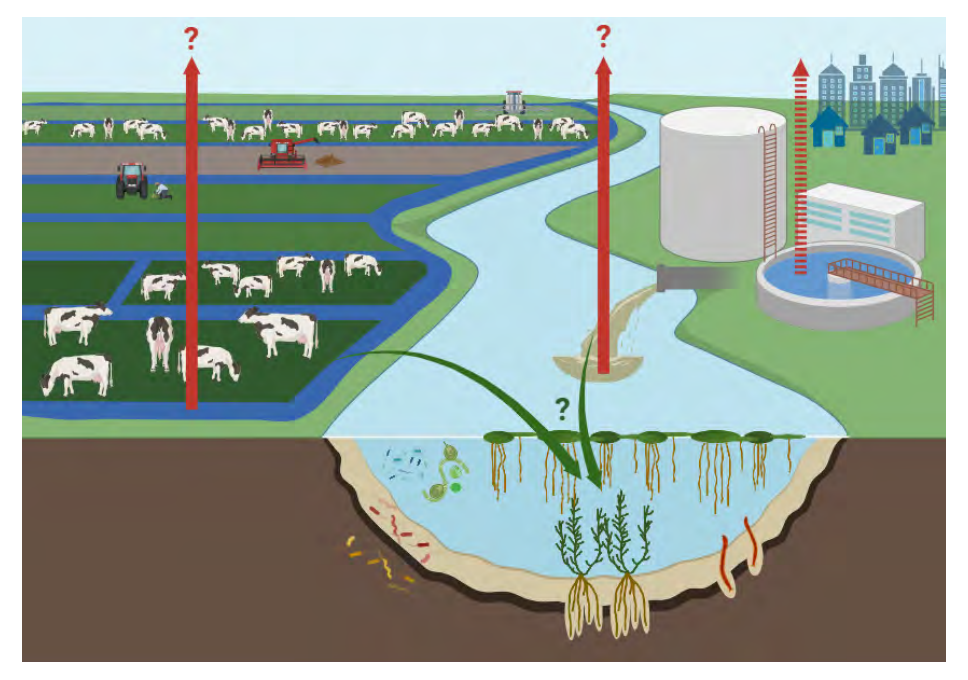


FIGURE 1.4 Different processes of the main nutrient input factors: agriculture and wastewater. Red arrows are greenhouse gas emissions, green arrows are mitigation processes in the (natural) waterbodies receiving these high nutrient inputs.

Due to this high input of N, P and C, many ditches and other freshwater systems, such as rivers, are (highly) eutrophic and are facing a bad water quality. In order to manage, protect and improve the quality of water resources across the European Union, the Water Framework Directive (WFD) came into force in 2000. It requires Member States to achieve good status in all waterbodies by 2027. Yet, in 2018, 60% of the waterbodies in Europe still failed to meet the objectives of the WFD and the question rises whether it is possible to achieve the goal in 2027 (EEA, 2018). Eutrophication in aquatic systems can be expected to also result in higher GHG emissions. Eutrophic drainage ditches may contribute substantially to global anthropogenic CH emissions, in some countries even up to 9% of national anthropogenic CH, emissions (Luan & Wu, 2015; Peacock et al., 2021; Wu et al., 2023). Furthermore, rivers that are polluted have shown, even though difficult to quantify, high emissions of CO,, CH, and N₂O (Yao et al., 2020; Upadhyay et al., 2023), which increases when wastewater effluent is discharged into these rivers (Alshboul et al., 2016; Hu et al., 2018). Yet, the emissions coming from these systems have been poorly quantified and are, in the case of ditches, not always taken into account in national GHG inventories. Omitting emissions from such systems may therefore underestimate GHG budgets. The aquatic systems themselves may to some extent mitigate N, P and C input and emissions through several processes, and the question rises how high this mitigation may be (Fig. 1.4).

1.4 NATURAL KEY PLAYERS INVOLVED IN NUTRIENT AND CARBON CYCLING

Aquatic organisms, such as plants, macroinvertebrates, algae and microorganisms, are found to remove nutrients, organic matter and toxic compounds from the surface water in nature. In eutrophic waters, highly competitive organisms outcompete slower growing species and the system transitions from a biodiverse system to a system dominated by only a few species. Yet, the nutrient and carbon cycling through these different groups of organisms could help combatting the high nutrient and carbon loading and GHG production within the waterbodies, both in natural waters and in constructed wetlands using different groups of plants, macroinvertebrates, algae and microorganisms.

1.4.1 Aquatic plants

Different forms of aquatic plants have different traits in which they alter the water and sediment conditions. The plants use N, P and C for photosynthesis and plant growth, and therefore take up these nutrients and inorganic C from the water column itself. Most submerged plants root within the sediment (Fig. 1.5a), and take up nutrients through their roots. Due to radial oxygen loss from their roots, they oxygenate the sediment in the rhizosphere (Lemoine et al., 2012; Tian et al., 2015). In this way, they limit CH, production. However, the CH, that is produced within the anoxic zones of the sediment could diffuse through the plants, acting as a chimney, and in this way enter the water column (Vroom et al., 2022). In the rhizosphere, the plants stimulate coupled nitrification-denitrification (Eriksson & Weisner, 1999), leading to N loss from the sytem but potentially also to N,O production diffusing to the water column. In addion, the decomposition of plant-produced OM leads to GHG and nutrient emission (Chingangbam & Khoiyangbam, 2023). In eutrophic systems, floating plants can form a dense mat on top of the water column (Fig. 1.5b), acting as a barrier between water column and atmosphere (Kosten et al., 2016). The plants take up high amounts of CO, for photosynthesis, and take up N and P directly from the water column. Although in the rhizosphere, radial oxygen loss increases oxygen concentrations (Kosten et al., 2016), the dense mat causes oxygen concentrations to

be low in the water below and thus most likely the sediment will be anoxic (Veraart et al., 2011). CH₄ production within the sediment might increase and CH₄ diffuses to the water column, where it gets trapped underneath the plant mat. In this usually oxygenated zone, CH₄ oxidation could take place (Moorhead & Reddy, 1988; Kosten et al., 2016). The heterogenous circumstances and alternations of oxic and anoxic sites, however stimulate coupled nitrification-denitrification and thus N loss to the atmosphere, by which N₂O may also be produced.

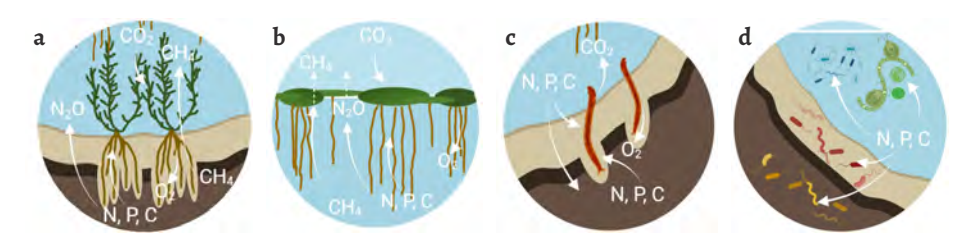


FIGURE 1.5 Processes of submerged plants (a), floating plants (b), macroinvertebrates (c), and algae and microorganisms (d).

1.4.2 Aquatic macroinvertebrates

Aquatic macroinvertebrates are small animals living in the water layer, on top of, or in the sediment (Fig. 1.5c). Especially the species that are burrowing in the sediment are oxygenating the sediment, leading to similar processes as described for submerged plants (Benelli & Bartoli, 2021). Burrowing additionally distributes nutrients and gases in or from the sediment (Boström et al., 1988; Chen et al., 2015; Gautreau et al., 2020; Benelli & Bartoli, 2021). Furthermore, macroinvertebrates feed on the organic matter within the sediment and in this way degrade this organic matter and take up and excrete N, P and C (Graça, 2001; Vos et al., 2004). Part of these substances is used for their growth, another part is being excreted and returned to the water column or sediment. As the animals respire, they release CO_2 to the water column which can then be emitted to the atmosphere. After death, OM is being decomposed leading to nutrient and GHG emission.

1.4.3 Algae and microorganisms

Algae and cyanobacteria take up high amounts of nutrients (Fig. 1.5d), and with excessive nutrient input may form algal blooms. They are then able to outcompete other organisms in terms of light and oxygen, resulting in organism die-off and consequently nutrient and carbon release. As these organisms die and decompose, nutrients are released back into the water column, perpetuating the cycle of eutrophication and algal proliferation (Paerl & Huisman, 2009). Additionally, the presence of algal blooms can lead to increased water turbidity, reducing water

clarity and light penetration, and altering aquatic systems (Schindler, 2006). Microorganisms use nutrients and carbon as substrate for multiple processes (Fig. 1.5d). Microorganisms could be present in the anoxic and oxic sediment, in the water column and in biofilms attached to surfaces of plants and other substrates. They convert organic carbon to CO_2 using oxygen or alternative electron acceptors such as NO_3^- , Fe(III) and SO_4^{-2-} , or convert organic C to CH_4 , which can in turn be converted to CO_2 again by oxic and anoxic methanotrophy (see section 1.2.3). Nitrogen is being used and converted in many forms (section 1.2.1).

1.5 THE USE OF AQUATIC PLANTS IN WATER TREATMENT

Aquatic plants have already been used in water treatment, for example in constructed wetlands. Constructed wetlands have emerged as a sustainable and effective approach for water treatment, removing various pollutants through natural processes. They mimic the functions of natural wetlands, making use of the interactions between plants, microorganisms, and environmental conditions to treat water. Aquatic plants play an important role in these constructed wetlands by facilitating physical, chemical, and biological processes, by providing surface area for biofilm formation and by the formation of heterogenous conditions within the water column and sediment. In this way, the plants enhance nutrient removal by increased nitrification-denitrification and P binding to the sediment (Vymazal, 2013; Sun et al., 2019). Despite the numerous benefits offered by constructed wetlands, several constraints and questions remain. Challenges include variability in treatment performance due to fluctuations in environmental conditions, such as temperature, hydraulic loading, and nutrient concentrations, and space requirement (Ghosh & Gopal, 2010; Sarmento et al., 2013). Additionally, plants in constructed wetlands are mostly indirectly involved in nutrient removal and it remains unclear which part of the removed nutrients can be released to the water column again, for example by plant decomposition (Menon & Holland, 2014). Furthermore, constructed wetlands can emit substantial amounts of GHGs, especially N₂O (Wu et al., 2017; Zhang et al., 2019), and may thereby not contribute to sustainable water treatment. Recently, water treatment in a hydroponic way has gained interest. Aquatic plants are grown directly on to-be treated water without a sediment layer, and thus nutrient removal is also directly influenced by plant-uptake (Magwaza et al., 2020). By harvesting the biomass, nutrients that have been taken up by the plants are permanently removed from the water column. Until now, focus has been on water treatment through nutrient removal, but not on GHG fluxes associated with this treatment, and the question remains whether hydroponic water treatment can aid in reducing GHG emissions from these waters.

1.6 AIMS AND SCOPE OF THIS THESIS

The present thesis has two general aims: I) to quantify links between eutrophication and GHG emission in aquatic systems, and II) to find novel ways to reduce nutrient and GHG emission in wastewater treatment using natural mechanisms. The main objectives within these aims were I) to quantify GHG emissions coming from two water types facing the highest nutrient loading from either agriculture or wastewater discharge: agricultural drainage ditches and wastewater effluent receiving rivers, and II) to develop a natural and low-emission technique to enhance nutrient removal from municipal wastewater, using aquatic organisms, that counteracts eutrophication and GHG emission. These objectives are divided into six chapters, depicted in Fig. 1.6.

In quantifying GHG emissions from eutrophic waterbodies, the aim of chapter 2 was to assess the role of drainage ditches in the GHG budget of agricultural landscapes, since GHG inventories strongly lack this information. Year-round diffusive emissions of CO,, CH, and N,O, and CH, ebullition were quantified in 10 drainage ditches located between heavily fertilized, peaty agricultural fields. Seasonal variations were assessed, as well as differences between ditches. Furthermore, water and sediment quality indicators were used to determine proxies for these differences in emissions. Next, in **chapter 3**, GHG emissions from another important source of eutrophication were assessed: effluent discharge within rivers. GHG emissions were measured in rivers being affected by wastewater effluent discharge. It is known that effluent discharge can increase emissions over the whole river, but the direct effect of this effluent remains understudied. Two rivers were sampled: one river with 5 effluent discharge locations and one river with one location. GHG flux was measured upstream, downstream and right at the effluent discharge points. Additionally, sediment and water samples were taken to describe the microbial community and to assess whether community composition changes after effluent discharge.

Next, different studies were performed on developing a natural water treatment technique using aquatic organisms, focussing especially on aquatic plants and wastewater effluent polishing. First, we assessed which plant growth form would be most efficient in wastewater effluent polishing. In **chapter 4**, two floating plant species were compared to two submerged species in nutrient removal efficiency, GHG reduction (CO₂ uptake, and CH₄ and N₂O emission reduction) and biomass

production when grown on wastewater effluent for two weeks. The floating species performed best in all three categories, so it was decided to continue with this plant growth form. Therefore, in **chapter 5** different floating plant species were compared to quantify the most efficient species for effluent polishing, focussing on nutrient removal, GHG balance and biomass production. Furthermore, it was studied whether a combination of the two most efficient floating plant species is removing nutrients more efficiently compared to a single cultivation of those species, and whether the sequence in which these species are placed matters.

Combinations of organisms are not limited to plant-plant combinations. Wastewater treatment plants are facing, next to excess of nutrients and carbon, the problem of sludge production and processing. This sludge is a sediment-like substance consisting of organic material, microorganisms and pollutants attached to this. Sludge processing is a costly process. Since aquatic animals, especially bioturbating macroinvertebrates, are feeding on sediment in natural waterbodies, a combination of these macroinvertebrates and floating plants was used in **chapter 6** to assess how well a cascading system of both organisms is able to degrade sludge, remove nutrients and decrease GHG emissions.

The above-mentioned experiments on water treatment were performed in batch systems, under controlled circumstances. To test whether effluent polishing using plants would also work on a larger scale, an experiment that lasted for a whole year was designed at a wastewater treatment plant, where the system was continuously fed with effluent coming directly from the plant (**chapter 7**). Here, it was assessed whether a combination of species results in higher effluent polishing efficiency on a bigger scale, and whether seasonal changes or effluent flow rate affects the efficiency of the system.

In **chapter 8**, I will synthesize all research chapters and show a broader perspective. Furthermore, I will outline implications and challenges of effluent polishing using aquatic organisms, upscaling of such system and a perspective on sustainability and circularity.

1

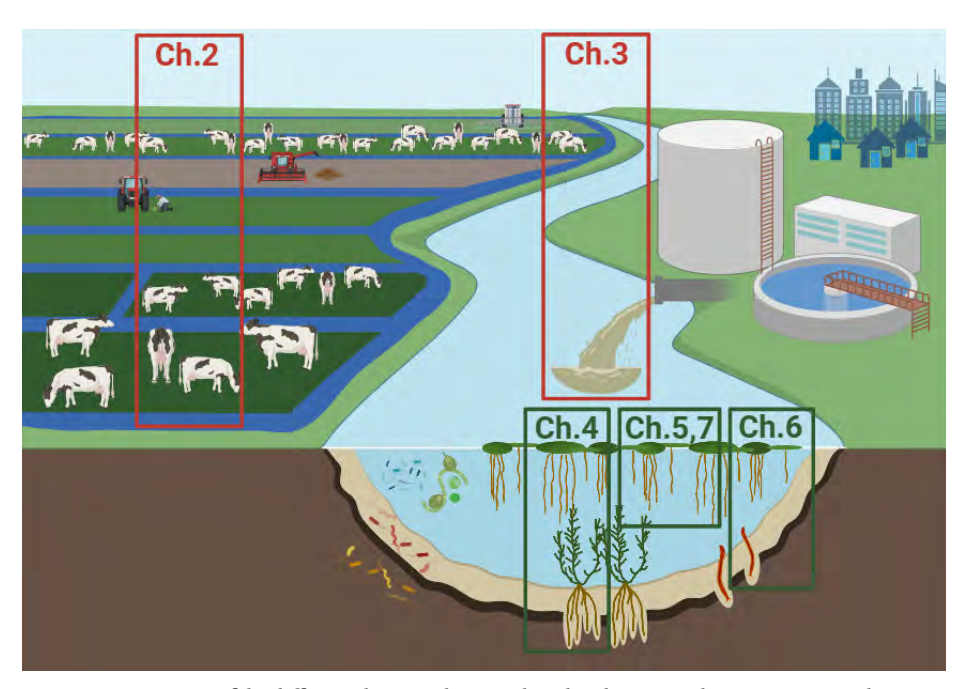


FIGURE 1.6 Overview of the different chapters showing the related topics with respect to eutrophication, greenhouse gas emissions and the natural processes involved. Note that chapters 4-7 are not taking place in the natural aquatic systems but in experimental settings.



Chapter 2 Drainage ditches are year-round greenhouse gas hotlines in temperate peat landscapes

Lisanne Hendriks, Stefan Weideveld, Christian Fritz, Tatiana Stepina, Ralf C. H. Aben, Ngum E. Fung, Sarian Kosten

Published in Freshwater Biology, 2024, 69 (1): 143-156doi: 10.1111/fwb.14200

ABSTRACT

Greenhouse gas (GHG) emissions from drained peatlands have been studied extensively. Considerably less attention has been paid to the emissions from the ditches used to drain peatlands. High within-ditch GHG production and lateral inflow of GHGs may lead to ditches emitting considerable amounts of GHGs on the landscape scale. We quantified annual emissions of ebullitive and diffusive methane (CH₂), carbon dioxide (CO₂) and nitrous oxide (N₂O) in 10 drainage ditches in intensively-used temperate peatlands used for dairy farming, in The Netherlands. Additionally, we assessed water and sediment quality to determine proxies for emissions via the two emission pathways. The mean annual emissions from the studied ditches varied between 3.57 and 60.1 g CO,-eq. $m^{\text{--}2}\ d^{\text{--}1}$ (based on a global warming potential over a 100-year timeframe), where CO₂ contributed on average 43% (ranging between 1.9 and 22.0 g CO $_2$ m $^{-2}$ d $^{-1}$) and diffusive CH $_4$ contributed 16% (0.1 – 16.5 g $\rm CO_2$ -eq. $\rm m^{-2}$ $\rm d^{-1})$ to the total GHG emission. Ebullition of $\rm CH_4$ made up nearly half of the total GHG emission (40%, 1.3 - 40.9 g CO $_2$ -eq. m $^{-2}$ d $^{-1}$). N $_2$ O emissions were mostly low. CO2 emissions were higher in winter months, while CH4 ebullition was higher during spring and summer. Diffusive CH, emissions did not show a seasonal pattern. The mean emission factor, the estimate of average emissions per unit area (EF), for CH4 was 2144 kg CH4 ha-1 yr-1, which is 2 times higher than the tier 1 EF reported by the IPCC (with underrepresented ebullition data), underlining the high variability of ditch emissions. Ditch emissions were also higher than the EF used for the surrounding drained peatlands indicating that ditch emissions can be important on the landscape scale and should be considered to be included in national greenhouse gas reporting.

2.1 INTRODUCTION

Drained peatlands are a substantial source of greenhouse gases (GHGs) to the atmosphere (IPCC, 2014; Tiemeyer et al., 2016). A total of 22.5–50.9 million ha of peatlands worldwide have been drained for agricultural use (Leifeld & Menichetti, 2018; Tubiello et al., 2016). Although natural and restored peatlands show net uptake or only minor emissions of GHGs, present-day emissions from global drained peatlands are estimated to be 1.9-2.5 Gt CO₂-eq. yr⁻¹ (Günther et al., 2020; Joosten, 2010; Leifeld & Menichetti, 2018). Most studies, however, focus on quantifying the emissions of carbon dioxide (CO₂), methane (CH₄) and nitrous oxide (N₂O) from the terrestrial area of the peatlands (e.g. Couwenberg et al., 2010; Günther et al., 2020; Hooijer et al., 2012; Ojanen et al., 2010).

Considerably less attention has been paid to GHG emissions from the drainage ditches in managed peatlands, that are used globally to drain the adjacent agricultural land (Cooper et al., 2014; Evans et al., 2016; Hensen et al., 2006; Koschorreck et al., 2020; Peacock et al., 2017). Ditch networks are used as drainage infrastructure in peatlands (e.g. to enable agriculture and forestry use, Joosten & Clarke, 2002; Connolly & Holden, 2017) and to irrigate peatlands with surface waters (e.g. furrow irrigation, Liu et al., 2022). Peatlands that are managed as nature areas may be (slightly) drained (e.g. when targetting meadow birds) as well, just as rewetted peatlands that often contain a dense network of (old) ditches (Kooijman et al., 2016; Lordkipanidze et al., 2019; Köhn et al., 2021). Hence, ommitting peatland ditches from emission inventories from a wide range of different peatlands may underestimate GHG budgets from these areas as ditches generally make up 6 to 43% of the total peat area (Vermaat & Hellmann, 2010). Ditch emission data, however, is scarce and particularly insights in the seasonal variation in emissions and data on CH, ebullition intensity i.e. the release of gas bubbles - is largely lacking. The available studies focussing on ditches, however point out that the emissions can be substantial (Evans et al., 2016; Köhn et al., 2021; Schrier-Uijl et al., 2011; Teh et al., 2011). The current IPCC default emission factors, global estimates of average emissions per unit area, for ditches in GHG inventories are 416 kg CH, ha-1 yr-1 for ditches on mineral soils (Lovelock et al., 2019) and 1165 kg $\mathrm{CH_4}$ ha $^{-1}$ yr $^{-1}$ for ditches on organic soils in deep drained boreal and temperate grassland and cropland (IPCC, 2014). These emission factors are 26 to 73 times higher – on an areal basis – than CH₄ emissions from deep drained (water table level >30 cm below surface) grasslands on drained peatlands in temperate regions (IPCC, 2014). Additionally, waters within agricultural areas can contribute 4% to 45% of total landscape N₂O emissions and therefore can play an important role in the GHG budget of drainage ditches (Outram & Hiscock, 2012; Turner et al., 2015). Also when compared to headwater streams and rivers (11 t CO, ha-1 yr-1 (Hotchkiss

et al., 2015), 664 kg $\rm CH_4$ ha⁻¹ yr⁻¹ (Rosentreter et al., 2021), 0.48 g $\rm N_2$ O ha⁻¹ yr⁻¹ (Yao et al., 2020)) ditch emissions tend to be in the upper range of the emissions. However, to enable upscaling from individual ditches to larger ditch networks, we need to better understand the major drivers of ditch GHG emissions. The lack of accurate emission data to extrapolate these emissions is likely the reason why ditch $\rm CH_4$ emissions are not yet always included in national $\rm CH_4$ emission inventories. This may lead to substantial inaccuracies of the national emission estimates. Koschorreck and colleagues (2020), for instance, found that Dutch ditch emissions possibly make up 16% of the Dutch national $\rm CH_4$ emission, still so far they are not incorporated in the national greenhouse gas emission inventory (Coenen et al., 2017).

High ditch emissions are explained by both intensive within-ditch GHG production and the strong and direct link with the phreatic groundwater in the adjacent land, the zone where the soil is saturated with water (Roulet & Moore, 1995). As ditches – regularly combined with drainage pipes - are designed to drain the surrounding area, there is a strong lateral inflow of dissolved and particulate organic carbon (DOC, POC) and dissolved GHGs derived from the agricultural peatland (Roulet & Moore, 1995). Studies in streams and rivers point out that lateral inflow can be responsible for up to 72% of riverine CO₂ outgassing (Hotchkiss et al., 2015). In addition, small streams, which resemble ditches most closely, tend to emit more CO2 than large rivers (Hotchkiss et al., 2015) suggesting that lateral inflow may even be more important in systems with higher shoreline to stream surface area ratios. Because most ditches drain organic soils - as due to their high water holding capacity more drainage is needed to enable traditional agricultural use as compared to clay and sandy soils-, the inflow of organic and inorganic carbon may be particularly high (Nieminen et al., 2018; Wilson et al., 2011). Erosion of the ditch banks and high aquatic primary production as a result of high nutrient loading are other important sources of organic carbon (Schrier-Uijl et al., 2011; Vermaat et al., 2011). High respiration rates in ditch sediments and waters generally lead to CO₂ oversaturation resulting in strong diffusive emissions to the atmosphere (Schrier-Uijl et al., 2011). High organic matter availability and high sedimentation rates increase CH, production by limiting oxygen exposure times, thereby increasing the fraction of highly reactive organic matter available for methanogenesis (Sobek et al., 2012). High temperatures, which often occur in ditches due to their shallow nature, promote surface water deoxygenation (Bartosiewicz et al., 2016) and raise CH₄ production rates (Marotta et al., 2014), explaining the high CH₄ emissions from eutrophic systems (Beaulieu et al., 2019; Li et al., 2021), particularly under warm conditions (Davidson et al., 2018; Van Bergen et al., 2019). Based on the strong temperature dependence of CH₄ emissions, earlier work shows that the warm summer season may be responsible for 70% of the annual ditch emission of CH, and CO, (Schrier-Uijl et al., 2011). The production of CO,

2

and $\mathrm{CH_4}$, as well as of $\mathrm{N_2O}$, is related to the decomposition of organic matter, yet $\mathrm{N_2O}$ production is overwhelmingly driven by nitrogen (N) loading from agricultural leaching and runoff (Tian et al., 2020). Therefore, $\mathrm{N_2O}$ emissions are likely strongly related to fertilizer application and hydrological conditions.

GHG emission from drainage ditches to the atmosphere occurs – just as in other surface waters - not only via diffusion, but also through release of gas bubbles (ebullition) (Bastviken et al., 2011; DelSontro et al., 2018; Köhn et al., 2021). Although quantitative data is still limited, recent studies in lakes, rivers, and mesocosms show that CH emissions via bubbles are highly variable (0-99.6% of the total CH₄ emission), but most often dominate CH₄ emissions (Aben et al., 2017; Bastviken et al., 2004; Davidson et al., 2018; Deemer and Holgerson, 2021; Van Bergen et al., 2019). Ebullition occurs episodically. Therefore, to reliably quantify ebullition, long-term measurements (weeks to months) are needed, and short measurements (minutes to days) tend to underestimate ebullition (Maeck et al., 2014; Wik et al., 2016). Long-term measurements are currently largely lacking for ditches (but see data on 4 ditches in Köhn et al., 2021). Short-term ebullition data, however, has been reported and these measurements suggest that also in streams and ditches ebullition can be an important pathway (Crawford et al., 2014; Vermaat et al., 2011). Therefore, current ditch emission estimates, which are primarily based on only diffusive fluxes or diffusive and short-term ebullition measurements may underestimate CH₄ release and, thus, total GHG emission from ditches.

Here, we assess the role of ditches in the GHG budget of peat landscapes. We therefore quantified the year-round emission of greenhouse gases from drainage ditches including diffusive fluxes of ${\rm CO_2}$, ${\rm CH_4}$ and ${\rm N_2O}$, and ${\rm CH_4}$ ebullition. We hypothesize H1) that ditch emission is dominated by ${\rm CH_4}$, especially via ebullition. Additionally, we expect that H2) GHG fluxes differ considerably among ditches with high temporal variability, in which most of the emissions occurring in summer, and that H3) the among-ditch variation can be explained by factors closely related to productivity, such as oxygen concentration and nutrient availability. Lastly, H4) GHG emissions in agricultural ditches per unit area are expected to be higher than published terrestrial emissions.

2.2 METHODS

2.2.1 Study sites

Ten ditches varying in trophic status and morphology were selected to obtain insight in the variability of GHG emissions. These ditches are located in the North of the Netherlands, which has a temperate oceanic climate with average annual

temperatures ranging from 0 °C in winter to 21 °C in summer. The ditches were all located in peatlands with the thickness of the peat layer varying from less than 1 meter to 2 meters. The peatlands are used for grass production for dairy farming, fertilized with cow manure between February 15th and September 1st (for more information about the farms, see Weideveld et al., 2021). The ditches are used to drain the meadows in case of a precipitation excess and used to transport water to the meadows in case of a water deficit. They are part of a complex system of canals and lakes that are connected to the largest water reservoir of the Netherlands: Lake IJsselmeer. During the growing season, submerged macrophytes (*Elodea spp., Myriophyllum spicatum*) and floating plants (*Lemna spp.*) were observed (but not quantified) in the ditches. On the shores of the ditch a narrow strip of helophytes (*Typha latifolia, Glycera maxima*) was present. The ditches are labelled A1–A3, K1–K2, S1–S3 and V1–V2 (first letter referring to the farm they were located on, Fig. 2.1). We selected a single sample point within each of the 10 ditches. The flow velocity in the ditches is low during most of the year (Table 2.1).

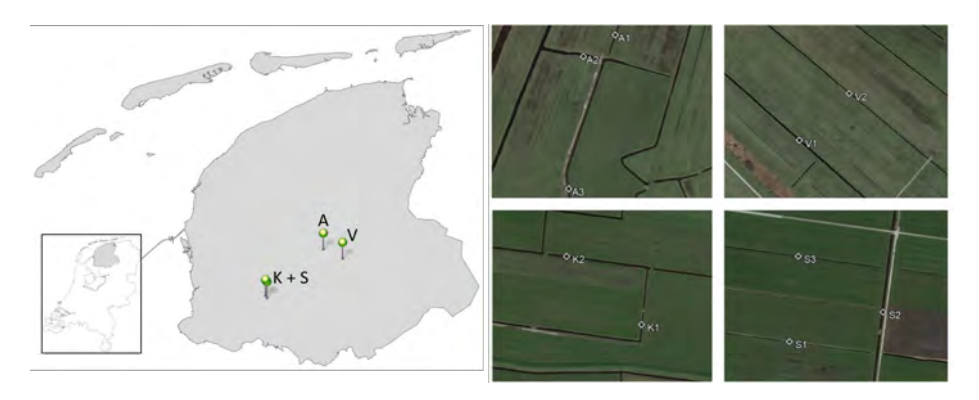


FIGURE 2.1 Locations of the four farms and of the 10 ditches in Friesland in the north of the Netherlands.

2.2.2 Field measurements

2.2.2.1 Greenhouse gas fluxes

Field measurements were performed every two to four weeks from May 2017 to June 2018 with the highest frequency in summer. The mean air temperature during measuring period was 10.5 °C (the mean air temperature over the past 30 years is 9.8 °C). During each field campaign diffusive fluxes of CO₂ and CH₄ were measured during the day with a transparent acrylic glass floating chamber (30 cm diameter, 30 cm height) connected to an Ultra-Portable Greenhouse Gas Analyzer (GGA-30EP, Los Gatos Research, Santa Clara, CA, USA). Diffusive flux measurements were conducted in triplicate, each measurement lasting at least 3 minutes, which was the time needed to obtain a linear

increase or decrease in CO₂ and CH₄ concentration in the chamber. When a sudden increase in CH₄ concentration was observed, due to ebullition, or when we observed a non-linear increase in gas concentrations, the measurement was discarded and repeated. In between measurements the chamber was aerated with atmospheric air. In addition to CO₂ and CH₄ fluxes, N₂O fluxes were measured from May until August 2017 and in April 2018, using a Greenhouse Gas Analyzer (G2508, Picarro, Santa Clara, CA, USA) for the measurements of all three gases. Our results were limited to day-time CO₂ fluxes only.

In each ditch four self-constructed bubble traps (Fig. S2.1) were installed within a stretch of ten meters, to measure ebullition. These traps consisted of a glass bottle varying in size between 100 and 1000 ml. The smaller bottles were connected to funnels of 9.5 cm diameter and placed in very shallow ditches. The larger bottles were connected to funnels of 20 cm diameter. The bubble traps were kept afloat by EVA foam boards. During periods of extreme low water levels, the water column in two ditches was too shallow to use funnels and we placed the bottles in the water without funnels. During each field visit the volume of the collected gas was determined. "Fresh bubbles" were collected with funnels while disturbing the sediment. This was done in summer and winter.

2.2.2.2 Surface water and pore water quality sampling and in situ measurements

HOBO Pendant® temperature data loggers (UA-001-64, Onset Computer Corporation, Bourne, MA, USA) recording the temperature each 2 hours were placed just above the sediment during the first field visit and removed during the last. During each field visit water temperature, pH and dissolved oxygen (O2) were measured at 3 depths (5 cm below surface, 20 cm below surface, just above sediment - with the deepest ditch being 70 cm deep, see Table 2.1) using a Portable Multi Meter (HQ40d, HACH, Loveland, CO, USA), resulting in 15-16 profiles over time per ditch. To monitor concentrations of cations and anions (including nutrients), surface water samples in the top 2 centimetres were taken approximately each month (n=9-10 per ditch) with 100 ml polyethylene bottles and transported refrigerated to the laboratory for further analysis. Additionally, in each ditch a 12 ml glass exetainer (Labco, high Wycombe, UK) containing 0.2 ml 2.5M H₂SO₄ was filled completely with surface water (*n*=10–12 per ditch), for dissolved CH₄ measurements in the laboratory. In November and February 2017 and April 2018, sediment pore water was sampled at a depth of 15 cm in the ditch sediment using a 60 ml syringe connected to a porous ceramic cup (Eijkelkamp Agrisearch Equipment, Giesbeek, the Netherlands) via a Teflon tube and stored at 4 °C until further analysis (see 'Laboratory analysis').

Water levels in the ditches are controlled by pumps and overflow weirs. During each visit we determined the water depth using a Secchi disk: the disk was slowly lowered

in the water until it 'landed' on the soft sediment after which we noted the length of the submerged part of the rope connected to the disk. Drainage level was determined as the difference between the water level and the average depth of the adjacent field. The hard-bottom of the ditch was estimated in June and December 2017 lowering a stick with cm-marks in the ditch until a hard soil layer was reached and the stick could not go deeper. Sediment thickness was estimated by subtracting the water depth from the hard-soil depth.

Sediment samples, used for analysis of loss on ignition (LOI) and $\mathrm{CH_4}$ and $\mathrm{CO_2}$ production rates, were taken once on December 2017 using a suction corer and gravity core sampler (UWITEC GmbH, Mondsee, Austria). We sampled approximately half a liter of sediment and placed it in zip bags of which all air was expelled. Samples were taken within a sediment depth of 5–10 cm, which is the most active depth for $\mathrm{CH_4}$ and $\mathrm{CO_2}$ production. The samples were refrigerated at 4 °C until further analysis.

2.2.3 Laboratory analysis

Surface water samples from the 100 ml polyethylene bottles were homogenized and filtered the day after sampling using a vacuum with 0.47 mm glass microfiber filters (Whatman International Ltd, Maidstone, England). 10 ml of filtered water was acidified (0.1 ml 10% nitric-acid) and, after storage at 4 °C, analysed for concentrations of the following ions: aluminium (Al³+), calcium (Ca²+), iron (Fe²+), potassium (K+), sodium (Na+), phosphorus (P), total sulphur (S_{tot}) (which includes elemental S, organically bound S and total S), silicon (Si) and zinc (Zn²+) (ICP-OES, iCap 6300, Thermo Fisher Scientific, Bremen, Germany). Another 10 ml was stored at -20 °C and analysed for concentrations of the following nutrients: ammonium (NH $_4$ +), nitrate (NO $_3$ -) and phosphate (PO $_4$ -) (Auto Analyzer (Seal Analytical XY – Z sampler, Bran + Luebbe GmbH, Norderstedt, Germany)).

Dissolved inorganic carbon (DIC, as CO₂, HCO₃ and CO₃ c) was measured by injecting 0.2 ml of filtered water in a closed glass chamber containing 0.2 M H₃PO₄ solution, converting all DIC into CO₂. A continuous flow of N₂ was used as carrier gas to transport the CO₂ to an AO2020 Continuous Gas Analyser (ABB, Zürich, Switzerland). The area under the curve of the raw instrument output was converted to CO₂ (equalling sample DIC) via a calibration curve that was made by injecting different volumes (0.1–1.0 mL) of 1.25 mM HCO₃ solution. Dissolved CO₂ concentrations were calculated according to the equations in Table 4.2 of Stumm and Morgan (1995) and using data from measurements of DIC, pH, water temperature, and dissociation constants of carbonic acid in pure water (taken from Dickson & Millero, 1987):

Where K_1 is dissociation constant calculated from p K_1 = -126.34048 + 6320.813/T + 19.568224lnT and p K_2 = -90.18333 + 5143.692/T + 14.613358lnT, resulting in a K_1 of 4.15*10⁻⁷ and K_2 of 4.20*10⁻¹¹ at 20 °C.

Dissolved $\operatorname{CH_4}$ was analysed by first making a 2 ml gas headspace in the 12 ml exetainers using nitrogen ($\operatorname{N_2}$), followed by vigorously shaking the exetainers for 30 seconds and measuring $\operatorname{CH_4}$ concentrations in the headspace using the above-mentioned GC. Original $\operatorname{CH_4}$ concentrations in the water were calculated using Henry's law and its solubility constant for $\operatorname{CH_4}$, taking the respective water temperature into account (Sander, 2015). The pore water samples were analysed for the same variables in the same way.

2.2.4 Sediment CH, and CO, production assays

Sediment CH_4 and CO_2 production was assessed in quadruplicate per ditch by placing 40 ml of carefully mixed sediment in a 120 ml glass vial. The vials were flushed with nitrogen gas, and sealed with red butyl rubber stoppers (Rubber BV, Hilversum, Netherlands) and aluminium crimp caps before dark incubation at a temperature of 25 °C. Headspace samples of 100 μ l were taken with use of a gas-tight glass syringe (Hamilton Company). Headspace samples for CO_2 were taken 3 times per vial, at intervals of 2–3 days and determined on the above mentioned infrared gas analyser. CH_4 samples were taken at intervals of 2 days for 2 weeks (6 samples per ditch sediment) and were measured with the above-mentioned GC. The CO_2 and CH_4 production rate was calculated by following the gas concentrations in the head space in time (as in Kosten et al., 2016) and subsequently expressed per gram of dry weight and per gram of organic matter.

For each vial sediment dry weight and LOI was determined at the end of the incubation. The sediment samples for LOI were dried at 70 °C for 3 days to obtain sediment moisture content and these dried samples were further incinerated at 550 °C for 24 hours. Loss on ignition, as a proxy for organic matter content, was determined as the difference between dry weight at 70 °C and 550 °C (as in Heiri et al., 2001).

2.2.5 GHG flux calculations

Each diffusive flux was calculated using linear regression of the three minute measuring period as in Vroom et al. (2018) using the following equation:

Where F is gas flux (mg m² d⁻¹); V_{ch} is chamber volume (m³); A_{ch} is chamber surface area (m²); slope is the slope of the measured CO_2 , CH_4 or N_2O concentration over time (ppm s⁻¹); P is the atmospheric pressure (kPa, obtained from the meteorological

station in Leeuwarden, approximately 20–35 km from the ditches (station number 85 Royal Netherlands Meteorological Institute (KNMI))); *M* is the molecular mass of CO₂, CH₄ or N₂O (g mole⁻¹); *F1* is the conversion factor of seconds to days; *R* is the gas constant (8.3144 J K⁻¹ mole⁻¹); and *T* is temperature (K, logged during the measurements (HOBO Pendant® temperature data loggers (UA-001-64, Onset Computer Corporation, Bourne, MA, USA))). CO₂ concentration changes during closed chamber deployment were checked visually for linearity in the field to ensure no disturbance by ebullition. All fluxes of CO₂, CH₄ and N₂O exceeded the minimum detectable flux (i.e. 4.2, 0.013 and 0.090 mg m⁻² d⁻¹ for CO₂, CH₄ and N₂O, respectively) by a large margin (Nickerson, 2016).

The ebullitive flux was determined by multiplying the gas volume with the mean concentration of CH₁ in fresh bubbles and subsequently divided by the area of the funnel (or bottle opening in case there was no funnel attached) and time of deployment. The CH₄ concentration was calculated using the ideal gas law. The average concentration of $CH_{_{A}}$ in the fresh bubbles was 35% (4 - 65%). As in Maeck et al. (2014) and Marcon et al. (2022), we used this percentage to convert the volumetric ebullition fluxes to CH, ebullitive fluxes again using the ideal gas law. We used the CH concentration of the fresh bubbles as we observed that a considerable CH loss from the bubble traps occurred during deployment (75% decrease in concentration in 23 days, unpublished data). Diffusion back into the water seems the most likely cause for this, potentially accelerated by CH₄ oxidation (which creates a steeper diffusion gradient). Using the CH₄ concentration of the gas in the bubble traps would therefore lead to an underestimation of the CH, that was emitted through ebullition. CH, concentrations were measured with a HP 5890 gas chromatograph (GC) equipped with a Porapak Q column (80/100 mesh) and a flame ionization detector (Hewlett Packard, Wilmington, DE, USA).

2.2.6 Data analysis

All statistical analyses were performed using R (version 4.1.3). Statistical significance was determined at P < 0.05. We follow the atmospheric sign convention, i.e. positive gas fluxes denote emission whereas negative fluxes denote uptake from the atmosphere.

We used linear interpolation of the average emission per time-point to estimate GHG emissions in between measurements for each ditch. We opted to interpolate, instead of using 'monthly values' as interpolation avoids setting trivial boundaries as to where a month starts or ends. Mean annual emissions per ditch were calculated by averaging the interpolated data (the same method was used to calculate means for water quality variables). A global warming potential of 27.2 for CH₄ and 273 for N₂O

was used (100-year time frame, IPCC, 2021) in order to get CO_2 equivalents (CO_2 -eq.). We then used the obtained annual emission data of the different pathways to assess the contribution of each pathway to the total GHG emission in CO_3 -equivalents (H1).

To study the effect of seasonality on diffusive fluxes of CO, and CH, and ebullitive CH, fluxes (H2), we first calculated the share of the annual emission occurring in different meteorological seasons: spring: March 1st - June 1st; summer: June 1st - September 1st; fall: September 1st - December 1st; winter: December 1st - March 1st. We visualized seasonal emission patterns for all 10 ditches using GHG emissions normalized to the highest emission in an individual ditch (i.e. emissions were expressed as a fraction of the highest emission). In addition, we used linear mixed-effects models (LMM) using the 'lme4' packages (Bates et al., 2015). Based on the measurement dates we attributed each measurement to their corresponding meteorological season. Subsequently, meteorological season was used as a fixed effect in the model with measurement date and ditch ID as crossed random effects on the intercept to account for nonindependence stemming from having multiple measurements per date and per ditch. To study spatial variation among ditches (H2), we used a similar analysis. Here, we used ditch ID as fixed effect with measurement date as a random effect on the intercept to account for nonindependence stemming from repeated measurements. Diffusive CH, fluxes and CH4 ebullition were log-transformed. Diffusive CO2 fluxes were square roottransformed after removing negative values by subtracting the minimum CO, flux and adding a value of one. Model assumptions of linearity, homoscedasticity and normality of residuals were checked using residual plots, histograms and Q-Q plots of residuals and a Shapiro-Wilk's test (function shapiro.test). The significance of fixed effects was statistically tested using a type-III ANOVA (function anova) with degrees of freedom and P-values calculated using the Kenward-Roger approximation (Kenward and Roger, 1997) via the 'lmerTest' and 'pbkrtest' packages (Halekoh and Højsgaard, 2014; Kuznetsova et al., 2017). Pairwise comparisons, using Tukey adjustment, were performed using the emmeans and pairs functions of the 'emmeans' package.

To get insight in which variables can explain – and potentially drive – the variation in GHG emissions among ditches (H3), we performed a partial least squares (PLS) analysis ('pls' package, *plsreg2*, Liland et al., 2021) using the mean annual emissions. We choose PLS as it can deal with multicollinearity among the variables and can test multiple response variables at once, in our case diffusive CO₂ and CH₄, and ebullitive CH₄ (in g CO₂-eq. m⁻² d⁻¹) (Höskuldsson, 1988). The following variables were tested: water depth; sediment thickness; ditch width (all in cm); O₂ (mg l⁻¹) and pH of the surface water; dissolved CH₄ and CO₂ in the water column (μmol l⁻¹); CH₄ and CO₂ production in the sediment (mg g⁻¹ dry weight d⁻¹); LOI; and concentrations (all in

 μ mol l⁻¹) of NH₄⁺, NO₃⁻, PO₄³⁻ in the surface water and pore water. To summarize the influence of those variables for the emission pathways, across the extracted PLS components, we used the variable influence on projection (VIP). Variables with VIP values larger than 1, were considered most influential for the model, variables with VIP values between 0.6 and 1.0 as moderately important. Variables with a lower VIP are considered less influential. We used scaled and centred PLS coefficients to interpret the influence of the variable on every emission pathway. The variables that were influential in the PLS, were tested for linear relationships with the different response variables ('stats' package, lm). Significantly related variables with an R² > 0.3 were plotted against the corresponding GHG variable.

2.3 RESULTS

2.3.1 Environmental conditions

The ten studied ditches varied strongly in water depth, thickness of the sediment layer, ditch width and nutrient concentrations in the water column as well as in the sediment (Table 2.1). Sediment thickness varied from 40 cm in ditch S1 to 103 cm in A1. Ditch S2 was, with a mean water level of 64 cm, the deepest ditch. The water level is regulated by farmers and the Water Authority and varied considerably in time, with the strongest variation occurring in ditch A1 where the maximum water depth occurred in summer (70 cm) and the minimum (15 cm) in winter. In ditch S3 the water level also fluctuated strongly, with minimum water levels of 5–10 cm from September to March, impeding funnel deployment (see also Table 2.1). Nutrient concentrations were higher in the pore water than in the surface water and varied strongly. Elemental concentrations in the water column and sediment also varied strongly among ditches (Table S2.1, S2.2).

Most elemental concentrations displayed a seasonal pattern, with Na⁺, S_{tot} and Si concentrations, for instance, peaking in winter, and Ca²⁺ concentrations being lowest in winter (Fig. S2.2, S2.3). Water temperatures showed clear seasonal patterns ranging between 0.5 °C in winter and 26 °C in summer in the surface water and between 3 °C and 22 °C near the sediment. O₂ concentrations showed the same seasonal patterns, with lowest concentrations from September until March, while pH did not show seasonal variation (Fig. S2.4).

2.3.2 Annual emissions

Mean annual emissions as well as the relative contribution of diffusive CO_2 , diffusive CH_4 and ebullitive CH_4 emission varied strongly and significantly among the ditches (Fig. 2.2, LMM: $F_{3,39} = 4.83$; P < 0.001 for diffusive CO_2 ; $F_{3,39} = 14.77$; P < 0.001 for diffusive

CH₄; F_{3,39} = 20.22; P<0.001 for ebullitive CH₄). Mean diffusive CO₂ fluxes ranged between 1.9 and 22.0 g CO₂ m⁻² d⁻¹ (overall mean 8.9 g CO₂ m⁻² d⁻¹), contributing only 12% to the mean annual GHG emission in ditch A1 while contributing 75% to the total emissions in ditch S2. The share of diffusive CH₄ emissions to total GHG emission varied between 1.3% in ditch A1 and 41% in ditch S3, with mean annual fluxes ranging from 0.1 to 16.5 g CO₂-eq. m⁻² d⁻¹ (overall mean 4.8 g CO₂-eq. m⁻² d⁻¹). Ebullitive CH₄ emissions varied between 1.3 and 40.9 g CO₂-eq. m⁻² d⁻¹ (overall mean 11.2 g CO₂-eq. m⁻² d⁻¹). The share of the ebullitive CH₄ fluxes to the total GHG emissions ranged from 5% in ditch K1 to 87% in ditch A1. Diffusive CH₄ emissions were correlated with diffusive CO₂ emissions yet not with ebullitive CH₄ emissions (Fig. 2.3).

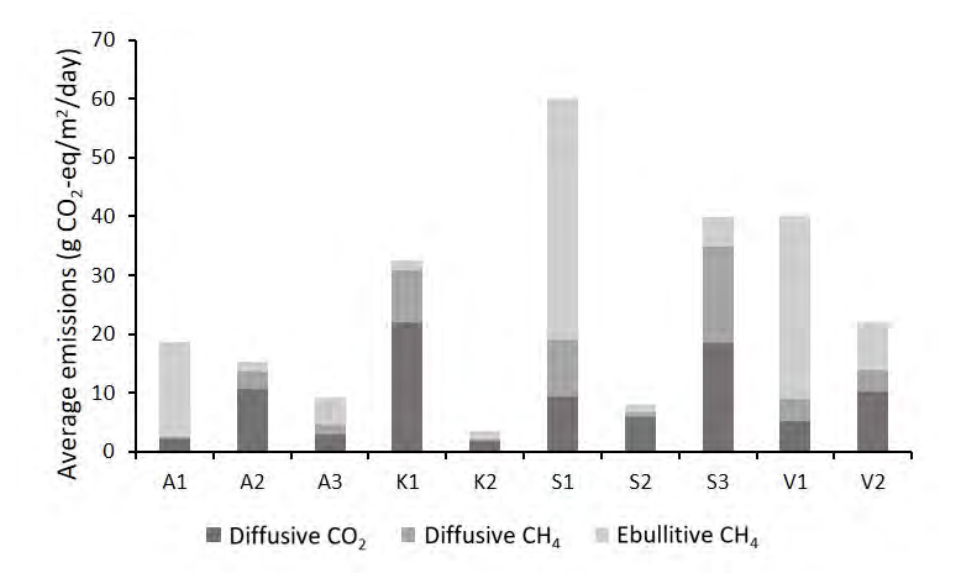


FIGURE 2.2 Mean annual CO, and CH, emissions between May 2017 and May 2018 in 10 ditches.

 $\rm N_2O$ emissions (measured from May until August in 2017 and in April 2018) were generally low (~ 0.3 mg m $^{-2}$ d $^{-1}$ equalling 82 mg $\rm CO_2$ -eq. m $^{-2}$ d $^{-1}$). The contribution of $\rm N_2O$ to the total greenhouse gas emission from ditches based on mean emissions was low (<0.9%) but depending on the frequency of occurrence and the duration of peak emissions the actual contribution may be higher.

Such a peak emission in the ditches of farm V occurred on June 29 when heavy showers followed a dry period. On this day we observed water from the humid grasslands flowing into the ditches from the drainage pipes, which resulted in ditch N_2O emissions of 3.0 g CO_2 -eq. m^{-2} d^{-1} (V1) and 10.4 g CO_2 -eq. m^{-2} d^{-1} (V2). Two single

measurements at the outlet of a drain even showed N_2O emissions of on average 142 mg m⁻² d⁻¹ (equalling 38.8 g CO_2 -eq. m⁻² d⁻¹), in addition to emissions of 45 g CO_2 m⁻² d⁻¹ and 110 mg CH_4 m⁻² d⁻¹ (equalling 3 g CO_2 -eq. m⁻² d⁻¹).

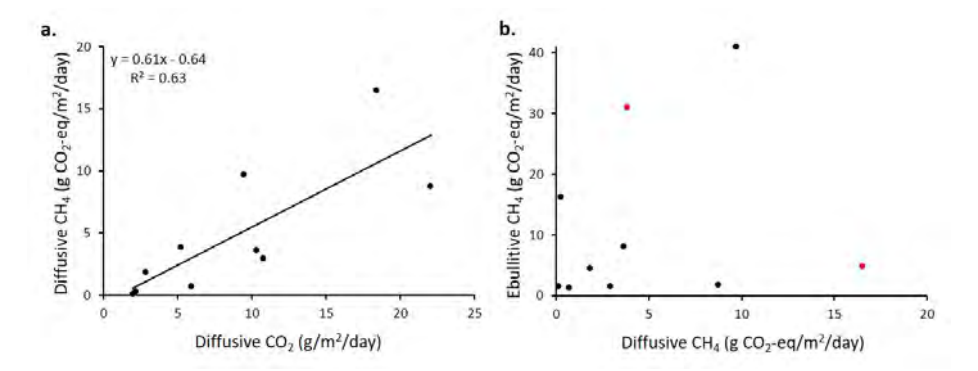


FIGURE 2.3 Relationships between the different gasses- and different emission pathways based on annual mean emissions (n=10). **a**. Relationship between diffusive CH_4 and CO_2 emission. P = 0.006. **b**. Relationship between ebullitive and diffusive CH_4 emission. P = 0.62. Red datapoints show ditch S3 and V1, where low water table hampered funnel deployment and ebullitive fluxes may be underestimated. Data from May 2017 to May 2018.

Variable	A1	A2	A3	K1	K2	S1	S2	S3	V1	V2
Sediment thickness (cm)	103	85	100	78	75	40	65	60	46	75
Mean water depth (cm)	43	39	33	46	52	24	64	10	34	24
Depth min-max (cm)	15-70	30-55	25-50	30-60	40-60	10-50	50-70	5-50	20-50	15-40
Width (m)	2.5	5.0	3.6	2.8	4.3	1.1	3.8	1.8	3.8	2.0
Flow	Low	Low	High	High	High	Low	High	No †	High	No†
pH surface	7.0	6.9	7.1	6.6	7.1	6.7	6.8	6.1	6.5	6.3
pH – 20 cm	6.7	6.3	6.8	6.1	6.4	5.3	6.6	6.2	6.1	5.9
O ₂ concentration surface (mg l ⁻¹)	6.0	5.5	6.6	4.9	7.6	3.7	5.7	2.5	3.8	3.0
O ₂ concentration – 20 cm (mg l ⁻¹)	3.3	4.3	4.9	3.6	6.2	0.3	5.5	1.7	0.9	0.2
O ₂ concentration sediment (mg l ⁻¹)	4.2	2.9	2.6	0.6	1.4	0.9	2.8	1.1	0.2	1.0
NH4 ⁺ surface water (µmol l ⁻¹)	52.6	50.1	39.3	68.1	66.2	80.6	86.2	496.3	71.9	76.3
NH4 ⁺ pore water (µmol l ⁻¹)	390.2	651.6	940.7	432.8	234.6	431.4	657.1	628.4	1080.1	1070.
NO3 surface water (µmol l-1)	48.5	46.5	62.0	11.0	21.5	15.5	28.4	17.4	15.0	12.5
NO ₃ · pore water (µmol l¹)	152.7	26.7	188.5	5.1	14.1	23.7	34.0	10.6	26.8	14.5
PO ₄ 3- surface water (µmol l ⁻¹)	2.4	3.6	4.7	2.5	2.5	1.6	1.7	4.6	6.3	3.7
PO ₄ ³ - pore water (µmol l ⁻¹)	11.2	51.1	78.4	5.5	7.2	0.3	3.4	1.5	119.5	17.6

TABLE 2.1 Characteristics and water column nutrient concentrations of the studied ditches. Mean annual concentrations and parameters calculated based on interpolated data between May 2017 and May 2018 (surface water samples n = 15; pore water samples n = 3).

2.3.3 Seasonal variation in GHG emissions

The CO₂ flux ranged between -4.04 and 138.1 g m⁻² d⁻¹. Although the variation among the ditches was strong, diffusive CO₂ fluxes were significantly affected by seasonality (Fig. 2.4a, LMM: $F_{3,39} = 13.51$; P<0.001). Fluxes in fall were significantly higher than those in spring (t = 2.99; P = 0.023) and summer (t = 5.13; P<0.001), and similar to those in winter (t = 0.31; t = 0.99). Spring and summer represented periods of either

 CO_2 uptake or very little emissions: during this time, four ditches – A1, A2, A3 and K2 – took up CO_2 and the remaining 6 ditches released only 13% (ranging between 2 and 24%) of their annual CO_2 emissions.

The observed diffusive CH_4 emissions ranged between 0.00 and 2.59 g m⁻² d⁻¹ over the year. We did not observe a seasonal pattern in diffusive CH_4 emissions (Fig. 2.4b, LMM: $F_{3,39} = 0.48$; P = 0.699), with on average 27% (5 – 60%) of the annual emissions occurring during summer months.

In contrast to the diffusive CH_4 fluxes, ebullitive CH_4 fluxes showed a seasonal pattern with emissions being highest in spring and summer, and lowest in winter (Fig. 2.4c, LMM: $F_{3,39} = 22.77$; P < 0.001). Ebullitive CH_4 fluxes ranged from 0.00 - 4.21 g m⁻² d⁻¹ over the year. Fluxes in summer were significantly higher than those in fall (t = 2.80; P = 0.04) and winter (t = 8.05; P < 0.001), and similar to those in spring (t = 1.41; t = 0.50). For 8 out of the 10 ditches 43% (t = 2.80) of t = 0.500. For 8 out of the 10 ditches t = 0.5010 of t = 0.5011 occurred during the summer months. Two ditches t = 0.5021 of t = 0.50222 with funnels. We therefore deployed bubble traps without funnels which most certainly lead to an underestimation of ebullition during summer (t = 0.50222 and t = 0.50323 and t = 0.50333 and t = 0.503333 and t = 0.50333 and t = 0.503333 and t = 0.5033333 and t = 0.50333333 and t = 0.5033333 and t = 0.5033333 and t = 0.50333333 and t = 0.5033333 and t = 0

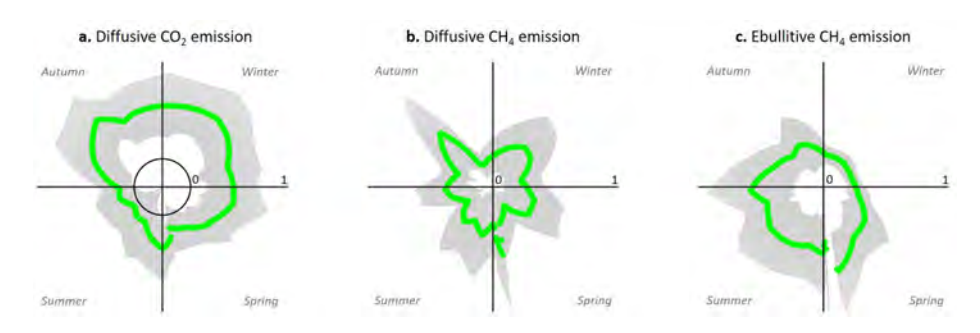


FIGURE 2.4 Year-round variation of diffusive CO₂ (a), diffusive CH₄ (b) and ebullitive CH₄ (a) emission, based on interpolated normalized emissions for each day of the year. The green line shows mean emission from the 10 ditches, the grey area depicts the standard deviations, where 1 is highest emission and values below 0 (in panel a, within circle) show an uptake. The emissions are depicted clockwise, with December 1st (first day of winter) located on the y-axis. Data from measuring period May 2017 to June 2018 (note for ebullition and total emissions measuring period started 3 weeks later due to bubble trap deployment).

2.3.4 Variables explaining among-ditch variability in greenhouse gas emissions

According to the PLS analysis, elemental concentrations in the surface water and pore water in the different ditches mostly co-vary (Fig. 2.5). While mean annual diffusive

fluxes of both ${\rm CO_2}$ and ${\rm CH_4}$ cluster with mean annual surface water concentrations – including dissolved ${\rm CH_4}$ and ${\rm CO_2}$ concentrations –, ${\rm CH_4}$ ebullition correlates positively with sediment loss on ignition and negatively with ditch characteristics (Fig. S2.5).

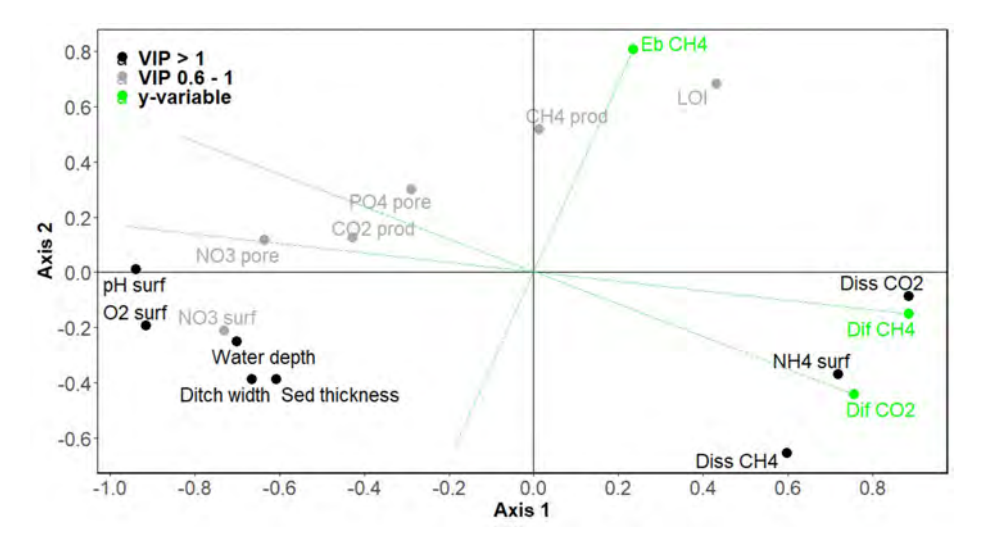


FIGURE 2.5 PLS plot showing how the mean annual X variables (black and grey) correlate with the different mean annual emission pathways (Y variables; green). The X variables are classified according to their VIPs: highly influential (black, VIP >1) and moderately influential (grey, VIP 0.6-1.0). Less influential variables are not shown for clarity. The plot can be interpreted by drawing a line from an emission pathway through the origin and across the plot (dashed green lines). The variables on or close to this line are closest related to the emission pathway. Explanation of abbreviations: eb = ebullitive; dif = diffusive; pore = pore water; surf = surface water; diss = dissolved;; prod = production.

2.4 DISCUSSION

The annual mean emissions in the 10 ditches were high and varied between 3.57 and $60.1\,\mathrm{g}$ CO $_2$ -eq. m⁻² d⁻¹. On an annual basis all ditches acted as a GHG source for CH $_4$ as well as for CO $_2$. Total CH $_4$ emissions contributed most (57%, ranging 25 – 88% among the ditches) to the overall GHG emission. Ebullition contributed 40% (5 – 87%) to the total GHG emission, supporting our first hypothesis with respect to the importance of ebullition. The diffusive CH $_4$ and CO $_2$ flux contributed 16% (3 – 41%) and 43% (12 – 75%) respectively. The emissions differed significantly among ditches (H2). Moreover, the estimated annual mean CH $_4$ emission of ~16 g CO $_2$ -eq. m⁻² d⁻¹ (and ~9 g m⁻² d⁻¹ for CO $_2$) from our ditches is among the highest reported world-wide (biased towards European and North American countries, Peacock et al., 2021) and roughly 2 times higher than the default emission factor for ditches on organic soils as reported by the IPCC (Lovelock et al., 2019) (H4).

2.4.1 Importance of ebullition

This is one of the first reports of year-round measurements of CH, ebullition in ditches. Our approach based on long-term deployment of bubble traps indicates that ebullition occurs year-round (Fig. 2.3) and forms a principal component of the total GHG emission (Fig. 2.1), responsible for up to 87% (min. 5%; mean 40%) of the annual GHG emission and up to 98% (min. 17%; mean 64%) of annual $\mathrm{CH_4}$ emission. This is higher than previous reports on ebullition form ditches based on shortterm summer measurements that indicated that ebullition contributes between 20 and 69% (Baulch et al., 2011; Tokida et al., 2007; Vermaat et al., 2011; Wilcock & Sorrell, 2008). Furthermore, this is also considerably higher than reported in the publication of Köhn et al., (2021), who found ebullition to contribute less than 10% to the total CH, emission in German drainage ditches after long-term deployment. The difference is striking and may be related to sediment structure which strongly impacts the ratio between diffusive and ebullitive fluxes (Langenegger et al., 2019). Strongly decomposed sediment generally has a low porosity and a relatively high gas storage capacity (Ramirez et al., 2015). Gas bubbles stored in the sediment can serve as a shortcut for diffusive CH, fluxes (Flury et al., 2015). Possibly, the German ditches had further decomposed sediment than the Dutch ditches, explaining the higher CH. diffusion rates and lower CH₄ ebullitive rates while the total CH₄ emission rates were within the same range.

We found a moderate correlation between organic matter content of the sediment and CH₄ ebullition (Fig. 2.5), but the explanatory power of models predicting among-ditch variation in CH₄ ebullition is low (Fig. 2.4b and 2.5 as also found by Liu et al., 2020 and McClure et al., 2020). Therefore, more insight in the contribution of potential drivers is needed to accurately upscale ebullitive fluxes. Until better predictive models are available, a high spatial and temporal resolution is needed to accurately assess this emission pathway. Our experiences show that to assess ebullition in shallow ditches of less than 10 cm deep, development of a different type of bubble traps is needed. We were unable, for instance, to measure ebullition accurately in our shallowest ditch (S3) during part of the year, which certainly has led to an underestimation of the annual emission. In addition, modelling approaches as in Langenegger et al. (2019) or Eddy co-variance approaches (Iwata et al., 2018) could be further developed to assess ebullition in these small and shallow systems.

2.4.2 Seasonal variability

While no seasonal pattern was found for diffusive $\mathrm{CH_4}$ emissions, ebullitive $\mathrm{CH_4}$ emissions peaked in summer. Summer emissions made up – on average – 43% of the annual $\mathrm{CH_4}$ ebullition, corresponding with earlier observations that summer

emissions are highest (Schrier-Uijl et al., 2010). While it is well-known that an increase in temperature stimulates CH₄ production, at the same time CH₄ oxidation rates increase, which may – in part – explain why we did not observe a seasonal trend in diffusive CH₄ emission (Fuchs et al., 2016). In addition, CH₄ diffusion from the sediment to the water column is limited by diffusivity (e.g. Flury et al., 2015) hampering a strong increase in diffusive sediment CH₄ release. Ebullition, on the other hand, is less affected by CH₄ oxidation and diffusion rates, generally leading to exponential increase with temperature rise (Aben et al., 2017). Clearly, other factors than temperature impact seasonal variation in CH₄ production and oxidation as well. Examples are seasonal changes in the availability of O₂, light (Thottathil et al., 2018) and alternative electron acceptors (Bastviken, 2009; Rissanen et al., 2017). In addition, seasonal differences in precipitation impact the inflow of dissolved gasses from the terrestrial area into the ditch, with higher diffusive emissions likely related to higher inflow – as further discussed below - which is largely independent of temperature.

CO₂ emissions were highest in fall and winter, with mean 35% of annual CO₂ emissions for both seasons. Higher primary production during spring and summer months due to algal and/or plant growth, combined with negligible inflow from the adjacent land as a result of lower gradients between peatland groundwater levels (evaporation losses) and high summer water levels in the ditches - to optimize grass production - likely explain this seasonal pattern in CO, emissions. Similar seasonal patterns in CO₂ emissions were found in lakes (e.g. Trolle et al., 2012). Most likely because of our day-time-only measurements, we largely underestimate CO, fluxes in spring and summer and therefore also their contribution to total GHG budgets from ditches, since high primary production leads to CO, release during the nights, that may lead to a net CO, release and that is possibly higher in summer than in winter. Night-time flux measurements are needed to assess this. We do not have data to infer night time diffusive emissions, but assuming a 39% higher night-time CO, emission compared to day-time emissions (Attenmeyer et al., 2021) and a 0.7 scaling factor to convert day-time diffusive CH, emissions to diel CH, emissions (Johnson et al., 2022), we find average diel GHG emissions are in the same range as day-time only measurements (mean 26.9 (17 sd.) g CO_3 -eq. m⁻² d⁻¹ vs. mean 24.9 (17 sd.) g CO_3 -eq. m⁻² d⁻¹). Note that our ebullitive CH₄ emission estimates are based on continuous bubble-trap deployment and therefore integrate day- and night-time fluxes.

Since in our study N₂O emissions were measured only four times and measurements were strongly biased towards the summer period, we did not obtain insights on potential seasonal variations in N₂O emission. N₂O emissions in winter have been

found to be substantially higher than in summer (Xiao et al., 2019) and strongly related to pulses in nitrogen addition (Meng et al., 2023). As we largely missed these events, we argue that our N₂O emission estimate is likely an underestimate.

While short term variability in GHG emissions was not the focus of the current study, we expect that variability in emissions within seasons may be strongly driven by lateral water inflow including GHG discharge of drains. The importance of drain discharge for GHG emissions was clearly illustrated by the high $\rm CO_2$, $\rm CH_4$ and $\rm N_2O$ emissions (respectively 45, 3 and 39 g $\rm CO_2$ -eq. m⁻² d⁻¹), measured near the outlet of the drain shortly after a rain event. The drains transport soil organic matter- and plant-derived $\rm CO_2$ and $\rm CH_4$ into the ditches (Kuzyakov & Gavrichkova, 2010; Van der Grift et al., 2016). The high $\rm N_2O$ emissions are likely related to the manure – containing high amounts of ammonium – applied to the adjacent fields (Hama-Aziz et al., 2017). $\rm N_2O$ may be produced by nitrification of ammonium and/or through denitrification of nitrate in different parts of the soil profile and washed out to the drains and eventually to the ditch.

2.4.3 Among-ditch variability

As hypothesized (H2) we found a strong and significant among-ditch variability in GHG emissions. This variation could not be explained by potential sediment $\mathrm{CH_4}$ and $\mathrm{CO_2}$ production rates – assessed using sediment incubations – nor with other sediment characteristics (in line with Wik et al., 2018) hinting at overriding importance of lateral inflow of GHGs or water column processes. In contrast, $\mathrm{O_2}$ concentrations did explain the variance in total ditch GHG emissions (supporting H3, see Fig. 2.5). $\mathrm{O_2}$ likely acts as an 'integrated proxy', representing the balance between aerobic respiration ($\mathrm{CO_2}$ production) and primary production ($\mathrm{CO_2}$ consumption). In addition, low $\mathrm{O_2}$ concentrations in the water column will reduce the oxygenated boundary layer of the sediment, where most of the $\mathrm{CH_4}$ oxidation occurs. Therefore, it may hamper $\mathrm{CH_4}$ oxidation and stimulate $\mathrm{CH_4}$ production likely explaining the negative relation between $\mathrm{O_2}$ concentration and both ebullitive and diffusive $\mathrm{CH_4}$ emissions.

In line with earlier studies (Vermaat et al., 2011) shallow ditches were found to have higher GHG emissions, especially diffusive emissions, than deeper ditches (Fig. 2.5). The underlying reason may that deeper ditches had higher dissolved $\rm O_2$ concentrations in the water column enhancing $\rm CH_4$ oxidation. A longer residence time of $\rm CH_4$ in the water column in deeper waters – with comparable gas exchange velocities – may also lead to a higher fraction of $\rm CH_4$ being oxidized before it leaves the water column (Bastviken et al., 2008; Holgerson, 2015). Overall, dead-end or

slow-flowing ditches (A1, A2, S1, S3 and V2, mean emission 31.1 (16.8 sd.) g CO_2 -eq. m⁻² d⁻¹) tended to emit more GHGs than connecting ditches (ditches A3, K1, K2, S2 and V1, mean emission 18.7 (14.7 sd.) g CO_2 -eq. m⁻² d⁻¹) that tended to have higher flow rates (visual observation). In this study we did not quantify the amount of carbon derived from the peatland outgassing downstream. This remains an important emission pathway that needs further attention to make a full assessment of landscape emissions (Casas-Ruiz et al., 2023).

2.3.4 Aquatic versus terrestrial emissions

The ditches emitted on average 24.9 g CO₂-eq. m⁻² d⁻¹ or 91 t CO₂-eq. ha⁻¹ yr⁻¹. Default emission factors for the highest emissions from the terrestrial area of drained Dutch peatlands (grassland on peat with a mean surface level lowering of 8.5 mm per year), are estimated to be 19 t CO₂-eq. ha⁻¹ yr⁻¹ with negligible CH₄ emissions (Arets et al., 2019). This indicates that aquatic emissions in our ditches, on a per area basis, are 4.8 times higher than the default values used for the national greenhouse gas reporting of drained peatlands, supporting our last hypothesis. In our study region the ditch surface area makes up 5% of the total area, implying that ditches represent roughly 20% of the total GHG emission on a landscape scale. Our data therefore highlight that ditch emissions are important on a landscape scale. We measured emissions from the open water of the ditches only, and did not include emergent littoral vegetation. Since these plants are known for direct CH₄ transportation from sediment to atmosphere (van den Berg et al., 2020), including the littoral area possibly results in even higher ditch emissions.

Extrapolating our mean CH₄ ditch emissions using a conservative estimate of the total Dutch ditch area of 300,000 km² (Koschorreck et al., 2020), indicates that roughly 10% of all Dutch annual CH₄ emissions can be attributed to ditches (based on the total national CH₄ emission estimate from Coenen et al., 2017). This percentage closely matches with an earlier estimate (16%) based on literature-derived data (Koschorreck et al., 2020) and points out that ditch emissions are not only important on a landscape scale, but on a national scale as well. We therefore argue ditch emissions should be considered in national greenhouse gas reporting conducted under the United Nations Convention on Climate Change (UNFCCC) and the Kyoto Protocol. This is currently not always the case, although recently an IPCC methodology for this has been accepted (IPCC, 2019). While GHG emissions from drainage infrastructure such as ditches are likely an important component of GHG emissions of peat areas across the globe, global estimates are, so far, hard to make because of unknown areal extent of ditches and the high variation in emissions (Peacock et al., 2021). We argue that future work on regional GHG emissions should explicitly incorporate emissions

from ditches and their potential drivers in order to improve the accuracy of modelled ditch emissions and to enable global upscaling.

Acknowledgements

We would like to thank the farmers for granting access to the field site. Furthermore, we are thankful for the technical staff and the people who helped gather data in the field: Roy Peters, Germa Verheggen, Paul van der Ven, Sebastian Krosse (both from the RU General Instrumentation), Nicolas Herbert, Weier Liu, Peter Schramm, Roel Jan Wijma and Hessel de Boer. We thank Daniël Tak for running a part of the gas analysis and Mandy Velthuis and Simone Cardoso for helping out with the data analyses. We thank the anonymous reviewers for their suggestions on the manuscript. Fieldwork was funded by Horizon 2020 Framework Programme: PeatWise, ERA-GAS. Part of this research was supported by Horizon Europe Grant Wet Horizons (GAP-101056848). SK was partially financed by NWO-VIDI 203.098.

SUPPORTING INFORMATION

TABLE S2.1 Surface water concentrations of chemical elements of the studied ditches. Average annual concentrations calculated based on interpolated data between May 2017 and May 2018 (*surface water samples n* = 15).

Ditch ID	Al (μmol/l)	Ca (μmol /l)	Fe (μmol /l)	K (μmol/l)	Na (μmol /l)	P (μmol/l)	S (µmol/l)	Si (μmol/l)	Zn (µmol /l)
A 1	7.24	1009.49	26.53	223.55	1351.61	8.04	378.89	126.94	1.19
A2	8.62	886.52	33.45	254.19	1340.27	10.89	395.70	163.78	1.48
A3	7.15	974.54	23.90	245.72	1311.22	9.13	486.69	167.13	2.07
K1	12.38	838.44	52.35	189.99	3036.52	9.62	803.94	151.78	2.09
K2	15.32	813.36	68.75	225.68	2336.97	9.28	584.04	127.53	3.62
Sı	11.32	1285.96	80.85	222.37	2725.51	8.34	705.79	172.71	1.36
S2	13.46	1031.86	59.03	207.56	2733.43	9.94	671.64	127.81	1.23
S 3	15.41	834.77	188.43	337.23	8342.77	42.39	590.43	230.41	1.06
V1	14.05	796.43	56.84	270.15	1111.84	16.81	379.40	100.53	2.53
V2	22.03	865.92	50.10	294.32	797.83	11.84	713.65	104.25	1.41

TABLE S2.2 Porewater concentrations of chemical elements of the studied ditches. Average annual concentrations calculated based on interpolated data between May 2017 and May 2018 (porewater samples n = 3).

Ditch ID	Al (μmol/l)	Ca (μmol /l)	Fe (µmol /l)	K (μmol/l)	Na (μmol /l)	P (μmol/l)	S (µmol/l)	Si (µmol/l)	Zn (µmol /l)
A 1	9.02	1218.01	33.18	266.17	2004.49	25.90	362.68	342.00	1.85
A2	7.67	1344.92	61.79	370.26	2331.63	68.38	203.52	508.49	1.06
A 3	9.44	1809.49	101.41	434.32	2293.25	55.56	210.28	646.92	1.89
K1	20.46	772.56	164.06	258.89	5372.88	43.90	252.88	417.75	5.04
K2	10.91	874.65	136.61	218.36	2398.63	26.48	162.92	302.31	2.20
Sı	22.82	1108.77	547.69	224.92	4219.02	8.70	290.39	267.90	1.40
S2	19.48	1113.52	286.48	317.42	9594.51	33.78	405.22	367.29	1.83
S 3	27.00	765.05	156.45	228.16	8721.76	16.87	284.97	303.94	2.02
Vı	6.14	1305.38	20.91	362.73	1284.25	55.88	168.61	522.89	0.27
V2	21.82	1203.62	61.66	420.73	1244.99	51.57	178.62	482.13	0.91

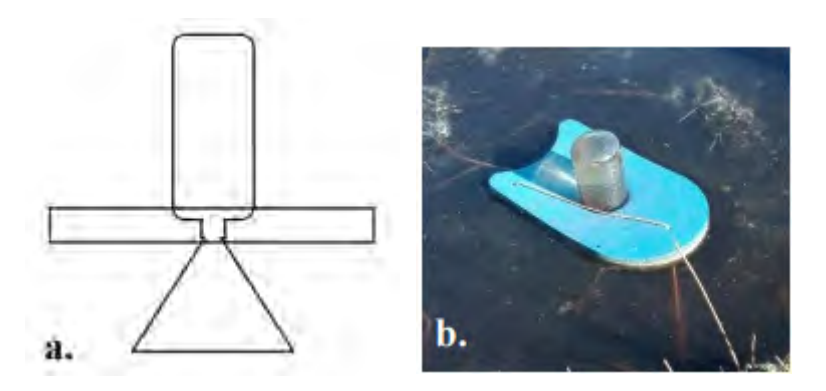


FIGURE S2.1 Self-constructed bubble-trap.

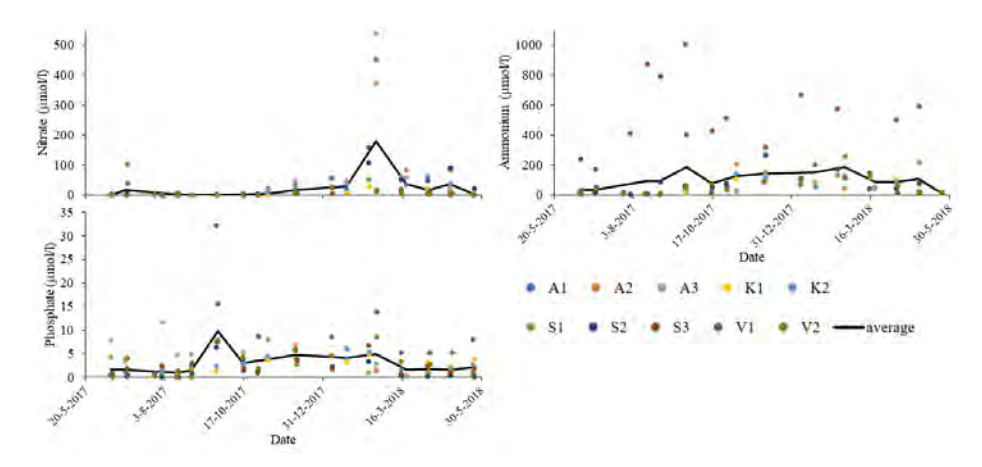


FIGURE S2.2 Seasonal variation of nutrient concentration in the surface water over the measuring period June 2017 to May 2018. Note the difference of y-axis values.

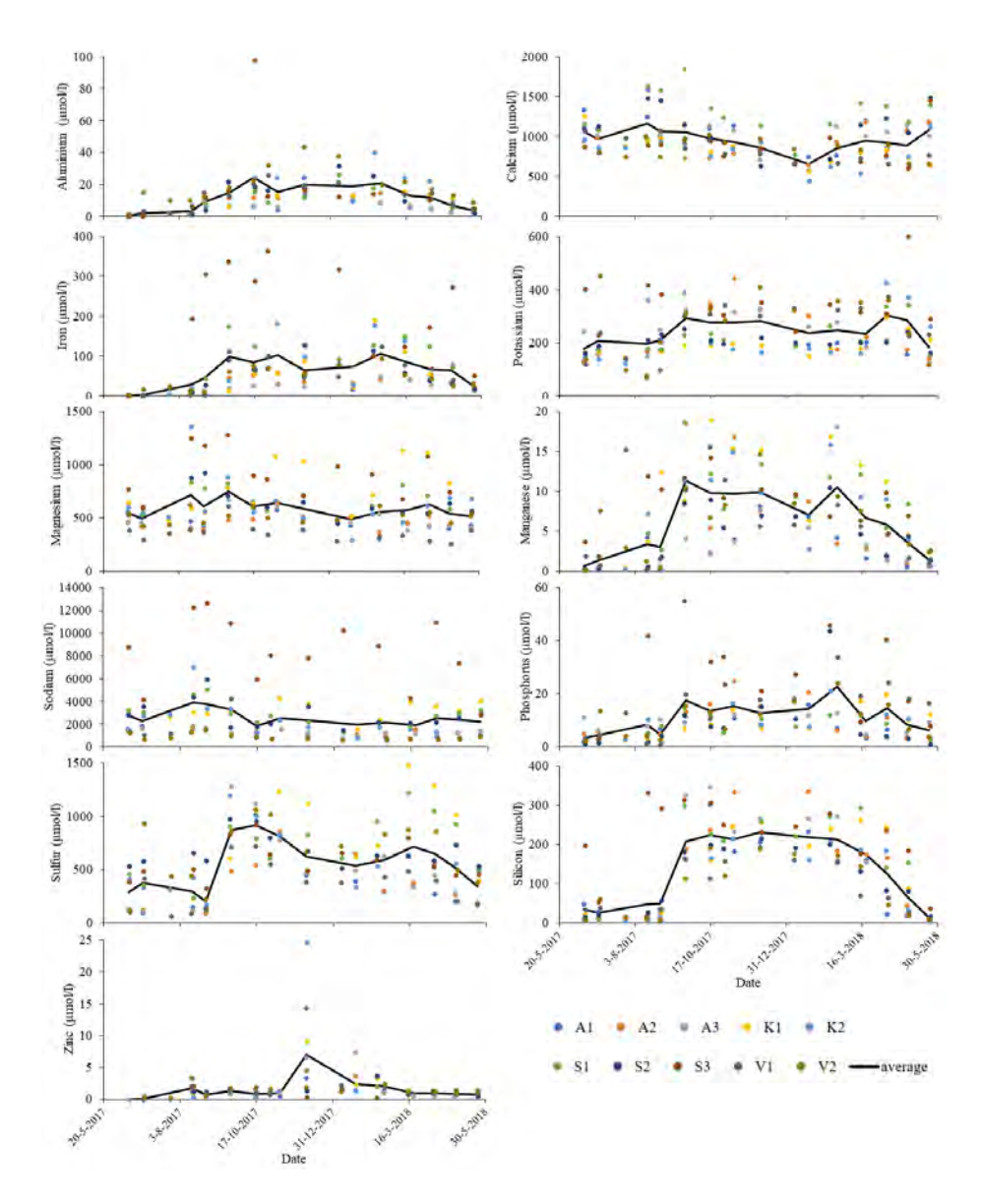


FIGURE S2.3 Seasonal variation of elemental concentration in the surface water over the measuring period June 2017 to May 2018. Note the difference of y-axis values.

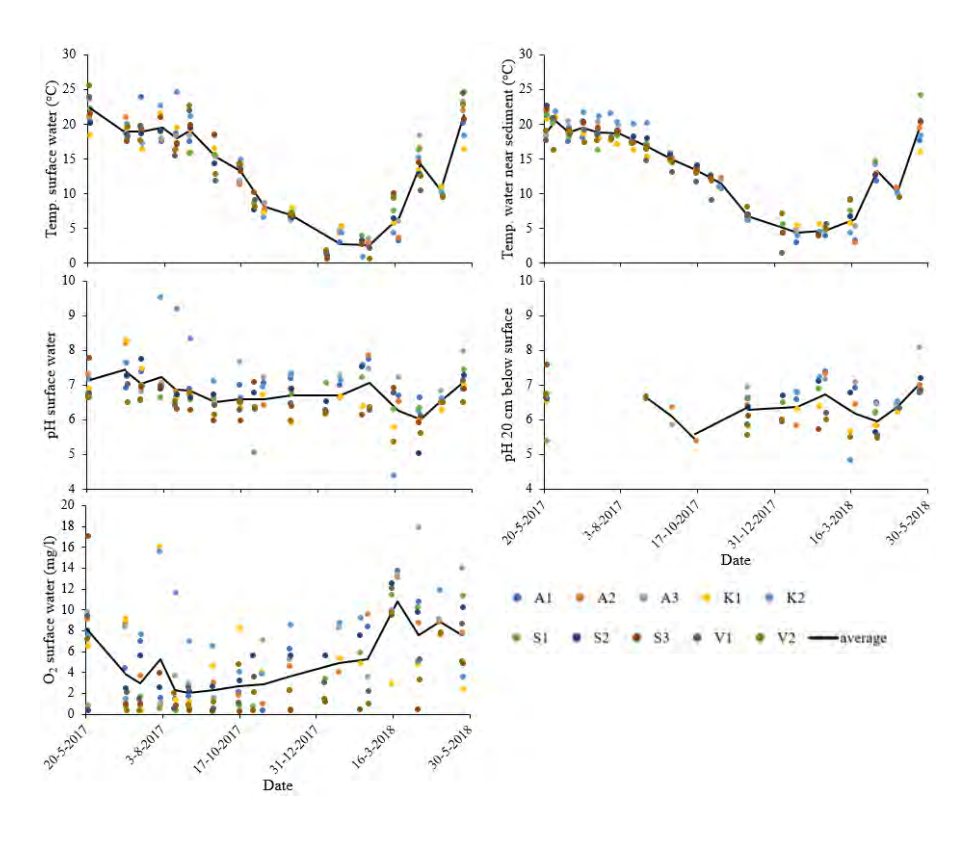


FIGURE S2.4 Seasonal variation of temperature, pH and O_2 concentration in the surface water (temperature, pH, O₂), near the sediment (temperature) and 20 cm below surface (pH).

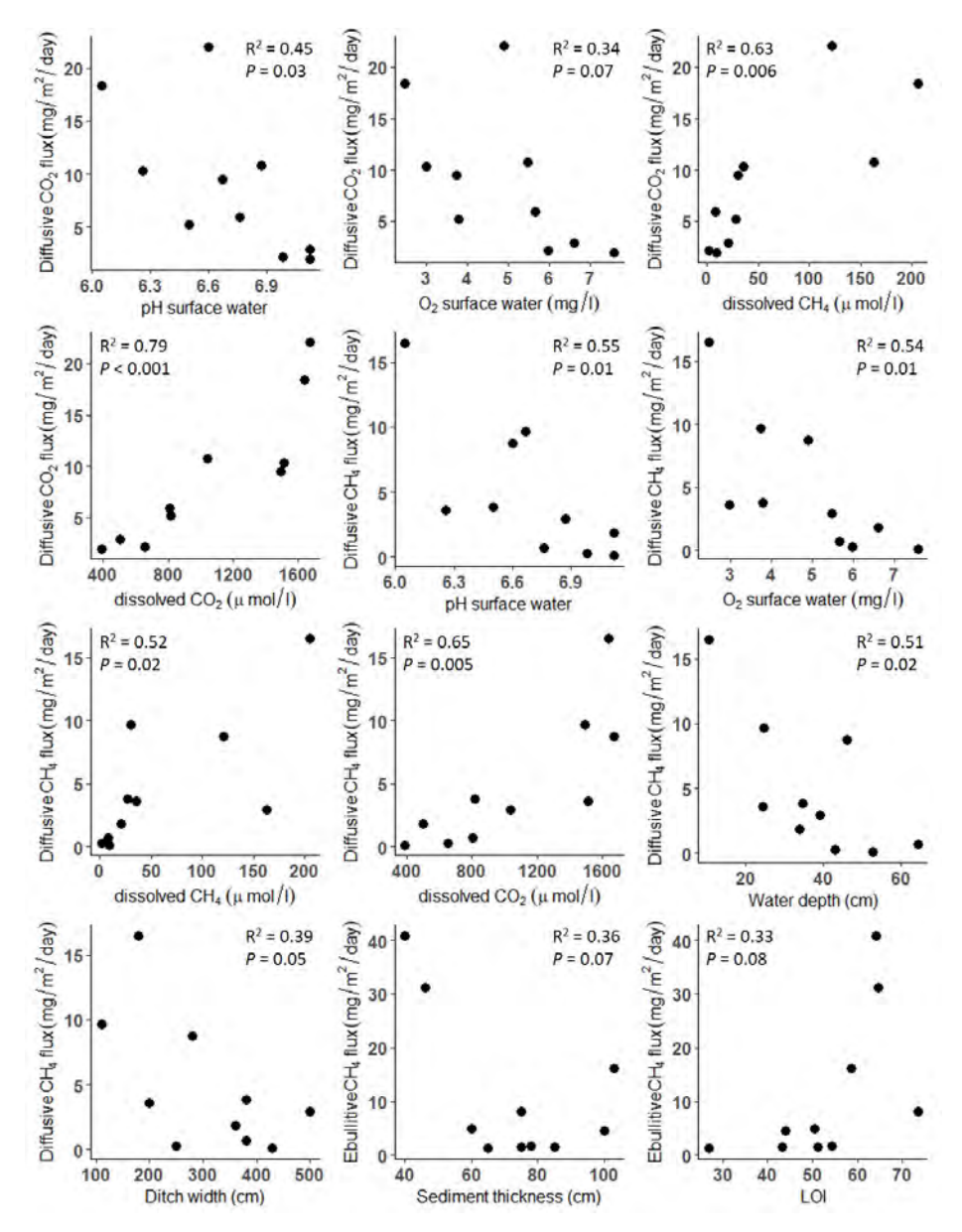


FIGURE S2.5 Linear relationships between diffusive CO_2 , diffusive CH_4 and ebullitive CH_4 emission, and different explanatory variables, that came out highly influential from the PLS analysis, and were correlated with an $R^2>0.3$ and a P-value < 0.08.



Chapter 3 Effects of wastewater effluent discharge on river greenhouse gas emissions and microbial communities

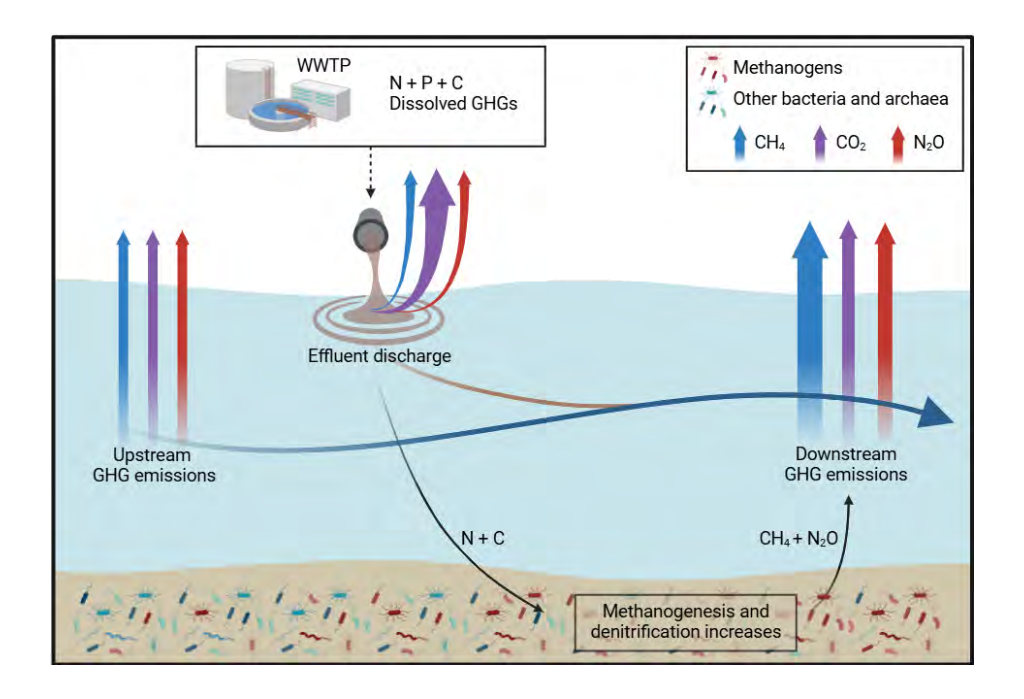
Ida F. Peterse*, **Lisanne Hendriks***, Stefan T.J. Weideveld, Alfons J.P. Smolders, Leon P.M. Lamers, Sebastian Lücker, Annelies J. Veraart *Equal contribution

Published in Science of the Total Environment, 2024, 951: 175797

doi:10.1016/j.scitotenv.2024.175797

Adapted version

GRAPHICAL ABSTRACT



ABSTRACT

Rivers are well-known sources of the greenhouse gasses (GHG) carbon dioxide (CO₂), methane (CH₂) and nitrous oxide (N₂O). These emissions from rivers can increase because of anthropogenic activities, such as agricultural fertilizer input or the discharge of treated wastewater, as these often contain elevated nutrient concentrations. Yet, the specific effects of wastewater effluent discharge on river GHG emissions remain poorly understood. Here, we studied two Dutch rivers which both receive municipal wastewater effluent; river Linge and river Kromme Rijn. Dissolved concentrations and fluxes of CH_4 , N_2O and CO_3 were measured upstream, downstream and at discharge locations, alongside water column properties and sediment composition. Microbial communities in the sediment and water column were analysed using 16S rRNA gene sequencing. In general, both Linge and Kromme Rijn exhibited high GHG emissions compared to other aquatic systems. CO₂ emissions peaked at most discharge locations, likely resulting from dissolved CO, present in the effluent. N₂O and CH₄ were highest 2 km downstream, suggesting biological production by methanogenic and denitrifying activity stimulated by the effluents' nutrient supply. Notably, methanogenic archaea were more abundant downstream of effluent discharge locations. However, overall microbial community composition remained relatively unaffected in both rivers. In conclusion, we demonstrate a clear link between wastewater effluent discharge and enhanced downstream GHG emission of two rivers. Mitigating the impact of wastewater effluent on receiving rivers will be crucial for reducing riverine GHG contributions.

3.1 INTRODUCTION

Rivers produce and emit greenhouse gases (GHGs), such as carbon dioxide (CO₂), methane (CH), and nitrous oxide (NO). These GHG emissions have increased in the last decade because of anthropogenic activities enlarging the organic matter and nutrient influx into rivers (Yao et al., 2020; Upadhyay et al., 2023). In addition to agricultural runoff, treated effluent discharged from wastewater treatment plants (WWTPs) impact the river nutrient balance, causing increased GHG emissions (Hu et al., 2018; Carey & Migliaccio, 2009; Tong et al., 2020; Alshboul et al., 2016). The discharge of WWTP effluent can affect GHG emissions in several ways. Firstly, effluent water itself contains dissolved GHGs produced during wastewater treatment, with concentrations up to 1 mmol L-1 for CO, 17 µmol L-1 for CH, and 0.9 µmol L-1 for N₂O, (Alshboul et al., 2016; Tumendelger et al., 2019). These GHGs are produced by microorganisms during the degradation of organic matter in the aeration tank and anaerobic sludge digester, or as intermediate or side products by autotrophic nitrification, nitrifier denitrification, and heterotrophic denitrification. During effluent discharge, these dissolved gases enter the river where they can be emitted or metabolized by the microbial community.

Moreover, wastewater effluent still contains substantial amounts of dissolved nutrients and organic matter, forming a source of ammonium, phosphate, and organic carbon, nitrogen and phosphorus (Hendriks et al., 2017; Kim et al., 2019; Meng et al., 2013). These compounds fuel microbial transformations, including (an) aerobic respiration, nitrification, denitrification, and methanogenesis, leading to GHG production. Nutrient influx also stimulates the growth of algae, cyanobacteria, and plants (Hendriks et al., 2023; Riis et al., 2019; Lu et al., 2018). While this results in CO₂ uptake during photosynthesis, plant senescence returns nutrients and organic carbon into the system, potentially enhancing microbial GHG production (Chingangbam & Khoiyangbam, 2023; Luo et al., 2020).

Lastly, effluent can contain considerable amounts of microorganisms (Cébron et al., 2004; Do et al., 2019; Lu & Lu, 2014; Servais et al., 1999). These microorganisms either originate from the initial sewage or are part of the WWTP microbial community, for example from the activated sludge. Microorganisms present in effluent water impact downstream river microbial diversity (Atashgahi et al., 2015; Drury et al., 2013; Price et al., 2018; Wakelin et al., 2008) and may play a part in biochemical processes downstream of the discharge location, possibly affecting GHG dynamics.

The amount of nutrients, dissolved GHGs, and microorganisms present in treated wastewater depends on the dimension and type of WWTP. The maximum allowed nutrient concentration in the effluent may also differ between WWTPs. For example, in the Netherlands, installations with higher capacity in terms of inhabitant equivalents must discharge effluent containing lower nutrient concentrations (714 and 32 µmol L-1 N and P, respectively) compared to smaller WWTPs (1070 and 64 µmol L-1) (Lozing van afvalwater uit rioolwaterzuiveringsinstallaties, n.d.). Unique properties of WWTP treatment lines, such as on-site sludge processing, may lead to large temporal variations in treated effluent. Lastly, a WWTP works most efficiently at temperatures above 20 °C and effluent nutrient concentrations thus can be elevated in winter months (Johnston et al., 2019; Johnston et al., 2023; Ju et al., 2013)

Due to the high complexity of river systems, it is difficult to quantify GHG emissions as a result of effluent discharge. To date, only a few studies have shown that WWTP effluent discharge is associated to an increase in GHGs, albeit with high variability (1.2-8.6 ×, 1.1-3.1 ×, and 1.2-10.9 × increase of CO₂, N₂O₃, and CH₄ emissions, respectively; Hu et al., 2018; Alshboul et al., 2016). Although the IPCC shows emission factors (EFs) for wastewater influence on receiving waters, they remain highly speculative due to a lack of data (IPCC, 2019). More research on the direct impact of WWTP effluent discharge on river GHG emissions is therefore needed to accurately estimate these emissions for better implementation in GHG inventories.

In this study, we assessed the influence of WWTP effluent discharge on GHG emissions from two rivers in the Netherlands. We quantified GHG emissions and characterized biochemical properties of multiple locations upstream and downstream of WWTP effluent discharge locations. On river Linge, we sampled over a length of 40 kilometer (km), with five discharge locations of five different WWTPs. On river Kromme Rijn a transect of 4 km was sampled, harboring one discharge location. In addition, we described the microbial community in both the water column and sediment upstream and downstream of these discharge locations.

3.2 METHODS

3.2.1 Study area

We tested the effect of effluent discharge in two rivers, river 'Linge' and river 'Kromme Rijn' (Fig. 3.1a, b). Both rivers are located in the Netherlands, which has a temperate marine climate, and are part of the river Rhine system. They are fed by water from the Rhine and their respective catchment areas. Both rivers are classified as slow-flowing (<50 cm s⁻¹), small rivers (CBS et al., 2024). The Linge starts near Doornenburg in the east of the Netherlands and ends 108 km downstream near Gorinchem in the river 'Beneden-Merwede'. It encounters multiple cities, small harbours, intensive agriculture, orchards, and reed beds. Upstream of the river crossing with the Amsterdam-Rijnkanaal the Linge is strongly canalized, downstream it continues as a meandering river. Between the cities of Geldermalsen and Gorinchem, there are five discharge locations of WWTPs treating municipal sewage water in a stretch of 40 km (Table 3.1). The Kromme Rijn starts at Wijk bij Duurstede where it splits off from the 'Nederrijn' and ends 26 km downstream in the urban outer-canal system of Utrecht. The Kromme Rijn has a meandering, natural flow path until it reaches Utrecht. This is also the section of the river where the discharge location of the WWTP of Bunnik is located. The Kromme Rijn flows past floodplains, urbanized areas, recreational harbors, pastures, agricultural fields and small forests.

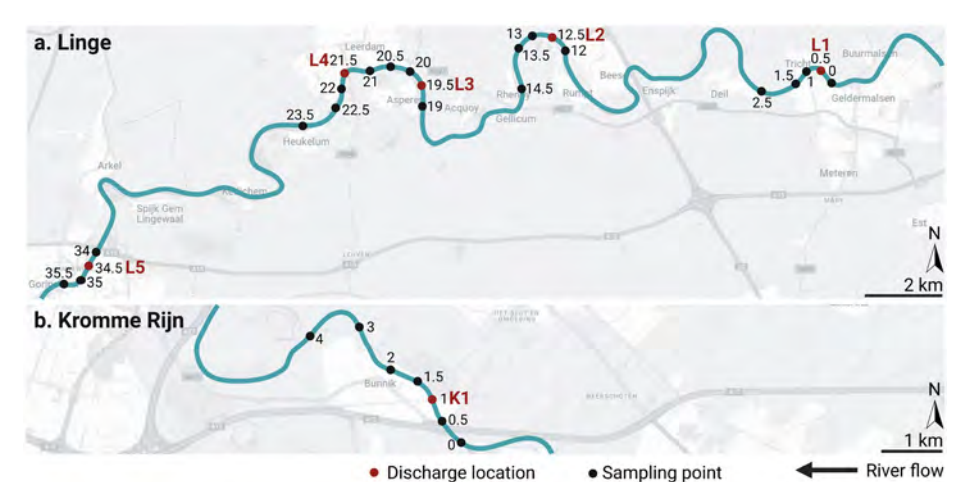


FIGURE 3.1 The sampling sites on the river Linge (a) and Kromme Rijn (b). Exact sampling locations can be found in Table S3.1.

TABLE 3.1 Properties of the six wastewater treatment plants (WWTPs). L= Linge, K= Kromme Rijn. TOD = total oxygen demand, N_{tot} = total nitrogen concentration, $P_{\rm tot}$ = total phosphorus concentration, BOD₅ = biological oxygen demand in five days.

	Geldermalsen (L1)	Beesd (L2)	Asperen (L3)	Leerdam (L4)	Gorinchem (L5) Bunnik (K1)	Bunnik (K1)
Construction year	1990	1987	1972	1986	1990	1972
Effluent discharge location	Linge	Linge	Linge	Linge	Linge	Kromme Rijn
Treatment type	Trickling filter bed + activated sludge	Oxidation ditch	Oxidation ditch	Carrousel system	Carrousel system	Biological phosphate removal, two two-step oxidation tanks
Biological capacity (inhabitant equivalent – gr. TOD d ⁻¹)	33,000 - 136 29,920 - 150 25,000 - 54	10,000 - 136 9,067 - 150 7,500 - 54	9,300 - 136 8,432 - 150 7,000 - 54	30,400 - 136 27,563 - 150 23,000 - 54	32,000 - 136 29,013 - 150 24,000 - 54	42,000 - 136 38,080 - 150
Hydraulic capacity ($\mathbf{m}^3\mathbf{h}^{\text{-1}}$)	12.70	350	400	1000	1150	006
Effluent discharge	Directly on Linge	Directly on Linge	Through ditch (600 m)	Directly on Linge	Through pipe (1400 m)	Through pipe (370 m)
$N_{_{ m tot}}$ effluent ($\mu mol~L^{-1}$)*	421.23	154.83	119.23	164.21	339.12	364.11
$\mathbf{P}_{ ext{tot}}$ effluent ($\mu ext{mol L}^{-1}$)*	46.91	25.28	72.09	24.31	113.0	18.89
$\mathbf{BOD}_{_{\mathrm{S}}}$ effluent (mg \mathbf{L}^{-1})*	3.80	3.45	3.50	1.75	3.40	2.30
Sampling time*	10:15 – 13:00	14:00 – 16:00	16:30 – 17:00 & 10:00 – 10:30	10:30 – 12:30	14:00 – 15:00	09:00 – 13:00
River flow rate (cm sec ⁻¹)**	9	11	10	11	7	8
River water depth (m)**	2.60 – 3.10	2.70 – 3.05	3.15 – 3.50	3.80 - 4.50	3.95 – 4.50	1.30 – 2.15
River width (m)**	21 – 33	28 – 35	31 – 58	38 – 58	33 – 85	11 – 18

*Measured in September 2023

^{**}In a range between 500 m upstream and 2000 m downstream of discharge location, approximated

3.2.2 Analysis of water composition

We sampled river Linge September 11th and 12th, 2023, and river Kromme Rijn September 15th, 2023. Before and during the 11 and 12th of September, a heat wave occurred, with maximum temperatures of ca. 30 °C. During the sampling of the river Kromme Rijn temperatures had dropped to 20 °C. Measurements and sampling were done from a small boat. Sampling locations were 500 m upstream of each effluent discharge location, at the discharge location itself (0 m), and 500, 1000, and 2000 m downstream of each discharge location.

3.2.2.1 Physical-chemical properties of the water column

On all sampling locations, we measured pH, dissolved oxygen (DO), electrical conductivity (EC), and temperature using a Portable Multi Meter (HQ2200, HACH, USA) with the appropriate probes (PHC20101, LDO1010, CDC401). River depth and water turbidity were estimated using a Secchi disk, and water flow was measured by a flow meter.

Water samples were taken by scooping ~2 L of water from the upper meter of the water column. All water samples were stored cool and in the dark during the sampling day. Part of the water sample was filtered directly after sampling (0.45 µm pore size, cellulose nitrate membrane Whatman™ filters, GE Healthcare, UK). Part of the unfiltered samples was fixated with 20 µl 2000 ppm HgCl₂ and stored at 4 °C directly upon return to the lab facilities. In these fixated samples, total organic carbon (TOC) and total nitrogen (TN_k) were determined in the lab, using a Focus Radiation NDIR detector (Multi N/C3100, Analytik Jena, Jena, Germany) after combustion at 780 °C. Other unfiltered water samples were treated with 0.1 ml 10% nitric acid and stored at 4 °C directly upon return to the lab facilities. These samples were analysed for the following elements by ICP-OES (iCap 6300, Thermo Fisher Scientific, Bremen, Germany): aluminium (Al), calcium (Ca), iron (Fe), potassium (K), sodium (Na), phosphorus (P), total sulphur (S_{tot} ; which includes elemental S and organically bound S), silicon (Si), and zinc (Zn). Additionally, non-treated, unfiltered water was analysed for total inorganic carbon (TIC, as CO₂, HCO₃ and CO₃ the day after sampling, on a AO2020 Continuous Gas Analyser (ABB, Zürich, Switzerland) as in Hendriks et al. (2024). Filtered water samples were stored at -20 °C and analysed for nutrients (ammonium [NH₄], nitrate + nitrite [NO₃ + NO₂], but since it is mostly NO₃, we refer to it as such, phosphate [PO $_{_4}^{3-}$]) on an auto analyser (III; Seal Analytical XY – Z sampler, Bran + Luebbe GmbH, Norderstedt, Germany). NH, was determined using the Berthelot reaction (NEN-EN-ISO 11732:2005), NO using NEN-EN-ISO 13395:1997, and PO_{A}^{3-} according to ISO 15681-2:2003.

3.2.2.2 Diffusive greenhouse gas fluxes

On each sampling location we measured diffusive greenhouse gas fluxes (N_2O , CH_4 , CO_2) using a transparent acrylic glass floating chamber (height 17 cm, surface area 0.07 m²) connected in a closed loop to two greenhouse gas analysers simultaneously: one for N_2O fluxes (MIRA Ultra N_2O /CO analyser, Aeris Technology, Hayward, CA, USA) and one for CH_4 and CO_2 fluxes (LGR-ICOSTM, model GLA131-GGA [extended range], ABB Inc, Quebec, Canada). The floating chamber was carefully lowered to the water surface after which an airtight lid was closed. Fluxes were measured in intervals of at least 3 minutes, counted from the first observation of a gas concentration change. Each measurement was checked visually for linearity. When a bubble entered the chamber, seen as a sudden increase in CH_4 concentration, the measurement was disregarded and repeated. In between measurements, the chamber was vented to lower gas concentrations to atmospheric concentrations.

Each diffusive flux was calculated using linear regression as in Hendriks et al. (2024A). Positive gas fluxes denote emission from water column to atmosphere, while negative fluxes denote fluxes from the atmosphere to the water column, following the atmospheric sign convention. We used global warming potentials of 27 and 273 (100-year timeframe; IPCC, 2021) to convert CH_4 and N_2O , respectively, to CO_2 -equivalents (CO_2 -eq). All fluxes exceeded the minimum detectable flux (i.e., 3.77, 0.12, and 1.18 mg CO_2 -eq $m^{-2}d^{-1}$ for CO_2 , CH_4 , and N_2O_2 , respectively) by a large margin (Nickerson, 2016).

3.2.2.3 Dissolved greenhouse gases

Dissolved greenhouse gas samples were collected in triplicate at each sampling location using the headspace method (Dean et al., 2020). Three 60 mL syringes were filled with 50 mL river water collected as described in section 2.2.1. In addition to river water, 10 mL of ambient air was aspirated to create a headspace of 10 mL in the syringe. Water and headspace were equilibrated by shaking the syringes for 1 minute directly after sampling, after which the 10 mL equilibrated headspace was injected in a pre-evacuated 5.9 mL borosilicate Exetainer® (Labco, Lampeter, United Kingdom) creating an overpressure. Additionally, we took one atmospheric air sample per sampling location to correct for the atmospheric GHG concentrations by directly injecting 10 mL air into evacuated exetainers.

 CH_4 and N_2O concentrations were measured in the lab by injecting 100 μ L gas from the exetainer into a gas chromatograph using a 100 μ L glass syringe (Hamilton, Reno, NV, USA). For CH_4 measurements an HP 5890 series II gas chromatograph was used, equipped with a Porapak Q-column and flame-ionisation detector (Agilent Technologies, Santa Clara, USA). N_2O concentrations were measured with a 6890A gas chromatograph equipped with an Electron Capture Detector (Agilent Technologies, Santa Clara, USA).

Concentrations of dissolved CH_4 and N_2O in river water were calculated as described by Aho and Raymond (2019). The headspace partial pressure of each gas was calculated using Henry's Law, taking the temperature of the river water into consideration. The ideal gas law was then used to calculate the amount of each gas in the post-equilibrated headspace. From this, we calculated the CH_4 and N_2O concentration in the preequilibrated water sample by summing the calculated amount of CH_4 or N_2O in the post-equilibrated headspace and the calculated post-equilibrated concentration in the water.

3.2.2.4 Data Analysis of water column properties

We constructed linear mixed effects models (LMM) to assess the effect of effluent discharge on the following physical-chemical properties of the river water: pH, dissolved O₂, EC, TOC, NH₄⁺, NO₃⁻ and PO₄³⁻. We performed the same analysis for fluxes of CO₂, CH₄ and N₂O and dissolved GHGs. Each unique discharge location was entered as a fixed effect, as well as distance from discharge locations, and sampling date was used as random effect. For river Kromme Rijn, data collected at distances –1000 and 3000 m from the discharge location were omitted, since these distances were not measured on river Linge. Model assumptions for linearity were checked visually using histograms. When linearity was not met, which was the case for EC, TIC, TOC, NH₄⁺, PO₄³⁻, N₂O flux, dissolved CO₂ and dissolved N₂O, log-transformations were performed. The significance of the fixed effects was tested using an Anova with degrees of freedom and p-values calculated using the Kenward–Roger method.

To assess the variables that best explained dissolved concentrations of CO₂, CH₄, and N₂O and their emissions, we constructed two partial least squares (PLS) analyses. PLS analysis can particularly deal with multicollinearity among variables and can test multiple dependent variables at once (Mevik and Wehrens, 2007; Hendriks et al., 2024). The analysis was performed for two sets of dependent variables: 1) concentrations of dissolved CO₂, CH₄, N₂O; and 2) CO₂, CH₄, N₂O fluxes. Both analyses included the following independent variables: distance from discharge location ('Point'), pH, dissolved O₂ (DO), temperature (Temp.), EC, TIC, TOC, DN_b, TN_b, NH₄, NO₃ and PO₄³. Scaled and centered PLS coefficients were used to interpret the influence of the independent variable on every dependent variable. To measure predictor importance of each dependent variable, the variable influence on projection (VIP) was extracted. Variables with VIP values larger than 1 were considered most influential for the model, whereas variables with VIP values between 0.7 and 1.0 were considered moderately influential. Variables with a lower VIP (0.4-0.7) were considered to have low influence.

All analyses were performed in R (version 4.3.3; R Core team, 2024), using packages 'lmerTest', 'emmeans', 'plsdepot'.

3.2.3 Analysis of sediment composition

Sediment samples were taken along the transects of both rivers. In the Linge, we sampled 500 m upstream of the first WWTP effluent discharge location, and 500 m downstream of each discharge location, resulting in six sampling locations. In the Kromme Rijn, samples were collected 500 m upstream, and 500 m and 2 km downstream of the only WWTP effluent discharge location, resulting in three sampling locations. Sediment was collected using a gravity corer system with transparent PVC core liners (60 cm length, 6 cm diameter; UWITEC GmbH, Mondsee, Austria). The sediment core was divided into three zones (0-2 cm, 2-5.5 cm, 5.5-15.5 cm), sliced immediately on the boat, after which slices were stored in Ziplock bags at 4 °C. On the same day, sediment samples were transferred to -20 °C, until further analysis.

In the sediment samples, we determined organic matter content, carbon, nitrogen, phosphorus and other elements, such as iron (Fe) and aluminum (Al) at the depths between 0-2 cm and 2-5.5 cm. First, the sediment was dried at 70 °C until completely dry, after which part of the sediment was incinerated at 550 °C for 24 hours. Loss on ignition (LOI), as a proxy for organic matter content, was obtained by the difference between the dry weight at 550 and 70 °C (as in Heiri et al., 2001). To obtain C and N content, approximately 40 mg of sediment was processed on a CNS elemental analyzer (Vario Micro Cube, Elementar, Langenselbold, Germany). For P, Fe and Al, approximately 200 mg of sediment was digested in Teflon vessels by adding 4 mL HNO₃ (65%) and 1 mL H₂O₂ (35%), after which they were heated in an Ethos One microwave (Milestone, Italy) for 20 minutes at 120 °C. The digested samples were subsequently analyzed on the previous-mentioned ICP-OES (2.2.1).

3.2.4 Analysis on the microbial community

We analysed the microbial community in both the sediment and the water column of the Linge and Kromme Rijn. At the same sampling locations as those where sediments were collected, we also collected 1 L of water from the upper ~1 meter of the river water column. On the same day, two ~400 mL water samples per sampling location were filtered using a vacuum pump until the filter (Supor® PES 0.22 μ m) clogged. The exact volume filtered was noted and filters were stored at -20 °C until further analysis.

3.2.4.1 DNA extraction

DNA of sediment samples was extracted using the DNeasy PowerSoil Isolation kit (Qiagen, Venlo, Netherlands) according to the manufacturer's instructions with minor modifications: Initial bead-beating was done with a TissueLyser LT (Qiagen, Venlo, Netherlands) for 10 minutes at 50 Hz and the final elution of purified DNA was done with two elution steps using 50 μ L Diethyl pyrocarbonate (DEPC)-treated water.

DNA of the water column was extracted from filters using the FastDNATM SPIN Kit for Soil (MP biomedicals, CA, USA). Filters were sliced with a sterile scalpel and added to the Lysing Matrix A tubes of the kit. Manufacturer's instructions were followed, with the alteration that a TissueLyser was used during homogenization for 3 x 40 s at 50 Hz and final DNA elution was done twice with 30 μ L DEPC water on the Spin filter and incubations for 5 minutes at 55 °C. Eluted DNA was diluted to a final concentration of 2 ng/ μ L and stored at 4 °C until sequencing. The initial concentration of DNA per gram dry weight of sediment and per milliliter of filtered river water was calculated as a proxy for microbial abundance (Table S3).

To analyze the microbial community composition of the samples, the V3-V4 region of the 16S rRNA gene was sequenced (Macrogen Inc, Amsterdam, Netherlands) on the Illumina MiSeq platform. Bacterial 16S rRNA genes were amplified with the primers Bac341F (5'-CCTACGGGNGGCWGCAG-3'; Herlemann et al., 2011) and Bac805R (5'-GGACTACHVGGGTWTCTAAT-3'; Caporaso et al., 2012). For amplification of the archaeal 16S rRNA gene the primers Arch349F (5'- GYGCASCAGKCGMGAAW-3'; Takai & Horikoshi, 2000) and Arch806R (5'-GGACTACVSGGGTATCTAAT-3'; Takai & Horikoshi, 2000) were used.

3.2.4.2 Data analysis on the microbial community

Using the FIGARO tool (Sasada et al., 2020), we determined trimming and filtering parameters for the sequencing reads of bacteria and archaea separately to maximize read retention. Reads were then filtered and trimmed according to the DADA2 pipeline (Callahan et al., 2016; version 1.13.0) in R (version 4.3.2), trimming bacterial reads at base positions 273 and 212 and archaeal reads at positions 269 and 212 for forward and reverse reads, respectively. The maximum number of expected errors for both forward and reverse reads was set to 2. Taxonomy of amplicon sequence variants (ASVs) was assigned using the SILVA 16S rRNA database (Quast et al., 2012; version 138.1). The microbial community was further analyzed with *phyloseq* (version 1.46.0; McMurdie & Holmes, 2013) and plots were generated with *ggplot2*. The raw reads are deposited on the European Nucleotide Archive under accession number PRJEB75265.

3.3 RESULTS

3.3.1 River water and sediment conditions

In both rivers, pH ranged from 7 to ~8. We observed a small decrease in pH at the WWTP effluent discharge locations and a subsequent increase after discharge over the 2 km stretch (p = 0.004). Dissolved O₂ (DO) concentrations in the river water were

generally above 6 mg L-1, except for discharge location K1, where DO concentrations decreased to 5.4 mg L-1. Downstream of the discharge locations, DO concentrations generally tended to increase over the 2 km stretch, although not significant (p = 0.29). Electrical conductivity peaked at discharge locations (p = 0.03), with highest EC at K1 (1100 mS m⁻¹) and L4 (940 mS m⁻¹). Water column TIC concentrations peaked at discharge locations L4, L5 and K1, although no significant effect of effluent discharge was found (p = 0.08). TOC concentrations were highest at the L5 and K1 discharge locations, and did not significantly differ between upstream and downstream sampling points (p = 0.49) (Fig. S3.1).

NH₄ concentrations in both rivers were significantly higher at discharge locations compared to the upstream and downstream sampling points (p = 0.03). This was especially observed at L1, L4, L5 and K1, with the highest concentration of 32 µmol L-1 occurring at L5. The NO, concentrations started high at ~75 μmol L-1 in the upstream section of river Linge, and decreased over the river transect but did not significantly change at or after effluent discharge (p = 0.95). In river Kromme Rijn, the measured NO, concentration was high (116.8 \pm 7.5 μ mol L⁻¹) compared to the Linge, and a slightly higher concentration was measured after WWTP effluent discharge at K1. In both rivers, PO3- concentrations were generally low but tended to peak at the discharge locations (p = 0.076). Highest peaks of PO₄ were observed at discharge locations L4 (16.0 μ mol L⁻¹) and L5 (28.0 μ mol L⁻¹, Fig. S3.2).

The C content of the sediment in river Linge increased 500 m downstream after every effluent discharge location until it peaked 500 m downstream of L3 (Table S3.2). This is in coherence with the higher organic matter content of the deeper sediment layer (2-5 cm) (Table S3.2). In addition, an increasing trend in N content was measured over the transect of river Linge. Downstream of L5 the lowest C and N and organic matter content was measured. P concentration was the highest 500 m downstream of L1 and decreased over the transect of river Linge. Fe and Al followed a similar pattern as P. For Kromme Rijn no pattern could be detected because upstream of the effluent discharge location it was hard to obtain an intact sediment core due to the numerous pebbles and stones. Instead, a scoop of sediment was taken on this location. This sample only contained 1% organic matter and differed greatly from the other samples.

3.3.2 Greenhouse gas fluxes on the river-transect

Although not significant (p = 0.35), CO₂ fluxes tended to peak at discharge locations. On the river Linge, CO, fluxes were highest at the WWTP effluent discharge locations L1 and L4, with a peak of 71.4 g CO, m-2d-1 at L4 (Fig. 3.2a). On the Kromme Rijn, a substantial peak of CO, of 24.1 g CO, m-2d-1 was observed at discharge location K1 (Fig. 3.2b). Over the whole transect, both rivers were a CO_2 source. The CH_4 flux increased after receiving WWTP effluent, and emissions tended to be highest two kilometres downstream of the discharge locations (p = 0.09) (Fig. 3.2a). In river Linge, two kilometres downstream of discharge locations, CH_4 flux was on average almost 5 times higher (4.9 ± 1.3 sd.) than right at the discharge location. On the Kromme Rijn, CH_4 flux was 3.48 times higher 1 kilometre downstream of the single discharge location (0.9 g CO_2 -eq m⁻²d⁻¹), after which fluxes decreased again. N_2O fluxes were also affected by effluent discharge, although not significant (p = 0.74), with highest emission (5.1 ± 3.4 times higher) two kilometres downstream of discharge locations, most prominently downstream of L2 (2.0 g CO_2 -eq m⁻²d⁻¹; Fig. 3.2a). On the Kromme Rijn, a peak in N_2O emission of 1.6 g CO_2 -eq m⁻²d⁻¹ was observed.

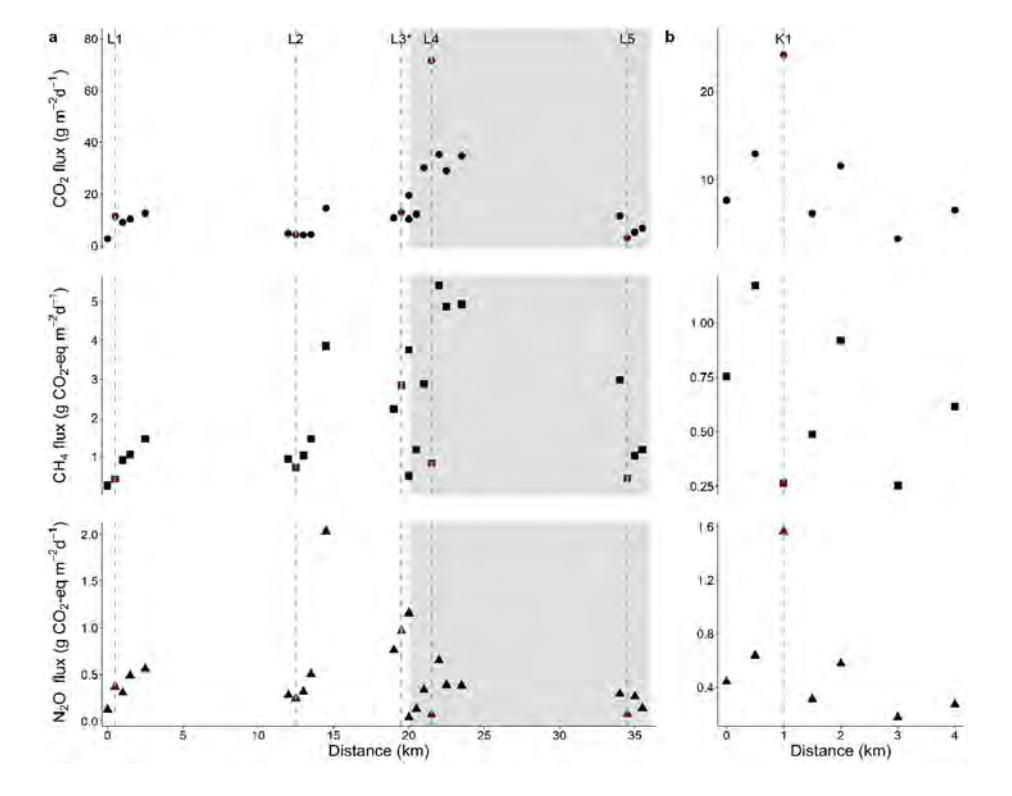


FIGURE 3.2 Greenhouse gas fluxes (CH_4 , CO_2 , and N_2O) over the transect of the rivers Linge (**a**) and Kromme Rijn (**b**). The white area is the first sampling day, the grey area in (**a**) indicates the second sampling day. The red points indicate the discharge locations. At location L3, we could not measure directly at the discharge location, confounding these measurements. The location 500 m downstream of L3 (20 km) was measured on both sampling days. Note the difference in y-axis values.

3.3.3 Dissolved greenhouse gas concentrations along the river transects

In both rivers, dissolved CO concentrations were highest at effluent discharge locations (p = 0.005), peaking at L4 (810 μ mol L-1) in the river Linge (Fig. 3.3a) and at K1 (1705 µmol L-1) in the Kromme Rijn (Fig. 3.3b). Dissolved CH, concentrations in the river water increased downstream of effluent discharge at L1 and L4. The highest dissolved concentration was measured 2 km downstream of L1 and 1 km downstream of L4. Dissolved CH, decreased after all the other discharge locations, although not significant (p = 0.76), and in the Kromme Rijn dissolved CH_4 concentrations were not correlated to effluent discharge. No effect of effluent discharge was found for dissolved N_2O concentrations (p = 0.30), except for discharge location L5 and K1, where N₂O concentrations peaked at the effluent discharge location.

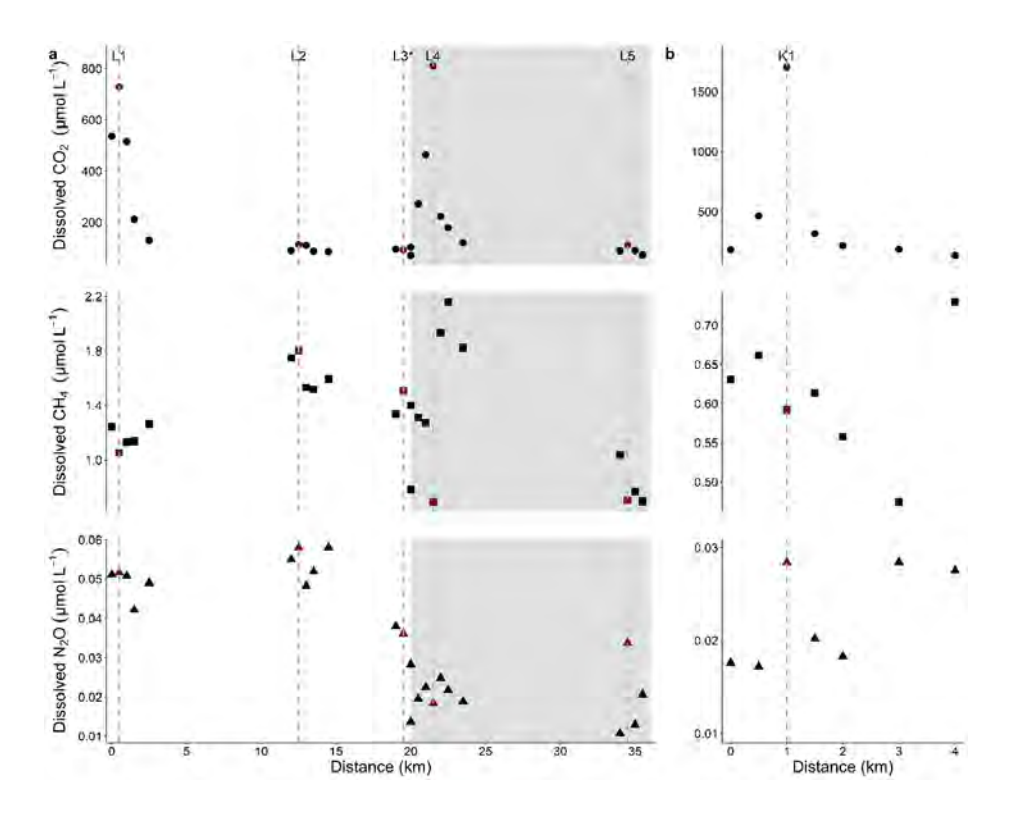


FIGURE 3.3 Dissolved greenhouse gas concentrations (CH,, CO,, and N,O) over the transect of river Linge (a) and Kromme Rijn (b). The white areas indicate the first sampling day, the grey area in (a) indicates the second sampling day. The red points indicate the discharge locations. At location L3 we could not measure directly at the discharge location, confounding these measurements. The location 500 m downstream of L3 (20 km) was measured on both sampling days. Note the difference in y-axis values.

3.3.4 Potential drivers of greenhouse gas emissions: physical and chemical conditions in the water column

We constructed PLS models to visualize drivers of greenhouse gas emissions. For dissolved GHGs, the two components of the PLS model explained 62% of the variance (Fig. 3.4a). Dissolved CO_2 positively relates to NH_4^+ , $\mathrm{PO}_4^{3^+}$ and EC in the water column, and negatively to pH, dissolved O_2 (DO) and the distance from the discharge location ('Point'). Dissolved CH_4 is associated to higher temperatures, TN and TOC, and to lower TIC in the water column. Dissolved $\mathrm{N}_2\mathrm{O}$ is explained positively by NO_3^- and negatively by TIC. The two components of the PLS model for GHG fluxes explained 43% of the variance (Fig. 3.4b), where CO_2^- flux is explained positively by TIC and EC, and negatively by DO and temperature. CH_4^- flux is mostly associated to the distance from discharge location, whereas $\mathrm{N}_2\mathrm{O}$ flux is explained positively by pH and negatively by nutrients in the water column.

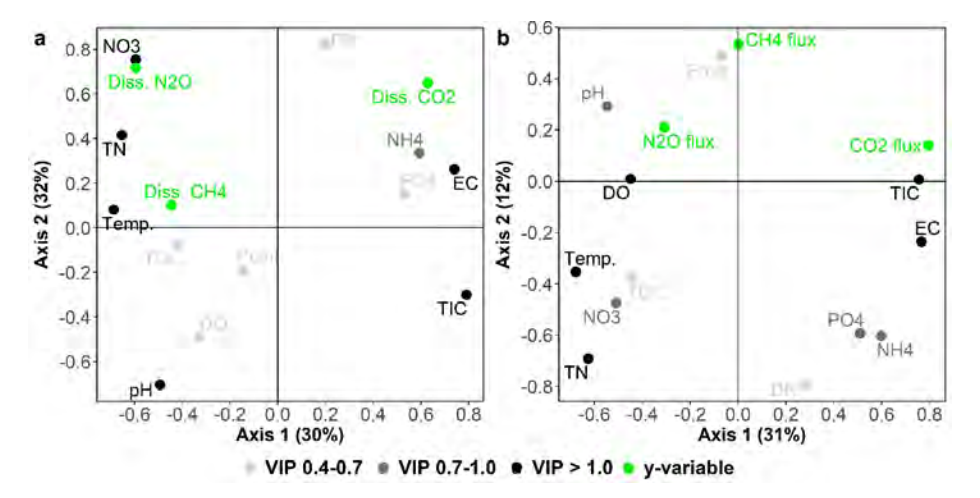


FIGURE 3.4 Partial least squares (PLS) analysis of water column predictors (x-variables, black and grey) for dissolved greenhouse gases (${\rm CO_2}$, ${\rm CH_4}$ and ${\rm N_2O}$) (**a**) and greenhouse gas fluxes (**b**) (y-variables, green). Predictors are classified according to their variable influences on projection (VIP), where predictors with VIP > 1.0 indicate 'High influence', with VIP 0.7-1.0 indicating 'Moderate influence' and with VIP 0.4-0.7 indicating 'Low influence'. 'Point' indicates the distance from a discharge location.

3.3.5 Microbial community on the river-transect

To identify potential correlations between the river water column, sediment microbiomes and greenhouse gas emissions, we explored archaeal and bacterial communities involved in the production and consumption of greenhouse gases. Using 16S rRNA gene amplicon sequencing, we identified microorganisms involved in methanogenesis (Fig. 3.5, Fig. S3.5), anaerobic methane oxidation (Fig. 3.5, Fig. S3.5), aerobic methane oxidation (Fig. S3.7), and nitrification (Fig. S3.5, Fig. S3.5, Fig. S3.7).

We observed shifts in the methane cycling community along the river transects of both Kromme Rijn and Linge. Methanogens were detected in all sequenced sediment samples (Fig. 3.5, Fig. S3.5) and the methanogenic families with highest relative abundance were Methanosaetaceae and Methanoregulaceae. These two families became more dominant in the sediment downstream of the first effluent discharge location on Linge (L1; Fig. 3.5), especially in the deeper sediment layers. Downstream of effluent discharge location L4, these two families constitute approximately 50% of the total archaeal community in the sediment. Downstream of L5 their relative abundance decreased again. Similarly to river Linge, Methanoregulaceae and Methanosaetaceae became more dominant after the only discharge location on the river Kromme Rijn (Fig. S3.5). Interestingly, in the water column of Kromme Rijn and Linge, the methanogenic community is abundant and rather stable over the sampled river transects (Fig. 3.5 and Fig. S3.5). Comparable to the sediment, Methanosaetaceae and Methanoregulaceae were the most abundant methanogens in the water column of both rivers.

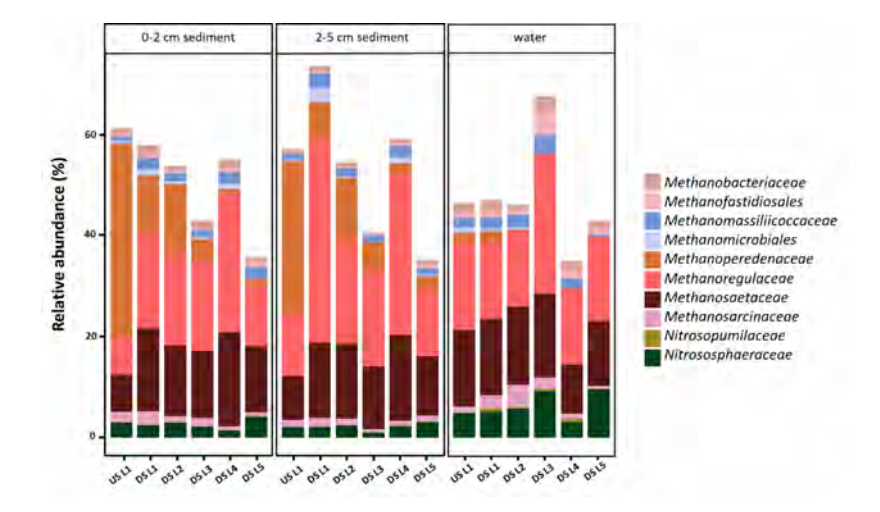


FIGURE 3.5 Relative abundances of methanogenic, anaerobic methane-oxidizing, and aerobic ammoniaoxidizing archaea in sediments (top 0-2 cm and 2-5 cm) and water column samples of the river Linge based on 16S rRNA gene amplicon sequencing. The initial community composition was assessed 500 m upstream (US) of the first WWTP effluent discharge location (L1). All other samples were taken 500 m downstream (DS) of each WWTP effluent discharge location. Taxonomy is presented at the family level.

Putatively anaerobic methane-oxidizing members of the family Methanoperedenaceae showed the highest relative abundance upstream of L1 in the archaeal fraction of river Linge sediment compared to all other detected families (Fig. S3.3). Their relative abundance lowered by almost 30% downstream of effluent discharge location L1 on river Linge, which is in contrast with the methanogenic community. This trend continued downstream across the whole transect of this river (Fig. 3.5). *Methanoperedenaceae* were detected in Kromme Rijn sediment too, but no similar trend could be detected.

The bacterial methanotrophic community composition was stable over the sampled transects of rivers Linge and Kromme Rijn. Both rivers contained multiple genera of methane oxidizing bacteria (MOB) (Fig. S3.7) with relative abundances in the sediment of up to 4%. Most sediment MOB sequences derived from classically filamentous members of the gammaproteobacterial genus *Crenothrix*. In the water column, methanotrophic bacteria were less dominant with a relative abundance of up to 2%, with Candidatus *Methylopumilus* representing the most abundant bacterial methylotroph in both rivers (Fig. S3.7).

Furthermore, sequences of the archaeal ammonia oxidizers *Nitrosopumilaceae* and *Nitrosophaeraceae* were present in the sediment and water column of both river Linge and Kromme Rijn (Fig. 3.5, S3.5). *Nitrobacter, Nitrosomonas, Nitrospira* and Candidatus *Nitrotoga* were the nitrifying bacteria detected, with *Nitrospira* constituting the most abundant nitrifier in the sediment with a relative abundance of up to 2% (Fig. S3.7). *Nitrospira* bacteria can either be complete ammonia oxidizers or canonical nitrite-oxidizers (Daims et al., 2015; Van Kessel et al., 2015). Like the ammonia-oxidizing archaea (Fig. S3.5), the bacterial nitrifiers were also decreasing in abundance in the Kromme Rijn mixed sediment downstream of the discharge location (Fig. S3.7b). In addition, in river Linge a lower abundance of *Nitrospira* and *Nitrosomonas* was detected after the first discharge location (L1) compared to the upstream sampling location (Fig. S3.7a). Bacterial nitrifiers in the water columns of the rivers amounted to less than 0.1% relative abundance in the overall bacterial communities (Fig. S3.7).

An NMDS analysis based on Bray-Curtis dissimilarities was performed to visualize how differences in the archaeal community of river Linge sediment relate to environmental drivers (Fig. S3.6a). The first sampling locations, upstream and downstream of L1 (distance 0 and 1 km) were positively related to NO₃⁻ concentrations in the water and the community composition of these locations was more dissimilar from other locations. The distance along the Linge and the number of effluent locations showed a significant effect on archaeal community composition, but were less predictive than NO₃⁻, NH₄⁺, and Fe concentrations in the water column. Contrastingly, the NMDS analysis on the bacterial community indicated a rather constant community structure, not heavily influenced by five WWTP effluent discharge locations except for downstream of L1 (Fig. S3.6b). Indeed, the bacterial alpha diversity (chao1 index) of both sediment and water column showed that species

richness remained constant except for a sudden peak after the first effluent discharge location in the water column of both rivers, but not in the sediment (Table S3.4 and S3.5). In addition, bacterial richness in river Linge was on average highest in the top 2 cm layer of sediment (3486 \pm 324 taxa) followed by the deeper sediment layer (3190 \pm 172 taxa) and the water column (1177 \pm 238 taxa). Archaeal richness was on average lower compared to bacterial richness with the highest number of taxa in the deeper layer (2-5 cm) of the sediment (Table S3.4 and S3.5). A further description of general bacterial and archaeal taxonomy (Fig. S3.4 and S3.5) of the sampling sites can be found in the supplementary information.

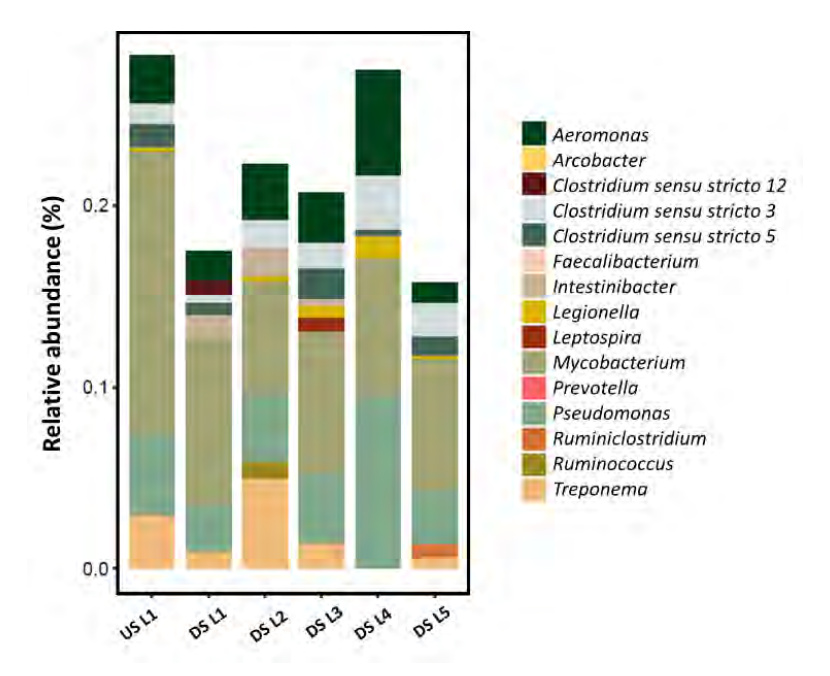


FIGURE 3.6 Relative abundance of bacterial faecal indicators and human pathogens in the top (0-2 cm) sediment of river Linge based on 16S rRNA gene amplicon sequencing. The initial community composition was assessed 500 m upstream (US) of the first WWTP effluent discharge location (L1). All other samples were taken 500 m downstream (DS) of each WWTP effluent discharge location. Taxonomy is presented at the genus level.

Lastly, to assess if microorganisms originating from wastewater treatment can be detected as part of the prokaryotic river community, we analysed the presence of faecal indicators and human pathogenic bacteria. The typical bacterial faecal indicator species Escherichia coli and Enterobacter were not detected among the retrieved 16S rRNA gene reads. However, in the river Linge, other faecal indicators such as Intestinibacter, Clostridium, and Ruminiclostridium were present. These species were detected in sediments collected downstream of WWTP effluent discharge locations but not upstream of the first discharge location (Fig. 3.6). In the water column of the Linge, the human faecal indicator *Feacalibacterium* and the pathogen *Acrobacter* also only appeared after WWTP effluent discharge, indicating that they originated from the effluent (Fig. S3.8a). Moreover, the pathogenic bacterium *Legionella* increased in abundance in the river water along the transect, peaking after discharge location L3, but was already present upstream of the WWTPs. For river Kromme Rijn, one *Clostridium* species, *Ruminiclostridum* which is related to animal rumens, and the human-gut related *Ruminococcus* appeared only after the effluent discharge location in the mixed sediment. In the water column, no changes in the bacterial communities were observed (Fig. S3.8b).

3.4 DISCUSSION

In this study, we assessed the influence of effluent discharge on GHG emissions from two Dutch rivers. To mechanistically understand changes in these emissions, we also assessed the chemical composition of water and sediment, as well as the microbial community composition. Overall, GHG emissions of the rivers Linge and Kromme Rijn were high. CO₂ emissions and dissolved CO₂ concentrations peaked at most effluent discharge locations, whereas CH₄ and N₂O gradually increased over the investigated distance of two kilometres downstream of the discharge locations. Although the microbial community composition in the river water and sediment was not strongly affected by the WWTP effluent, indicator species of wastewater treatment effluent were detected downstream of discharge locations. Moreover, the relative abundances of methanogenic archaea - methane producers - increased after discharge locations in the sediments of both rivers.

3.4.1 High emissions from riverine systems

Emissions of CO₂, CH₄, and N₂O (2.7-71.6, 0.1-5.4, 0.04-2.03 g CO₂-eq m⁻²d⁻¹, respectively) in the two investigated rivers were in the same range as emissions observed in eutrophic rivers in temperate urban and agricultural areas (0.8-30.8, 0.09-6.5, 0.54-12.3 g CO₂-eq m⁻²d⁻¹ for CO₂, CH₄, and N₂O, respectively; Upadhyay et al., 2023). Moreover, the river emissions observed were in the same range as those reported for estuaries influenced by WWTPs (N₂O: 0.06-3.7 g CO₂-eq m⁻²d⁻¹; Dong et al., 2023) as well as emissions from eutrophic, agricultural drainage ditches and canals (CO₂ and CH₄: 1.9-22.0 and 0.007-28.6 g CO₂-eq m⁻²d⁻¹; Hendriks et al., 2024a; Peacock et al., 2021). The emissions reported here probably underestimate CH₄ fluxes, as, even though bubbles were observed, we did not quantify CH₄ ebullition.

Ebullition may contribute substantially to total CH₄ emissions in rivers, but its quantification in rivers is still challenging (Hendriks et al., 2024a; Maeck et al., 2014). Furthermore, besides spatial variation, as observed in this study, GHG emissions show large diel and seasonal fluctuations, where CH, emissions are highest in summer and CO₂ emissions are highest in winter (Hendriks et al., 2024a; Galantini et al., 2021). Moreover, effluent composition may differ over time as well, depending on wastewater treatment performance and weather conditions. Performing multiple measurements a day, within different seasons, could further improve how riverine GHG emissions are affected by effluent discharge.

3.4.2 Effects of effluent discharge on physical-chemical properties of river water and sediment

Physical-chemical properties of the river water differed at the discharge locations compared to locations upstream and downstream of the WWTPs. At discharge locations, a lower pH, and higher EC, NH₄+, PO₄3- and TIC concentrations were observed compared to points upstream and downstream of effluent discharge. River NH,+ concentrations at the discharge locations were lower than average concentrations measured in the WWTP effluent being discharged (119-421 µmol L-1; Table 1), which can be explained by effluent dilution at the discharge location, and possibly nitrification in the effluent pipes.

The river GHG emissions and nutrient concentrations were most likely not only influenced by WWTP effluent discharge, but also by agricultural nutrient influx. As the two rivers are located in agricultural areas, agricultural runoff and erosion of fertilized land can increase the nutrient load of the rivers too. Supporting this, Yao et al. (2020) identified that N fertilizers were responsible for nearly 90% of the global increase of riverine N₂O emissions during the 1990s. Furthermore, high NO₂ levels in the first 20 km of river Linge, with a gradual decline along the transect, point to a source of NO₃ upstream of the first sampling location.

Changes in sediment characteristics as a result of effluent discharge could only be determined for river Linge, since sediment sampling upstream of discharge location at the Kromme Rijn was hampered by its stony sediment structure. Although we were only able to measure upstream of the first effluent discharge location in River Linge, and 500 m downstream of each discharge location, some general patterns could be observed. Organic matter content of Linge sediment, as well as N and C content, increased after the first discharge location, and tended to increase along the river transect, up to the sampling location downstream of L5. This discharge location was located at an industrial site, where sediment composition differed from the other

locations. P concentrations within the sediment increased after the first discharge location, whereafter it tended to decrease along the river transect. The same pattern was observed for Fe and Al, suggesting that P was less able to bind to those metals, and therefore released to the water column (Tammeorg, 2020; Golterman, 2004). The peak in PO₄³⁻ concentrations after L5 indicates this release as well.

3.4.3 Drivers of riverine GHG emissions in relation to WWTP effluent discharge

River GHG emissions tended to increase after receiving WWTP effluent, even though emissions were already substantial before the first discharge locations. CO_2 emissions peaked in at least half of the discharge locations. After effluent discharge, CH_4 and N_2O emissions increased simultaneously, with emissions being ~5-fold higher 2 km after discharge locations. Enhanced CH_4 emissions downstream of effluent discharge locations have been reported previously, in a study of well-mixed river sections where effects were monitored up to 100 m after discharge locations (Alshboul et al., 2016). Our results indicate that the impact of effluent discharge may occur for at least 2 km after discharge points, and potentially cause effects over larger distances.

Most likely, CO₂ emissions at discharge locations are derived from dissolved CO₂ already present in the effluent, as indicated by the high dissolved CO₂ concentrations at these locations, and their strong correlation with EC, TIC and (inversely) DO (Fig. 3.4, Fig. S3.1). Such CO₂ outgassing was also observed by Alshboul et al. (2016). CO₂ is produced biologically during wastewater treatment as a product of organic matter degradation. Within the anoxic sediment or, less likely, in anoxic microhabitats in the water column, both organic carbon and dissolved CO₂ can be used as substrates for methane generation, as also suggested by the relation between dissolved CH₄ and TOC (Fig. 3.4). In addition, the relative abundance of methanogens and CH₄ emissions increased simultaneously with the carbon content of the sediment. This indicates that the increase in CH₄ emissions downstream of discharge locations is likely produced in the river itself, stimulated by carbon and nutrients present in discharged effluent, and not a result of dissolved CH₄ loads originating from the WWTP effluent.

In rivers, N_2O can be produced in both anoxic and (sub)oxic habitats, mainly through denitrification, and as side product of nitrification in oxic habitats (Quick et al., 2019). Emission of N_2O from freshwater ecosystems usually occurs in specific locations ('hot spots') or short bursts ('hot moments') (Groffman et al., 2009). In this study, the largest N_2O peak at the Linge was observed immediately after the highest water column TOC concentration (1.1 mmol L^{-1}) measured in this river. This indicates

3

that at this location N₂O is likely produced via denitrification with organic carbon as electron donor, or that the organic carbon led to anaerobic microhabitats where denitrification took place. Availability of nitrate and other DIN sources are the main driver of denitrification in freshwater ecosystems (Seitzinger et al., 2006; Veraart et al., 2017, Kreiling et al., 2019). In our rivers, the highest dissolved N₂O concentrations were measured on locations with high NO₃ concentrations (Fig. 3.4). This points towards denitrification as the main N₂O source, with excess NO₃ resulting in incomplete denitrification (van de Leemput et al., 2011). In the river Kromme Rijn, CO₂ and N₂O emission patterns were more aligned; they both peaked at the effluent discharge location.

3.4.4 Microbial community change due to effluent discharge

Because microorganisms drive the production and cycling of GHGs, we investigated potential differences in microbial community composition before and after effluent discharge locations, using 16S rRNA gene sequencing. Overall, downstream of WWTP effluent discharge locations methanogenic archaea dominated the archaeal community in the sediment of both rivers. Methanogens were also the dominant archaeal groups in the river water, either indicating the presence of anoxic microhabitats in the turbid water column, or some sediment influence reaching higher water layers. Interestingly, downstream of the first WWTP effluent discharge location on the river Linge, the archaeal community shifted from being Methanoperedenaceae-dominated to a Methanoperedena is an anaerobic methane-oxidizing archaeon which couples CH₄ oxidation to NO₃ reduction (Haroon et al., 2013). Hence, the abundant availability of both dissolved CH₄ and NO₃ in the first 20 km of the river Linge may allow for the proliferation of Methanoperedenaceae.

Downstream of L1, the relative abundance of *Methanoperedenaceae* decreased greatly. Here, dissolved CO₂ concentrations are high and thus might be a driver for methanogenic archaea, assuming concomitant hydrogen (H₂) production by fermentative bacteria. However, as we only determined relative abundances these results should not be interpreted as a competition between methanogenic and methanotrophic archaea, as absolute numbers of *Methanoperedenaceae* may remain constant. At discharge location L4, a dissolved CO₂ concentration equally high as at L1 was measured, and especially *Methanoregulaceae* which is known as a hydrogenotrophic methanogen (Sakai et al., 2012) increased in relative abundance in the river sediment downstream. Similarly, in river Kromme Rijn an increase in methanogenic abundance after WWTP effluent discharge was observed, but overall *Methanoperedenaceae* were less dominant in this river.

The general community composition of methane-oxidizing and nitrifying bacteria, and the bacterial community overall, were not heavily influenced by the treated wastewater effluent, when comparing microbial samples taken 500 m downstream of discharge locations. This is in contrast with previous research showing a positive impact of effluent discharge on downstream microbial diversity (Price et al., 2018; Wakelin et al., 2008). Notably, Wakelin et al. (2008) observed the highest diversity 150 meters downstream compared to 400 and 1040 meters downstream. A different study reported lower bacterial diversity 50 meters downstream compared to upstream (Drury et al., 2013). These findings highlight the potential influence of the sampling location. Lastly, although the signature of wastewater was present in the rivers after discharge locations, as seen from the presence of *Intestinibacter* and *Arcobacter*, true faecal indicators like *E. coli* and *Enterococci* were not observed 500 meters downstream in river Linge and Kromme Rijn.

3.5 CONCLUSION

Here, we investigated the effect of wastewater effluent on the GHG emissions and GHG-cycling microbial communities of small, slow flowing rivers. High dissolved CO₂ concentrations originating from WWTP effluent likely drive CO₂ outgassing at discharge locations. Furthermore, we observed a ~5-fold increase in CH₄ and N₂O emissions 2 km downstream of discharge locations, potentially due to stimulated biological production within the river itself, due to effluent-enhanced nutrient concentrations. Besides the possible effects of effluent discharge on N₂O emissions, the dissolved N₂O concentration of both rivers was strongly influenced by other upstream sources of NO₃⁻. Overall, this study shows that wastewater treatment discharge is a potential cause of enhanced riverine GHG emissions. Acknowledging the complexity of river ecosystems and the multifaceted nature of GHG dynamics, we propose that mitigating nutrient loads to rivers, by targeting both point sources such as WWTPs, and diffuse sources such as agriculture, is a crucial strategy to reduce riverine GHG emissions.

Acknowledgements

We would like to thank Sebastian Krosse and Paul van der Ven from the Radboud University General Instrumentation lab and Roy Peters and Germa Verheggen from the Ecology department of Radboud University for sample analysis. Furthermore, we thank Sarah Schrammeck for performing analyses on the dissolved greenhouse gas samples.

SUPPORTING INFORMATION

TABLE S3.1 Overview of the sample locations on river Linge and river Kromme Rijn. WWTP effluent discharge locations are indicated between parentheses.

River	Distance (km)	Distance from discharge location (m	Coordinates
Linge	0	-500	51°53'06"N 5°16'49"E
Linge (L1)	0.5	0	51°53'15"N 5°16'34"E
Linge	1	500	51°53'15"N 5°16'07"E
Linge	1.5	1000	51°53′05″N 5°15′51″E
Linge	2.5	2000	51°53′01"N 5°15′02"E
Linge	12	-500	51°53'36"N 5°10'22"E
Linge (L2)	12.5	0	51°53′47″N 5°10′08″E
Linge	13	500	51°53'46"N 5°09'41"E
Linge	13.5	1000	51°53'36"N 5°09'23"E
Linge	14.5	2000	51°53'01"N 5°09'25"E
Linge	19	-500	51°52'47"N 5°07'06"E
Linge (L3)	19.5	0	51°53'03"N 5°07'01"E
Linge	20	500	51°53'16"N 5°06'44"E
Linge	20.5	1000	51°53'19"N 5°06'15"E
Linge	21	-500	51°53'16"N 5°05'55"E
Linge (L4)	21.5	0	51°53'18"N 5°05'21"E
Linge	22	500	51°53'03"N 5°05'14"E
Linge	22.5	1000	51°52'47"N 5°05'07"E
Linge	23.5	2000	51°52'26"N 5°04'22"E
Linge	34	-500	51°50'41"N 4°59'29"E
Linge (L5)	34.5	0	51°50'29"N 4°59'22"E
Linge	35	500	51°50′17″N 4°59′03″E
Linge	35.5	1000	51°50'08"N 4°58'45"E
Kromme Rijn	0	-1000	52°03'24"N 5°13'27"E
Kromme Rijn	0.5	-500	52°03'36"N 5°13'01"E
Kromme Rijn (K1)	1	0	52°03'48"N 5°12'49"E
Kromme Rijn	1.5	500	52°04'01"N 5°12'35"E
Kromme Rijn	2	1000	52°04'08"N 5°12'10"E
Kromme Rijn	3	2000	52°04'33"N 5°11'38"E
Kromme Rijn	4	3000	52°04'22"N 5°11'00"E

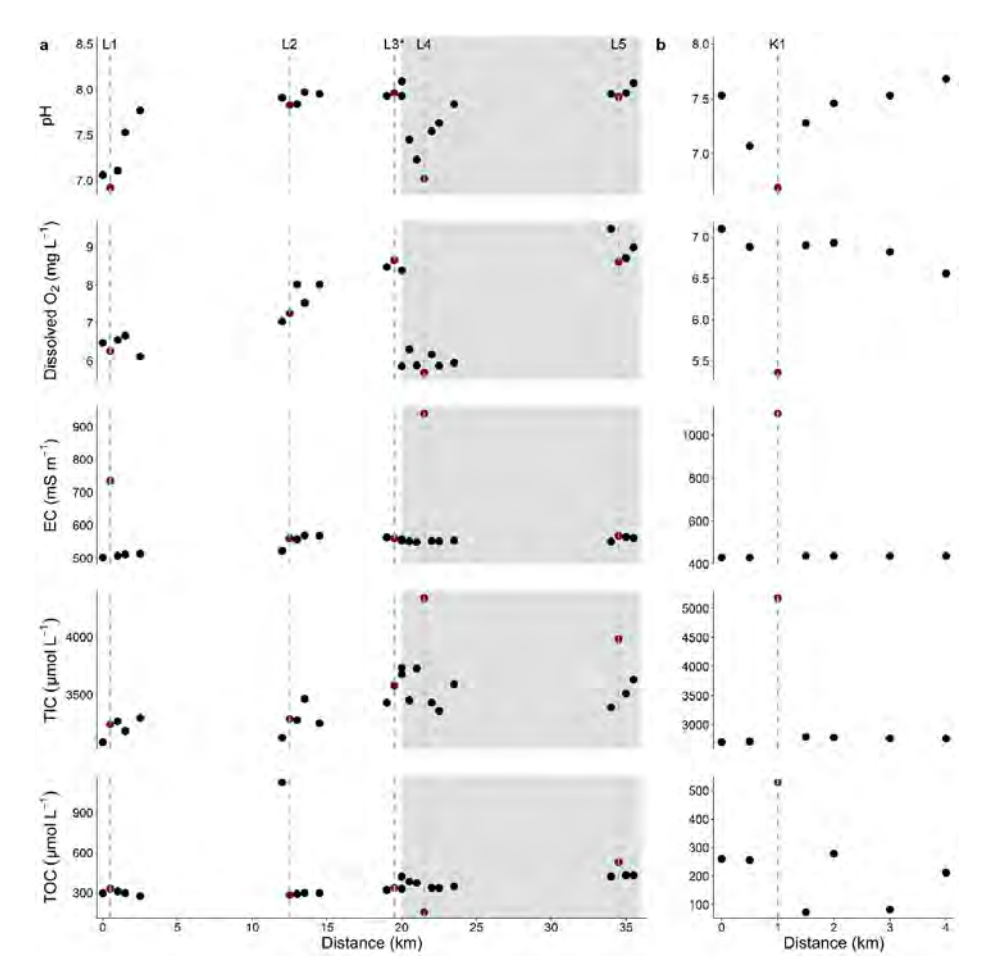


FIGURE S3.1 Water column conditions (pH, dissolved O₂, electrical conductivity (EC), total inorganic carbon (TIC) and total organic carbon (TOC)) over the transect of river Linge (a) and river Kromme Rijn (b). The white area is the first sampling day, the grey area in (a) indicates the second sampling day. The red points indicate the discharge locations. At location L3, we could not measure directly at the discharge location, confounding these measurements. The location 500 m downstream of L3 (20 km) was measured on both sampling days. Note the difference in y-axis values.

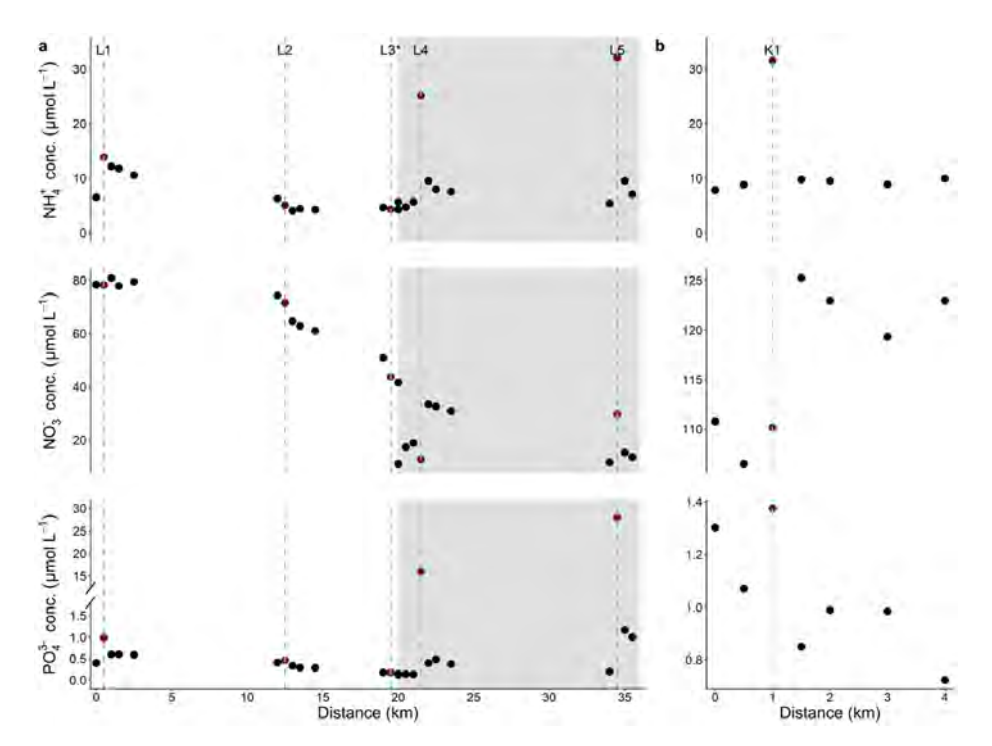


FIGURE S3.2 Dissolved nutrient concentrations (NH $_4^+$, NO $_3^-$ and PO $_4^{3*}$) over the transect of river Linge (a) and river Kromme Rijn (b). The white area is the first sampling day, the grey area in (a) indicates the second sampling day. The red points indicate the discharge locations. At location L3, we could not measure directly at the discharge location, confounding these measurements. The location 500 m downstream of L3 (20 km) was measured on both sampling days. Note the difference in y-axis values and the y-axis break at PO $_4^{3*}$ concentration (a).

TABLE S3.2 Biochemical characteristics of the different sediment depths of river Linge and Kromme Rijn. Nitrogen (N), carbon (C), phosphorus (P), Iron (Fe), Aluminium (Al) concentration of the sediment was determined 500 m upstream of the first discharge effluent location on Linge and Kromme Rijn and 500 m downstream of every effluent location.

River	Distance (km)	Depth (cm)	LOI (%)	N**	C**	P***	Fe***	Al***
L	0	0-2	7	0.33	4.43	134	887	745
L	0	2-5	11	0.27	3.95	129	708	456
L	1	0-2	13	0.44	5.07	187	1019	872
L	1	2-5	13	0.42	4.81	237	1027	661
L	13	0-2	15	0.49	5.49	147	972	842
L	13	2-5	13	0.44	4.89	173	1040	1134
L	20	0-2	14	0.41	5.81	83	632	539
L	20	2-5	20	0.41	7.16	110	630	436
L	22	0-2	14	0.49	5.55	114	816	818
L	22	2-5	14	0.51	5.55	131	892	1190
L	35	0-2	7	0.22	3.13	52	401	379
L	35	2-5	4	0.16	2.56	39	362	436
KR	0.5	M*	1	0.04	0.62	32	173	92
KR	1.5	M*	1	0.03	0.50	14	132	74
KR	1.5	0-2	14	0.44	6.22	101	748	873
KR	1.5	2-5	12	0.44	5.91	101	702	616
KR	3	M*	7	0.21	3.47	75	441	371
KR	3	0-2	10	0.25	4.33	108	521	291
KR	3	2-5	11	0.26	4.49	115	586	449

^{*} For KR no sediment core could be taken upstream of the effluent discharge location, instead a sediment sample was scooped and is indicated as "mixed sediment" (M). For the other two locations on KR both sediment cores and mixed sediment samples were taken.

^{**}Concentration is shown as mmol/g dry weight

^{***}Concentration is shown as µmol/g dry weight

TABLE S3.3 DNA concentration of two sediment layers and the water column of river Linge (L) and Kromme Rijn (KR).

River	Distance (km)	Depth (cm)	Sediment (µg DNA/g dry weight)	Water(ng DNA/mL)
L	0	-	-	5.2
L	0	0-2	43.8	-
L	0	2-5	37.8	-
L	1	-	-	5.1
L	1	0-2	42.1	-
L	1	2-5	36.7	-
L	13	-	-	7.5
L	13	0-2	77.2	-
L	13	2-5	29.5	-
L	20	-	-	6.9
L	20	0-2	34.3	-
L	20	2-5	5.1	-
L	22	-	-	7.2
L	22	0-2	121.2	-
L	22	2-5	16.1	-
L	35	-	-	10.5
L	35	0-2	42.4	-
L	35	2-5	4.3	-
KR	0.5	-	-	4.1
KR	0.5	M*	3.5	-
KR	1.5	-	-	5.0
KR	1.5	0-2	35.9	-
KR	1.5	2-5	28.3	-
KR	1.5	M*	1.3	-
KR	3	-	-	4.8
KR	3	0-2	19.5	-
KR	3	2-5	8.4	-
KR	3	M*	6.3	-

^{*} For KR no sediment core could be taken upstream of the effluent discharge location, instead a sediment sample was scooped and is indicated as "mixed sediment" (M). For the other two locations on KR both sediment cores and mixed sediment samples were taken.

Supplementary description of archaeal and bacterial 16S rRNA gene amplicon sequencing

The archaeal fraction in the water column and sediment of river Linge and Kromme Rijn consisted mainly of the orders Micrarchaeales and Woesearchaeales which both are poorly studied, and the classes Bathyarchaeia, Lokiarchaeia and Thermoplasmata (Fig. S3.3), in addition to the previously described methanogens archaeal ammonia oxidizers (Fig. 3.4 and Fig. S3.5). Batyarchaeota are often highly abundant and widespread in anoxic sediments but also appear in the water column of freshwater environments (Zhou et al., 2018). This is in accordance with our findings as they are abundant in the sediment but also in the water column of both Linge and Kromme Rijn.

Furthermore, in the water column of both rivers Actinobacteria, Bacteroidota and Proteobacteria were the most abundant phyla of the bacterial population (Fig S3.4). Although less abundant than the aforementioned phyla, Verrucomicrobiota and Cyanobacteria were also relatively abundant in river Linge. Interestingly, the relative abundance of Cyanobacteria increases downstream of the first four WWTP discharge locations. Proteobacteria was the most dominant phylum in the sediment of both Kromme Rijn and Linge, followed by Bacteroidota, Chloroflexi, Acidobacteriota, Desulfobacterota, Nitrospirota and Verrucomicrobiota (Fig. S3.4). The anaerobic methane oxidizing phylum Methylomirabilota was detected in the 2 to 5 cm sediment layer 500 m downstream of L3 in river Linge and 2 km downstream of the WWTP in river Kromme Rijn. These bacteria are known to couple the oxidation of methane to the reduction of nitrite (Ettwig et al., 2010).

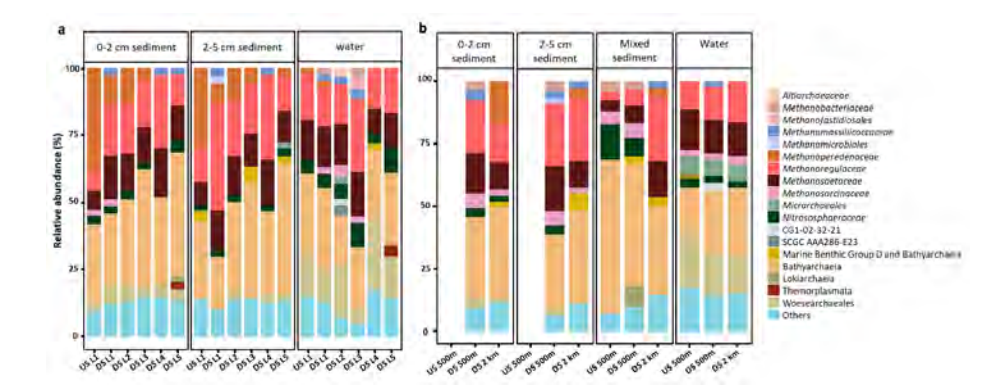


FIGURE S3.3 Archaeal community composition in sediment and water column of river Linge (a) and Kromme Rijn (b) based on 16S rRNA gene amplicon sequencing. A sample for the initial community composition 500 m upstream (US) of the first WWTP effluent discharge location was taken. For river Linge (a) all other samples were taken 500 m downstream (DS) of each WWTP effluent discharge location. For river Kromme Rijn (b) the other two sample locations were taken 500 m and 2 km downstream of the WWTP effluent discharge location. Upstream of the WWTP no sediment core could be taken, instead a sediment sample was scooped and is indicated as "mixed sediment". Taxonomy is presented at family level when available. ASVs representing less than 2% of all reads in a sample were grouped into 'Others'.

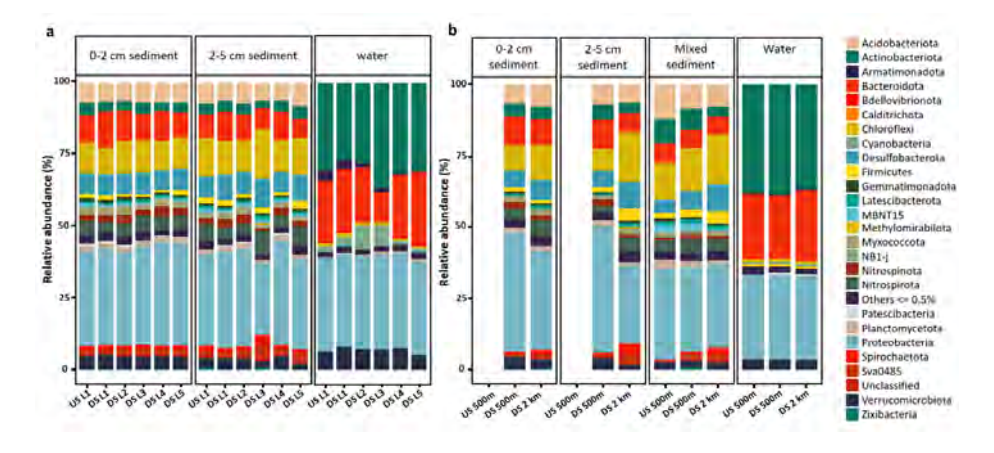


FIGURE S3.4 Bacterial community composition in sediment and water column of river Linge (a) and Kromme Rijn (b) based on 16S rRNA gene amplicon sequencing. A sample for the initial community composition 500 m upstream (US) of the first WWTP effluent discharge location was taken. For river Linge (a) all other samples were taken 500 m downstream (DS) of each WWTP effluent discharge location. For river Kromme Rijn (b) the other two sample locations were taken 500 m and 2 km downstream of the WWTP effluent discharge location. Upstream of the WWTP no sediment core could be taken, instead a sediment sample was scooped and is indicated as "mixed sediment". Taxonomy is presented at phylum level. ASVs representing less than 0.5 % of all reads in a sample were grouped into 'Others'.

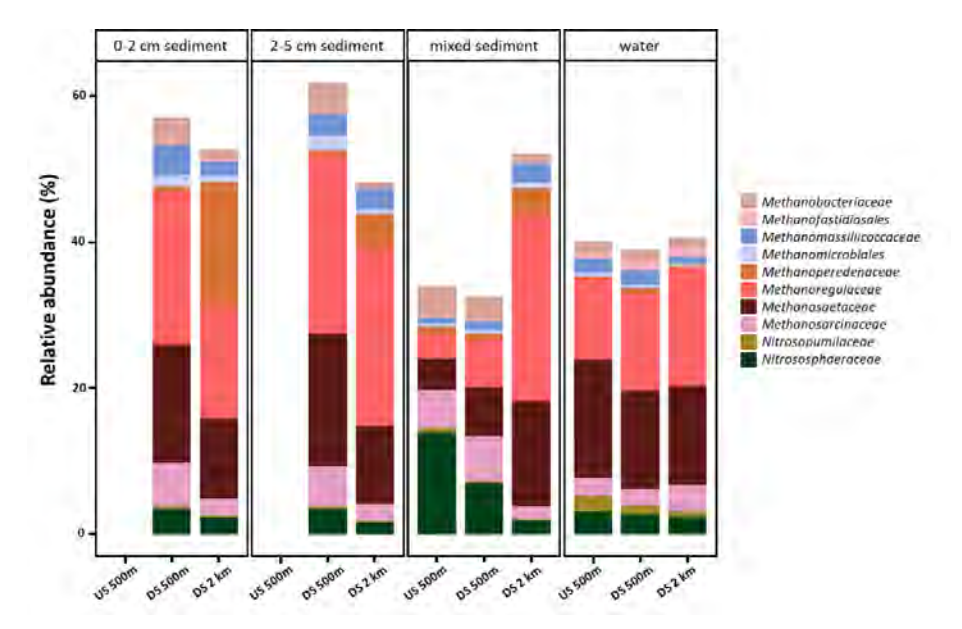


FIGURE S3.5 Relative abundance of methanogenic archaea, anaerobic methane oxidizing archaea and ammonia oxidizing archaea in sediment and water of river Kromme Rijn based on 16S rRNA gene amplicon sequencing. Upstream of the WWTP no sediment core could be taken, instead a sediment sample was scooped and is indicated as "mixed sediment". The other two sample locations were 500 m downstream (DS) and 2 km DS of the WWTP effluent discharge location. Taxonomy is presented at family level.

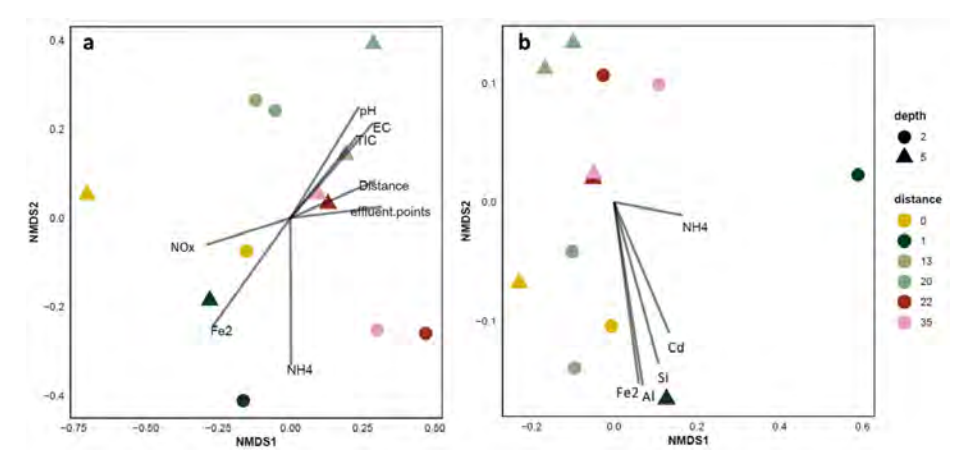


FIGURE S3.6 Ordination of the total archaeal (**a**) and bacterial (**b**) community in the sediment of river Linge based on 16S rRNA gene amplicon sequencing. Ordination of every sample was calculated with Bray-Curtis distance as non-metric two-dimension NMDS plot. Environmental variables were scaled based on significance of the correlations and only displayed when p < 0.05.

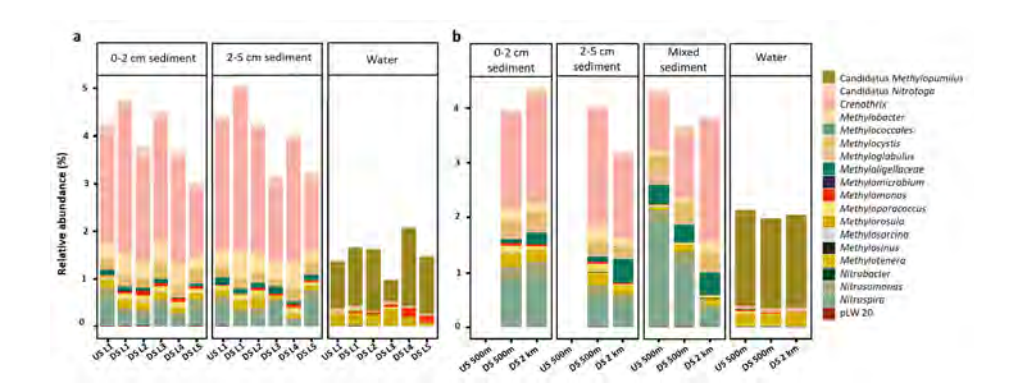


FIGURE S3.7 Relative abundance of nitrifying and methanotrophic bacteria in sediment and water of river Linge (a) and Kromme Rijn (b) based on 16S rRNA gene amplicon sequencing. A sample for the initial community composition 500 m upstream (US) of the WWTP effluent discharge location was taken. For Kromme Rijn (b) no sediment core could be taken US, instead a sediment sample was scooped and is indicated as "mixed sediment". The other sample locations were 500 m downstream (DS) of each WWTP effluent discharge location. For Kromme Rijn (b) an additional sample was taken 2 km DS. Taxonomy is presented at genus level.

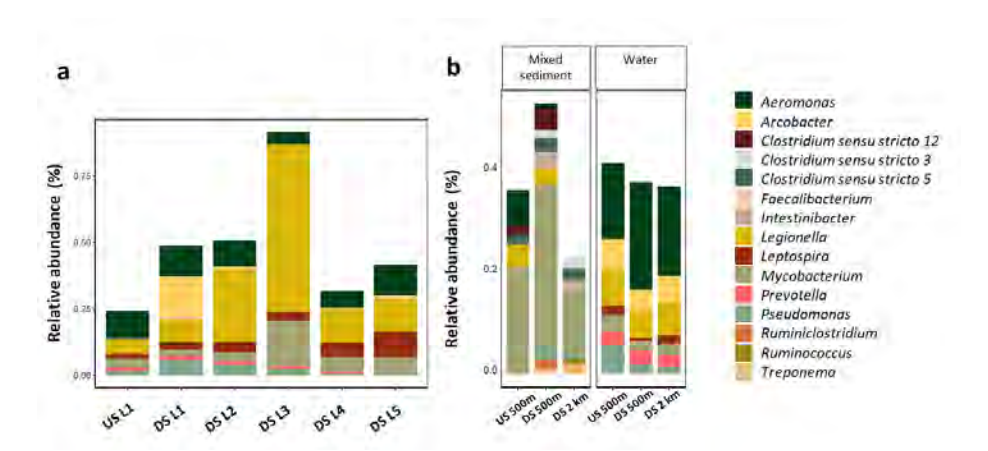


FIGURE S3.8 Relative abundance of bacterial faecal indicators and human pathogens in the water column of river Linge (a) and in mixed sediment and the water column of river Kromme Rijn (b) based on 16S rRNA gene amplicon sequencing. A sample for the initial community composition 500 m upstream (US) of the WWTP effluent discharge location was taken. For Kromme Rijn (b) no sediment core could be taken US, instead a sediment sample was scooped and is indicated as "mixed sediment". The other sample locations were 500 m downstream (DS) of each WWTP effluent discharge location. For Kromme Rijn (b) an additional sample was taken 2 km DS. Taxonomy is presented at genus level.

TABLE S3.4 Alpha diversity indexes (Chao1 and Shannon) of bacterial (bact) and archaeal (arch) fraction calculated for the water column of river Linge (L) and Kromme Rijn (KR).

River	Distance (km)	Fraction	Number of Taxa	Chao1 index	Shannon index
L	0	arch	394	398	4.7
L	1	arch	464	468	4.9
L	13	arch	215	218	4.4
L	20	arch	155	156	4.1
L	22	arch	316	320	5.0
L	35	arch	139	141	4.2
KR	0.5	arch	632	637	5.4
KR	1.5	arch	674	680	5.3
KR	3	arch	711	716	5.4
L	0	bact	1003	1073	5.3
L	1	bact	1364	1660	5.5
L	13	bact	991	1072	5.5
L	20	bact	1043	1115	5.4
L	22	bact	1044	1110	5.6
L	35	bact	974	1033	5.6
KR	0.5	bact	1200	1313	5.4
KR	1.5	bact	1466	1585	5.5
KR	3	bact	1339	1433	5.4

TABLE S3.5 Alpha diversity indexes (Chao1 and Shannon) of bacterial (bact) and archaeal (arch) fraction calculated for the different sediment layers of river Linge (L) and Kromme Rijn (KR).

River	Distance (km)	Depth (cm)	Fraction	Number of Taxa	Chao1 index	Shannon index
L	0	0-2	arch	1008	1018	4.9
L	1	0-2	arch	1087	1103	5.1
L	13	0-2	arch	849	863	5.2
L	20	0-2	arch	1072	1090	5.4
L	22	0-2	arch	647	654	4.9
L	35	0-2	arch	586	595	5.3
L	0	2-5	arch	1215	1232	5.2
L	1	2-5	arch	586	594	4.5
L	13	2-5	arch	1051	1067	5.2
L	20	2-5	arch	1088	1104	5.6
L	22	2-5	arch	808	814	4.9
L	35	2-5	arch	1158	1174	5.4
KR	1.5	0-2	arch	820	834	5.1
KR	3	0-2	arch	883	891	5.3
KR	1.5	2-5	arch	680	696	4.8
KR	3	2-5	arch	1015	1034	5.5
KR	0.5	\mathbf{M}^*	arch	522	525	4.9
KR	1.5	\mathbf{M}^*	arch	936	940	5.5
KR	3	\mathbf{M}^*	arch	1174	1191	5.4
L	0	0-2	bact	3528	3672	7.3
L	1	0-2	bact	3647	3805	7.3
L	13	0-2	bact	3345	3539	7.3
L	20	0-2	bact	3064	3336	7.2
L	22	0-2	bact	2672	2906	7.0
L	35	0-2	bact	3521	3654	7.2
L	0	2-5	bact	3217	3349	7.3
L	1	2-5	bact	3108	3264	7.1
L	13	2-5	bact	3158	3343	7.2
L	20	2-5	bact	2929	3080	7.2
L	22	2-5	bact	3028	3200	7.0

River	Distance (km)	Depth (cm)	Fraction	Number of Taxa	Chao1 index	Shannon index
L	35	2-5	bact	2783	2904	7.1
KR	1.5	0-2	bact	3157	3357	7.1
KR	3	0-2	bact	3083	3278	7.3
KR	1.5	2-5	bact	2907	3070	7.0
KR	3	2-5	bact	3274	3427	7.4
KR	0.5	\mathbf{M}^*	bact	2648	2796	7.1
KR	1.5	\mathbf{M}^*	bact	3532	3688	7.4
KR	3	\mathbf{M}^*	bact	2849	2973	7.2

^{*} For KR no sediment core could be taken upstream of the effluent discharge location, instead a sediment sample was scooped and is indicated as "mixed sediment" (M). For the other two locations on KR both sediment cores and mixed sediment samples were taken.



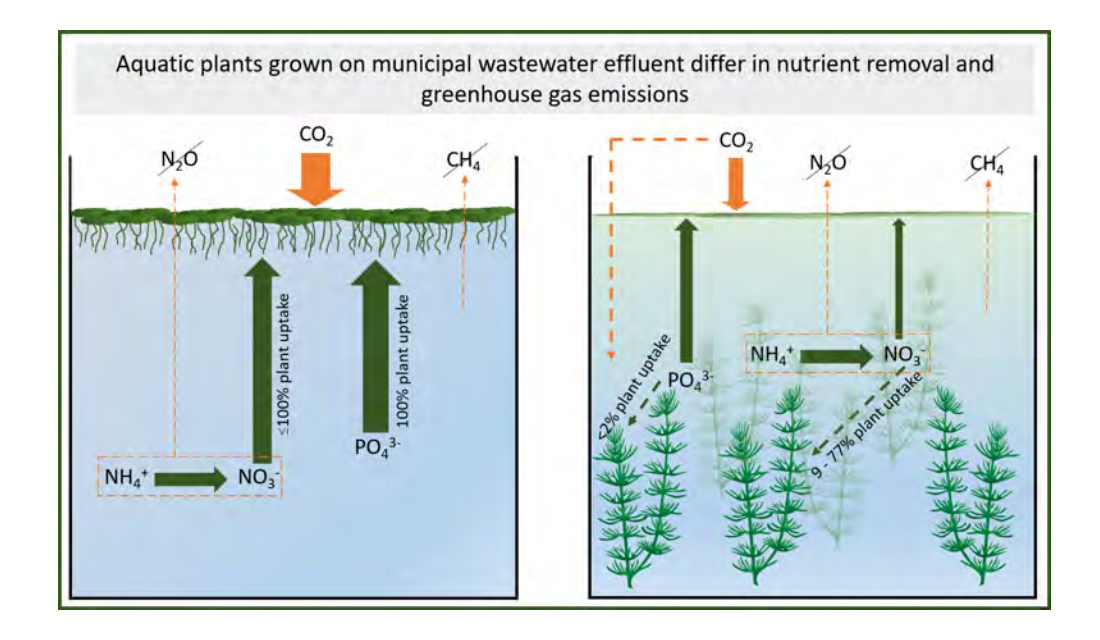
Chapter 4

Polishing wastewater effluent using plants: floating plants perform better than submerged plants in both nutrient removal and reduction of greenhouse gas emission

Lisanne Hendriks, Alfons J. P. Smolders, Thom van den Brink, Leon P. M. Lamers, Annelies J. Veraart

Published in Water Science & Technology, 2023, 88 (1): 23-34 doi: 10.2166/wst.2023.203

GRAPHICAL ABSTRACT



ABSTRACT

While research on aquatic plants used in treatment wetlands is abundant, little is known about the use of plants in hydroponic ecological wastewater treatment, and its simultaneous effect on greenhouse gas emissions. Here, we assess the effectiveness of floating and submerged plants in removing nutrients and preventing greenhouse gas (GHG) emissions from wastewater effluent. We grew two species of floating plants, Azolla filiculoides and Lemna minor, and two species of submerged plants, Ceratophyllum demersum and Callitriche platycarpa, on a batch of domestic wastewater effluent without any solid substrate. In these systems, we monitored nitrogen and phosphorus removal and fluxes of CO2, CH2 and N2O, for two weeks. In general, floating plants produced most biomass, whereas submerged plants were rapidly overgrown by filamentous algae. Floating plants removed nutrients most efficiently; both floating species removed 100% of the phosphate while Lemna also removed 90-100% of the inorganic nitrogen, as opposed to a removal of 41-64% in submerged plant with algae treatments. Moreover, aquaria covered by floating plants had roughly three times higher GHG uptake than the treatments with submerged plants or controls without plants. Thus, effluent polishing by floating plants can be a promising avenue for climate-smart wastewater polishing.

4.1 INTRODUCTION

Wastewater treatment plants (WWTPs) can account for up to 45% of the total nutrient loading in surface waters (e.g. Groenendijk et al. 2016). Because nutrient levels in domestic wastewater treatment effluents are relatively high (330 – 700 μ mol/l N; 18 – 50 μ mol/l P; Carey & Migliaccio 2009; CBS 2021), WWTPs contribute substantially to eutrophication of natural waterbodies (Carey & Migliaccio 2009), and furthermore contribute to high greenhouse gas (GHG) emissions from these waterbodies (Beaulieu et al. 2019). Reducing WWTP-derived nutrient loads can therefore reduce GHG emission in receiving waterbodies. GHG emissions are set to be reduced by 55% in 2030 (European Commission 2021) and regional water authorities and wastewater managers can have a substantial role in this reduction.

4.1.1 Aquatic plants in hydroponic effluent polishing

Since the 1990s the concept of ecological water treatment using aquatic plants (macrophytes) has gained interest (Wang 1987), but despite its many benefits it is not yet widely used. Moreover, the focus has been on effluent polishing through nutrient uptake, but not yet on low GHG-emission polishing. Next to constructed wetlands, a relatively new treatment of effluent has now started to gain interest, in which a closed system without a sediment layer is used for macrophyte growth, and effluent treatment takes place in a hydroponic way (e.g. Magwaza et al. 2020). By using the self-purification principle of natural water bodies – the uptake and transformation of nutrients mediated by aquatic plants – effluent can be treated to reach nutrient concentrations below the critical values set by the European Water Framework Directive (WFD) (Norström et al. 2004).

4.1.2 Trait-specific effects on nutrient removal and GHG fluxes

Aquatic plants mediate nutrient removal both directly and indirectly. Directly, plants can extract inorganic phosphorus (P) and nitrogen (N) from wastewater, incorporating them into their biomass, and thus enabling N, P and C harvesting and reuse (e.g. Norström et al. 2004). Indirectly, they alter conditions in water and sediment. For example, they alter oxygen concentrations and provide surface for biofilm formation, thereby favouring coupled nitrification-denitrification and altering the production and emission of CH₄ (Danhorn and Fuqua 2007; Veraart et al. 2011; Law et al. 2012). During nitrification and denitrification N₂O can be formed (Law et al. 2012), and aquatic plants have multiple ways in which they directly and indirectly affect this emission. At the same time, their photosynthesis removes CO₂ from the atmosphere or water layer while fixing carbon (C) in their biomass.

Different aquatic plant growth forms have their own characteristics in removing nutrients and altering GHG emissions (Attermeyer et al. 2016; Christiansen et al. 2016). Submerged plant species can provide a large surface for epiphytic biofilm formation, altering microbial processes in these biogeochemically heterogeneous sites (Eriksson & Weisner 1999). At the same time, submerged macrophytes may inhibit denitrification by their oxygen leakage and by competing for nitrate with denitrifying bacteria (Toet et al. 2003). Floating plants, on the other hand, can form a dense mat on top of the water column, creating a reaeration barrier. Local conditions determine whether this barrier favours oxygen depletion or oxygen trapping. Although lower oxygen concentrations under such mats induce higher denitrification rates and CH₄ production (Veraart et al. 2011), the O₃ trapped under the macrophytes through radial oxygen loss (ROL) may enhance nitrification and CH₄ oxidation, making the outcome in terms of nutrient removal and GHG emission system specific (Kosten et al. 2016). Since floating plants can only cover the top layer of the water column, their growth easily becomes space-limited. Consequently, N and P uptake may stall when floating plants achieve full coverage (Si et al. 2019). Additionally, reduced surface for epiphytic biofilm formation potentially lowers the potential for microbial nutrient conversions, especially in systems without a sediment layer. Lastly, the floating fern Azolla filiculoides has a symbiosis with N-fixing microorganisms, which makes them less efficient in removing N, but highly efficient in removing P, because their growth does not stall once N is depleted in the water column (Brouwer et al. 2018).

The goal of this study was to explore the nutrient-removal efficiency of two different macrophyte growth forms, floating vs. submerged, and their potential to lower GHG emissions when grown on WWTP effluent. We compared floating plants covering only the water column surface with submerged plants filling the entire water column. We expected that floating plants would stimulate denitrification, because they lower O, concentrations in the water column, and that submerged plants can stimulate nitrification because of their O₂ release. We expected the highest nutrient removal in systems with submerged plants because of their high uptake combined with a large surface area for biofilm formation. In addition, we expected that CO2 uptake by photosynthesis would fully compensate for CO, production from respiration of organic carbon present in the wastewater effluent, leading to net CO, uptake. N,O emission was expected during both nitrification and denitrification, where we expected highest emissions from systems covered by floating plants due to higher denitrification rates. Lastly, CH₄ emission was expected to be low in all cases, because of the lack of strictly anoxic habitats.

4.2 METHODS

4.2.1 Experimental setup

We quantified nutrient removal and GHG emissions of two floating plant species (Azolla filiculoides (hereafter: Azolla) and Lemna minor (Lemna)) and two submerged species (Ceratophyllum demersum (Ceratophyllum) and Callitriche platycarpa (Callitriche)). Additionally, a control of effluent without plants was included, resulting in a total of 5 experimental treatments, each consisting of 4 replicates. The experiment was performed at the Radboud University greenhouse facility, in glass aquaria of 24x24x30 cm, distributed in a randomized block design to avoid confounding microclimatic effects in the greenhouse. We maintained a light/dark cycle of 16 h/8 h, by using 400 W high-pressure sodium lamps (Hortilux-Schréder, Monster, The Netherlands), which turned on when the natural daylight intensity fell below 250 W/m².

Wastewater effluent originated from the municipal wastewater treatment plant in Remmerden, the Netherlands, which has a 2100 m³/hour hydraulic capacity and serves 46,000 households. It is a UCT (University of Cape Town) carrousel (Østgaard et al. 1997) which had the following effluent concentrations in 2021, ranging between: 80–500 μ mol/l NH $_4^+$ -N; 20–220 μ mol/l NO $_3^-$ -N; 1–30 μ mol/l PO $_4^3$ --P; 17–56 mg/l chemical oxygen demand (COD) and 1.9–8.9 mg/l biological oxygen demand (BOD $_5$) (Hoogheemraadschap de Stichtse Rijnlanden, WWTP Rhenen).

At the start of the experiment we added 15 litres of domestic wastewater effluent to each aquarium and introduced the assigned plant species to this effluent. Because of their different growth strategies and different morphological traits, floating plants were introduced to a surface area coverage of 25%, whereas submerged plants started at 25% volume in the water column. For each of the treatments, wet weight of this 25% cover was determined, and an extra batch of plants was used to obtain the wet to dry ratio, to estimate initial dry biomass.

In each aquarium, we monitored nutrient concentrations and GHG emissions for fourteen days, as well as physical-chemical properties of the water (temperature, pH, dissolved O₂). We measured three times on the first day, once a day during days 2-5, and every other day in the remaining period. On the last day, all plants were harvested to determine wet and dry biomass and plant nutrient content. We additionally harvested the filamentous green algae that started to grow in some of the treatments.

4.2.2 Water quality measurements

Concentrations of NH,+-N, NO,-N and PO,3--P were measured colorimetrically in rhizon-filtered samples (membrane pore size $0.12/0.18~\mu m$, Rhizon SMS 10 cm, Rhizosphere Research, Wageningen, The Netherlands) on an auto analyser III (Bran and Luebbe GmbH, Norderstedt, Germany) after being stored at -20 °C. Total phosphorus was measured in acidified water (0.1 ml 10% nitric-acid) on an ICP-OES (IRIS Interpid II, Thermo Fisher Scientific, Franklin, MA, USA) after being stored at 4 °C. Total inorganic carbon (TIC) was measured in unfiltered samples (ABB Advance optima Infrared Gas Analyzer (IRGA), Frankfurt, Germany) immediately after sample collection. The pH, temperature (°C) and dissolved O2 (mg/l) concentrations in the water column of each aquarium was measured using a Portable Multi Meter (HQ2200, HACH, Loveland, CO, USA).

4.2.3 Elemental concentrations in plant tissue

The plants that were harvested at the end of the experiment as well as the extra batch of each plant species at the beginning of the experiment were dried at 70 °C for four days, after which they were ground manually. The same was done for the filamentous algae that were collected on the last day. N and C contents were determined in plant material (3 mg) using an elemental CNS analyser (NA 1500, Carlo Erba; Thermo Fisher Scientific, Franklin, USA). P content was determined on the ICP-OES after microwave digestion, adding 4 ml HNO_{2} (65%) and 1 ml $H_{2}O_{2}$ (35%) to 200 mg dried plant material in Teflon vessels, followed by heating in an EthosD microwave (Milestone, Sorisole Lombardy, Italy).

4.2.4 GHG measurements

GHG fluxes (CO₂, CH₄, N₂O) were measured using a Greenhouse Gas Analyser (G2508, Picarro, Santa Clara, CA, USA) connected to a transparent acrylic glass floating chamber (7.1 dm³ headspace). In each aquarium, we measured diffusive fluxes of CO₂, CH₄ and N₂O over a period of four minutes, counted from when concentrations started to change. In between the measurements the chamber was aerated until gas concentrations returned to atmospheric levels.

4.2.5 Data analysis

Total dissolved inorganic N (TDIN) was obtained by summing NH_4^+-N and NO_3^--N . Total dissolved P (TDP) concentrations were obtained from elemental ICP analysis of the filtered water samples (µmol/l).

GHG fluxes (mg/m²/day) were calculated according to Almeida et al. (2016). A global warming potential of 29.8 for CH₄ and 273 for N₂O was used (100-year time frame; IPCC 2021) to convert fluxes to CO₂ equivalents (g CO₂-eq/m³).

For element stocks (C, N and P), the plant content was multiplied by the dry weight of the plants. The total uptake of C, N and P (in μ mol) were then obtained by subtracting total mass of each element at the end of the experiment from the total mass at the start.

Plant growth was calculated by the difference in dry weight between start and end of the experiment. Dry weight of filamentous algae harvested on the last experimental day was added to the plant growth data. Differences in plant growth and C, N and P plant-uptake between treatments were analysed using ANOVA with a Tukey post hoc test (R 4.1.1 (R Core Team 2021), stats::aov; multcompView::TukeyHSD (Graves et al. 2019)).

Efficiency of N and P removal by plant-uptake for the different plant species was calculated from the change in plant N and P content compared to dissolved inorganic N and P uptake from the water column. Efficiency was shown as a percentage, in which 100% indicated a complete removal due to plant-uptake. A negative percentage showed a net release of N or P to the water column.

4.3 RESULTS

4.3.1 Effluent conditions

Dissolved O_2 concentrations and pH were stable (4–6 mg/l and 7.3 respectively) until day 4, when filamentous algae started to appear (Fig. S4.1). After this, pH rose to 8.5 for the floating plants, 8.7 for *Callitriche* and 9.5 for the *Ceratophyllum* and the control treatment. Dissolved O_2 concentrations increased as well and ended at concentrations of 8–9 mg/l for the floating plants, 10 mg/l for *Callitriche*, and 13–15 mg/l for *Ceratophyllum* and the control treatment.

4.3.2 Nutrient removal, greenhouse gas emission and biomass production over time

In less than 8 days, all NH₄+-N was removed from the water column in all treatments (Fig. 4.1a). NO₃-N concentrations increased during the first few days and decreased during the remainder of the experiment (Fig. 4.1b), with differences in timing and removal efficiency between treatments. This resulted in a small initial increase, rapidly followed by a decrease in total dissolved inorganic nitrogen (TDIN) concentrations (Fig. 4.3a). In fact, water treatment with *Lemna* resulted in 100% removal of TDIN, while the other treatments were less efficient, with *Azolla* having little to no N removal.

 $PO_4^{3^{-}}$ -P concentrations were below 0.3 µmol/l after 8 days for *Lemna*, *Azolla* and the control treatment (Fig. 4.1c). *Ceratophyllum* treatments started with higher $PO_4^{3^{-}}$ -P

concentrations, yet after 10 days all PO₄ ³⁻-P was removed. Treatment with Callitriche resulted in PO_4^{3-} -P increase in the first 3 days, followed by PO_4^{3-} -P uptake. However, after 2 weeks still a considerable amount of PO $_4^{3-}$ -P (average 2.3 μ mol/l) was present. Total dissolved P (TDP) concentrations were lowered from 9.0 (±1.3 sd.) to 3.3 (±0.8 sd.) umol/l in treatments with Azolla, Lemna and Ceratophyllum, while Callitriche initially showed an increase and later a decrease in TP concentration, but plateaued around 7.8 $(\pm 4.7 \text{ sd.}) \mu \text{mol/l}$ (similar as the start concentration) after two weeks (Fig. 4.3b).

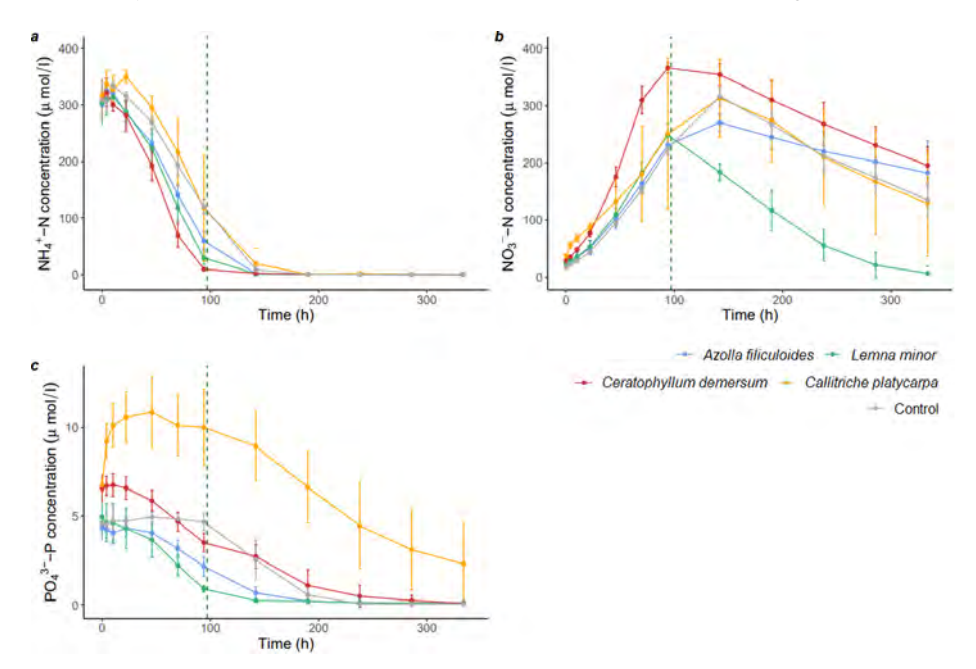


FIGURE 4.1 NH, +-N, (a) NO, -N (b) and PO, 3--P (c) concentration over time for the different treatments (mean values \pm sd.). The vertical dashed green line indicates the date in which algae started to appear in treatment Ceratophyllum, Callitriche and Control. Note the difference in y-axis scale.

GHG flux measurements started on day 3 (after 49 hours). Fluxes of CH, were low in all treatments (max. CH, flux 0.15 mg/m³/day), and from day 4 onwards no CH, fluxes were observed (Fig. 4.2a). At the start of the measurements, only Lemna and Azolla were taking up CO, and had highest CO, uptake during the whole experiment (Fig. 4.2b). Control treatments had similar CO₂ uptake as Ceratophyllum and Callitriche. CO, uptake only took place after day 4 for these treatments, which was at the onset of algal growth. N₂O emissions were low overall, with only a small peak after day 4 for Callitriche and the control treatment (Fig. 4.2c). Lemna and Azolla showed a net GHG uptake, having negative fluxes in CO₂-equivalents, while the other 3 treatments first emitted GHGs, followed by net uptake (Fig. 4.3c).

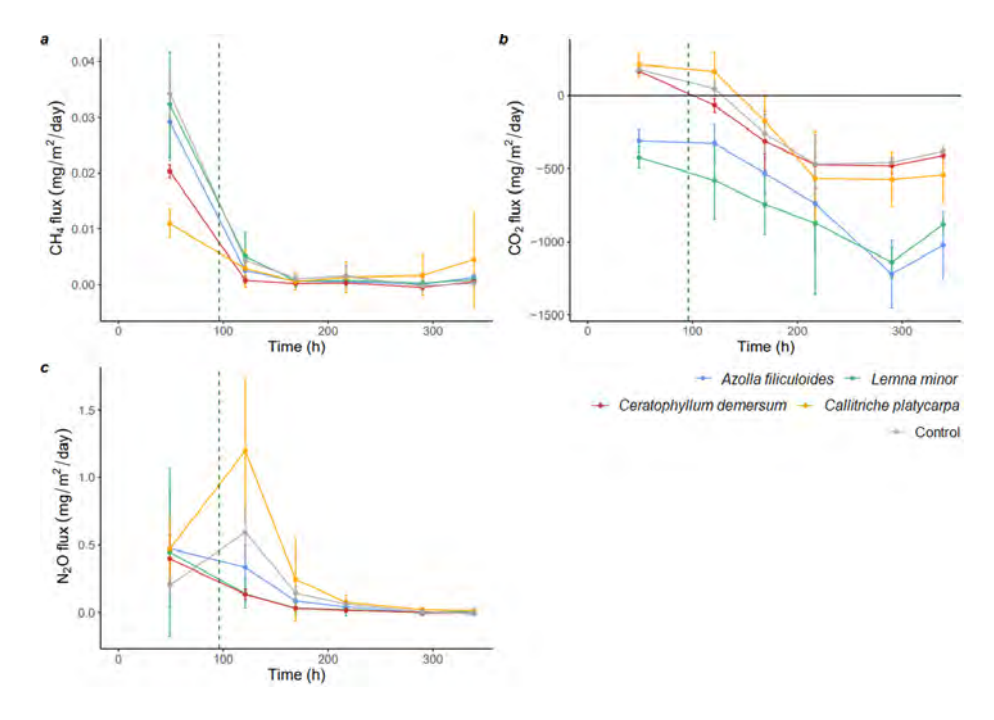


FIGURE 4.2 CH₄, (a) CO₂ (b) and N₂O (c) fluxes over time for the different treatments (mean values \pm sd.). The vertical dashed green line indicates the date in which algae started to appear in treatment *Ceratophyllum*, *Callitriche* and Control. Note the difference in y-axis scale.

The plants differed significantly in how well they grew on wastewater effluent (P<0.001; Fig. 4.3d). Azolla and Lemna had the highest biomass increase, although Lemna did not differ significantly from Ceratophyllum (P=0.06). The Callitriche treatment had little to no growth, with algae accounting for 46 (11–75)% of its total biomass gain. In control treatment aquaria, an increase in algal biomass was observed as well (up to 0.15 g).

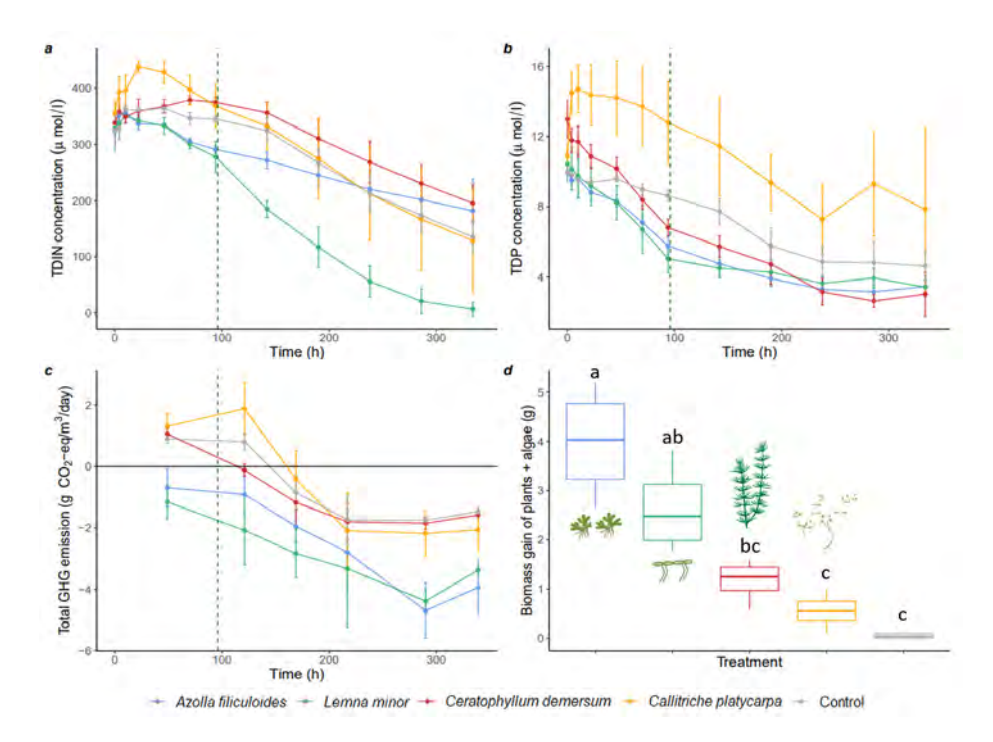


FIGURE 4.3 Total dissolved inorganic N (TDIN) concentration (a), total dissolved P (TDP) concentration (b) and total greenhouse gas (GHG) fluxes (in g CO,-eq/m³) (c) over time for the different treatments (mean values ± sd.), and average growth of the plants (d) (P<0.001 (one-way ANOVA), letters indicate significant differences between the treatments, Tukey HSD P<0.05). The dashed green line indicates the date on which algae started to appear in treatment Ceratophyllum, Callitriche and Control. Note the difference in y-axis scale. In (d), boxplots show the median values and 25th and 75th percentiles, whiskers indicate largest and smallest values.

4.3.3 Nutrient removal efficiency

The plants significantly differed in N and P removal efficiency (P=0.001 and P=0.04, respectively). Lemna was most efficient in removing TDIN, on average removing 97.4 (90.2-99.8)%, even though it was not significantly different from the Callitriche treatment (P=0.08). All treatments resulted in high TDIN removal (ranging from average 40.7% in Ceratophyllum treatment to 64.4% in Callitriche treatments) after two weeks (Fig. 4.4a). Treatment with *Ceratophyllum* resulted in highest TDP removal (77.0 (64.5-82.4)%) but was not significantly higher than Azolla, Lemna and the control treatment (*P*=0.94, *P*=0.95 and *P*=0.56, respectively; Fig. 4.4b).

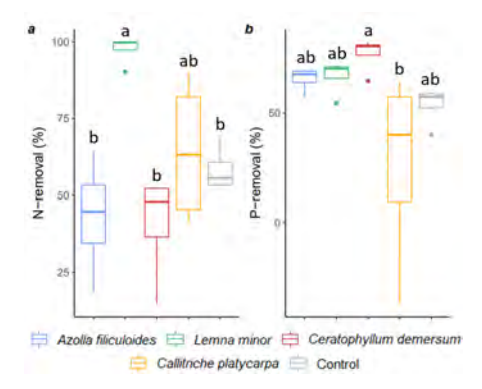


FIGURE 4.4 Nutrient removal efficiency of nitrogen (P=0.002 (one-way ANOVA), letters indicate significant differences between the treatments, Tukey HSD P<0.05) (a) and phosphorus (P=0.04 (one-way ANOVA), letters indicate significant differences between the treatments, Tukey HSD P<0.05) (b) for the different treatments. Note the difference in y-axis scale. Boxplots show the median values and 25th and 75th percentiles, whiskers indicate largest and smallest values.

4.3.4 Elemental plant-uptake

The plant species differed in the way they incorporated amounts of C, N and P in their tissues (*P*<0.01; Fig. 4.5). *Azolla* and *Lemna* showed highest sequestration of all three elements, including N-fixation by *Azolla*. *Azolla* did not differ significantly from *Ceratophyllum* in C-uptake (*P*=0.05). Both submerged plants had significantly lower elemental sequestration than the floating plants (*P*<0.001).

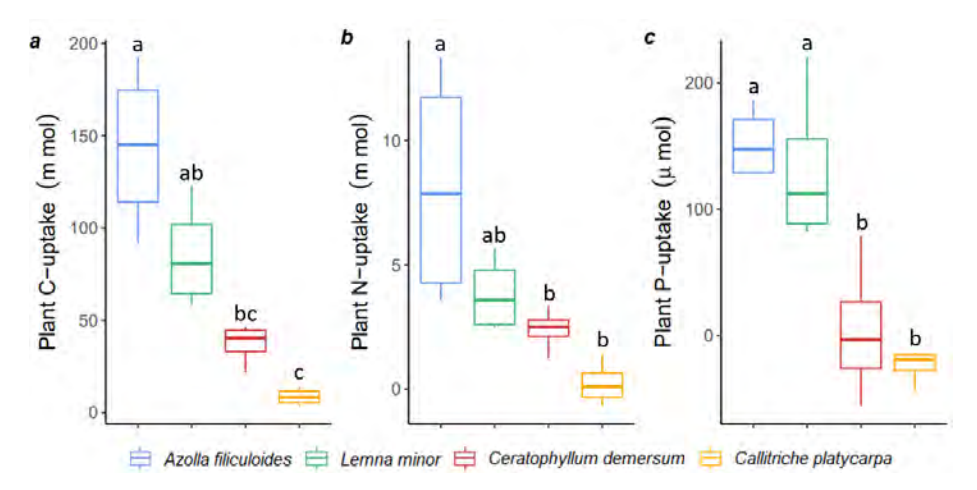


FIGURE 4.5 Total carbon (C) (*a*), total nitrogen (N) (*b*) and total phosphorus (P) (*c*) uptake by the different plant species at the end of the experiment (P<0.01 for all elements (one-way ANOVA), letters indicate significant differences between the treatments, Tukey HSD P<0.05). Note the difference in y-axis scale. Boxplots show the median values and 25th and 75th percentiles, whiskers indicate largest and smallest values.

N- and P-sequestration by the different plant species corresponded with N- and P-removal from the water column for the floating plants, whereas N- and P-removal in the submerged macrophyte treatments can only for a small part be explained by plant-uptake (Table 4.1).

TABLE 4.1 Efficiency of N and P removal by plant-uptake for the different plant species.

	N efficiency (mean % (min – max %))	P efficiency (mean % (min – max %))
Azolla filiculoides	616.3 (140.6 – 1644.8)	155.8 (120.6 – 184.8)
Lemna minor	83.0 (47.1 – 109.8)	142.3 (68.5 – 304.1)
Ceratophyllum demersum	130.3 (88.0 – 200.7)	2.1 (-34.6 – 47.9)
Callitriche platycarpa	7.3 (-14.3 – 37.1)	-23.3 (-78.1 – 15.3)

A negative percentage shows a net release of N or P. A percentage of above 100% can be explained by sampling variation when measuring plant uptake. Note that for Azolla, N efficiency also includes N-fixation, which explains why an uptake percentage of over 100% is reached.

4 DISCUSSION

In this study we tested the nutrient-removal efficiency of floating and submerged macrophytes grown on WWTP effluent, and their potential to capture CO2 and supress CH, and N,O emission. We compared the effects of two floating plants, Azolla filiculoides and Lemna minor, and two submerged macrophytes, Ceratophyllum demersum and Callitriche platycarpa. In this experiment, systems covered by the floating plants Azolla or Lemna, had highest N- and P-removal efficiency - resulting from plant-uptake - and captured most CO, while emitting the least CH, and N,O, thus resulting in net GHG uptake. Submerged plants Ceratophyllum and Callitriche did not grow well on WWTP effluent, and therefore contributed less to both nutrient removal and CO, uptake.

4.4.1 Effects of floating and submerged plants on nutrient removal and greenhouse gas emission

All treatments, including unvegetated controls, caused TDIN concentrations to decrease to on average ≈ 130 μmol/l, which is well below the average concentrations observed in the water bodies to which WWTPs discharge their effluent (≈ 285 μmol/l; Carey & Migliaccio 2009; van Puijenbroek et al. 2010). However, coverage by Lemna caused the largest decrease, resulting in almost complete TDIN removal after two weeks (Fig. 4.2a).

For water treated with Azolla, Lemna and Ceratophyllum, P concentrations were reduced to on average 3.3 (\pm 0.8 sd.) μ mol/l P after two weeks, which is similar to P concentrations occurring in the potential receiving water bodies (Carey & Migliaccio 2009; van Puijenbroek et al. 2010). In both floating plant treatments, plant P-uptake resulted in immediate P-removal from the water column, whereas Ceratophyllum P-uptake could not explain all P-removal from the water column. PO₄ -P concentrations increased in systems with Callitriche, likely due to plant senescence, observed from its lack of growth and visible signs of decay.

While submerged macrophytes were hampered in their growth by algal dominance, and presumably also by the high pH leading to very low CO_2 concentrations in the water layer, floating macrophytes showed high growth rates of 4.9 (\pm 1.2 sd.) and 3.3 (\pm 1.0 sd.) g/m²/day for *Azolla* and *Lemna*, respectively. This is in line with, and for *Azolla* even in the high range of, maximum growth rates found for these species (Reddy & DeBusk, 1985a).

After six days, all treatments resulted in net GHG uptake, with systems covered by Azolla or Lemna showing the highest uptake (Fig 4.2c). In treatments containing Ceratophyllum and Callitriche, CO₂ uptake only took place after four days, similar to the control treatment and starting at the moment filamentous algae became visible. Combined with poor growth of these submerged plant species, we expect at least part of the CO₂ uptake to be due to algal growth rather than macrophyte growth. Little to no CH₄ emission was detected in all treatments, which can be explained by the high O₂ concentrations in the water and lack of sediment. A small peak in N₂O emission occurred at the time when NO₃ -N concentrations were at its highest and NH₄ +-N was depleted. Yet, the highest emission of 1.88 mg N₂O/m²/day (occurring in Callitriche treatments), was still well below emissions observed in constructed wetlands, which can reach 3.12 mg N₃O/m²/day (e.g. Mander et al. 2014).

4.4.2 The importance of nitrification-denitrification in nitrogen removal

After 4 to 5 days, in all plant treatments all $\mathrm{NH_4^{+-}N}$ was removed. It was expected that due to their larger surface area and thus expected higher biofilm production, submerged plants would facilitate a higher $\mathrm{NH_4^{+-}N}$ removal, which was not the case. Because similar $\mathrm{NH_4^{+-}N}$ removal rates were found for the control treatment, in the absence of algae, the $\mathrm{NH_4^{+-}N}$ removal is most likely caused by nitrification performed by microorganisms in the water column and in biofilms on the aquaria walls, rather than by plant uptake. The coincidence with an increase in $\mathrm{NO_3^{--}N}$ in these first days confirms this. This is in line with other hydroponic systems, in which nitrification was also the predominant process of $\mathrm{NH_4^{+-}N}$ removal (Vaillant et al. 2003).

Our calculations show that all NO3-N removal from aquaria treated with Lemna as well as those with Azolla can be explained by plant N-uptake (Fig. 4.5), which is contrasting to other studies where Lemna and Azolla species only take up a fraction of NO :- N (Singh et al. 1992). In our systems, denitrification was not significantly contributing to N-removal from the effluent. Moreover, Azolla coverage resulted in higher plant N-uptake than N-removal from the effluent, which indicates N₂-fixation from the atmosphere by the Azolla-Nostoc symbiosis.

4.4.3 N-fixation causes less efficient N-removal by Azolla

Whereas Lemna had up to 100% NO3-N (and thus TDIN) removal after 2 weeks, Azolla hardly removed any of the produced NO3-N. This is most likely because of its symbiosis with the cyanobacterium Nostoc azollae that fixates nitrogen from the atmosphere (Brouwer et al. 2018). Normally, N-fixation is a costly process which only takes place when N is limited. Yet, it is found that N-fixation by the microbial symbiont occurs even when Azolla is grown on water containing substantial amounts of inorganic N, and N fixation is only inhibited by much higher concentrations of nitrogen than present in our experiment (Ito & Watanabe 1983). Azolla showed highest N plant-uptake (Fig. 4.5) combined with lowest TDIN removal, suggesting that almost all N that Azolla took up was derived from N-fixation from the atmosphere.

4.4.4 Algal growth affected the performance of submerged plants, and facilitated nutrient removal

In treatments containing submerged plants, as well as the unvegetated controls, algae started to appear after four days, which was facilitated by the abundance of light and nutrients in these treatments. Likely, light-limitation suppressed algal growth in the floating plant treatments. As a result, N- and P-uptake by submerged plants was negligible (Fig. 4.5 and Table 4.1). Most likely, in these treatments N-removal took place via algal uptake and coupled nitrification-denitrification by the microbial community, while P removal was mostly caused by algal uptake, especially in the Callitriche treatments.

4.4.5 High nutrient-removal efficiency and GHG reduction by floating macrophytes

Our systems including Azolla and Lemna were more efficient in removal of N and P than other hydroponic systems (Shah et al. 2014) as well as constructed wetlands (Tang et al. 2017; Hernández et al. 2018), and are performing better than, or similar to floating treatment wetlands (Prajapati et al. 2017). In line with these findings, floating macrophytes were more efficient in removing nitrogen and phosphorus than

emergent macrophytes in floating treatment wetlands (Prajapati et al. 2017) and are therefore considered good candidates in treatment of wastewater effluent.

Where constructed wetlands can emit up to 500 mg/m²/day $\rm CH_4$ and 25 mg/m²/day $\rm N_2O$ (Hernández et al. 2018), our systems did not show any significant $\rm CH_4$ emissions (lower than 0.04 mg/m²/day) and $\rm N_2O$ emissions of only 1.5 mg/m²/day at one specific point in time. Where some studies also indicate $\rm CO_2$ emission in constructed wetlands (Badiou et al. 2019), our treatments showed $\rm CO_2$ uptake, resulting in a total net uptake of GHG. Although our measurements are based on treated wastewater effluent, while constructed wetlands often deal with untreated wastewater – inherently having higher potential for GHG emission – our data show the potential to mitigate part of the WWTP emissions in the process of hydroponic effluent polishing. Moreover, nutrient reduction in WWPT effluent most likely lowers GHG production in receiving water bodies, by decreasing eutrophication effects (Beaulieu et al. 2019).

4.4.6 Use of floating plants to contribute to a circular economy

Ideally, plants used in effluent-polishing are used in added-value applications, to contribute to the circular economy. One prerequisite for growing plants on wastewater effluent is that algal growth should be limited, unless algae are the main product to be cultured. Floating plants that prevent light penetration in the water column can suppress algal growth. When using other plant types, algal growth can be suppressed by using UV light or by adding aquatic animals such as snails to counteract formation of floating algae beds; while zooplankton or mussels can be used to minimize phytoplankton density. But, it remains to be tested if such animals can also be used in wastewater effluent polishing systems.

Both floating plants tested in our experiment have economic value. *Azolla* and *Lemna* are rich in proteins and amino acids, potentially containing even more protein than soybeans (Brouwer et al. 2018). However, non-food applications are preferred because plants grown on domestic wastewater may contain contaminants such as heavy metals and traces of pharmaceuticals. *Azolla* can be used to produce potting soil for ornamental plants, substituting peat, thereby contributing to the protection of C-storing peatland ecosystems (Khomami et al. 2019). Both species can be digested to bioethanol or biogas as well. Although this would offset the negative carbon footprint of phytoremediation, saving on fossil fuels is always beneficial.

4.4.7 Conclusions

Based on our results we conclude that the floating plants Azolla and Lemna are promising for use in effluent polishing, due to their ability to lower nutrient

concentrations in the effluent while at the same time sequestering carbon and limiting the emission of other greenhouse gases. Where the growth of submerged macrophytes was strongly affected by competition with algae, both of the floating plants showed the highest biomass production, and were most efficient in removing nitrogen and phosphorus from the water column. Note, however, that nutrients taken up by the plants are only permanently removed after harvesting. When combining Azolla with Lemna, or other high value floating plants, excess P and N can be removed from wastewater effluent, while taking up GHGs and producing plant biomass with commercial value, contributing to a circular economy. Moreover, by lowering the nutrient load derived from discharged WWTP effluent, effluent polishing can also contribute to mitigation of eutrophication and GHG emission from natural waterbodies.

Acknowledgements

We would like to thank Koos Janssen, Harry van Zuijlen and Walter Hendrickx from the greenhouse facility at Radboud University for their help during the experiment. Thanks to Jiry de Waal (Adviesbureau de Waal/Vijvermeester.nl) for plant advice and delivery. We thank Sebastian Krosse and Paul van der Ven from the Radboud General Instrumentation for performing the elemental analyses, and Germa Verheggen en Roy Peters for help during other lab analyses.

SUPPORTING INFORMATION

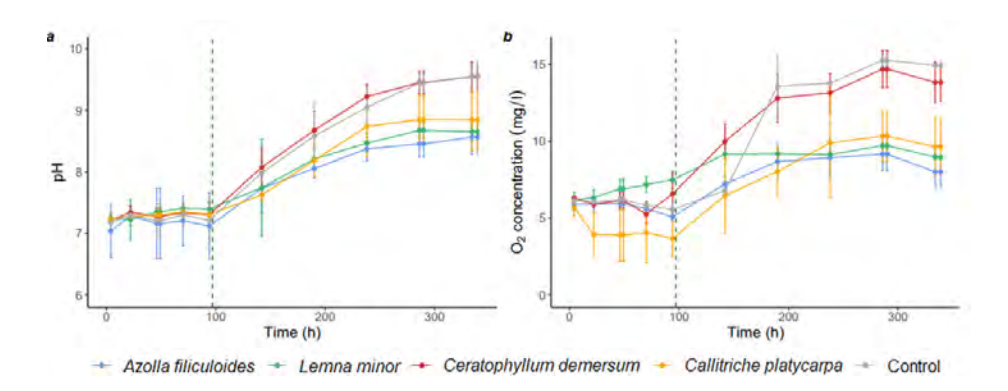


FIGURE S4.1 pH (*a*) and dissolved O_2 concentration (mg/l) (*b*) over time for the different treatments (mean values +/- SD). The vertical dashed green line indicates the date in which algae started to appear in treatment *Ceratophyllum*, *Callitriche* and Control.



Chapter 5 Combining different floating plants for optimal wastewater effluent polishing and carbon-capture

Lisanne Hendriks, Alfons J. P. Smolders, Inez van Erp, Leon P. M. Lamers, Annelies J. Veraart

In revision

ABSTRACT

Treated wastewater effluent is still a major source of nitrogen (N) and phosphorus (P) pollution to inland waters, causing greenhouse gas (GHG) emissions in discharge waters. Here, we propose effluent polishing using floating plants. We tested the efficiency of four different plant species (Azolla filiculoides, Azolla pinnata, Lemna minuta and Trapa natans) in N and P removal and how this affects GHG emissions when grown on municipal wastewater effluent over a period of four weeks. After two weeks, effluent was refreshed. All species completely removed ammonium via nitrification. Lemna minuta and Trapa natans efficiently removed nitrate. Both Azolla species showed highest P uptake. All systems hardly emitted methane or nitrous oxide, and captured CO2, with both Azolla species having the highest CO2 uptake. Next, we tested if combining the most efficient P-removing plant and the most efficient N-removing plant would increase effluent polishing efficiency. We sequentially cultivated Azolla filiculoides and Lemna minor using the same effluent, and compared this to single species cultivation. Although the single cultivation of Lemna minor removed all nutrients most efficiently, we argue that - because of the high carbon sequestration of Azolla filiculoides - combining both species works best as a low-emission effluent polishing technique.

5.1 INTRODUCTION

Conventional municipal wastewater treatment is facing multiple challenges. Nutrient concentrations in the treated wastewater, or effluent, need to be further reduced. In addition, wastewater treatment plants (WWTPs) need to become energy neutral and have to contribute to a circular economy, for example by reuse of the different substances present in wastewater (European Commission, 2022). Conventional wastewater treatment comes to its limits in achieving these goals, and high-tech post treatment technologies may be too costly especially in developing countries. Therefore, natural and low-cost alternatives to technical solutions could make a valuable contribution.

Municipal wastewater effluent is a potential source of nutrients for plant growth, and could be used for the production of high quality products. At the same time, plants can be used as wastewater polisher to obtain a higher purity of the effluent (Hendriks et al., 2023), since nitrogen (N) and phosphorus (P) are essential plant nutrients (Li et al., 2013). Therefore, plant-captured nutrients form a potential avenue of resource recycling, while minimizing the considerable CO₂ footprint of wastewater treatment by absorbing CO₂, and potentially mitigating CH₄ and N₂O emission (Wang et al., 2015; Attermeyer et al., 2016; Kosten et al., 2016; Hendriks et al., 2023).

Whereas helophytes, usually used in constructed wetlands, are mostly indirectly related to nutrient removal from the water column, because they take up nutrients from the sediment rather than the water itself (Gacia et al., 2019), hydrophytes, especially floating species, directly take up nutrients from the water column. Also, using hydrophytes in wastewater effluent polishing has the advantage that no soil or sediment substrate is needed, which minimizes maintenance, facilitates harvesting and minimizes carbon emission.

Different floating plants have different characteristics in how they remove nutrients and how they alter greenhouse gas (GHG) emissions. Plants forming a dense mat on top of the water, such as Azolla and Lemna species, may provide a barrier between water layer and atmosphere (Kosten et al., 2016) which can affect GHG emissions in different ways. On the one hand, reduced re-aeration and shading of the watercolumn by these floating plants lowers O_2 concentrations in the water column, while respiration continues to consume O_2 (Kosten et al., 2016). Lowered O_2 availability can stimulate microbial denitrification and methanogenesis while inhibiting aerobic methane oxidation, which could lead to increased N_2O and CH_4 emission (Veraart et al., 2011). On the other hand, the barrier potentially traps the formed CH_4 , and the

 O_2 released from roots by radial oxygen loss (ROL) can then stimulate CH_4 oxidation (Kosten et al., 2016). Moreover, hydrophytes with bigger root systems, like Trapa species, provide a larger surface for biofilm production and therefore may increase coupled nitrification-denitrification rates (Han et al., 2018). A bigger root system additionally means a higher net ROL (Moorhead and Reddy, 1988), which can enhance nitrification rates as well as N_2O emissions, but can also increase CH_4 oxidation.

While N can be removed from aquatic systems through various microbial transformations as well as by plant uptake, plant uptake is the only natural P-removing pathway, and is therefore dependent on plant growth rate (Körner et al., 2003; Shilton et al., 2012). In addition, all plants take up CO₂ as part of photosynthesis, with highest uptake during plant growth. Lastly, plants differ in their nutrient uptake efficiency. For example, *Azolla* lives in symbiosis with a nitrogenfixing cyanobacterium, facilitating growth using atmospheric N (Baker et al., 2003). Because of this symbiosis, *Azolla* has been used historically as a natural N-fertilizer, and as a tool in aquatic P-removal (Wagner, 1997).

Studies on these aquatic plants have mainly focused on water quality improvement and nutrient and metal-removal performance (e.g. Reddy & DeBusk, 1985b; Sooknah and Wilkie, 2004). However, how hydrophytes used in effluent polishing affect greenhouse gas (GHG) emissions remains largely unclear. A recent study, however, has shown that floating macrophytes perform better than submerged macrophytes in both removing nutrients from wastewater and mitigating GHG emission during effluent polishing (Hendriks et al., 2023). Moreover, until now focus has been mostly on nutrient removal using single plant species (but see e.g. Tripathi and Upadhyay et al., 2003). Since the efficiency in which plants remove specific nutrients depends on plant-specific traits, a combination of different species might enhance nutrient removal.

Aquatic plants may be suitable to address the challenges water authorities have to meet in the near future. They are able to directly and indirectly remove nutrients from wastewater and can alter GHG emission. Additionally, their biomass could be used in a circular economy. Here, we compare nutrient (N, P) removal and GHG fluxes between floating macrophytes with different plant-specific traits to assess which plants are suitable to address the different goals of conventional and circular wastewater treatment plants. Next, we assess whether a combination of two plant species is more efficient in nutrient removal compared to a single cultivation of those species, and we determine the optimal growth sequence when combining these species in different effluent-polishing compartments.

5.2 MATERIALS AND METHODS

Two experiments were carried out. First we tested the effluent polishing ability of four different floating plants during a four-week experiment, where we refreshed effluent after two weeks. Next, to achieve optimal nutrient removal, we tested if the use of two plant species would be more effective than a single cultivation of plant species, and if this depended on the growth sequence when plants were applied after each other on the same batch of wastewater. To this end, we used the plant species that removed most nitrogen from the water column and the one that removed the most phosphorus, and grew these one after the other on the same batch of effluent, to simulate a compartmented effluent polishing system.

5.2.1 Experimental setup

Both experiments were performed at the Radboud University greenhouse facility. The greenhouse is equipped with 400 W high-pressure sodium lamps (Hortilux-Schréder, Monster, The Netherlands), and maintains a light/dark cycle of 16 h/8 h. During the experiments, lights turned on when the natural light intensity fell below 250 W m⁻². We used tanks (polypropylene – food-grade) of 40 x 60 x 30 cm for our treatments. The effluent used for both experiments originated from WWTP Remmerden, The Netherlands, which is a UCT carrousel serving 46,000 households (see Hendriks et al., 2023), with effluent concentrations of NH₄⁺, NO₃⁻ and PO₄³⁻ ranging from 182.9-385.3, 7.74-25.64 and 2.32-5.90 µmol L⁻¹ at the time of the experiments.

5.2.1.1 Effluent polishing efficiency of four floating plant species

In the first experiment we quantified biomass production, nutrient removal and greenhouse gas emissions of the following plant species grown on municipal wastewater: two species of water fern (Azolla filiculoides (A. filiculoides) and Azolla pinnata (A. pinnata)), duckweed (Lemna minuta (L. minuta)) and water caltrop (Trapa natans (T. natans)) (Fig. 5.1a). These species were chosen because of their ability to thrive on water containing high nutrient concentrations and because of their potential market value.

To limit algal growth, we continuously circulated the effluent (-2 L h⁻¹) through an ultraviolet-C (UV-C) sanitation system (UV7, 7 Watt, Kos, Van Cranenbroek, The Netherlands). To make sure the microbial community was able to establish on the plants, we only turned on the UV-C lights after four days. To test nutrient removal in the absence of plants, we set up two different controls, one in which effluent was applied without further (plant) treatment (Control), allowing for the development of algae, and one where no plants were added and algal development was inhibited by

applying UV-C lights (UV-C Control). All treatments were set-up in quadruplicate, resulting in 24 tanks, that were placed randomly, to avoid potential confounding factors of microclimatic effects in the greenhouse.

At the start of the experiment, each tank was filled with municipal wastewater effluent (60L per tank), and inoculated with its assigned plant species. Because of the similar growth strategies, yet different morphological traits of floating plants, we standardized starting conditions for each plant by surface area coverage rather than wet or dry biomass, inoculating each tank with 10% coverage of its assigned plant species. For each of the treatments, wet weight of this 10% cover was determined, and an extra batch of plants was used to obtain the wet to dry ratio of this inoculum, to estimate initial dry biomass.

After two weeks, the effluent was refreshed and the plants were placed back into the new batch of effluent. For A. filiculoides, A. pinnata and L. minuta, 50% surface area was placed back, since these plant species covered more than 100% of the surface area — by growing on top of each other - in the first two weeks. For T. natans, all plants were placed back. After another two weeks, the plants were removed from the effluent.

5.2.1.2 Efficiency of combinations of plant species

In the second experiment we assessed whether a combination of two species is more efficient in nutrient removal than a single cultivation of those species and whether the sequence in which the species are placed matters. We chose the best P-removing plant and the best N-removing plant from experiment 1 (Plant 1 (P1) and Plant 2 (P2), respectively) and performed an experiment with five different treatment groups: a single cultivation of the best P-removing plant (treatment P1-P1), a single cultivation of the best N-removing plant (P2-P2), a combination of two cultivations over time in which Plant 1 was replaced by Plant 2 after two days (P1-P2), a combination of two cultivations over time in with Plant 2 was replaced by Plant 1 (P2-P1). A mixed culture of both Plant 1 and Plant 2 was represented by treatment group MIX (Fig. 5.1b). Each treatment consisted of four replicates, and the experiment was repeated three times to take into account changes in effluent composition.

At 'to', 25 litres of effluent were added to each tank after which 50% surface cover of plants, according to their treatment group, were added. After two days, at 't2', all plants were removed from the water, and 50% surface coverage of the second assigned plant species was added to the same effluent, to simulate a flow-through system. After another two days, at 't4', the second batch of plants was removed again (Fig. 1b).

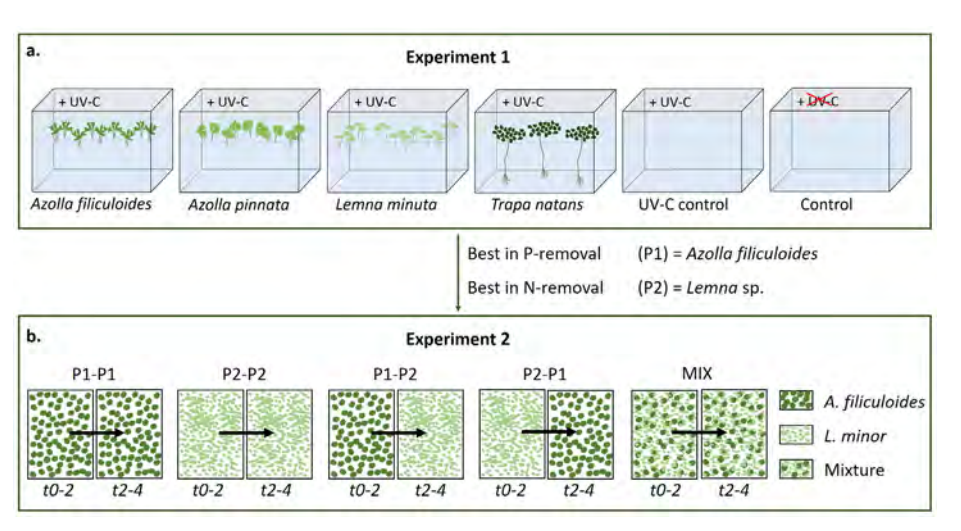


FIGURE 5.1 Schematic overview of experimental set-up for both experiments. a) Experiment 1: efficiency of four different floating plant species in effluent polishing; b) Experiment 2: efficiency of combinations of plant species, P1 = Azolla filiculoides, P2 = Lemna minor.

5.2.2 Measurements

In the first experiment, we measured nutrient concentrations, plant growth and greenhouse gas emission in each tank, for one month. We measured nutrient uptake, physical-chemical properties of the water (temperature, pH, dissolved O, (DO); Fig. S5.1), plant growth and GHG emission daily during the first 7 days, and every other day in the second week. After two weeks, effluent was refreshed and we performed the same measurements for another two weeks. At the end of the experiment, all plants were weighed again.

In the second experiment, each day we measured nutrient concentrations, plant growth and the above-mentioned physical-chemical properties of the water.

5.2.2.1 Water quality measurements

In both experiments, filtered water samples were taken to monitor nutrient concentrations and physico-chemical conditions. Concentrations of NH₄+, NO₃and PO33 were measured colorimetrically in rhizon-filtered samples (membrane pore size 0.12/0.18 µm; Rhizon SMS 10 cm, Rhizosphere Research, Wageningen, The Netherlands) on an Auto Analyser III (Bran and Luebbe GmbH, Norderstedt, Germany) after storage at -20 °C. Total dissolved P (TDP) concentration was measured in acidified water (0.1 ml 10% nitric-acid added to 10 ml) on an ICP-OES (iCap 6300, Thermo Fisher Scientific, Bremen, Germany) after being stored at 4 °C. The temperature, pH and DO concentrations in the water column of each aquarium were measured using a Portable Multi Meter (HQ2200, HACH, Loveland, CO, USA).

5.2.2.2 Biomass measurements

In experiment 1, harvested plants were dried at 70 °C until completely dry. This was done after two weeks for A. filiculoides, A. pinnata and L. minuta, and after four weeks for all plant species, as well as the extra plant batches for all species at the start of the experiment. After drying they were weighed and ground. N and C content within the plants was determined from 3 mg ground material, using a CNS elemental analyser (Vario Micro Cube, Elementar, Langenselbold, Germany). To determine P content in the plants, 200 mg of ground material was digested in Teflon vessels by adding 5 ml HNO₃ (65%) and 2 ml H₂O₂ (35%), and heated in an Ethos One microwave (Milestone, Italy) for 20 minutes at 120 °C. The digested samples were subsequently analysed on the previous-mentioned ICP-OES.

5.2.2.3 Greenhouse gas measurements

Only in the first experiment, Greenhouse gas fluxes (${\rm CO_2}$, ${\rm CH_4}$, ${\rm N_2O}$) were measured starting from day 2, using a Greenhouse Gas Analyser (G2508, Picarro, Santa Clara, CA, USA) connected to a transparent acrylic glass floating chamber (7.1 dm³ headspace). In each tank, we measured diffusive fluxes of ${\rm CO_2}$, ${\rm CH_4}$ and ${\rm N_2O}$, until a linear change was observed for a period of four minutes. In between the measurements, the chamber was aerated to set back the gas concentrations to atmospheric levels.

GHG fluxes (mg m⁻² d⁻¹) were calculated according to Hendriks et al. (2023):

$$F = \frac{V_{ch}}{A_{ch}} * slope * \frac{P * M * F1}{R * T}$$

Where F is gas flux (mg m⁻² d⁻¹), $V_{\rm ch}$ is chamber volume (m³), $A_{\rm ch}$ is chamber surface area (m²), slope is the slope of the measured CO_2 , CH_4 or N_2O concentration over time (ppm s⁻¹); P is the atmospheric pressure (kPa); M is the molecular mass of CO_2 , CH_4 or N_2O (g mol⁻¹); F1 is the conversion factor of seconds to days (86400); R is the gas constant (8.3144 J K^{-1} mol⁻¹); and T is temperature (K). When indicating fluxes, we follow the atmospheric sign convention; positive gas fluxes denote emission whereas negative fluxes denote uptake from the atmosphere. All fluxes of CH_4 , CO_2 and N_2O were checked to confirm that they exceeded the minimum detectable flux (i.e. 0.05, 8.62 and 0.36 mg m⁻² d⁻¹ for CH_4 , CO_2 and N_2O , respectively) and otherwise were noted as 'O' (Christiansen et al., 2015; Nickerson, 2016). A global warming potential of 27 for CH_4 and 273 for N_2O was used (100-year time frame; IPCC, 2021) in order to get CO_2 equivalents (CO_2 -eq).

5.2.3 Data analysis

Cumulative GHG emissions (experiment 1) were obtained by calculating the area under the curve. Total plant-C, -N and -P uptake (experiment 1) was calculated from the rise in C, N and P concentration within the plant tissue, multiplied by their biomass gain, in the first and second two weeks separately.

All statistical analyses were performed in R (version 4.2.0). Statistical significance was determined at p < 0.05. We used analysis of variance to test for differences between plant species in nutrient removal rates as well as nutrient concentrations at the end of the experiment, after confirming normality and homogeneity of variance. Differences between species were then tested using a Tukey post-hoc test.

5.3 RESULTS

5.3.1 Nutrient removal of the four floating plants

The plant species differed in nitrogen removal from the water column (Fig. 5.2). In all treatments, NH, was removed in the first days of both the first and second two weeks, at an average rate of 96.4 \pm 4.8 (sd) and 120.2 \pm 25.4 μ M d⁻¹, respectively. Removal rates differed between plant species in both the first and second two weeks (batch 1 $F_{5,18}$ = 3.15, p = 0.032; batch 2 $F_{5,18}$ = 11.35, p < 0.001). However, a Tukey post-hoc test did not show any differences between treatments for the first two weeks. In the second two weeks, on a fresh batch of effluent, the UV-C control had a significantly lower removal rate than the other treatments.

As NH₄ concentrations declined, NO₃ concentrations started to rise, first at an average rate of 98.3 \pm 2.9 μ M d⁻¹ and after two weeks at an average rate of 77.5 \pm 24.1 μ M d⁻¹. The NO3 increase differed between plant species in both the first and second two weeks (batch 1 $F_{5,18}$ = 7.77, p < 0.001; batch 2 $F_{5,18}$ = 65.3, p < 0.001), with the control treatments having the highest rates, and the UV-C Control having the lowest. The plants differed significantly in NO₃ removal rates starting from day 3 and 19 in respectively the first and second two weeks (batch 1 $F_{5,18} = 8.73$, p < 0.001; batch 2 $F_{5,18} = 16.39$, p < 0.001). Additionally, NO, concentrations at the end of each batch (day 13 and 27) differed significantly (batch 1 $F_{5.18}$ = 8.68, p < 0.001; batch 2 $F_{5.18}$ = 20.32, p < 0.001), where Azollacontaining treatments had the highest final concentrations.

The plant species differed in the way they affected effluent phosphorus concentrations (Fig. 5.2c). PO $_{_{A}}^{_{3^{-}}}$ concentrations were low at the start (0.91 \pm 0.92 μ mol L $^{\text{--}1}$) and after refreshing the effluent (2.60 \pm 0.69 μ mol L⁻¹). In the first two weeks, PO $_{3}^{3}$ -concentrations increased for all treatments (max 0.24 μ M d⁻¹) except for the *A. filiculoides*, *A. pinnata* and Control treatments. PO₄³⁻ concentrations after the first two weeks differed significantly between plant species ($F_{5,18} = 5.13$, p = 0.004), where *A. filiculoides*, *A. pinnata* and Control treatments had the lowest final PO₄³⁻ concentrations. After 27 days, no significant difference was found in PO₄³⁻ concentrations between treatments (p > 0.05). However, *A. filiculoides*, *A. pinnata* and *L. minuta* removed all PO₄³⁻ already in the first two days.

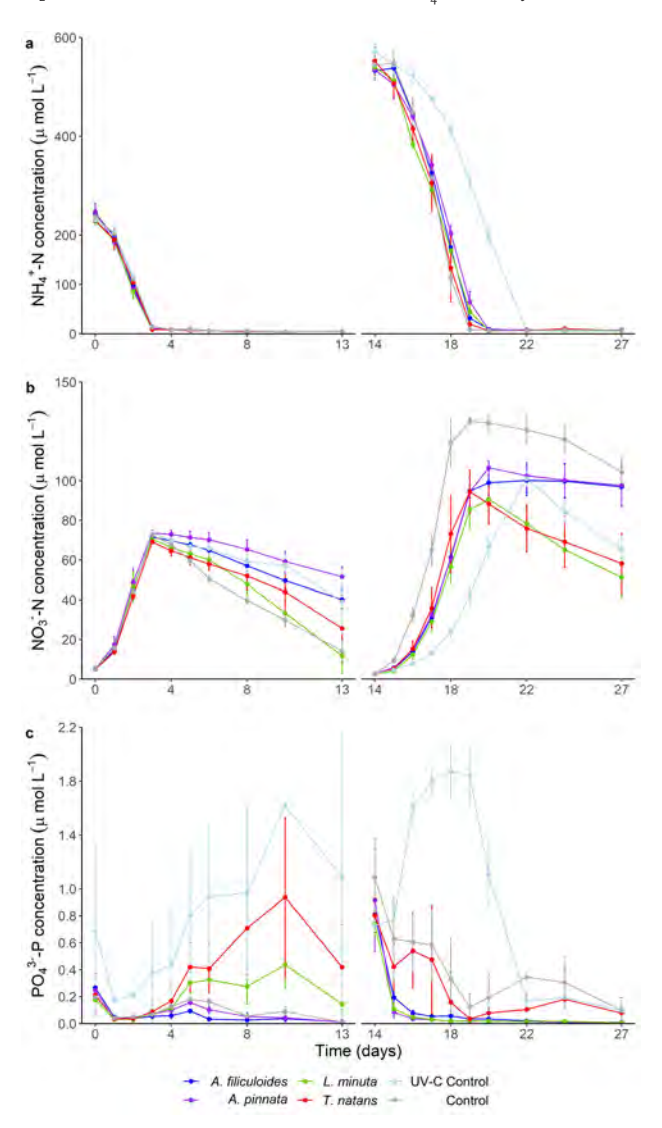


FIGURE 5.2 Concentrations of NH_4^+ (a), NO_3^- (b) and $PO_4^{3^-}$ (c) in wastewater effluent treated by different plant species in a 28-day batch experiment. After 14 days, effluent was refreshed. The UV-C control is a control treatment without plants, but with UV-C light to limit algal growth. Error bars denote standard deviation.

5.3.2 Plant-C, -N, and -P uptake of the four floating plants

Carbon capture and nutrient incorporation from the effluent differed between species (Fig. 5.3). The highest C and N uptake was observed for A. filiculoides and A. pinnata treatments (C $F_{3,21} = 27.55$, p < 0.001; N $F_{3,21} = 31.69$, p < 0.001), but did not differ between the first two weeks and the second two weeks (p > 0.05).

Total plant-P uptake differed between the first and second two weeks ($F_{1,21} = 10.73$, p = 0.004) with the first two weeks having a higher P uptake than the second two weeks. Additionally, plant-P uptake differed between plant species ($F_{3,21} = 17.39$, p < 0.001), with A. filiculoides having the highest uptake in the first two weeks, and T. natans having the lowest P uptake and in two cases even a net P release.

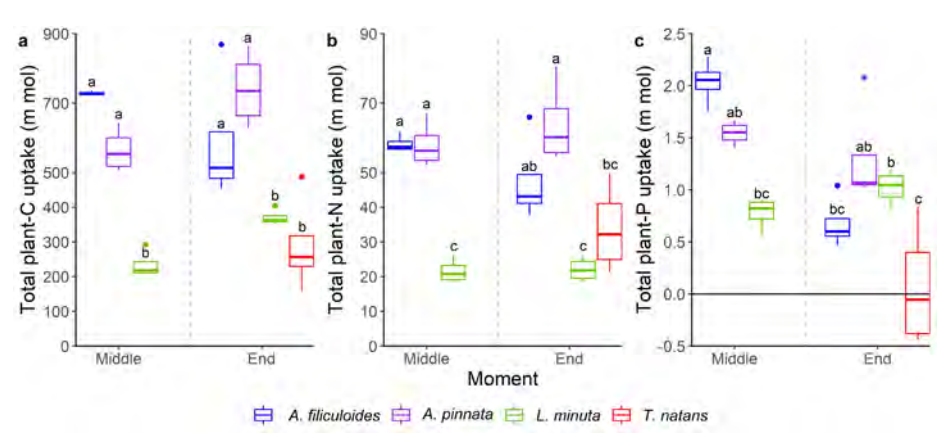


FIGURE 5.3 Total plant-C (a), -N (b), and -P (c) uptake by the different plant species. Different letters indicate significant differences between groups (Tukey HSD post hoc test). Boxes show interquartile range, bold lines represent the median, whiskers indicate the lowest and highest values within a 1.5 x interquartile range from the box, dots represent outliers.

5.3.3 Greenhouse gas fluxes of the four floating plants

The plants differed in the way they facilitated CH₄ and N₂O emission and took up CO₂ (Fig. 5.4). Although CH₄ fluxes were very low and only showed a peak at the very beginning after effluent addition, cumulative CH₄ emissions differed between treatments for both the first two and second two weeks (batch 1 $F_{5.18}$ = 6.89, p < 0.001; batch 2 $F_{5.18}$ = 9.32, p < 0.001). The lowest CH₄ emissions were found in both control treatments.

Plant presence resulted in a significantly (4 - 6 times) higher CO, uptake than the unplanted controls (batch 1 $F_{5,18}$ = 48.95, p < 0.001; batch 2 $F_{5,18}$ = 45.70, p < 0.001). Unplanted controls both also showed a slight CO₂ uptake over time, likely due to biofilm development and algal growth. The highest CO_2 uptake (up to 34.5 g m⁻² d⁻¹) was found in A. filiculoides and A. pinnata treatments during the whole experimental period.

 N_2O emissions were generally low, however when taking their global warming potential (GWP-100) into consideration, emissions were considerable for all treatments, with a peak at day 18-20. Emissions did not differ between treatments in the first two weeks (p > 0.05), but did in the second two weeks ($F_{5,18} = 4.73$, p = 0.006), where A. filiculoides and A. pinnata show higher N_2O emissions than L. minuta treatments.

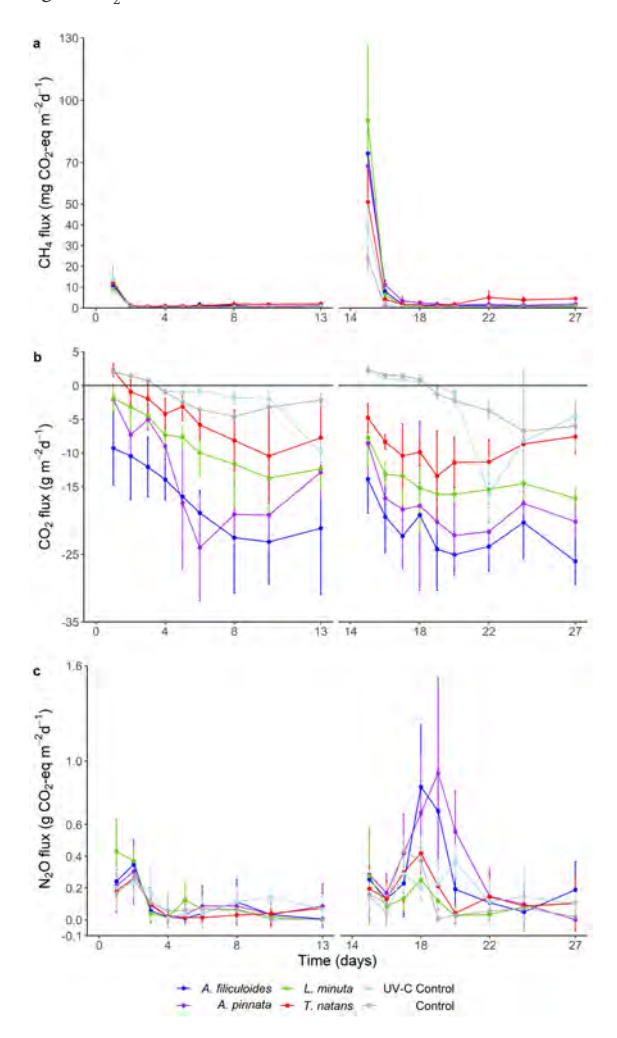


FIGURE 5.4 Average CH_4 (a), CO_2 (b) and N_2O (c) fluxes for the different floating plants during the 28-day experimental period. CH_4 and N_2O fluxes are noted in CO_2 -equivalents based on GWP-100 (27 and 273 times CO_2 , respectively). Note that CO_2 and N_2O flux is reported in g and CH_4 in mg, and CO_2 flux shows negative values, corresponding to CO_2 -uptake.

All GHG fluxes combined, we found that all treatments show a net uptake of total GHGs, with A. filiculoides and A. pinnata having the highest uptake, and L. minuta showing a significantly higher uptake than Control and UV-C Control treatments $(F_{5.18} = 48.88, p < 0.001; Fig. S5.2).$

5.3.4 The effect of plant-order in effluent polishing efficiency

To test the effect of plant combinations, we added the plant species with the highest N-removal rate from the water (Fig. 5.2), Lemna, and the best P-removing plant species, Azolla, to a next experiment. Restricted to the availability of the plant species at the time of the experiment, we used Lemna minor instead of Lemna minuta as the N-removing plant (P1) - hereafter referred to as 'L' -, and Azolla filiculoides as the P-removing plant (P2) - hereafter 'A'.

During the four-day experiments with different plant species combinations, NH, + concentrations in the water column decreased from ~180 µmol L-1 to ~5 µmol L-1 (Fig. 5.5a). After the first 2 days, NH + concentrations were higher in Azolla treatments (AA and AL) compared to the other treatments ($F_{4.55}$ = 35.4, p < 0.001), yet final concentrations did not differ between all treatments.

Water column NO₂ concentrations started at ~3 µmol L-1 and increased in the first days, after which they decreased to ~3 μ mol L-1 again (Fig. 5.5b). After two days, concentrations were highest in *Azolla* treatments ($F_{a \in S} = 43.3, p < 0.001$), with the MIX treatment in between Azolla and Lemna. After four days, the treatments still differed $(F_{acc} = 14.9, p < 0.001)$, with the lowest NO₂ removal in treatment AA.

PO $_4^{3\text{-}}$ concentrations in the water column started at ~11 μ mol L $^{\text{-}1}$ (Fig. 5.5c). After two days water column concentrations were significantly higher in Azolla treatments (AA and AL) compared to the other three treatments ($F_{a.s.}$ = 32.0, p < 0.001). After four days, PO $_{_4}^{_{3^{\text{-}}}}$ concentrations were decreased to ~0 $\mu mol~L^{\text{--}1}$ in all treatments.

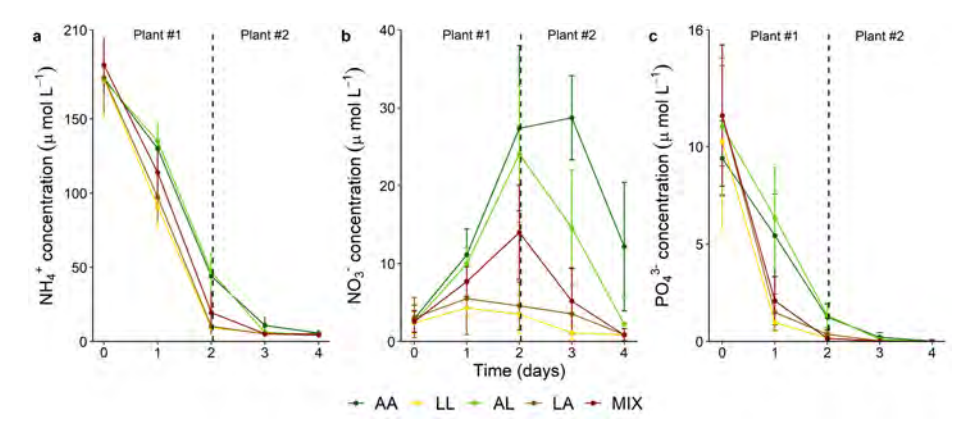


FIGURE 5.5 Concentrations of NH₄⁺ (**a**), NO₃⁻ (**b**) and PO₄³⁻ (**c**) in the water column of the different treatments during the four-day experiments. Plant #1 is the first plant that was added to the effluent from 'to-t2', Plant #2 is the second plant ('t2-4'). The dashed line indicates when the first plant species were harvested and the second species were added to the system. Experiments were replicated three times, shown here is the average between the three experiments. Error bars show standard deviations.

5.4 DISCUSSION

Here, we explored the suitability of four species of floating plants, for different aspects of effluent treatment: nutrient removal, total nutrient plant uptake and reduction of greenhouse gas emission. We show that nutrient concentrations in effluent can be reduced by using floating macrophytes as a natural and low-emission effluent polishing technique. The plant species differed in the way they contribute to effluent treatment and some plants appeared to be more promising than others. Therefore, the most promising inorganic N-removing and P-removing plant species were combined to optimize removal efficiency.

5.4.1 Efficient, low-emission, nutrient removal by floating plants

Already after three days of plant growth, as well as in the control treatment, NH₄⁺ in the effluent was depleted. Nitrification resulted in rapid NH₄⁺ removal, as seen from the corresponding initial rise in NO₃⁻ concentrations. The overall N-budget and NH₄⁺ and NO₃⁻ dynamics show that N-loss was likely a combination of coupled nitrification-denitrification and plant-uptake (Veraart et al., 2011; Körner and Vermaat, 1998), with some of these losses compensated for by N-fixation in the *Azolla* treatments (Baker et al., 2003). Since O₂ was not limited (Fig. S5.1), nitrification occurred in all treatments, including both control treatments. NO₃⁻ removal likely resulted from plant-uptake, or from algal uptake in the unplanted controls. Algal biofilms observed on plant surfaces and attached to tank walls may have contributed to NO₃⁻ removal. All treatments

reduced inorganic N to such extent that final inorganic N concentrations were well below the European norm for concentrations of receiving water bodies with high ecological potential (<271 µmol L⁻¹; Evers et al., 2018).

In contrast to the rapid onset of NH, removal, in the first few experimental weeks, PO₄³⁻ concentrations in the treated effluent increased in all treatments except those containing Azolla. This increase may arise from the microbial liberation of inorganic P from particulate P present in the effluent, and hence final P concentrations will reflect the overall balance between P-release and plant and algal P-uptake. Overall, both Azolla species (A. filiculoides and A. pinnata) performed best in terms of P-uptake, with Lemna minuta also showing near complete P-removal in the second experiment. Azolla is known to effectively remove P from aquatic ecosystems, as its symbiosis with diazotrophs prevents N-limitation (Temmink et al., 2018). Due to its rapid growth rate and high nutrient content, Lemna has also been found to efficiently remove P (Körner and Vermaat, 1998). However, its capacity for P-uptake may be more sensitive to inhibition by wastewater components, as observed in the first two weeks of the present experiment and also noted by Sudiarto et al. (2019), who observed growth inhibition after 13 days.

 $\mathrm{CH_{_{4}}}$ and $\mathrm{N_{_{2}}O}$ emission were low in all treatments. The low $\mathrm{CH_{_{4}}}$ emission can be explained by the lack of sediment and high O concentrations in the water, limiting CH, production. If CH, would have been produced at all, it would most likely be oxidized in the rhizosphere of the floating plant mats (Kosten et al., 2016). The peak in N₂O emission coincides with a dip in NH₄ concentration and a peak in NO₂ concentration, pointing at coupled nitrification-denitrification as primary N₂O source (Sabba et al., 2017). All treatments led to CO, sequestration, but A. filiculoides and A. pinnata showed highest uptake, which can also be seen in the plant-C uptake by these plant species (Fig. 3a).

5.4.2 Combinations of plant species for most efficient effluent polishing

In experiment 2, Lemna and Azolla both completely removed P within two days. Due to its N-fixing symbiosis, we expected Azolla to outperform Lemna in P-removal efficiency. But, due to the short duration of experiment 2 (four days), nitrogen had not yet been depleted resulting in similar performance of both plant species in terms of P-uptake. By contrast, in experiment 1 Azolla indeed removed P after N had been depleted. In longer term experiments, we therefore expect the combination of Lemna and Azolla to be most beneficial. Moreover, A. filiculoides has shown to have the highest CO, uptake of all tested species, and may therefore be an interesting species to add to the treatment process. A set-up in which A. filiculoides is placed after L. minor in a

treatment sequence will therefore likely lead to the most efficient effluent polishing and greenhouse gas reduction, without N-limitation for *L. minor*.

5.4.3 Applicability of effluent polishing by floating plants

In experiment 2, *A. filiculoides* and *L. minor* were found to be very effective in effluent polishing – having a removal efficiency of >99% for PO₄³⁻ and >95% for NH₄⁺ within four days. The tested set-ups with floating plant species were able to remove NO₃⁻ from the effluent by up to 98%. Thus, the tested floating plants showed a higher removal efficiency of PO₄³⁻, NH₄⁺ and NO₃⁻ compared to microalgal effluent polishing and biofilm reactors (Xu et al., 2015; Hu et al., 2017; Sheng et al., 2017; Kawan et al., 2022). To maximize nutrient uptake, upscaled polishing systems using small floating plants are ideally shallow, and potentially stacked to minimize space requirements.

Yet, nutrient removal and greenhouse gas reduction is not the only challenge to tackle. To permanently remove nutrients from the water system, the produced biomass has to be harvested. To avoid harvested resources going to waste, or leading to new GHG emissions, ideally this biomass is used in other applications. Based on European restrictions, only non-food products are a suitable option. A. filiculoides for example is an excellent green fertilizer. Moreover, it is rich in protein, and can be used as a peat substitute in potting soil, for example to grow ornamental plants. Although T. natans was least efficient in nutrient removal, its current market value as pond or aquarium plant might still make it a profitable addition in circular wastewater treatment systems, enabling optimal resource reuse. Especially in low-income countries, it would be beneficial to explore circular wastewater treatment as a cost-efficient strategy.

5.4.4 Conclusion

Effluent polishing using floating plants, either as monoculture or in plant combinations, is a promising technique for effluent polishing. It can lead to nearly complete removal of inorganic nitrogen and phosphate from treated effluent, while having a minimal - or even a negative - greenhouse gas footprint. When using the produced biomass in non-food applications, plant-mediated effluent polishing can also contribute to a circular economy.

Acknowledgements

We thank Germa Verheggen and Roy Peters from the department of Ecology, and Paul van der Ven and Sebastian Krosse from the General Instrumentation at Radboud University for their help in plant processing and lab analyses. We thank Koos Janssen, Harry van Zuijlen and Walter Hendrickx from the greenhouse facility at Radboud

University for their assistance during the experiment. Thanks to Jiry de Waal (Adviesbureau de Waal/Vijvermeester.nl) for plant advice and delivery, and to Teunis Roelofsen for his assistance at the WWTP in Remmerden.

Statements and Declarations

This work was funded by the Dutch water authorities Hoogheemraadschap de Stichtse Rijnlanden, Waterschap Rivierenland and Hoogheemraadschap Hollands Noorderkwartier (Grant Aquafarm 2.0). Lisanne Hendriks has received financial support from the above-mentioned Dutch water authorities. The data that support the findings of this study are openly available in DANS EASY at doi: 10.17026/dans-zs6-53v5.

SUPPORTING INFORMATION

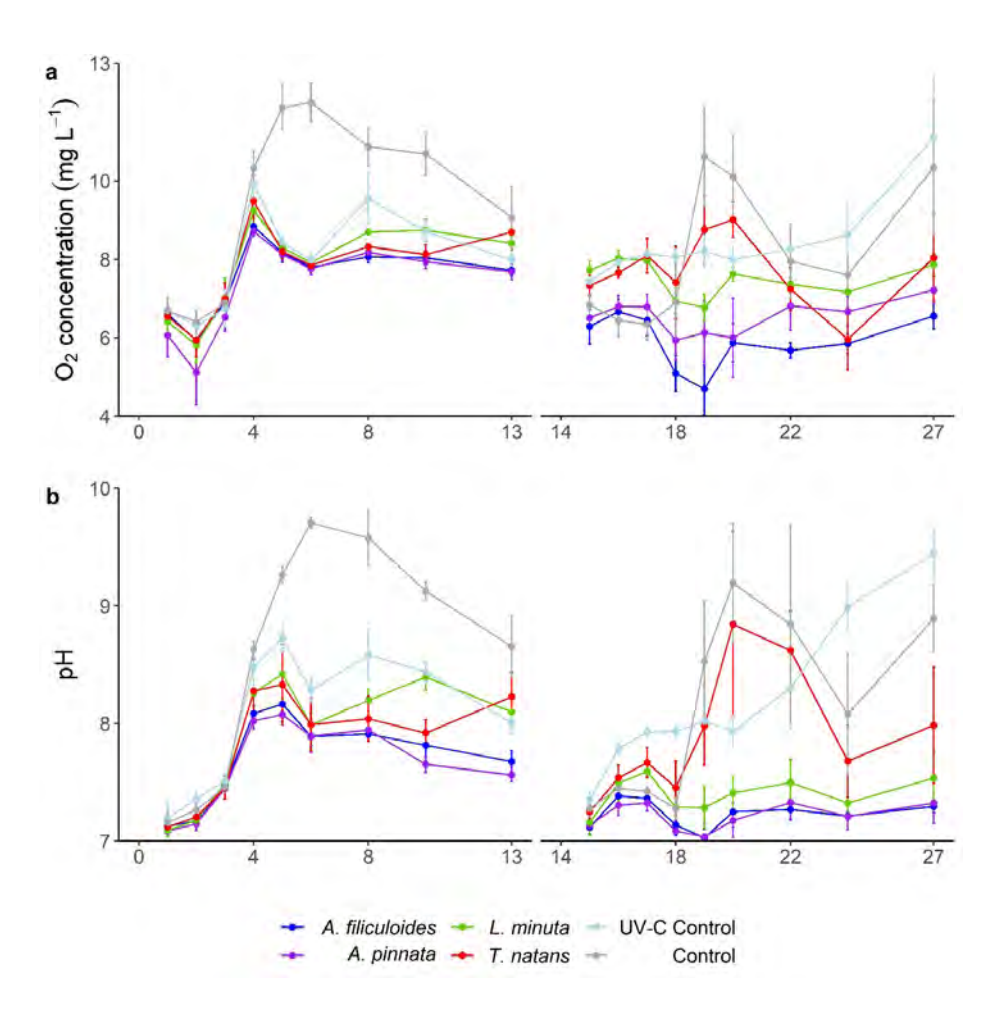


FIGURE S5.1 Dissolved oxygen concentration (a) and pH (b) in wastewater effluent treated by different plant species in a 28-day batch experiment. After 14 days, effluent was refreshed. UV-C Control is a control treatment without plants, but with UV-C light to limit algal growth. Error bars denote standard deviation.

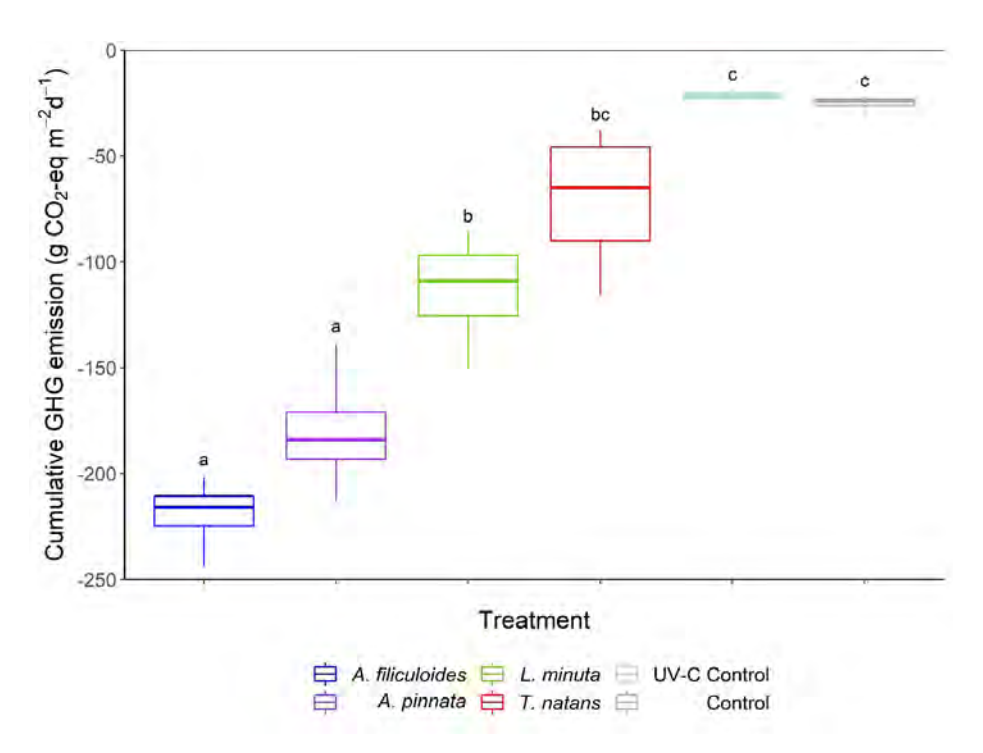


FIGURE S5.2 Cumulative greenhouse gas emission from the different treatments for the 28-day experimental period combined. Different letters indicate significant differences between groups (Tukey HSD post hoc test). Boxes show interquartile range, bold lines represent the median, whiskers indicate the lowest and highest values within a 1.5x interquartile range from the box.



Chapter 6

Sludge degradation, nutrient removal and reduction of greenhouse gas emission by a *Chironomus-Azolla* wastewater treatment cascade

Lisanne Hendriks*, Tom V. van der Meer*, Michiel H.S. Kraak, Piet F.M. Verdonschot, Alfons J.P. Smolders, Leon P.M. Lamers, Annelies J. Veraart

*Equal contribution

Published in PLOS ONE, 2024, 19 (5): e0301459 doi:10.1371/journal.pone.0301459

ABSTRACT

Wastewater treatment plants (WWTPs) are a point source of nutrients, emit greenhouse gases (GHGs), and produce large volumes of excess sludge. The use of aquatic organisms may be an alternative to the technical post-treatment of WWTP effluent, as they play an important role in nutrient dynamics and carbon balance in natural ecosystems. The aim of this study was therefore to assess the performance of an experimental wastewater-treatment cascade of bioturbating macroinvertebrates and floating plants in terms of sludge degradation, nutrient removal and lowering GHG emission. To this end, a full-factorial experiment was designed, using a recirculating cascade with a WWTP sludge compartment with or without bioturbating Chironomus riparius larvae, and an effluent container with or without the floating plant Azolla filiculoides, resulting in four treatments. To calculate the nitrogen (N), phosphorus (P) and carbon (C) mass balance of this system, the N, P and C concentrations in the effluent, biomass production, and sludge degradation, as well as the N, P and C content of all compartments in the cascade were measured during the 26-day experiment. The presence of Chironomus led to an increased sludge degradation of 44% compared to 25% in the control, a 1.4 times decreased transport of P from the sludge and a 2.4 times increased transport of N out of the sludge, either into Chironomus biomass or into the water column. Furthermore, Chironomus activity decreased methane emissions by 92%. The presence of Azolla resulted in a 15% lower P concentration in the effluent than in the control treatment, and a CO uptake of 1.13 kg ha⁻¹ day⁻¹. These additive effects of Chironomus and Azolla resulted in an almost two times higher sludge degradation, and an almost two times lower P concentration in the effluent. This is the first study that shows that a bio-based cascade can strongly reduce GHG and P emissions simultaneously during the combined polishing of wastewater sludge and effluent, benefitting from the additive effects of the presence of both macrophytes and invertebrates. In addition to the microbial based treatment steps already employed on WWTPs, the integration of higher organisms in the treatment process expands the WWTP based ecosystem and allows for the inclusion of macroinvertebrate and macrophyte mediated processes. Applying macroinvertebrate-plant cascades may therefore be a promising tool to tackle the present and future challenges of WWTPs.

6.1 INTRODUCTION

About half of all wastewater produced globally is treated in wastewater treatment plants (WWTPs), but their efficiencies to degrade organic matter and to reduce nutrient concentrations vary substantially (Jones et al., 2021). Hence, WWTPs remain a point source of organic and inorganic contaminants and nutrients, negatively impacting the discharge-receiving surface waters (Burdon et al., 2020; Dos Reis Oliveira et al., 2020; Mor et al., 2019; Pereda et al., 2020). Moreover, during the treatment process, greenhouse gases (GHGs) are emitted, contributing to climate change (Parravicini et al., 2016), and large volumes of excess sludge are produced. The costs of processing and disposal of this excess sludge can make up to 60% of the total operational costs of a WWTP (Buys et al., 2008). Therefore, new high-tech post-treatment technologies are being developed with higher nutrient removal rates (Gutierrez et al., 2010; Zietzschmann et al., 2014), but these are often expensive and energy demanding, contributing to global carbon emissions (Bunce et al., 2018). In response to these expensive and energy demanding technologies, the European Commission advocated that wastewater treatment should be cost-effective and energy neutral (European Commission, 2022). Moreover, as 48% of the global wastewater is not being treated at all, mostly in regions with limited sanitation infrastructure (Jones et al., 2021), these high-tech post-treatments may have a limited contribution to attaining the global Sustainable Development Goals (SDGs). Therefore, there is an urgent need for low-budget WWTP post-treatment techniques that further reduce the nutrient concentrations in the effluent, as well as the amount of produced sludge, while having a minimal GHG footprint. Moreover, such low-budget solutions may pave the way for application in regions still lacking any wastewater treatment.

As an alternative to technical solutions, we here argue that aquatic organisms have the potential to aid in sludge degradation and nutrient removal, as they also degrade organic matter and take up nutrients, especially nitrogen (N) and phosphorus (P), in their natural environment. Indeed, multiple species of macroinvertebrate collectorgatherers can feed on WWTP sludge, thereby affecting fluxes of nutrients and metals (Van der Meer et al., 2021; Van der Meer et al., 2022a). They can also reduce GHG emissions from organically rich sediments, for example through burrowing, thereby oxygenating deeper layers and thus limiting methane (CH₂) production and favouring CH, oxidation (Benelli & Bartoli, 2021). A similar effect of benthic invertebrate bioturbation on WWTP sludge may be expected, because redox conditions in WWTP sludge are similar to those in organically enriched sediments. Chironomus riparius is a macroinvertebrate with a high sludge degradation capacity (Van der Meer et al., 2022b) occurring in high densities in organically enriched sediments (Groenendijk et al., 1998), which makes it a suitable candidate for the treatment of wastewater. Macrophytes, including floating plants, can effectively remove nutrients from WWTP effluent (Hendriks et al., 2023; Selvaraj & Velvizhi, 2021), and can affect GHG emissions positively or negatively by altering oxygen concentrations in the water column (Kosten et al., 2016; Rassamee et al., 2011). Compared to other plants, *Azolla filiculoides* has a high nutrient removal potential (100% PO₄³⁻ removal) and a high growth rate when grown on WWTP effluent (Hendriks et al., 2023). Since it lives in symbiosis with a N fixing cyanobacterium, *Nostoc azollae*, it can overcome N limitation (Brouwer et al., 2017) and still remove P when N is limited. The produced biomass (doubling in 5 days; Janes, 1998) may then be removed, permanently extracting the nutrients from the system and preventing nutrient discharge into the environment. Afterwards, this biomass can be sustainably post-processed. A cascaded setup may further allow for positive effects of both species, as well as facilitative interactions (Schuijt et al., 2021).

The aim of the present study was therefore to assess how well an experimental wastewater treatment cascade of bioturbating macroinvertebrates and floating plants is able to degrade sludge, remove N and P, and decrease GHG emission. To this end, an experiment was designed using a recirculating cascaded setup consisting of a wastewater treatment sludge compartment with or without bioturbating *Chironomus riparius* larvae, and an effluent container with or without the floating plant *Azolla filiculoides*. To calculate the N, P and carbon (C) mass balance of this system, we measured nutrient concentrations, biomass production, and sludge degradation, as well as the N, P and C content of all compartments in the cascade.

Bioturbating macroinvertebrates were hypothesized to promote the transfer of N and P into their own biomass and from the sludge into the overlying water, and to lower sludge CH₄ emissions (Hypothesis (H)1). Furthermore, floating plants were expected to increase the transport of N and P from the water column into plant biomass, increase CO₂ uptake, and decrease the emission of nitrous oxide (N₂O) (H2). Lastly, it was hypothesized that the combination of bioturbating macroinvertebrates and floating plants would result in an increased transport of N and P into plant biomass, by invertebrate mobilisation of nutrients and subsequent uptake by plants, leading to a net lowering of N and P in the water column (H3a). As invertebrates and plants may affect GHG formation differently, the combination of organisms was expected to further limit GHG emissions from the two-compartment cascade (H3b).

6.2 MATERIAL AND METHODS

6.2.1 Outline of the study

To determine the effect of Chironomus and Azolla on sludge degradation, nutrient dynamics and GHG emission during the polishing of activated sludge and effluent from a WWTP, sixteen recirculating cascades were created, each consisting of two containers. In each of these cascades, the first container contained WWTP effluent and a small compartment with settled activated sludge, while the second container contained effluent (Fig. 6.1). An overflow pipe connected the two containers, while water from the second container was pumped back into the first container by a peristaltic pump, creating a recirculating system. The full 2x2 experimental design consisted of four treatments: a Chironomus-Azolla (midge-plant; MP) treatment, a Chironomus-control (MC) treatment, a control-Azolla (CP) treatment and a controlcontrol (CC) treatment, containing neither Chironomus nor Azolla. Ten-day old Chironomus larvae and egg ropes were added to the sludge compartment of the first container of the Chironomus containing treatments MC and MP, while Azolla was added to the second container of the Azolla containing treatments CP and MP. Each treatment consisted of four replicates. The experiment lasted for 26 days, during which dissolved nutrients and GHG emissions were measured twice a week, and emerging Chironomus adults and Azolla were harvested intermittently. At the end of the experiment, all biomass and remaining sludge were collected, weighed and C, N and P contents were determined.

6.2.2 Methods

6.2.2.1 Collection of WWTP sludge and effluent

One day before the start of the experiment, 80 L activated sludge and 1000 L effluent were collected from the municipal wastewater treatment plant in Remmerden, The Netherlands, a UCT carrousel (Østgaard et al., 1997) with a 2100 m³ hour-1 hydraulic capacity that serves 46,000 households. In 2022, the sludge from the aeration tank had a (mean \pm SD) dry weight of 3.75 \pm 0.37 g L⁻¹, and the effluent contained 390.6 \pm 177.4 μ mol L⁻¹ N and 24.6 \pm 8.1 μ mol L⁻¹ P.

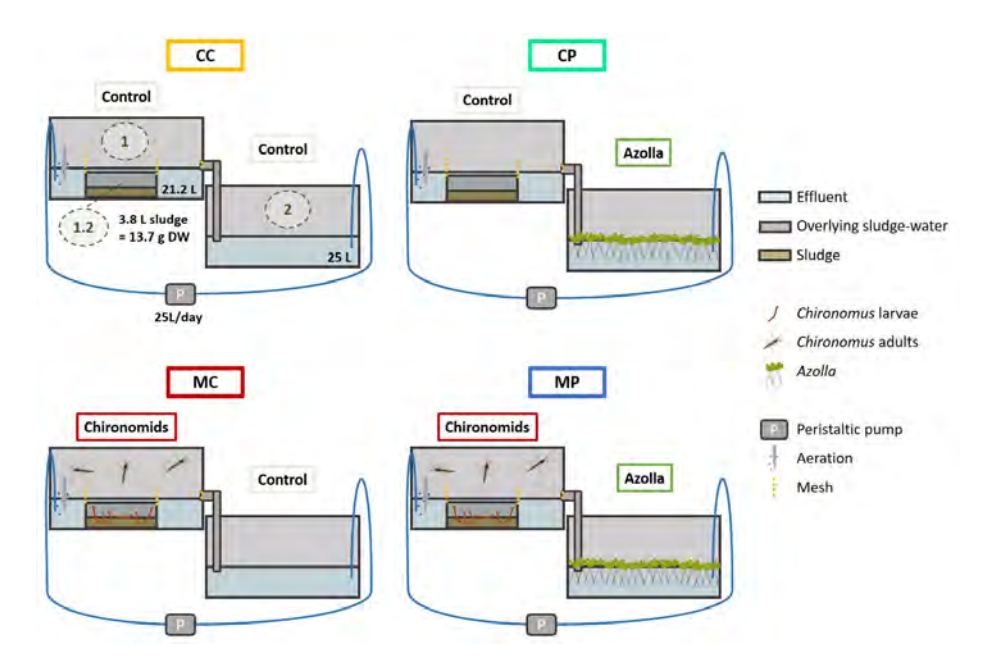


FIGURE 6.1 Schematic overview of the experimental setup. Cascades consisted of container 1 (1), filled with effluent and a sludge compartment (1.2), connected with a pipe to container 2 (2) which was also filled with effluent. A peristaltic pump (P) pumped the water from container 2 back into container 1. *Chironomus* larvae and egg ropes were added to container 1 of the MC and MP treatments, and *Azolla* was added to container 2 of the CP and MP treatments. To assess microbial sludge degradation, nutrient dynamics and GHG emissions, a control treatment without *Chironomus* and *Azolla* (CC) was also included in the setup.

6.2.2.2 Test organisms

Chironomus riparius

The non-biting midge *Chironomus riparius* (further referred to as *Chironomus*) is a common detritivorous macroinvertebrate, occurring in very high densities in organically enriched systems (Groenendijk et al., 1998), where they construct burrows, thereby affecting sediment characteristics and nutrient dynamics (Gautreau et al., 2020).

Chironomus larvae and egg ropes originated from an in-house culture at Wageningen Environmental Research. Chironomus larvae were cultured in tanks containing a 3 cm sediment layer consisting of commercially available sand (63-210 µm), water column of Dutch Standard Water (DSW; deionized water 200 mg L⁻¹ CaCl₂•2H₂O, 180 mg L⁻¹ MgSO₄•7H₂O, 100 mg L⁻¹ NaHCO₃, and 20 mg L⁻¹ KHCO₃). Chironomus larvae were fed three times a week with a 9:1 Tetramin:Tetraphyll© (Tetrawerke, Germany) mixture. Half of the culture medium was renewed twice a month.

To obtain egg ropes and larvae, Chironomus adults were collected from the four culture tanks and placed in a flight cage, where they could mate and deposit their egg ropes in a small container containing sand and DSW. For the 10-day old larvae, these egg ropes were placed in freshly prepared culture tanks, where the eggs could hatch, and the larvae were collected after 12 days, as the mean hatching time was 2 days. These larvae were fed with the same food as the cultures.

Azolla filiculoides

Azolla filiculoides (further referred to as Azolla), is a floating plant occurring in eutrophic systems. Azolla can take up high amounts of carbon and nutrients resulting in a high maximal growth rate, outcompeting other plant species under eutrophic circumstances (Hendriks et al., 2023).

Azolla originated from an in-house culture at Radboud University, and was cultured in a greenhouse facility in large tubs (100 L) with a 16h/8h light dark cycle at 20.1 (16.2-25.2) °C. Before adding the plants to the experiment, they were transferred into smaller containers (40x60x10 cm) and grown on rainwater for two weeks, to ensure a low N, P and C content in the plants at the start of the experiment.

6.2.2.3 Experimental setup

The four replicates of each of the four treatments were distributed in a randomised block design to avoid confounding microclimatic effects in the greenhouse. Each cascade consisted of two polypropylene containers of 40x60x30 cm (l*w*h) with recirculating water. On the bottom of container 1 a smaller compartment (26.7x16.6x9.3 cm; 3.8 L) was placed containing WWTP sludge. To prevent detrimentally low oxygen concentrations for the Chironomus larvae, aeration was provided in two corners of container 1. An overflow pipe at a height of 12.5 cm allowed a maximum volume of 25 L. Excess water flowed into the second container, which was situated 15 cm lower. The outlet of this pipe was located 2 cm under the water level of container 2, which contained a volume of 25 L of effluent. The water from container 2 recirculated into container 1 via a Masterflex L/S peristaltic pump (Model No. 7528-30, Masterflex LLC, USA) equipped with a standard pump head (Model No. 7015-20), including high-performance precision platinum-cured silicone 4.88 mm tubing, with a hydraulic retention time (HRT) of 0.5 days (50 L day¹ -35 mL min⁻¹). To prevent algal growth in the tubing, all tubes were wrapped in aluminium foil. To prevent the Chironomus adults from escaping, containers 1 from the Chironomus containing treatments were covered with a mosquito net. Additionally, a mesh (1 mm mesh size) was attached to the sides of the sludge compartment, to prevent larvae from escaping from this compartment. Furthermore, all containers 1 and all containers 2 without plants (CC and MC treatments) were covered with white cloth to limit algae

growth. The experiment was conducted in a greenhouse facility at Radboud University. To maintain a light/dark cycle of 16 h/8 h with sufficient light intensity, 400 W high-pressure sodium lamps (Hortilux-Schréder, The Netherlands) switched on when the natural daylight intensity was below 250 W m⁻² during the 16h light period.

6.2.3 Experimental procedures

6.2.3.1 Start of the experiment

One day before the start of the experiment WWTP sludge (3.8 L) was added to the sludge compartment of container 1, which was allowed to settle for 30 minutes. Thereafter, 21.2 L of effluent was carefully added to container 1, taking care not to disturb the settled sludge. The water in container 1 was high enough (12.5 cm) to also cover the 10 cm-high sludge compartment (Fig 1). To container 2, 25 L of effluent was added, resulting in a water level of 12.5 cm. To determine the initial dry weight per litre of sludge, as well as the N, P and C content of the dry mass and of the watery part of the sludge, six 2 L containers were filled with sludge, which was allowed to settle, after which water samples of water overlying the sludge were collected, excess water was removed, and all remaining sludge was collected. To determine initial nutrient concentrations of the effluent, a further six initial effluent water samples were collected. All samples were frozen at -20 °C until analysis. At the start of the experiment, Azolla was introduced into container 2 of the Azolla containing treatments, covering 50% of the surface area. To the Chironomus containing treatments, 200 10-day old Chironomus larvae and 8 egg ropes were added to the sludge compartment of container 1. To determine the initial dry weight of both Azolla and Chironomus larvae, four additional plant batches (dry weight 5.6 \pm 0.1 g), and three additional batches of 200 10-day old Chironomus larvae were collected from the culture, dried at 70 °C and weighed. The experiment lasted for 26 days, and measurements of nutrient content and greenhouse gas fluxes were done biweekly.

6.2.3.2 Water quality measurements

To determine the dissolved nutrient concentrations (PO $_4^{3-}$, NH $_4^+$, NO $_2$, NO $_3^-$, together NO $_x^-$) in the overlying water, filtered water samples were collected (pore size 0.12/0.18 μ m, Rhizon SMS 10 cm, Rhizosphere Research, The Netherlands) of both containers from each replicate per treatment at the start of the experiment, before adding the organisms, and subsequently every 3 to 4 days. Samples were stored at $-20~^{\circ}$ C until further analysis. The pH, temperature and dissolved O $_2$ concentrations in the water column of each container were measured using a Portable Multi Meter (HQ2200, HACH, USA) with the appropriate probes (PHC20101, LD01010). Due to practical constraints, filtered water samples to determine the dissolved organic carbon

(DOC) and dissolved nitrogen (DN) content were only collected at the start of the experiment, after 12 and 19 days and at the end of the 26-day experiment. Samples were stored at 4 °C until further analysis (see 'nutrient analysis').

6.2.3.3 Greenhouse gas fluxes

Diffusive greenhouse gas (CH, CO, N,O) emissions from all containers were measured at the start of the experiment, before adding Chironomus and Azolla, and subsequently every 3 to 4 days. Fluxes were measured using a Greenhouse Gas Analyser (G2508, Picarro, USA) connected to a transparent acrylic flux-chamber placed over the container. The edges of the flux-chamber were inserted 2 cm into the water column of the containers to seal the 10.4 dm³ headspace from the surrounding air. In each container, diffusive GHG fluxes were measured for 3 minutes, beginning at the moment that concentrations started to change. In-between the measurements, the chamber was aerated to return gas concentrations to atmospheric levels. To accurately calculate GHG fluxes, chamber air temperature was logged using HOBO Pendant® temperature data loggers (UA-001-64, Onset Computer Corporation, USA). Measurements were performed between 10:00 and 15:00 h.

6.2.3.4 Biomass collection

After 8, 15, 22 days and at the end of the 26-day experiment Azolla was harvested, reducing the plant coverage in each container to the original 50%. Exact coverage was ensured by creating a 100% coverage in a "harvesting container" of half the original container size, collecting the remaining Azolla from container 2, and returning all Azolla from the harvesting container into the original container 2. The collected biomass was dried at 70 °C until completely dry. Chironomus adults started to appear after 8 days, which were collected by a customized vacuum-driven Chironomuscollector (adapted Turbo-Tiger, Princess™; Fig. S6.1). Chironomus adults floating on top of the water, exuviae and egg ropes were collected and counted as well. All Chironomus samples were stored at -20 °C until further processing.

6.2.3.5 Ending the 26-day experiment

At the end of the 26-day experiment, all plants of the Azolla containing treatments were harvested. The overlying water from all containers, including the controls, was poured through a 38 µm sieve and all additional material (algae in control containers, Chironomus larvae that escaped from the sludge compartment in Chironomus containers, and Azolla-roots in Azolla containers) were collected. Thereafter, the overlying water of the sludge compartment was removed, and all remaining sludge was collected into 2 L pots. Sludge, Chironomus and additional accumulated leftover material were freeze dried. Azolla biomass was dried at 70 °C until completely dry.

6.2.4 Nutrient analysis

6.2.4.1 Dissolved nutrients

Concentrations of NH₄⁺, NO_x⁻ and PO₄³⁻ in the filtered water samples were measured colorimetrically on an auto analyser (III, Seal Analytical, Norderstedt, Germany). NH₄⁺ was determined using the Berthelot reaction (adapted NEN-EN-ISO 11732:2005), PO₄³⁻ using an adapted ISO 15681-2:2003, and NO_x⁻ according to an adapted version of NEN-EN-ISO 13395:1997. Total dissolved phosphorus (DP) and trace elements were measured in filtered acidified water (0.1 ml 10% nitric-acid) on an ICP-OES with a radial plasma observation, a V groove nebulizer and a cyclonic spray chamber (iCap 6300, Thermo Fisher Scientific, Bremen, Germany). DOC and DN concentrations were measured in rhizon-filtered samples on a total organic carbon analyser, using combustion catalytic oxidation at 680 °C (TOC-L CPH/CPN analyser, Shimadzu). Each DOC and DN sample was measured twice.

6.2.4.2 N, P and C content in sludge, Azolla and Chironomus

Dried plant material was weighed and ground. Sludge, *Chironomus* adults, *Chironomus* larvae, exuviae and additional accumulated leftover material were freeze-dried at –90 °C until completely dry. *Chironomus* larvae still present in the sludge at the end of the experiment were taken out from the freeze-dried sludge by hand, counted and weighed. *Azolla* and *Chironomus* larvae present in the leftover material were also manually separated and processed. Ground material (10 mg for sludge, 3 mg for other samples) was used to determine N and C concentrations using a CNS elemental analyser (Vario Micro Cube, Elementar, Langenselbold, Germany). To determine P and trace element concentrations, duplicate sample material (200 mg for *Azolla*, sludge and leftover material, 8–200 mg for *Chironomus* samples) was digested in Teflon vessels by adding 4 mL HNO₃ (65%) and 1 mL H₂O₂ (35%). These samples were then heated in an Ethos One microwave (Milestone, Italy) for 20 minutes at 120 °C. The digested samples were subsequently analysed on the previous-mentioned ICP-OES.

6.2.5 Data analysis

6.2.5.1 Nutrient concentrations in water, and calculation of mass balances

The nutrient concentrations in the overlying water of both containers 1 and 2 were averaged per replicate and per day. DN concentrations were not measured one day before the start of the experiment. However, because DN was strongly related to DIN $(NH_4^+ \text{ and } NO_x^- (R^2 = 0.96))$, we were able to estimate these missing DN values. To calculate the mass balances of N, P and C of all treatments at the start and the end of the experiment, the start and final amount of N, P and C was determined for each

compartment in the system: water, sludge, Chironomus, Azolla and leftover material. To determine the start and final amount of N, P and C in the water, the concentrations in the water at day 0 and 26 were multiplied by the volume of the system (50 L). To determine the start and final amount of N, P and C in the sludge, Chironomus, Azolla and leftover material, the start and final dry weight of the sludge, the total harvested Chironomus and Azolla, and the leftover material with their respective nutrient contents were multiplied, using the following equation:

$$N_{tot} = \sum ([N_w] \times V_w) + ([N_S] \times DW_S) + ([N_C] \times DW_C) + ([N_A] \times DW_A) + ([N_L] \times DW_L)$$
 (1)

Where N_{tot} is the total amount of N (mmol) in the cascade system, N_{W} (mmol L-1) and V_{w} (L) the N concentration and volume of the overlying water, N_{g} , N_{c} , N_{L} , (mmol g⁻¹) the N content and DW_{s} , DW_{c} , DW_{h} and DW_{L} (g) the dry weight of respectively the sludge, the Chironomus biomass, the Azolla biomass, and the leftover material. The same formula was used for the mass balances of P and C.

6.2.5.2 Greenhouse gas fluxes

GHG fluxes (mg m⁻² day⁻¹) were calculated according to Hendriks et al., 2024a. To convert the CH₄ and N₂O emissions into CO₂ equivalents, multiplication factors were used of 27 and 273 respectively (global warming potential over a 100-year time frame (IPCC, 2021). Fluxes of CO₂, CH₄ and N₂O below the minimum detectable flux (13.3, 2.4 and 151.9 mg CO₂-eq m⁻² day⁻¹ for CO₂, CH₄ and N₂O, respectively) were denoted as 0 (Christiansen et al., 2015; Nickerson, 2016). Measurements that were not useable due to sharp spikes in GHGs as a result of ebullition were counted as ebullition events. Cumulative GHG fluxes were calculated by the area under the curve divided by the 26-day period, expressing GHGs in CO, equivalents.

6.2.5.3 Statistical analysis

Differences in DN, DP and DOC concentrations in the overlying water between the four treatments were assessed for every sampling date. Differences were assessed using one-way ANOVAs or non-parametric Kruskal-Wallis tests, followed by either a TukeyHSD or Dunn's post-hoc test (with a Benjamini-Hochberg correction), depending on the occurrence of deviations from normality (Shapiro-Wilk test) and/ or homogeneity (Levene's test).

Differences in sludge DW, C, N, and P content between the treatments were assessed using a Welch One-Way analysis of means, with treatment as explanatory variable, followed by a Dunnett T3 post-hoc test to determine which treatments differed from each other. Since the data were normally distributed, but homogeneity of variance

was not met, this is a robust and conservative method for a dataset with a small sample size (Welch, 1951; Shingala et al., 2015).

To determine if GHG emissions differed between experimental treatments, linear fixed models (*lmer*) were used, where both the day and the container were defined as random effects, and the presence of *Chironomus* larvae and *Azolla* were included as fixed effects. The complete model was compared to models only containing *Chironomus* or *Azolla* as fixed effects, and the best performing model was selected. Differences in CH₄ emissions between container 1 and container 2 were also assessed using the same method, but with container as a fixed effect. As the CH₄ emissions from container 2 and the effects of *Azolla* on CH₄ emissions were non-significant, finally the effect of *Chironomus* on the CH₄ emissions in container 1 was also assessed using an *lmer*, with the presence *Chironomus* as a fixed effect.

Between-treatment differences in ebullition observed in container 1 were assessed using Pearson's chi square test for count data.

The effects of *Chironomus* and *Azolla* on the final mass balances of C, N and P were assessed by two-way multivariate ANOVAs (MANOVA), with C, N or P content in the sludge and in the overlying water as response variables, and the presence of *Chironomus* or *Azolla* as explanatory variables. N content was log transformed to meet the assumptions of (multi-variate) normality and homoscedasticity, which were tested using multivariate Shapiro-Wilk tests, and Box's M tests respectively. When the results of the MANOVA were significant, two separate two-way ANOVAs were performed. This way we assessed whether significant changes were due to effects on either the sludge, the overlying water or both. All statistical analyses were performed in R 4.3.3 (R Core Team, 2022) using the packages lme4 (Bates et al., 2015), lmerTest (Kuznetsova et al., 2017) and emmeans (Lenth, 2022) for linear fixed models, dunn. test (Dinno, 2017) for Dunn's tests, car (Fox & Weisberg, 2019) for Levene's tests. The packages heplots (Friendly et al., 2022) and mynormtest (Jarek, 2012) were used to check assumptions for the MANOVAs. For the creation of the figures, the ggplot2 (Wickham, 2009) and ggpubr (Kassambara, 2020) packages were used.

6.3 RESULTS

6.3.1 Experimental conditions

Water temperature increased over time from 20.6 ± 0.4 °C to 24.3 ± 0.3 °C (Fig. S6.2a), and the pH ranged between 6.7 and 8.6 (mean = 7.6 ± 0.3 ; Fig. S6.2b) during the 26-day experiment. Dissolved O₂ concentrations were always above 6.2 mg L⁻¹ (Fig. S6.2c).

6.3.2 Sludge degradation

Sludge dry weight at the start of the experiment was 13.7 g (SE=0.06) per container and decreased during the 26-day experiment in all treatments ($F_{4,7}$ = 367.08, p < 0.001; Fig. 6.2a). Sludge dry weight at the end of the experiment in the Chironomus containing treatments (7.7 g, SE=0.26) was significantly lower than in the treatments without *Chironomus* (10.3 g, SE=0.10) (all p < 0.001), revealing that the presence of *Chironomus* caused a 1.8 times higher sludge degradation during the 26-day experiment (Fig. 6.2a). Sludge N-content was affected by treatment ($F_{4.7}$ =13.23, p=0.001; Fig. 6.2b). Moreover, the N-content in the Chironomus containing treatments tended to be lower compared to the treatments without Chironomus (S1 Table). Sludge P-content also differed between treatments ($F_{4.7}$ = 327.07, p < 0.001; Fig. 6.2c). P-content in the treatments without Chironomus tended to be lower than in the treatments with Chironomus (Table S6.1). Lastly, sludge C-content also differed between treatments $(F_{47} = 31.07, p < 0.001; Fig. 6.2d)$. Sludge C-content tended to be higher in treatments without Chironomus compared to treatments with Chironomus (Table S6.1).

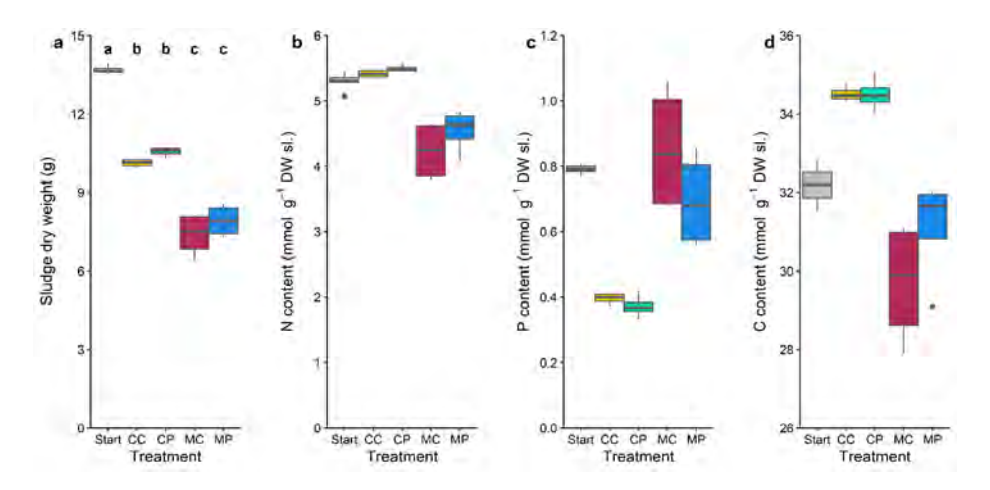


FIGURE 6.2 Sludge dry weight (a), N content (b), P content (c) and C content (d) of the initial sludge, and at the end of the 26-day experiment for the CC, CP, MC and MP treatments. Boxes show interquartile ranges, bold lines represent the median, whiskers indicate the lowest and highest values within a 1.5x interquartile range from the box, dots represent outliers.

6.3.3 Nutrient dynamics in the overlying water

At the start of the experiment dissolved nitrogen (DN) concentrations in the water ranged between 287.9 \pm 7.0 μ mol L⁻¹, and differed between treatments after 12 days ($F_{3,28} = 59.0$, p < 0.001). The *Azolla* containing treatments had a lower DN concentration than the *Chironomus* only treatment, which in turn was lower than the control treatment (all p < 0.001). At the end of the 26-day experiment, treatment still had an effect on the DN concentration ($X^2(3, N = 32) = 13.6$, p = 0.003), since the DN concentration was lower in the control and CP treatment than in the *Chironomus* containing treatments (all p < 0.05; Fig. 6.3a). NH₄ and NO_x concentrations in the overlying water showed the same pattern (Fig. S6.3a, b).

Dissolved phosphorus (DP) concentrations in the water were highest on day 8, and were affected by treatment ($F_{3,28}=60.2$, p<0.001). Both *Azolla* containing treatments (CP and MP) had a lower DP concentration than the treatments without *Azolla* (CC and MC; all p<0.001). After 19 days, when the lowest mean DP concentrations were observed, DP concentration was still affected by treatment ($F_{3,28}=54.6$, p<0.001), but by then, the treatments without *Chironomus* (CC and CP) had a higher DP concentration than both *Chironomus* containing treatments (MC and MP), while in turn the MP treatment had a lower DP concentration than MC (all p<0.001). Although at the end of the 26-day experiment, treatment still had an effect on DP concentration ($X^2(3, N=32)=16.2$, p=0.001; Fig. 6.3b), only the treatment containing both organisms (MP) had a significantly lower DP concentration than the other treatments (all p<0.02). PO $_4^{3-}$ concentrations in the overlying water showed the same pattern (Fig. S6.3c).

After 12 days, approximately halfway the experiment, the DOC concentration in the overlying water was not affected by treatment, while at the end of the 26-day experiment the control treatment (CC) had a lower DOC concentration than the other treatments ($X^2(3, N = 32) = 15.6, p = 0.001, \text{ all } p < 0.03; \text{ Fig. 6.3c}$).

6.3.4 Dynamics of Chironomus and Azolla biomass and NPC content

From the moment that the *Chironomus* adults started to emerge, the harvested adult *Chironomus* biomass increased over time (t=3.06, p=0.004), but did not differ between treatments (t=0.76, p=0.46; Fig. S6.4a). Likewise, the presence of *Azolla* did not affect the biomass of any of the *Chironomus* life stages (Fig. S6.4b). Furthermore, the *Chironomus* N, C, and P content did not differ between treatments, but P content in *Chironomus* adults increased over time (t=3.25; p=0.003) (Fig. S6.4c-e). This resulted in an average P removal rate by *Chironomus* in the MC treatment of 410 \pm 159 μ mol P day 1 m 2 sludge and in the MP treatment of 276 \pm 48 μ mol P day 1 m 2 sludge.

During the experiment the Chironomus adults produced on average 110.5 \pm 23.6 and 148.8 ± 18.1 egg ropes per replicate in the MC and MP treatments, respectively.

Harvested Azolla biomass also increased over time (t = 7.54, p < 0.001), with an interaction effect of treatment (t = -2.61, p = 0.02), since the increase in Azolla biomass (Fig. S6.5a) and the total produced Azolla biomass at the end of the experiment (Fig. S6.5b) in the plant-only treatment (CP) was significantly higher than when *Chironomus* was also present ($F_{2,0} = 143.2$, p < 0.001). Azolla N and P contents decreased over time, while the C content increased (N: t = -2.16, p = 0.04; P: t = -13.31, p < 0.001; C: t = 3.67, p = 0.001), but the N and P contents did not differ between treatments (N: t = 1.97, p = 0.96; P: t = -0.19, p = 0.83). The C content of Azolla differed significantly between treatments (effect size = 0.5; t = 2.25, p = 0.03; Fig. S6.5c-e). This resulted in an average P removal rate by Azolla in the CP treatment of 813 \pm 23 μ mol P day m⁻² Azolla cover and in the MP treatment of 669 \pm 71 μ mol P day ⁻¹ m⁻² Azolla cover. The trace element and metal contents of Ca, Fe, Mn, Si, Zn and Cu in Azolla grown in the MP treatment were lower than in Azolla grown in the CP treatment. Concomitantly, concentrations of these elements and metals were lower in the overlying water and higher in the remaining sludge when Chironomus was also present (Table S6.2).

6.3.5 Reduction of Greenhouse gas emissions

CH₄ emissions were only observed in the sludge containing containers 1 (2.4 (SE=0.6) mg CO₂-eq m⁻² day⁻¹; df = 221.7, t = 4.1, p < 0.001), while CH₄ fluxes in containers 2 did not exceed the minimum detection limit. The best fitting lmer model included only Chironomus as an explanatory variable, while Azolla did not increase the model fit, which was thus excluded. The emission of CH₄ in containers 1 in the presence of Chironomus (0.384 (SE=1.07) mg CO₂-eq m⁻² day⁻¹) was significantly lower than in the absence of *Chironomus* (4.939 (SE=1.14) mg CO₂-eq m⁻² day⁻¹) (df = 14.0, t = 3.5, p = 0.004; Fig. 6.4a), a reduction of 92%. Moreover, in total 13 out of 64 CH₄ measurements were not usable because of ebullition in containers 1, which in 12 out of 13 cases appeared in treatments without Chironomus larvae (CC and CP; $X^2(1, N = 13) = 9.31, p = 0.002$).

CO₂ uptake occurred only in containers 2 (-148.2 (SE=1.9) mg m⁻² day⁻¹, df = 225.56, t = -13.6, p < 0.001), whereas no uptake nor emission of CO₂ was observed in the sludge containing containers 1 (1.2 (SE=16.2) mg m⁻² day⁻¹, df = 18.5, t = 0.1, p = 0.94; Fig. 6.4b). The best fitting lmer model included only Azolla as an explanatory variable, while Chironomus did not increase the model fit, which was thus excluded. Azolla presence significantly increased CO, uptake in containers 2 (112.7 (SE=7.4) mg m-2 day-1, df = 14.2, t = 15.2, p < 0.001), while treatments without Azolla did not show a significant CO₂ emission, nor uptake (-14.6 (SE=9.7) mg m⁻² day⁻¹, df = 6.3, t, = 1.5 p = 0.18).

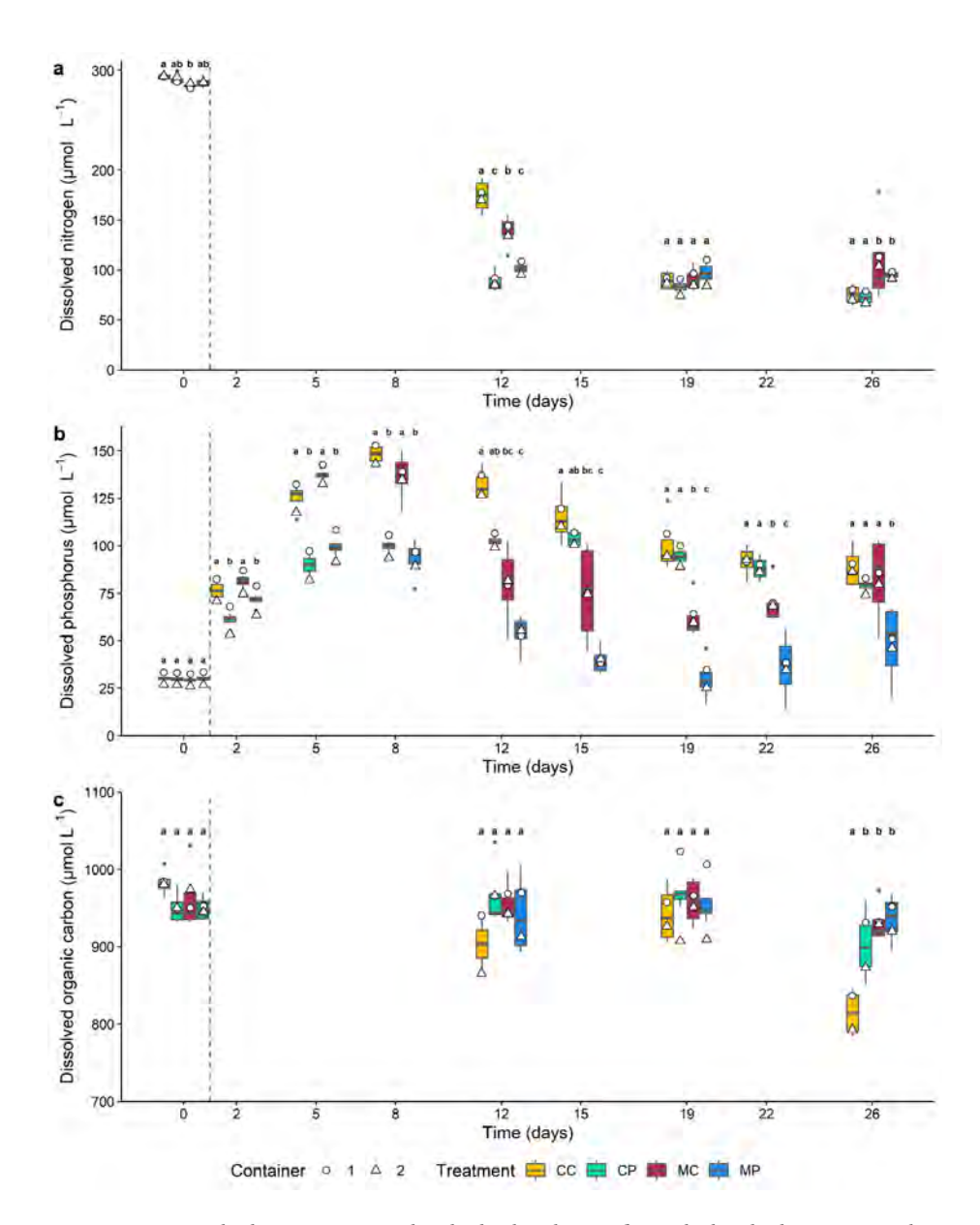


FIGURE 6.3 Dissolved nitrogen (a), dissolved phosphorus (b) and dissolved organic carbon (c) concentrations in the overlying water (μ mol L⁻¹) during the 26-day experiment for the CC, CP, MC and MP treatments. Boxes show interquartile ranges, bold lines represent the median, whiskers indicate the lowest and highest values within a 1.5x interquartile range from the box, dots represent outliers. White circles and triangles represent the average concentrations in respectively container 1 and container 2.

During the entire 26-day experiment, NO emissions did not exceed the minimum detectable flux in any of the treatments or containers.

When combining the cumulative contribution of the two GHGs, a net GHG-uptake (in CO, equivalents) was observed in the Azolla containing treatments CP (-122.2 $(SE=12.0) \text{ mg CO}_2 - \text{eq m}^{-2} \text{ day}^{-1}) \text{ and MP (-135.3 (SE=10.4) mg CO}_2 - \text{eq m}^{-2} \text{ day}^{-1}), \text{ whereas } \text{ otherwise}$ a very limited net effect on GHG emissions was observed for the CC (-13.2 (SE=4.1) mg CO $_3$ -eq m $^{-2}$ day $^{-1}$) and MC (-17.5 (SE=3.9) mg CO $_3$ -eq m $^{-2}$ day $^{-1}$) treatments. The net GHG emission of the CC and CP treatment are less accurate, because ebullition from these treatments was not taken into account.

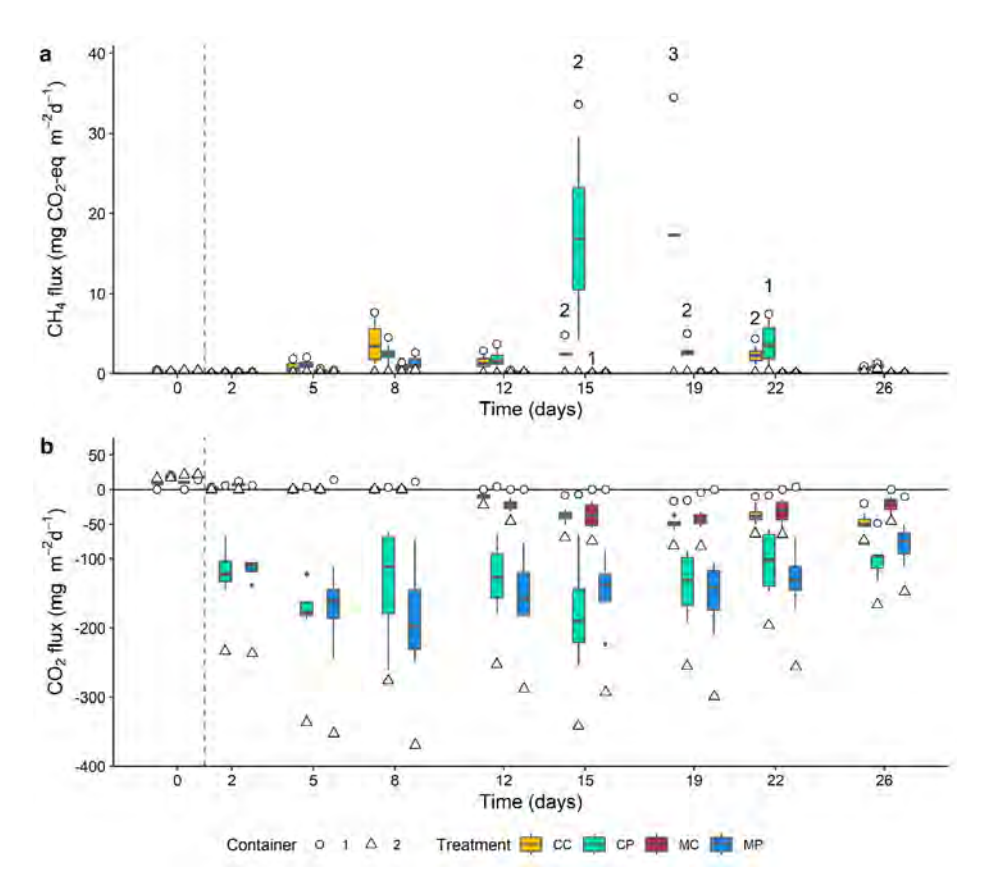


FIGURE 6.4 CH, (a) and CO, (b) fluxes for all treatments during the 26-day experimental period. Note the numbers given above some CH, fluxes, which correspond to the number of flux measurements unusable due to ebullition in container 1. Boxes show interquartile ranges, bold lines represent the median, whiskers indicate the lowest and highest values within a 1.5x interquartile range from the box, dots represent outliers. White circles and triangles represent the average concentrations in respectively container 1 and container 2.

6.3.6 N, P and C mass balance

Chironomus affected the distribution of N between the sludge and the overlying water (Pillai's Trace = 0.8, $F_{1,12}$ = 27.6, p < 0.001; Fig. 6.5a), whereas Azolla did not affect this distribution. The effect on the N distribution by Chironomus could largely be attributed to the lower final amount of N in the sludge in the presence of Chironomus larvae ($F_{1,12}$ = 59.8, p < 0.001), which was partly due to the uptake by the larvae, whereas the amount of N in the overlying water was only marginally higher in the presence of Chironomus larvae ($F_{1,12}$ = 7.4, p = 0.01).

The P distribution between the sludge and the overlying water was affected by both the presence of *Chironomus* (*Pillai's Trace* = 0.9, $F_{1,12}$ = 35.9, p < 0.001; Fig. 6.5b) and Azolla (*Pillai's Trace* = 0.8, $F_{1,12}$ = 26.6, p < 0.001), which showed an interactive effect (*Pillai's Trace* = 0.6, $F_{1,12}$ = 11.0, p = 0.002). This was the result of the higher amount of P in the sludge in the presence of *Chironomus* larvae ($F_{1,12}$ = 37.4, p < 0.001) and the lower amount of P in the overlying water in presence of the Azolla ($F_{1,12}$ = 6.5, p = 0.025).

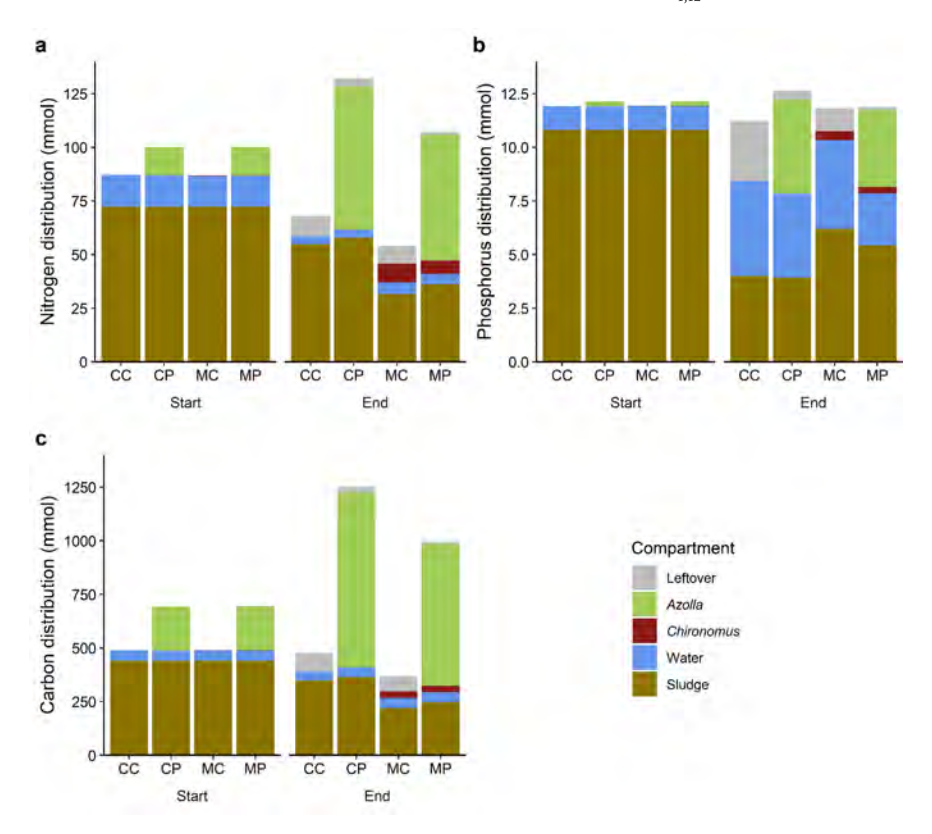


FIGURE 6.5 Mass balance of the treatment cascades for N (**a**), P (**b**) and C (**c**) in mmol at the start and the end of the 26-day experiment. Compartments include leftover material (grey), *Azolla* biomass (green), *Chironomus* biomass (red), overlying water (blue) and sludge mass (brown).

The C distribution in the cascades was also affected by both the presence of Chironomus (Pillai's Trace = 0.9, $F_{1,12}$ = 48.7, p < 0.001; Fig. 6.5c) and Azolla (Pillai's Trace = 0.6, $F_{112} = 7.1$, p = 0.011). This was mostly due to the lower C amount in the sludge in the presence of *Chironomus* ($F_{1,1}$ = 105.9, p < 0.001), and the lower amount of C in the water in the presence of Azolla ($F_{1,12} = 7.90$, p = 0.021), and/or the higher amount of C in the overlying water in the presence of *Chironomus* ($F_{1,12} = 18.2$, p = 0.001).

6.4 DISCUSSION

The present study assessed to what extent an experimental wastewater treatment cascade of Chironomus and Azolla was able to enhance sludge degradation, enhance nutrient removal and reduce GHG emissions. In line with our hypotheses, the presence of Chironomus led to increased sludge degradation, increased transport of N from the sludge into the overlying water and decreased CH₂ emission (H1). However, contrary to our expectations, the transport of P from the sludge into the overlying water was limited in the presence of Chironomus larvae (H1). The presence of Azolla resulted in a lower TP concentration in the water column, and a higher uptake of CO as expected (H2). Interestingly, although the amount of P in the water column and GHG emission was indeed lowest in the treatment where both species were present (MP), this was not due to a facilitative effect where each organism altered waterconditions favourable to the other species, but rather due to the additive effects of the joint presence of both species (H3a and b).

6.4.1 The effect of Chironomus on sludge degradation, nutrient dynamics and GHG emissions

Chironomus larvae almost doubled the sludge degradation compared to the control systems, which is in line with previous work on sludge degradation by Chironomus larvae (Van der Meer et al., 2022a). Chironomus larvae could enhance sludge degradation even up to five times, when using higher densities of third instar larvae (Van der Meer et al., 2022b). Furthermore, uptake of C and N by Chironomus larvae did not explain all C and N removed from the sludge. It is therefore likely that their bioturbation activity also stimulated the transport of C and N into the overlying water and subsequently to the atmosphere, leading to net C and N losses throughout the experiment. The release of C and N, for example in the form of CO, or N, from the sludge could have been caused by the bioturbation induced enhanced flux of oxygen into deeper layers of the sludge, which stimulated aerobic decomposition and coupled nitrification-denitrification (Chen et al., 2015). P on the other hand, remained largely associated to the sludge. Apparently, the Chironomus

larvae limited the transport of P from the sludge into the overlying water, most likely because the increased O concentration in the sludge resulted in effective binding of P to metal-oxides (Smolders et al., 2006; Patrick Jr et al., 1974). The effect of bioturbation on the redistribution of P is highly dependent on the species-specific type of bioturbation, as well as on sediment characteristics. For instance, while the present study and Chen et al. (2015) observed a reduced P concentration in the overlying water due to iron-coupled inactivation, Gautreau et al. (2020) reported a 21-fold increase in P concentration in overlying waters. This discrepancy may be explained by differences in OM contents, since the present study used sludge, which was very rich in organic matter, but also by the different type of burrows and bioturbation activity of the different benthic invertebrates. While C. riparius, used in our experiment, constructs J-shaped burrows, C. plumosus, used by Gautreau et al. (2020), makes U-shaped burrows, which they ventilate, thereby transporting P rich pore water into the overlying water. During the first 8 days of the experiment, the DP concentration increased in all treatments, due to the initial release from the sludge when this started to degrade, but also due to the presence of a deep anoxic layer. No effects of Chironomus were observed during this period, likely due to their small size. Interestingly, after this initial peak, in the presence of Chironomus the DP concentration in the overlying water decreased until day 19, after which it started to increase again until the end of the experiment. Possibly, after initial bioturbationmediated P-binding until day 19, sediment-binding sites were saturated, while at the same time P continued to be excreted due to feeding activity. This would indicate that bioturbation and feeding activity are antagonistic processes simultaneously mediated by Chironomus. As previously observed for metals (Van der Meer et al., 2022a), bioturbation by Chironomus larvae resulted in a greater change in the distribution of P and N in the system than the bioaccumulation within the organisms.

Bioturbation by *Chironomus* larvae also decreased $\mathrm{CH_4}$ emissions from the sludge by 92% and prevented $\mathrm{CH_4}$ ebullition. This emission-suppressing effect would be even stronger than presently calculated when considering the emitted GHGs by ebullition, which was especially happening when *Chironomus* was not present (Hendriks et al., 2024a). These observations indicate that in our experiment *Chironomus* burrows were likely an important $\mathrm{CH_4}$ oxidation site, and that their burrowing activity also prevented the built-up of GHGs as bubbles in the sludge (Benelli & Bartoli, 2021). *Chironomus* larvae did not affect $\mathrm{CO_2}$ emission, suggesting that the $\mathrm{CO_2}$ produced by their respiration was compensated for by reduced $\mathrm{CO_2}$ production of the microbial community.

Chironomus larvae can thus greatly affect the distribution of elements and processes in their benthic environment, having a positive effect on the three pillars of the present study: enhanced sludge degradation and nutrient removal, and reduced GHG emission.

6.4.2 The effect of Azolla on nutrient dynamics and GHG emissions

During the first 12 days of the experiment, DN removal from the overlying water column was highest in the Azolla treatments. Although at the beginning of the experiment the NO_x concentration in the water increased, this was compensated for by the removal of NH,+, pointing at nitrification rather than plant uptake as main NH₄ removing pathway. From day 8 onward, NO_x concentrations in the water decreased, which proceeded faster in the presence of Azolla, suggesting either denitrification or NO, uptake. Even though earlier work on Azolla grown on wastewater effluent suggested that it did not decrease NO, concentrations, and therefore total N concentrations remained rather high (Hendriks et al., 2023), in the present cascade N concentrations in the water column were further reduced when Azolla was present. Besides NH, and NO, uptake, Azolla likely also fixed N from the atmosphere, as shown by the overall nitrogen balance, where the final amount of N exceeded the initial amount when Azolla was present. Although N fixation during $\mathrm{NH_{_{4}}^{+}}$ abundance may seem counterintuitive, this has been previously observed in the Azolla-cyanobacteria symbiosis. In other experiments, the N content in Azolla was more related to N fixation from the atmosphere than to N assimilation from NH, the same of (Okoronkwo et al., 1989). P uptake by Azolla removed DP from the overlying water column. Removal rates (669-813 µmol P day 1 m-2 Azolla cover) were in the same range as those reported for duckweed (450-2400 µmol P day⁻¹ m⁻² plant cover; Körner & Vermaat, 1998), but lower than Azolla-mediated P removal observed in other studies (745-1100 μmol P day¹ m⁻² Azolla cover; Costa et al., 2009). This is likely because Azolla growth and P uptake in the treatment including Chironomus was limited by the low concentrations of trace elements in the water column, due to their increased binding to the sludge as a result of the Chironomus activity. Nonetheless, even though initial removal of N and P by Azolla was high, the final concentrations of these nutrients did not differ from those in the control treatments. Possibly, after 12 days, filamentous algae growing in control treatments started to affect the N and P dynamics and balance, since these algae are also known for their high N and P removal potential (Ge & Champagne, 2017). The presence of Azolla, however, prevented the growth of algae by blocking light penetration into the water column.

Azolla presence drastically reduced GHG emission. No CH, was emitted from the Azolla containers, as was also observed in previous studies on hydroponically grown Azolla (Hendriks et al., 2023). Additionally, even when CH₄ would have been produced, harvesting the Azolla biomass limited the formation of a reaeration barrier, and thus O₂ levels decreased only slightly. Moreover, Azolla captured high amounts of C, reflected by high CO₂ uptake (1.13 kg ha. day: Fig. 6.4b), and subsequent C incorporation into their biomass. Under optimal growth conditions, this uptake might even be up to five times higher, up to 5800 mg m⁻² day⁻¹ (Hamdan & Houri, 2022).

As Azolla increased nutrient removal from the effluent and sequestered high amounts of GHGs, this plant may be a suitable option to use in a WWTP polishing cascade.

6.4.3 Combined effects of *Azolla* and *Chironomus* on nutrient balances and GHG budget

No facilitative interactions were observed between Chironomus and Azolla regarding growth, which contrasts the findings of Schuijt et al. (2021), who observed increased growth of Azolla when Tubifex worms were present in a preceding compartment in a comparable experimental cascade. This was attributed to a lowered pH of 4 and increased Fe water concentrations due to Tubifex sludge consumption. In our experiment, however, no effect of Chironomus activity on pH was observed, and the pH remained therefore relatively high in the Azolla containers, thereby possibly limiting Azolla growth (Schuijt et al., 2021). Azolla sequestered less N, P and C in the presence of Chironomus, likely due to the lower growth rate of Azolla. Yet, the sludge P binding due to Chironomus activity compensated for this, resulting in the lowest overlying water P concentration in the presence of both Chironomus and Azolla. Contrasting to this additive effect of Chironomus and Azolla on the P distribution, Chironomus larvae stimulated the transfer of C from the sludge into the overlying water, whereas the Azolla removed C from the water column. Hence, Chironomus larvae and Azolla both affected specific GHGs at specific places in the cascade, and therefore also showed additive effects in the overall GHG dynamics, resulting in the highest carbon sequestration when they were both present. Therefore, the combination of both species, despite present in different compartments, resulted in the largest removal of P and N from the overlying water, as well as the largest GHG reduction through their additive, but not facilitative, effects on the P and N distribution in the system.

6.4.4 Implications and challenges for future wastewater treatment

Our *Chironomus-Azolla* treatment cascade was able to efficiently redistribute the nutrients present in the experimental wastewater system. The N and P in the original wastewater remained either associated with the sludge or were incorporated into organism biomass, limiting the amount of nutrients present in the overlying effluent. These lower effluent nutrient concentrations were in concord with lower amounts of

remaining sludge and lower GHG emissions, thus tackling three urgent challenges of WWTP operators: limiting excess sludge production and lowering GHG emissions and nutrient rich effluent discharges into surface waters, which are key for future proof WWTPs. Moreover, the remaining sludge contained a higher amount of P, which makes it more suitable to extract P to use it as a fertilizer, which is in line with the stated EU proposals (European Commission, 2022).

Our experimental setup was primarily focused on assessing the effects of Chironomus and Azolla on the N, P and C dynamics, and the joint presence of the two species resulted indeed in the highest P removal from the water column, with the P concentration being almost two times lower than in the control treatment. Nonetheless, the final P concentration in the water was higher than at the start of the experiment. Hence, to increase the effectivity of the cascade, the dimensions should be adjusted to allow for a larger surface area of Azolla to take up the nutrients released during Chironomus sludge degradation.

To achieve a well-functioning real-life treatment cascade, the next focus should be on how to scale up these processes, both in time and space. Our experiment was performed under favourable conditions for the organisms, at 20-24 °C with 16 hours of daylight, but in practice temperatures and light conditions may be less optimal during winter periods at more northern locations. Nonetheless, both Azolla and Chironomus can grow and reproduce at 4 and 14 °C, respectively (Janes, 1998; Foucault et al., 2018), but under these conditions their growth rates are lower. Increasing light and temperature might then be an option, although this would increase costs and GHG emissions. Optimizing growth conditions for Azolla could lead to a P extraction of 1100 µmol P day⁻¹ m⁻² Azolla cover (Costa et al., 2009). Furthermore, the larval density (Hooper et al., 2003) and the harvesting rate of Azolla would also affect the efficiency of nutrient removal and sludge degradation and should be a focus of future chronic multi-generational experiments.

The proposed treatment does not require high-tech nor expensive equipment and may therefore be suitable to complement conventional wastewater treatment, especially at locations lacking the infrastructure to apply such high-tech wastewater treatment techniques. Depending on climate, water quality and sludge composition, other species combinations may be more, or less efficient in sludge degradation (Van der Meer et al., 2022b), assimilation of nutrients or GHG emission reduction (Hendriks et al., 2023). The processes described here with Chironomus and Azolla may therefore be replicated in other climates using local species. As an alternative for Azolla, phytoplankton could be used to remove nutrients and contaminants from

WWTP effluent (Mohsenpour et al., 2021), and the use of macroalgae is gaining attention as well (Ge & Champagne, 2017). The growth of filamentous algae in our experiment did indeed show that the employment of macroalgae could be a suitable option. Moreover, algae-filter feeder cascades have already been applied successfully on an experimental scale (Van der Meer et al., 2023).

The harvested *Chironomus* and *Azolla* biomass may be used as a resource for novel products, but in choosing the most appropriate application, the contaminant concentrations should be considered. For instance, *Azolla* and other floating plants are already used as feed, renewable fuels and biofertilizer (Prabakaran et al., 2022). To limit risks associated to bioaccumulation of contaminants (Liu et al., 2021), nonfood applications are preferred. Bioaccumulation of contaminants in sludge-grown *Chironomus* seems to be limited, but nonetheless contaminant concentrations did sometimes exceed allowable levels for feed and foodstuff (Van der Meer et al., 2022a).

6.4.5 Conclusions

There is an urgent need for low-budget WWTP post-treatment polishing techniques that further reduce the nutrient concentrations in the effluent, as well as the amount of produced sludge, while having a minimal GHG footprint. Here, we showed for the first time that a *Chironomus-Azolla* treatment cascade can indeed reduce P and N concentrations in wastewater treatment effluent and degrade wastewater treatment sludge, while having a minimal GHG footprint and even showing GHG sequestration. Effects of *Chironomus* and *Azolla* on greenhouse gas emission reduction and nutrient removal were additive, highlighting the benefit of a cascaded two-species system. Thus, applying cascades of organisms in wastewater treatment may be a promising tool in conforming to new EU proposed guidelines for wastewater treatment and could lead to the design of low-cost, low-tech, widely applicable treatment systems.

Acknowledgements

We would like to thank Teunis Roelofsen for assistance with collection of WWTP material, employees of the Radboud greenhouse facility, especially Harry van Zuijlen, for practical preparation before and during the experiment. Furthermore, Roy Peters, Germa Verheggen, Sebastian Krosse and Paul van der Ven for sample analysis. We'd also like to thank Arjan de Kleine for the construction of the sludge compartments, and lastly, we greatly appreciate the help with collection of samples and measurements during the experiment by Annalieke Bakker, José Paranaíba, Yvet Telgenkamp, Aniek Roelofs, Maite Erdociain and Roy van Swam.

SUPPORTING INFORMATION



FIGURE S6.1 Adult Chironomid collection device. 1: Suction hose that is aimed at adult Chironomid. 2: Collection chamber and mesh bag, mesh bag can quickly be closed after vacuuming the Chironomids. 3: Tubing with valves to allow for the adjustment of suction power. 4: Vacuum device (Princess Turbotiger).

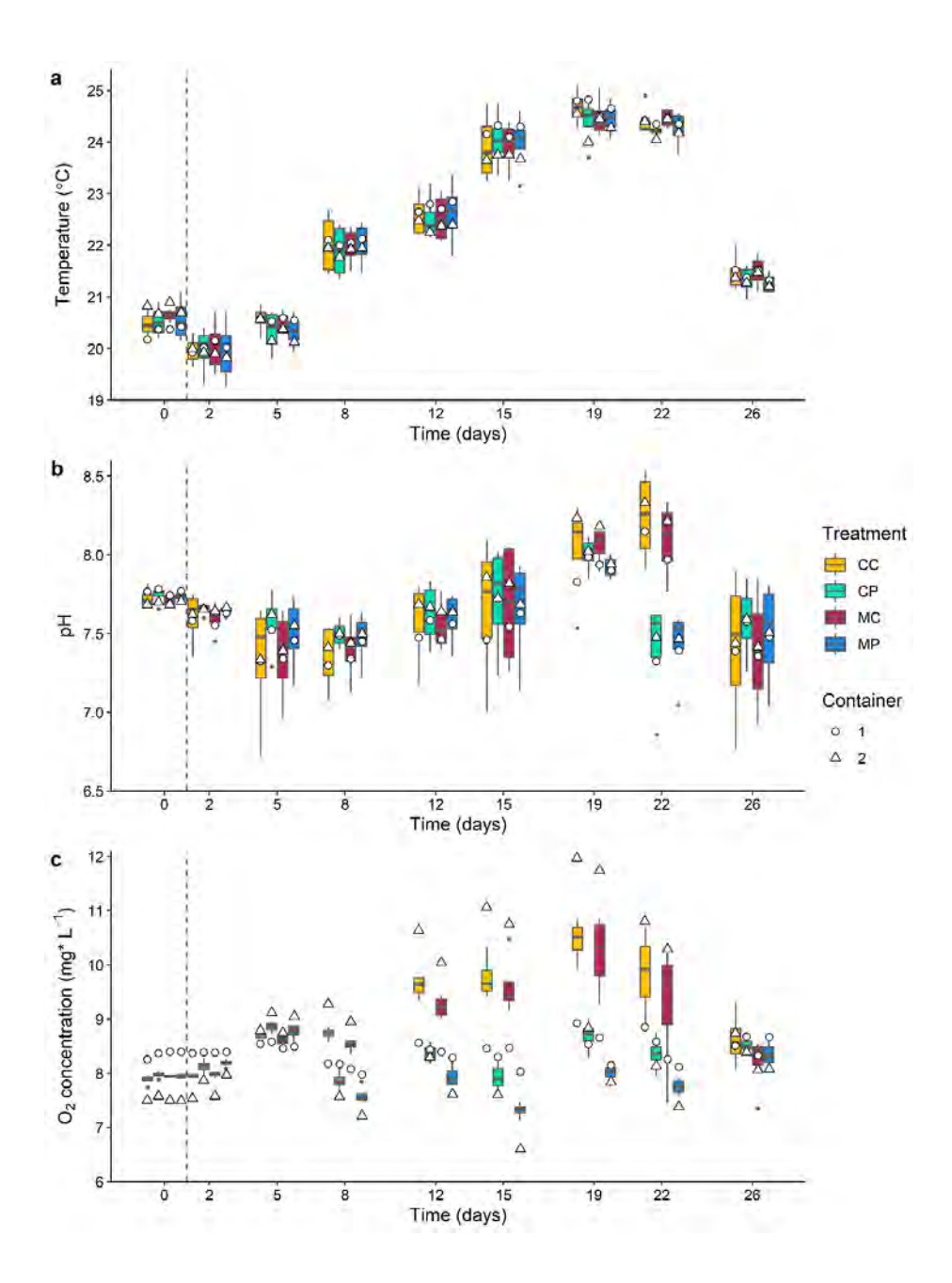


FIGURE S6.2 Temperature (°C) (a), pH (b) and dissolved O_2 concentration (mg L^{-1}) (c) in the overlying water during the 26-day experiment for the CC, CP, MC and MP treatments. Boxes show interquartile ranges, bold lines represent the median, whiskers indicate the lowest and highest values within a 1.5x interquartile range from the box, dots represent outliers. White circles and triangles represent the average concentrations in respectively container 1 and container 2.

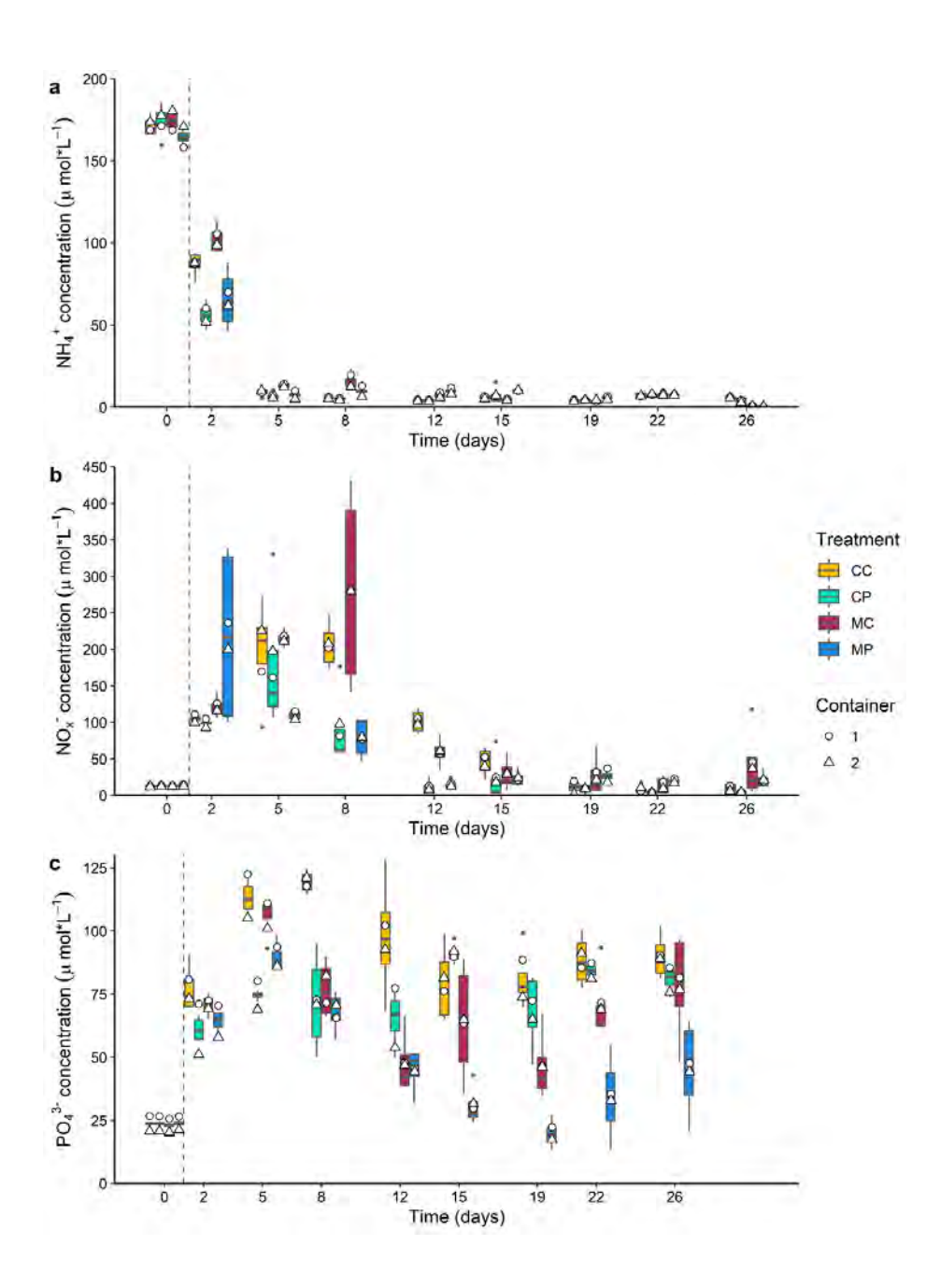


FIGURE S6.3 Dissolved NH₄⁺ (a), dissolved NO_x⁻ (b) and dissolved PO₄³⁻ (c) concentrations in the overlying water (µmol L-1) during the 26-day experiment for the CC, CP, MC and MP treatments. Boxes show interquartile ranges, bold lines represent the median, whiskers indicate the lowest and highest values within a 1.5x interquartile range from the box, dots represent outliers. White circles and triangles represent the average concentrations in respectively container 1 and container 2.

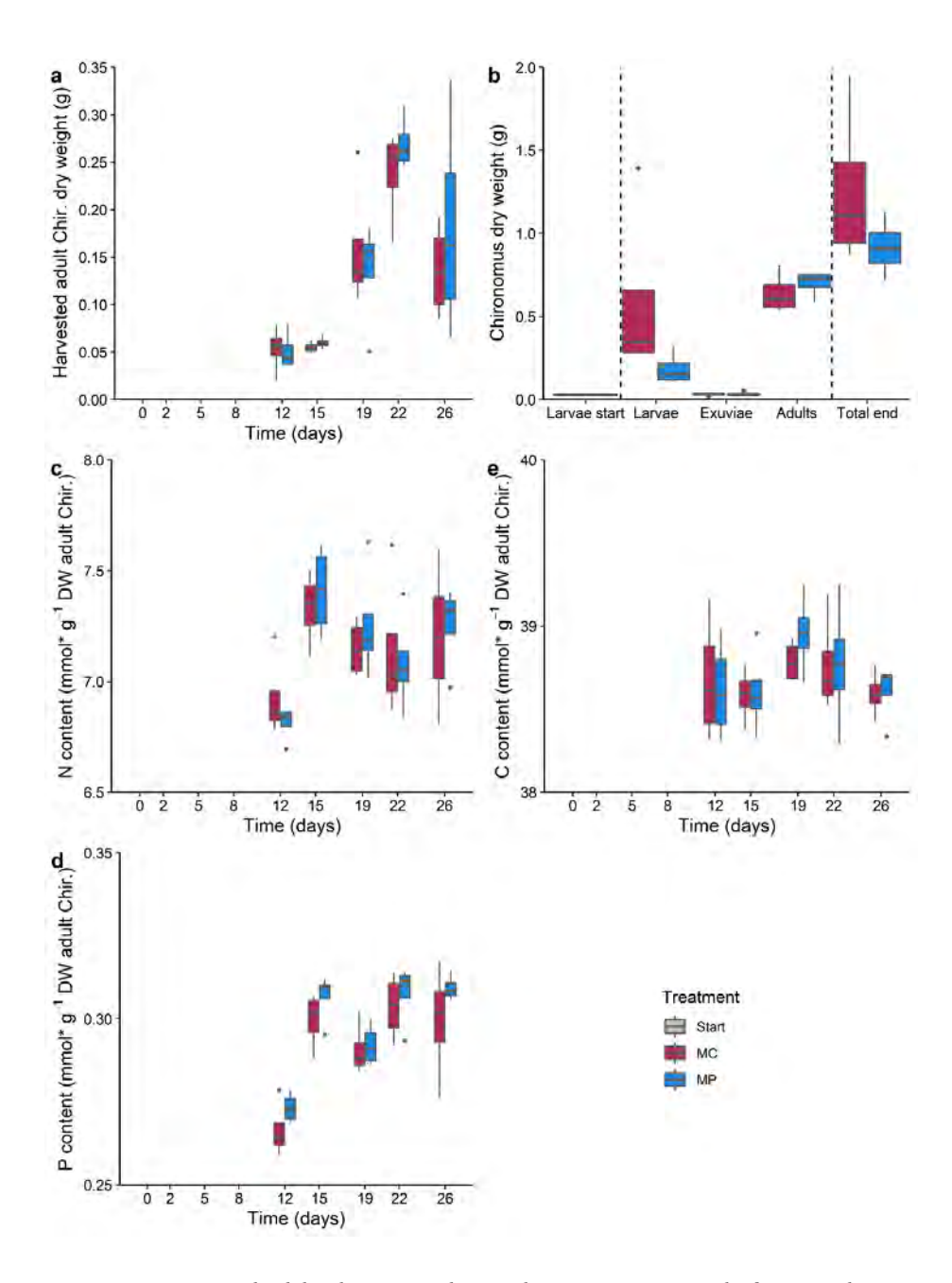


FIGURE S6.4 Harvested adult Chironomus dry weight over time (a), total *Chironomus* biomass (larvae, adults, exuviae) (b), nitrogen (c), phosphorus (d) and carbon (e) content over time, during the 26-day experimental period. Note only treatment MC and MP are shown, since these are the only treatments harbouring *Chironomus*. Boxes show interquartile ranges, bold lines represent the median, whiskers indicate the lowest and highest values within a 1.5x interquartile range from the box, dots represent outliers.

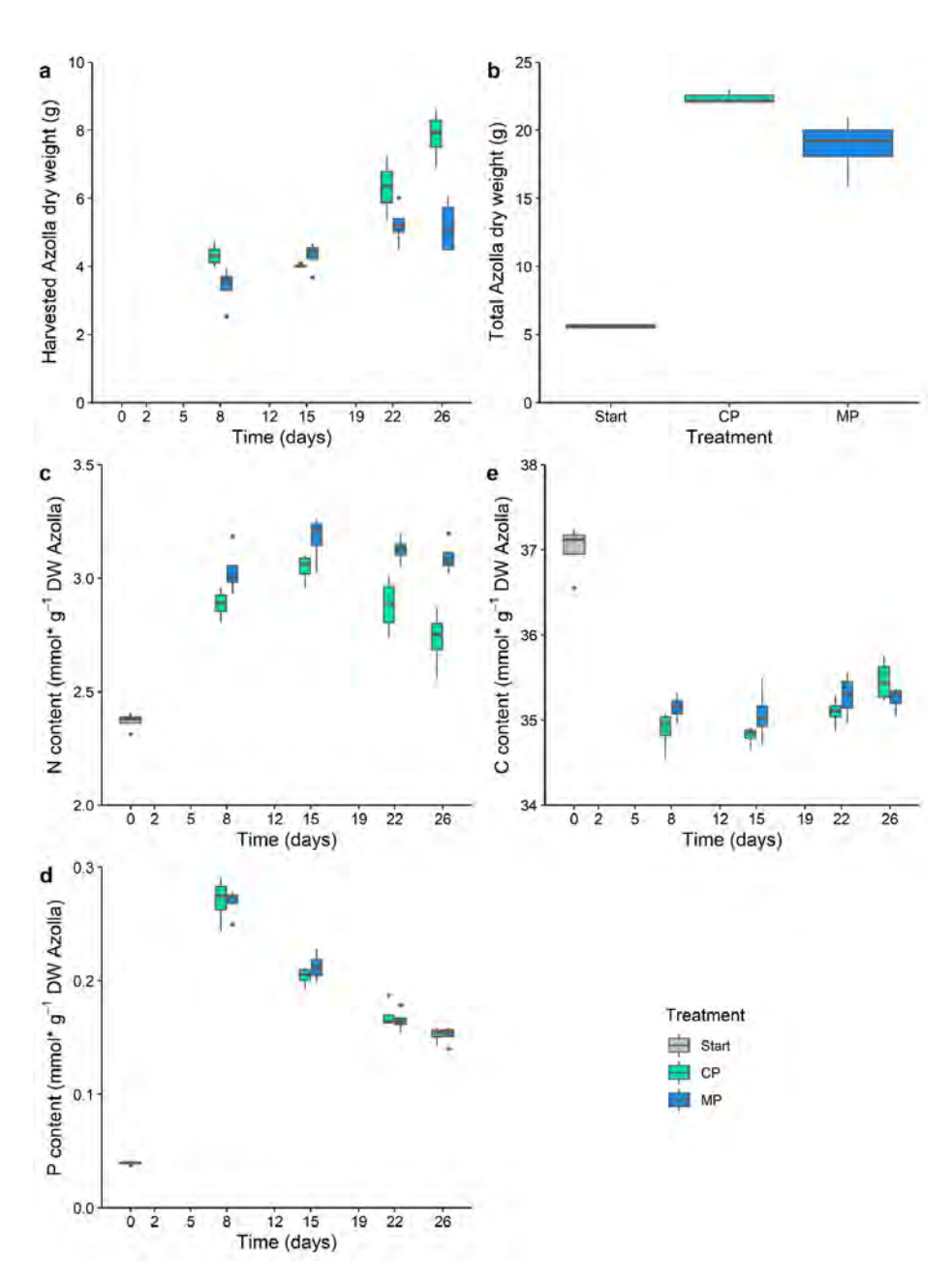


FIGURE S6.5 Harvested Azolla dry weight over time (a), total Azolla biomass (b), nitrogen (c), phosphorus (d) and carbon (e) content over time, during the 26-day experimental period. Note only treatment CP and MP are shown, since these are the only treatments harbouring Azolla. Boxes show interquartile ranges, bold lines represent the median, whiskers indicate the lowest and highest values within a 1.5x interquartile range from the box, dots represent outliers.

TABLE S6.1 Results from the Dunnett T3 post-hoc test.

Compound				t value	Pr (> t)	Signif.
Nitrogen	СР	-	CC	1.838	0.4346	
	MC	-	CC	-5.103	0.0535	
	MP	-	CC	-5.103	0.0535	
	MC	-	CP	-5.433	0.0452	*
	MP	-	CP	-5.557	0.0425	*
	MP	-	MC	1.109	0.8263	
Phosphorus	CP	-	CC	-1.178	0.7905	
	MC	-	CC	4.580	0.0712	
	MP	-	CC	3.996	0.1010	
	MC	-	CP	4.757	0.0645	
	MP	-	CP	4.219	0.0880	
	MP	-	MC	-1.278	0.7387	
Carbon	CP	-	CC	-0.017	1.0000	
	MC	-	CC	-6.068	0.0334	*
	MP	-	CC	-4.910	0.0593	
	MC	-	CP	-5.887	0.0363	*
	MP	-	CP	-4.720	0.0385	*
	MP	-	MC	1.353	0.6961	

Nitrogen, phosphorus and carbon content within the sludge is compared between treatments. t-, p-values and their significance are given. Significance (Signif.) codes: 0.001.44

TABLE S6.2 Elemental concentrations in different compartments of the experimental setup at the end of the 26-day experiment.

Trace element	Treatment	Mean ± SE in Sludge (μmol*g ⁻¹)	Mean ± SE in Water (μmol*L-1)	Mean ± SE in Azolla (μmol*g-¹)
Al	СР	128.0 ± 5.3	0.61 ± 0.11	5.47 ± 0.18
	MP	159.3 ± 6.0	0.66 ± 0.12	6.14 ± 0.85
Ca	CP	352.1 ± 13.3	897.2 ± 14.0	196.3 ± 5.3
	MP	402.3 ± 12.8	921.1 ± 6.3	157.5 ± 1.9
Fe	CP	44.2 ± 1.9	0.86 ± 0.02	4.94 ± 0.41
	MP	53.9 ± 3.1	0.79 ± 0.03	3.58 ± 0.26
K	CP	74.0 ± 3.6	219.8 ± 12.2	1018.5 ± 44.6
	MP	164.8 ± 21.9	157.3 ± 15.1	1097.2 ± 25.7
Mg	CP	116.9 ± 5.6	220.9 ± 1.9	95.0 ± 2.2
	MP	229.8 ± 30.6	185.7 ± 5.2	93.7 ± 0.7
Mn	CP	1.13 ± 0.02	0.01 ± 0.00	0.47 ± 0.03
	MP	1.02 ± 0.02	0.00 ± 0.00	0.29 ± 0.03
Na	CP	151.7 ± 5.0	2657.1 ± 27.8	331.6 ± 12.8
	MP	116.2 ± 12.5	2363.4 ± 17.7	404.8 ± 18.7
S	CP	295.9 ± 8.2	498.6 ± 2.8	128.7 ± 7.0
	MP	283.6 ± 13.4	495.8 ± 4.9	136.5 ± 7.1
Si	CP	27.1 ± 1.4	2.10 ± 0.05	11.5 ± 1.9
	MP	33.7 ± 1.6	1.57 ± 0.14	5.85 ± 0.78
Zn	CP	13.6 ± 0.5	0.67 ± 0.04	2.04 ± 0.13
	MP	19.9 ± 1.0	0.63 ± 0.03	1.45 ± 0.07
As	CP	0.05 ± 0.01	0.00 ± 0.01	0.03 ± 0.02
	MP	0.04 ± 0.01	0.00 ± 0.01	0.00 ± 0.03
В	CP	2.41 ± 0.10	3.51 ± 0.02	2.06 ± 0.03
	MP	3.14 ± 0.14	3.49 ± 0.11	1.95 ± 0.01
Cd	CP	0.01 ± 0.00	0.00 ± 0.00	0.00 ± 0.00
	MP	0.01 ± 0.00	0.00 ± 0.00	0.00 ± 0.00
Co	CP	0.03 ± 0.00	0.02 ± 0.00	0.01 ± 0.00
	MP	0.03 ± 0.00	0.01 ± 0.00	0.01 ± 0.00
Cr	CP	0.29 ± 0.01	0.00 ± 0.01	0.04 ± 0.02
	MP	0.38 ± 0.02	0.00 ± 0.00	0.00 ± 0.02

TABLE S6.2 Continued.

Trace element	Treatment	Mean ± SE in Sludge (μmol*g¹)	Mean ± SE in Water (μmol*L-1)	Mean ± SE in Azolla (μmol*g ⁻¹)
Cu	CP	3.06 ± 0.10	0.11 ± 0.01	0.39 ± 0.01
	MP	4.37 ± 0.17	0.07 ± 0.01	0.25 ± 0.01
Hg	CP	0.00 ± 0.00	0.00 ± 0.00	0.00 ± 0.00
	MP	0.00 ± 0.00	0.00 ± 0.00	0.00 ± 0.00
Мо	CP	0.06 ± 0.00	0.00 ± 0.00	0.01 ± 0.00
	MP	0.04 ± 0.00	0.00 ± 0.00	0.01 ± 0.00
Ni	CP	0.23 ± 0.01	0.04 ± 0.00	0.03 ± 0.00
	MP	0.29 ± 0.01	0.04 ± 0.01	0.03 ± 0.00
Pb	CP	0.24 ± 0.01	0.00 ± 0.00	0.01 ± 0.00
	MP	0.30 ± 0.01	0.00 ± 0.00	0.01 ± 0.01
Sr	CP	0.55 ± 0.01	1.25 ± 0.01	0.33 ± 0.01
	MP	0.63 ± 0.02	1.26 ± 0.02	0.28 ± 0.01



Chapter 7

Combination of Azolla Filiculoides and duckweed for municipal wastewater effluent polishing in a year-round pilot at a wastewater treatment plant

Lisanne Hendriks, Hugo Beekelaar, Mandy Velthuis, Jeroen J.M. de Klein, Roy Peters, Stefan T.J. Weideveld, Alfons J.P. Smolders, Leon P.M. Lamers, Annelies J. Veraart

In preparation

ABSTRACT

Since municipal wastewater effluent discharge still contributes to eutrophication in receiving water bodies, there is a need for effluent polishing to remove excess nutrients. Here, we propose a natural effluent polishing technique using floating plants in a controlled system without any sediment. To test the nutrient uptake efficiency and CO2 uptake of two functional groups of floating plants, we grew the water fern Azolla filiculoides and duckweed (a mix of Spirodela polyrhiza, Lemna minor, and L. minuta) on wastewater effluent in a year-round experiment at a wastewater treatment plant. The floating plants were grown in cascading tanks of 300 L, containing either one single plant-type or both plant-types in different sequences. All four treatments were run in duplicate. We assessed nutrient removal efficiency for a full seasonal cycle (October - October) and with two different flow rates: 24 or 12 L h-1. To determine the climate impact of plant-mediated effluent polishing, we measured greenhouse gas fluxes (carbon dioxide, methane and nitrous oxide) on six occasions during the year. Furthermore, we constructed a model to assess the effect of hydraulic residence time and harvesting frequency on phosphorus removal efficiency. Plant growth and nutrient removal took place throughout the experiment, including colder winter months. Plant growth was higher in summer, but this did not increase nutrient removal efficiency. A lower flow rate increased nitrogen removal by 20-60%, probably due to higher nitrification rates, while it did not increase phosphorus removal, which was in accordance with low phosphorus content of the plants. Yet, modelled phosphorus removal did increase at a longer hydraulic residence time. Azolla showed highest carbon sequestration, especially in summer where carbon dioxide uptake resulted in a net greenhouse gas uptake of 25 g CO2-eq m-2d-1. In winter, however, peak emissions of nitrous oxide were observed, leading to a net emission of greenhouse gases of 8 g CO2-eq m-2d-1. The cascades in which duckweed was placed before Azolla had highest mean nutrient removal rates, showing that dual-plant cascades perform better than single-plant cultivation, and that the plant sequence matters. Modelled phosphorus removal rates peaked at weekly harvesting. Nutrient removal efficiency was on average 40% but peaked at 97% at different times during the year. Thus, effluent polishing combining floating plant species may be a promising low-cost, low-emission, effluent polishing solution.

7.1 INTRODUCTION

While an estimated 360 × 109 m3 yr-1 of wastewater is produced globally, only 52% of this wastewater is being treated before discharge. Especially in low-income countries only 4% of wastewater receives treatment (Jones et al., 2021). Consequently, untreated or poorly treated wastewater causes eutrophication at discharge sites, impacting human health, ecosystems and freshwater quality (WWAP, 2017). Furthermore, eutrophication increases greenhouse gas (GHG) emissions from those receiving waterbodies (Upadhyay et al., 2023; Hu et al., 2018; Alshboul et al., 2016; Peterse et al., in prep.).

Yet, rather than seeing wastewater only as a problem, it can also be seen as a source of energy, nutrients and other useful products and thereby wastewater treatment and reuse can contribute to a circular economy (WWAP, 2017; Qadir et al., 2020). Wastewater treatment and reuse is gaining momentum, and high-tech solutions, such as direct membrane separation or membrane bioreactors, are gaining interest (Hube et al., 2020; Ahn et al., 2001). However, such solutions may be unsuitable for low-income countries, that cannot afford these types of treatment. Additionally, these high-tech treatments contribute to GHG emissions (Chen, 2019). Therefore, a low-cost and efficient wastewater treatment process could help in reaching the sustainable development goal (SDG) 6.3, which states to reduce the proportion of untreated wastewater and to increase reuse (Alcamo, 2019).

Aquatic plants can be used in water treatment. They are adapted to achieve optimal uptake of nutrients such as nitrogen (N) and phosphorus (P) and have high potential growth rates. This results in high biomass yields when nutrients are abundant. Additionally, they influence the production and emission of GHGs. In the past decades, constructed wetlands (CWs) have been successfully applied in areas lacking conventional sanitation infrastructure, but upscaling of these systems poses some challenges (Vymazal et al., 2021). The plants in CWs are mostly indirectly removing nutrients, by stimulating nitrification-denitrification and enhancing P binding to the sediment (e.g. Sun et al., 2019; Vymazal, 2013), and it is unclear which part of the removed nutrients or other toxic compounds are being released to the water column again, for example by plant decomposition (Menon and Holland, 2014). CWs are found to substantially emit GHGs, especially N2O (Wu et al., 2017; Zhang et al., 2019). Also, treatment by CWs needs a long residence time of the pre-treated wastewater, called effluent, meaning it needs a lot of space which is in most cases limited (Sarmento et al., 2013; Ghosh and Gopal, 2010). By using aquatic plants in a more controlled system, the plants can directly take up nutrients and by harvesting the plants, the nutrients can be permanently removed from the water column to be re-used. Furthermore, residence time of the effluent in such controlled system may be reduced, making it more efficient. Floating plants are very efficient in removing nutrients from effluent and additionally reduce GHG emissions through carbon uptake and lowered methane (CH4) and nitrous oxide (N2O) production (Hendriks et al., 2023).

Different floating plant-types have different specific plant-traits. For example, Azolla can efficiently remove P from the water column, because it overcomes potential N-limitation by its symbiosis with diazotrophs (Temmink et al., 2018). Duckweed species, such as Lemna and Spirodela (belonging to the Araceae family), are efficient N removers (Hendriks et al., 2023, Ng and Chan, 2018). A combination of these floating plant-types can therefore result in community trait-combinations leading to optimal N and P removal and CO2 uptake. To prevent interspecific competition and to optimise growth conditions for specific plant-types, the plants can be grown in a cascade set-up. The sequence in which the plants are placed may play a role: Azolla first – duckweed second is hypothesized to optimize N-removal, but duckweed is predicted to grow less biomass due to P limitation. Duckweed first – Azolla second will likely optimize P-removal - or P harvesting and biomass production - but will potentially lead to reduced N-removal (Hendriks et al., subm).

Plant treatment efficiency and plant-type combinations have mostly been tested in batch experiments under controlled circumstances (e.g. Garcia Chance et al., 2020; Sudiarto et al., 2019). In these cases, seasonal changes are not considered, even though these may affect nutrient-removal efficiency and plant growth, as these vary with temperature and light availability. Therefore, the goal of this study was I) to determine the efficiency of a pilot-scale cascade with two plant-types (Azolla and duckweed) and assess its optimal sequence, II) to determine the effect of seasonality on treatment efficiency and GHG emission, and III) to assess the impact of effluent residence time and harvesting frequency on the treatment efficiency of the cascade. We expected that a cascade including both plant-types would work better than one with one plant-type, and that the most efficient sequence depends on the way both plant-types take up N and P (hypothesis(H)1). Furthermore, we expected effluent polishing to be more efficient during warmer months due to a higher growth rate of the plants (H2) and expected an increase in nutrient removal with a longer residence time (H3a) and increased amount of harvesting (H3b). In addition, we expected GHG sequestration, especially during the growing season (H4).

7.2 METHODS

This study assessed whether a combination of Azolla filiculoides (further referred to as Azolla) and duckweed (a mix of Spirodela polyrhiza and Lemna spp.) enhances nutrient removal in municipal wastewater effluent polishing compared to a single cultivation of those plant-types and quantified differences in species-sequence. It was tested whether such effluent polishing is possible on a pilot scale at a Wastewater Treatment Plant (WWTP) and assessed the effects of season, hydraulic residence time and harvesting frequency on such a system. During this experiment GHG fluxes were additionally measured to assess emissions during effluent polishing.

7.2.1 Experimental setup

Four treatments were used: a single cultivation of *Azolla* (AA), a single cultivation of duckweed (DD), *Azolla* followed by duckweed (AD) and duckweed followed by *Azolla* (DA). All treatments were run in duplicates (Fig. 7.1a).

This experiment took place in a polytunnel greenhouse located at a municipal WWTP in Remmerden, The Netherlands (for details, see Hendriks et al., 2023). A total of eight cascading tanks (8 x 0.31 x 0.12 m) were set up, each harbouring ~300 L of municipal wastewater effluent (Fig. 7.1). To avoid confounding microclimatic effects in the greenhouse, one cascade of each treatment was placed in a group (a or b), in which treatment location was randomly distributed. The greenhouse was not heated and did not have extra lighting. The experiment ran for 12 months, from October 20th 2022 till October 31st 2023.

The cascades were set up as a flow-through system, with effluent entering in point 1 at plant-type 1 (*Azolla* or duckweed), followed by plant-type 2 after point 2 and leaving the cascade at point 3, where the water was collected and recirculated back to the WWTP. Each cascade had its own peristaltic pump (EcoAdd-ES-12003M-PFC-00S-1S-SO, EcoLab, Wallisellen, Switzerland), adding effluent directly from the WWTP at a speed of 24 L h⁻¹, resulting in a residence time of 12 hours for one cascade. In the last month of the experiment (October 2023), the water flow rate in half of the cascades (replicate a) was reduced to 12 L h⁻¹ to determine the difference in growth and nutrient removal with a longer hydraulic residence time.

Azolla filiculoides used in the experiment was harvested from cultures maintained at Radboud University Nijmegen, The Netherlands. Starting duckweed species Spirodela polyrhiza was collected from a local pond (51°50′02.2″N 5°51′52.2″E). Both plant-types were grown on nutrient poor rainwater for two weeks before being grown in effluent

at the greenhouse facility in Remmerden for 6 weeks to acclimatize. On day '-1', the cascades were filled with effluent water directly from the WWTP. At day 0, 50% of the surface area of the tanks were covered by their assigned plant-type, corresponding to a dry biomass of approximately 44.0 (±2.5) gram of *Azolla* and 26.5 (±1.5) gram of *Spirodela*, after which the plants were dispersed over the entire tank surface.

7.2.2 Treatment performance measurements

To test the performance of the treatment cascades, in terms of nutrient removal and biomass production, water column total and dissolved nutrient concentrations, trace metals, and plant biomass were monitored at regular intervals. From October 2022 to January 2023 measurements were done every week, after which measurements were done every two weeks for the remainder of the experiment, with the exception of the period between 28-02 and 21-03-2023, in which measurements were done at a three-week interval. Additionally, GHG fluxes were measured in the cascades on six occasions, spread over the seasons. Four measuring points were chosen in each cascade: at the inflow, receiving fresh wastewater treatment effluent (*inflow*), *Point 1* directly after the inflow, *Point 2* at the intersection between plant-type 1 and 2, and *Point 3* at the outflow of the cascade (Fig. 7.1b). Furthermore, two water samples from the intermediate bulk container (IBC) were taken as start effluent concentrations.

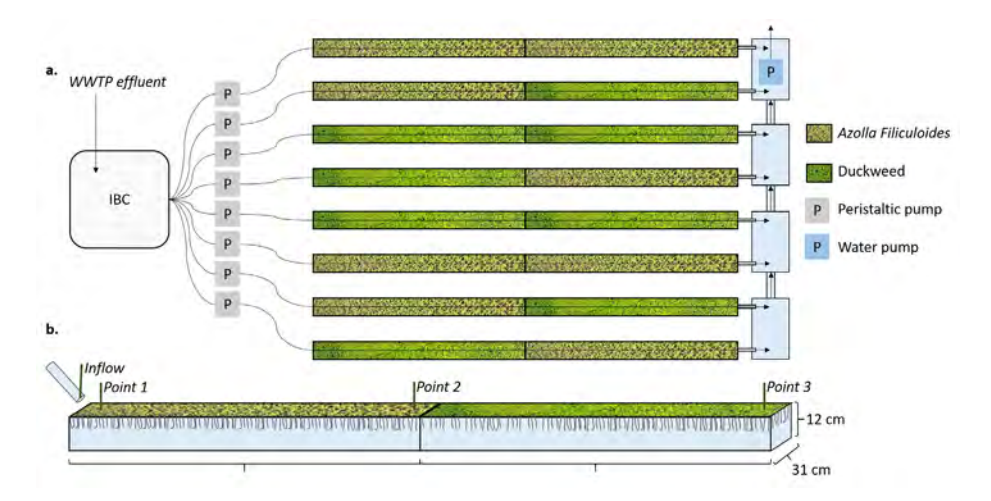


FIGURE 7.1 Schematic overview of the experimental set-up from above (a) and a side-view of a cascade-example, including dimensions and sampling points (b). Effluent flowed directly from the WWTP through an intermediate bulk container (IBC), after which it was led through eight peristaltic pumps into the different cascades. Treated water at the end of the cascades was collected in containers and pumped back to the WWTP system.

7.2.2.1 Water column conditions

Concentrations of NH $_4^+$, NO $_3^-$ and PO $_4^{3^-}$ were measured colorimetrically in rhizon-filtered samples (membrane pore size 0.12/0.18 µm, Rhizon SMS 10 cm, Rhizosphere Research, Wageningen, The Netherlands) on an auto analyzer III (Bran and Luebbe GmbH, Norderstedt, Germany) after being stored at -20 °C. Trace elements (Al, Ca, Fe, K, Mg, Mn, Na, P, S, Si, Zn, As, B, Cd, Co, Cr, Cu, Ni, Sr, Hg) were measured in unfiltered, acidified water (0.1 ml 10% nitric-acid) on an ICP-OES (IRIS Interpid II, Thermo Fisher Scientific, Franklin, MA, USA) after being stored at 4 °C. Total organic carbon and total bound nitrogen (TOC and $\mathrm{TN_b}$) were measured in unfiltered, fixated water (20 µl 2000 ppm HgCl $_2$) after being stored at 4 °C, by combustion at 780 °C with a Focus Radiation NDIR detector (Multi N/C3100, Analytik Jena, Jena, Germany). Samples were measured 2-3 times and averaged. The pH, temperature (°C) and dissolved O $_2$ concentrations (mg L $^{-1}$) in the water column of each point in the cascades were measured using a Portable Multi Meter (HQ2200, HACH, Loveland, CO, USA).

7.2.2.2 Biomass production and nutrient uptake

After water sampling and physico-chemical measurements, part of the plants was harvested manually. Most times this was 50% of the total biomass, but occasionally this was changed to 25%, 33%, 66% or 75%, depending on the growth that was observed in the weeks before with the goal to set the biomass back to such a state that no space limitation would occur within the 2-week growth period between harvests. The harvested biomass was dried at 70 °C for two weeks and the dry weight was measured. The dry weight was then multiplied by the percentage harvested to estimate the total biomass that was present in the cascades before harvest.

The plants harvested on November 1st 2022, March 21st 2023, July 11th 2023 and October 31st 2023 (spread over the seasons), were used for further analysis of C, N, P and trace element uptake. C and N content was determined in ground plant material (3 mg) using an elemental CNS analyser (NA 1500, Carlo Erba; Thermo Fisher Scientific, Franklin, USA). Elemental content was determined on the above mentioned ICP-OES after microwave digestion, adding 5 ml HNO $_3$ (65%) and 2 ml H $_2$ O $_2$ (35%) to 200 mg ground material in Teflon vessels, followed by heating in an EthosD microwave (Milestone, Sorisole Lombardy, Italy).

7.2.2.3 Greenhouse gas fluxes

Measurements of CO₂, CH₄ and N₂O were done on November 1st 2022, December 6th and 12th 2022, June 13th 2023 and October 31st, 2023. GHG fluxes were measured at point 1, 2 and 3 of every cascade using a Greenhouse Gas Analyser (G2508, Picarro, Santa Clara, CA, USA) connected to a transparent acrylic glass floating chamber

(3.18 dm³ headspace). At each point, diffusive fluxes were measured over a period of four minutes, counted from when concentrations started to change, which happened in each case. In between measurements, aeration took place to return gas concentrations to atmospheric levels. GHG fluxes (mg m⁻² d⁻¹) were calculated according to Hendriks et al. (2024a). All fluxes of CH₄, CO₂, and N₂O were checked to exceed the flux detection limit (i.e. 0.05, 8.62 and 0.36 mg m⁻² d⁻¹ for CH₄, CO₂ and N₂O, respectively) and otherwise noted as 'o' (Christiansen et al., 2015; Nickerson, 2016). A global warming potential of 27 for CH₄ and 273 for N₂O (100-year time frame; IPCC 2021) was used to convert fluxes to CO₂ equivalents.

7.2.3 Data analysis

All data analysis was performed in R (version 4.2.0; R Core team, 2021). Removal efficiency was calculated from concentrations at point 1 and point 3, in each cascade, on each timepoint. Mean nutrient and trace element removal efficiency was then calculated by averaging the linear interpolation between datapoints for each individual cascade followed by averaging between the replicates. Linear interpolation was also used to obtain C, N and P content of the plants.

For PO $_4^{3-}$, 16 out of the 807 PO $_4^{3-}$ datapoints were removed because the measured PO $_4^{3-}$ concentrations were more than 2.5 times higher than TP concentrations, and hence considered analytical outliers. Furthermore, on November 23rd 2022, all PO $_4^{3-}$ were unexpectedly high (> 200 μ mol L $^{-1}$), probably due to malfunctioning of the WWTP on that day. Therefore, data obtained on this date were not used in statistical analysis.

Seasonal patterns of physico-chemical conditions in the water column, plant biomass and GHG emissions were assessed using linear mixed-effects models (LMM (*lmer*), package *lme4*; Bates et al., 2015). Based on the measurement date, each sample was attributed to their corresponding meteorological season: spring: 1 March–1 June; summer: 1 June–1 September; autumn: 1 September–1 December; winter: 1 December–1 March. In the model, meteorological season was used as fixed effect and day and treatment as crossed random effects. Normality of the residuals of the model was visually checked using a histogram. The significance of fixed effects was statistically tested using a type-III ANOVA (*anova*, package *stats*) with degrees of freedom (*df*, approximated) and *p*-values calculated using the Kenward–Roger approximation (package *lmerTest*; Kenward & Roger, 1997) via the lmerTest and pbkrtest packages (Kuznetsova et al., 2017). Pairwise comparisons, using Tukey adjustment, were performed using *emmeans* (package *emmeans*; Lenth, 2022). The same method was used for comparison of physico-chemical conditions in the water column and GHG fluxes between treatments, with day as random effect.

The effect of flow rate on nutrient removal efficiency was analysed by a t-test (t.test, package stats) when the data were normally distributed (PO_4^{3-} , NH_4^+ , TP) or by a Mann-WhitneyWilcoxon test (wilcox.test, package stats) when normality was not met (TN_b). The effect of flow rate and plant-type on plant C, N and P content was analysed by a Mann-Whitney-Wilcoxon test since all data were not normally distributed. The relationship of temperature with plant biomass was calculated using a linear model (lm, package stats) for each plant-type. The effect of plant-type and position within the cascade on plant biomass was analysed by a Mann-Whitney-Wilcoxon test.

7.2.4 P-removal and plant uptake model

To better understand the impact of changes in hydraulic residence time and harvesting frequency on P-removal efficiency in our experimental system, we constructed a model in Duflow[®], which is a one-dimensional modeling package for water quality and movement (STOWA / MX-systems, 2004). For simplicity, we only focused on P-removal, as this excludes complex microbial interactions involved in nitrogen cycling. Here, we assume that PO_4^{3-} loss from the cascade is solely due to plant uptake, and particulate P (PP, defined as $PP = TP - PO_4^{3-}$) settles down in cascade-compartments over time. Briefly, species-specific plant growth was assumed P-dependent, following Monod equations. Maximum growth rates and plant P-content were based on experimental data, while half-saturation constants were based on literature values. The entire model description can be found in S7.1.

7.3 RESULTS

7.3.1 Physico-chemical conditions in the water column

During the one-year experiment, pH ranged between 6 and 7.5 (av. 6.47) and did not differ between seasons (LMM: p=0.09), but did between treatments (LMM: $F_{3.537}=5.333$, p=0.001). The pH of treatment AA was significantly higher than that of treatment DD (t=3.665, p=0.0015) and DA (t=3.218, p=0.0075). Dissolved O₂ concentrations were always lower than 7 mg L⁻¹ and on average 3.08±1.36 (sd.) mg L⁻¹, with treatment AD having the lowest dissolved O₂ concentrations in the complete cascade (av. 2.96 mg L⁻¹). No seasonal difference in dissolved O₂ concentration was found (LMM: p=0.07). Water temperature did not differ between treatments (LMM: p=0.29), but did differ between seasons (LMM: $F_{3,20}=10.979$, p<0.001), with highest temperatures of av. 28.6 °C in June and lowest of av. 7.5 °C in January (Fig. S1).

7.3.2 Change in duckweed species during the year

Starting duckweed species was *Spirodela polyrhiza*, but this changed during the experiment. After two weeks *Lemna minor* appeared, and in January the whole compartment was covered by *Lemna minor* and *L. minuta*. Both species co-existed until the end of the experiment. In the *Azolla* compartment, the dominant species was *Azolla filiculoides*, but underneath the plants some *L. minor* and *L. minuta* was growing.

7.3.3 Nutrient and trace element removal efficiency

The mean interpolated removal efficiency for N and P over the whole experimental period differed between treatments (Fig. 7.2). Over the year, removal of $PO_4^{\ 3^-}$, $NH_4^{\ +}$, TP and TN_b took place for respectively 77.5, 87.9, 84.7 and 85.6% of the time. Mean end concentrations of $PO_4^{\ 3^-}$ ranged between 7.7 and 10.3 μ mol L⁻¹, whereas for TP, this was between 14.3 and 16.8 μ mol L⁻¹. Mean final concentrations of $NH_4^{\ +}$ and $TN_b^{\ -}$ ranged between 76.1 and 96.3 and between 184.4 and 210.6 μ mol L⁻¹, respectively (Table 7.1). Treatment DD had the highest mean $PO_4^{\ 3^-}$ removal efficiency with a removal of 43.55% and removal rate of 17.71 μ mol L⁻¹d⁻¹ (Table 7.1). Treatment DA had highest mean removal efficiency for $NH_4^{\ +}$ (44.21%), $TN_b^{\ -}$ (30.82%) and TP (33.04%). No clear seasonal pattern in removal efficiency of N was observed, while a dip in efficiency of $PO_4^{\ 3^-}$ and TP removal was found in summer.

TABLE 7.1 Mean start concentration, final concentration and removal rate of $PO_4^{3^-}$, TP, NH_4^+ and TN for each treatment during the one-year experiment.

Treatment					
Element		AA	DD	AD	DA
PO ₄ 3-	Start (µmol L-1)	11.64	21.26	13.80	16.75
	Final (μmol L ⁻¹)	10.33	7.65	8.54	8.59
	Removal rate (μmol L ⁻¹ d ⁻¹)	5.06	17.71	8.19	10.82
TP	Start (µmol L-1)	20.51	21.44	21.21	21.87
	Final (μmol L ⁻¹)	15.04	14.90	16.81	14.34
	Removal rate (μmol L-1d-1)	10.46	13.76	5.52	13.08
$\mathbf{NH}_{_{4}}^{^{+}}$	Start (µmol L-1)	124.52	140.95	151.61	163.61
	Final (μmol L ⁻¹)	76.09	96.27	80.02	86.82
	Removal rate (μmol L-1d-1)	96.85	89.38	103.32	83.74
TN	Start (µmol L-1)	254.73	263.35	232.15	250.88
	Final (μmol L ⁻¹)	201.78	210.55	188.94	184.36
	Removal rate (µmol L-1d-1)	105.91	105.60	86.42	133.04

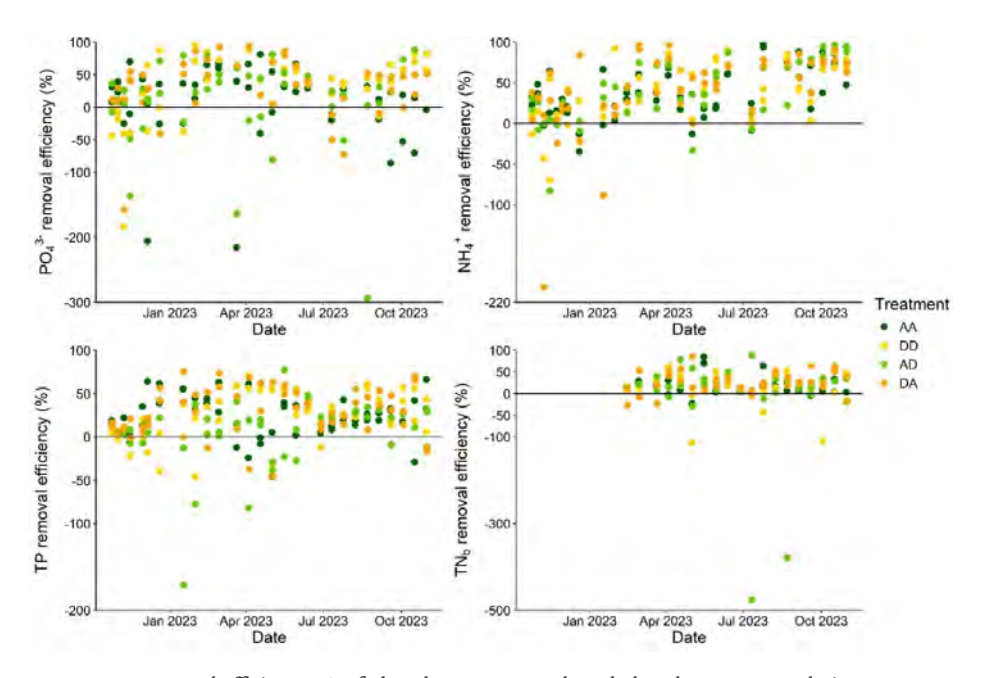


FIGURE 7.2 Removal efficiency (%) of phosphorus (PO $_4^{3-}$ and total phosphorus (TP)) and nitrogen (NH $_4^{+}$ and total nitrogen bound (TN $_b$)) during the one-year experimental period. Each treatment consisted of duplicates, both are shown in the figures. Note the differences in Y-axes. Negative removal efficiency indicates a net release of nutrients.

Flow rate affected NH₄⁺ (t(11) = 2.87, p = 0.01) and TN_b (W = 107, p = 0.04) removal efficiency, where a lower flow rate and thus longer hydraulic residence time, resulted in a 21% and 58% higher removal efficiency of NH₄⁺ and TN_b, respectively. A lower flow rate did not increase PO₄³⁻ or TP removal efficiency (p = 0.47; p = 0.31), although visibly there is a trend in a higher PO₄³⁻ removal efficiency at a lower flow rate in treatment AA (Fig. 7.3).

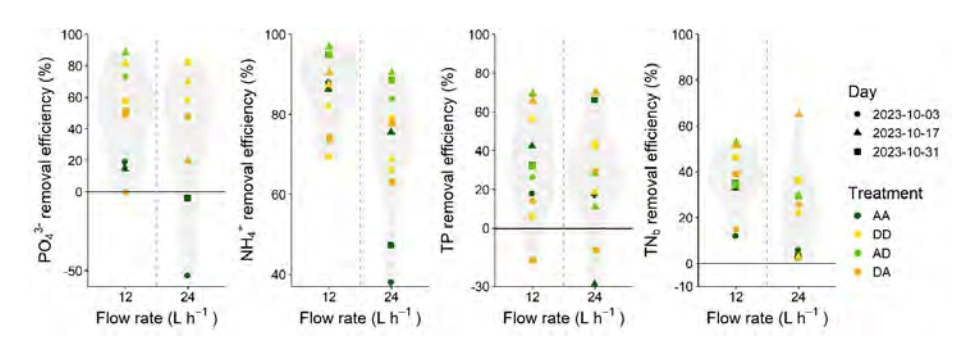


FIGURE 7.3 Difference in nutrient removal efficiency between a flow rate of 12 L h^{-1} (replicate a) and 24 L h^{-1} (replicate b) in the last month of the one-year experimental period. Note the differences in Y-axes.

Modelled PO $_4^{3^{\circ}}$ removal efficiency differed with hydraulic residence time, where a longer residence time, and thus a lower flow rate, resulted in a higher P removal efficiency. Modelled treatments including only duckweed achieved highest removal rates (Fig. 7.4). Since the model did not account for differences in growth resulting from plant position in the cascade, treatment AD and DA show the same removal efficiency. Modelled average particulate P removal due to settling was 33% at a flow rate of 24 L h $^{-1}$ and 53% at 12 L h $^{-1}$, and was independent of treatment.

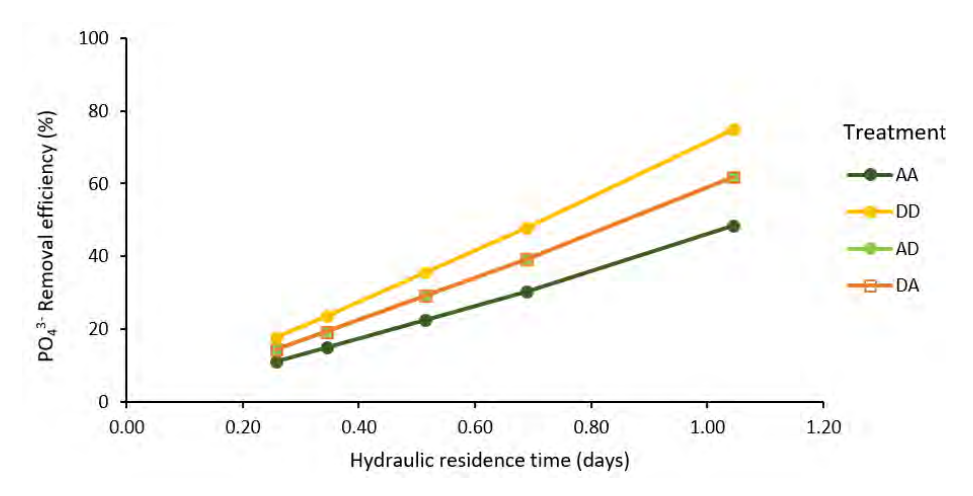


FIGURE 7.4 Modelled PO $_4^{3^{\circ}}$ removal efficiency for each treatment on different flow rates. A hydraulic residence time of 0.51 days (24 L h $^{\circ}$) is taken as baseline.

Concentrations of As, Cd, Co, Cr, Cu, Hg and Ni were below detection limit (0.063, 0.002, 0.020, 0.016, 0.037, 0.005 and 0.039 μ mol L⁻¹, respectively) during the year. Al, Fe, Si, Mn, K and Zn removal efficiency was generally low, but with peaks respectively up to 94, 85, 89, 88, 78 and 94%. Other trace elements (Ca, Mg, Na and S) were only removed for up to 47% (Fig. S7.2). No seasonal pattern was found for trace element removal efficiency.

7.3.4 Biomass production and C, N and P uptake

Independent of the position within the cascade, *Azolla* had the highest biomass compared to duckweed over the whole year (V = 17005, p < 0.0001; Fig. 7.5). *Azolla* reached a biomass of up to 300 g dryweight (dw) m⁻², whereas for duckweed this was up to 200 g dw m⁻². In both plant-types, its position affected biomass production and lowest biomass was found with plants later in the cascade (*Azolla*: V = 3901, p < 0.0001; duckweed: V = 3137, p = 0.0001). A peak in biomass presence occurred in June and July, correlating with temperature (*Azolla*: p < 0.0001, $R^2 = 0.59$; duckweed: p < 0.0001, $R^2 = 0.47$; Fig. S7.3). Highest plant growth (biomass production) was observed in

June (av. 11.07 and 7.63 g dw m $^{-2}$ d $^{-1}$ for *Azolla* and duckweed, respectively; Fig. S7.4). Biomass production continued in winter, albeit at low growth rates of on average 1.00 and 0.17 g dw m $^{-2}$ d $^{-1}$ for *Azolla* and duckweed, respectively.

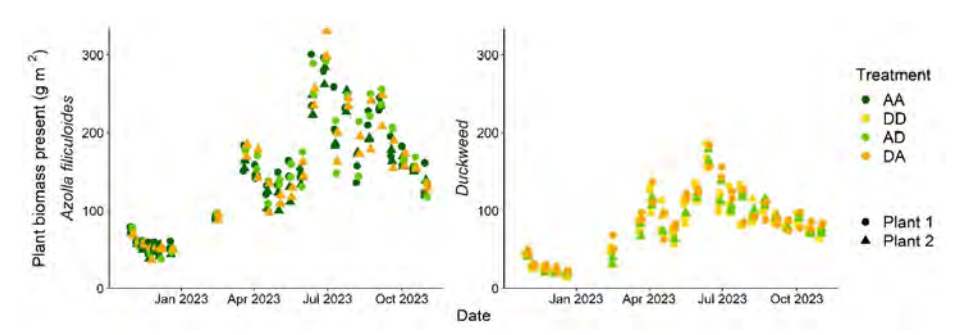


FIGURE 7.5 Azolla filiculoides and duckweed biomass (gram dryweight m⁻²) in the cascade during the one-year experimental period. Plant 1 is the first plant in the cascade, Plant 2 is second plant in the cascade.

Plant content of carbon, nitrogen and phosphorus differed between plant species (Fig. S7.5), where Azolla had highest C content per gram plant (W = 1024, p < 0.0001), and duckweed had highest N and P content (N: W = 311.5, p = 0.007; P: W = 14, p < 0.0001). The same is found when looking at total C, N and P incorporated in biomass per m^2 of the total treatment cascades (Fig. 7.6). Plant C, N and P content tended to be lower at a lower flow rate in treatments AA and DD, yet no significant difference between flow rate and C, N and P content was found (p = 0.80; p = 0.88; p = 0.80; Fig. S7.6).

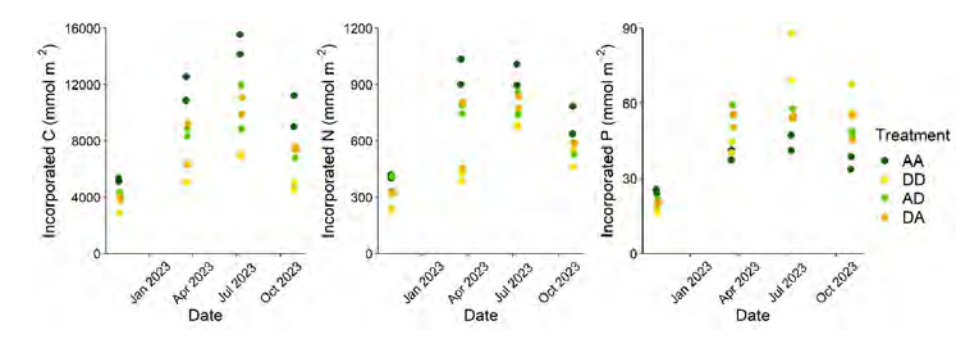


FIGURE 7.6 The amount of carbon (C), nitrogen (N) and phosphorus (P) incorporated within the total biomass in each treatment cascade during the one-year experimental period. Note the differences in Y-axes.

7.3.5 Harvesting frequency contribution to removal efficiency

Modelled PO $_4^{3-}$ removal efficiency differed between treatments, with treatment DD being the highest (Fig. 7.4; 7.7a). Even though *Azolla* produced more biomass (fig. 7.7b), modelled P removal in duckweed treatments was higher than in *Azolla*

treatments, due to the higher P-content of duckweed (Fig. S7.5). P-removal efficiency also differed between different harvesting frequencies, with optimal removal efficiency at weekly harvesting (Fig. 7.7a).

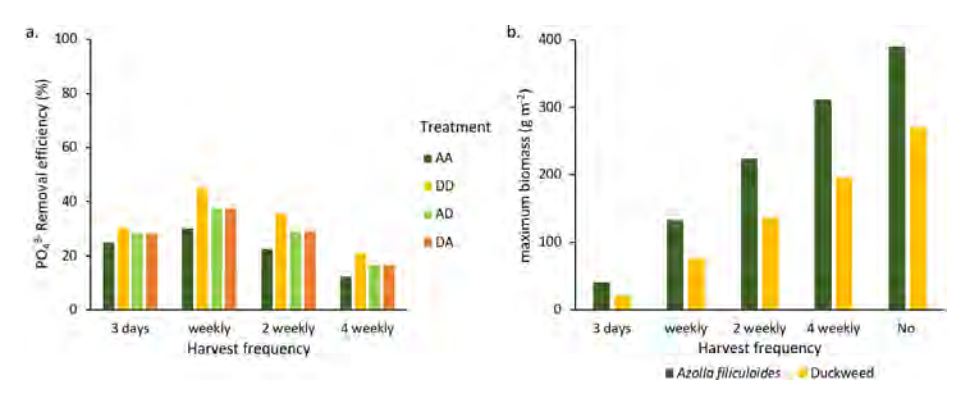


FIGURE 7.7 PO $_4$ removal efficiency for each treatment when harvesting every 3 days, every week, two weeks or four weeks (a), and maximum biomass presence at these harvesting frequencies (b).

7.3.6 Greenhouse gas emission

Total greenhouse gas fluxes (CO_2 , CH_4 and N_2O combined) followed a visual seasonal pattern, although fluxes did not significantly differ between seasons (p=0.08; Fig. 7.8). In summer, all treatments showed a net uptake of GHGs, with treatment AA having the highest total GHG uptake, corresponding to the highest uptake of CO_2 within this treatment (Fig. S7.7a), despite a higher CH_4 emission in summer (Fig. S7.7b). In winter, all treatments showed a net GHG emission, mainly corresponding to a peak in N_2O emission at that time (Fig. S7.7c). Overall, GHG fluxes differed between treatments (LMM: $F_{3,120} = 4.857$, p=0.003), where treatment AA had significantly lower GHG fluxes than treatment DD (t=-3.744, t=0.001).

7.4 DISCUSSION

Here we have assessed effluent polishing using floating plants on a bigger scale during a year-round pilot study. We showed that plant growth and nutrient removal can take place during the whole year and that a sequence in which duckweed is placed before Azolla results in the highest average removal efficiency of NH_4^+ , TN_b and TP. Although cultivation of only duckweed showed highest $PO_4^{3^+}$ removal, Azolla had highest carbon sequestration (H4). Indeed, including both species therefore results in a higher combined nutrient removal and carbon sequestration compared to cultivation of single species (H1). As expected, in summer, the plants grew faster (H2),

however this did not directly result in higher nutrient removal efficiency. While a longer hydraulic residence time did increase N removal, it did not increase P removal, although theoretically P removal should have increased according to our model (H3a). Weekly harvesting resulted in a modelled higher P removal compared to harvesting every 2 or 4 weeks. Moreover, the model results showed that harvesting every 3 days can decrease biomass to such extent that removal of P decreases as well (H3b).

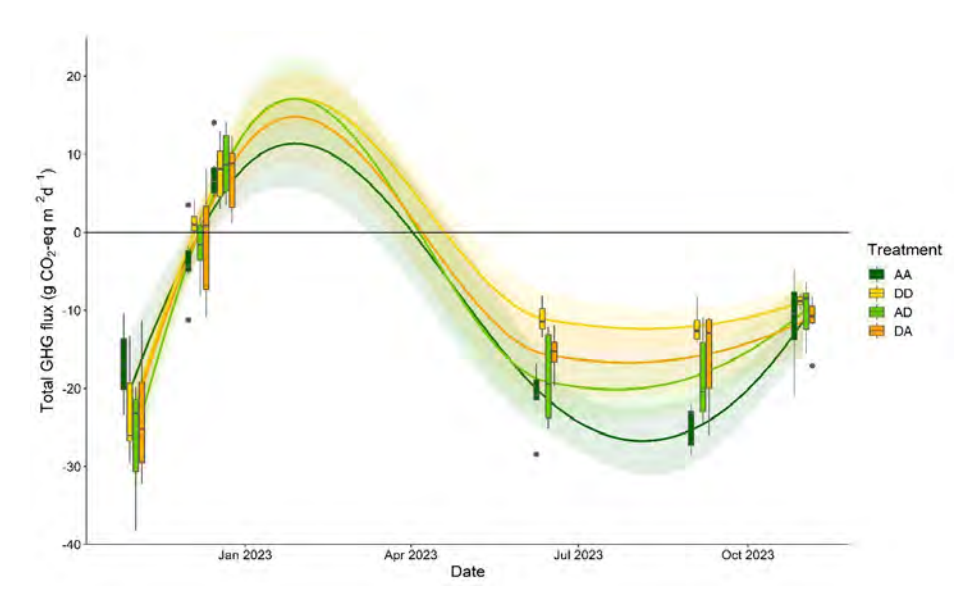


FIGURE 7.8 Flux of all three greenhouse gases combined, expressed in CO₂ equivalents, for all treatment cascades during the one-year experimental period. Lines represent polynomial regression models, capturing the overall seasonal trend while accounting for variability within the data. Boxes show interquartile ranges, bold lines represent the median, whiskers indicate the lowest and highest values within a 1.5x interquartile range from the box, dots represent outliers.

7.4.1 Efficiency of the different treatments

Although we expected the duckweed-Azolla treatment to have highest P removal efficiency, due to the fact that Azolla can overcome N-limitation by N-fixation and thus is able to still remove P at low N concentrations, we observed highest P removal by the treatments containing only duckweed. Treatments with combinations of both plant-types had the highest N removal. The highest N-content is found within Azolla plants, in line with expected N-fixation. Although one would not expect N-fixation under high NH₄+ concentrations, N-content in Azolla has previously been found to be more related to N-fixation than to N-assimilation (Okoronkwo et al., 1989). Although Azolla is known for its high P uptake (Vermaat & Hanif, 1998), in our study duckweed had higher P incorporation in their biomass, which has also been found in earlier work (Reddy & DeBusk, 1985a). It is known that Azolla needs high P concentrations

and is capable of luxury uptake (Peeters et al., 2016). The 10 µmol PO₄ ³⁻ L⁻¹ in the effluent of this WWTP may therefore be too low and *Azolla* may thus not be the most suitable candidate for P removal in effluent polishing if PO₄ ³⁻ concentrations are low. Yet, *Azolla* did take up the most carbon, as also seen in the highest CO₂ uptake. Combining both species therefore takes all the benefits: high nutrient removal, biomass production and carbon sequestration, and low CH₄ and N₂O emission. Since most concentrations of trace elements were below detection limits, it is unclear whether the plants removed any of those elements. The exception here is iron, an essential nutrient for both plant-types (Temmink et al., 2018). Sewage discharge of heavy metals in this particular WWTP might be negligible. Yet, it is known that duckweed and *Azolla* can remove heavy metals (Tel-Or & Forni, 2011) and thus may help in heavy metal removal from different wastewater types.

7.4.2 Seasonal variation

We saw a peak in biomass growth for both plant-types in summer months when temperature and light availability was high. C- and N-content within the plants did not differ during the year, while the P-content of duckweed increased throughout the year. One would therefore expect that a higher biomass production would result in higher nutrient removal. Yet, we did not see this seasonal pattern in removal efficiency. In fact, P removal tended to be lower in summer months, corresponding to a small dip in plant P-content of Azolla. It could be that decomposition of dead plant material that accumulated at the bottom (unquantified) led to nutrient release back into the water column. However, the cascades were cleaned in April, yet no increase in removal efficiency was found after that. Possibly, particulate N and P may be more prone to transformation in summer due to higher microbial activity, and therefore resulted in higher N and P concentrations in the water column.

In summer there was a net uptake of GHGs, mostly caused by the high uptake of CO_2 and low emission of N_2O . The high emission peak of N_2O in winter resulted in net GHG emission in every cascade. Seasonal N_2O peaks have been observed on other wastewater treatment facilities (STOWA, 2012), and may be related to changes in the N-cycling microbial community. Hence, peaks in N_2O might be related to incomplete denitrification in the treatment cascade or influx of N_2O -rich wastewater. CH_4 emissions were generally low. Although dissolved O_2 concentrations were low, O_2 was present in the water column at all times and thus CH_4 production was likely limited. Plants may also have trapped produced CH_4 at the oxic rhizosphere, enhancing CH_4 oxidation (Kosten et al., 2016).

7.4.3 Effect of flow rate

A higher hydraulic residence time, and thus a lower flow rate, increased NH₄⁺ and TN_b removal efficiency, but did not affect PO₄³⁻ and TP removal efficiency in our treatment cascade. Since N-content within the plants decreased for most of the treatments, the higher N-removal may be caused by higher nitrification rates. Although dissolved O₂ concentrations did not rise with an increase in residence time, there was more time for microbial processes to remove N from the system. This did not result in higher N₂O emissions. Generally, P-removal did not increase with a lower flow rate. Yet, when modelling PO₄³⁻ removal with different hydraulic residence times, theoretical removal increases with a longer residence time. This difference can be explained by the fact that the P-content within de plants decreased with an increase in residence time, which is not taken into account in the model. However, treatment AD showed higher P-incorporation into biomass, and as a result also higher P-removal at a lower flow rate.

7.4.4 Effect of harvesting frequency

Despite their high growth rates, plants were harvested every two weeks (except for the first 2 months), as this is a realistic and doable harvesting frequency when scaling up. It regularly happened that the plants covered more than 100% of the cascades and plants therefore may have been space limited, stalling biomass production. Consequently, nutrient uptake is expected to decrease with lower plant growth. To assess when the treatments were most productive, we modelled PO₄³⁻ removal efficiency under different harvesting frequencies, in which 50% of the biomass was harvested. Optimal removal efficiency occurred at weekly harvesting. Less frequent harvesting hampered nutrient uptake, whereas more frequent harvesting, every 3 days, decreased biomass too much and therefore decreased nutrient uptake as well.

7.4.5 Implications and challenges for upscaling

With a short hydraulic residence time of 12 hours, we could reach average nutrient removal of 40%. Reducing flow rate does not immediately mean a higher efficiency of the effluent-polishing system, although it did in our model. Additionally, seasonal effects on removal efficiency, although visible on plant growth, were not observed and thus effluent polishing using floating plants could be used during the whole year. However, the challenge of the presented cascade-system is its use of valuable space. A simple calculation of a small WWTP, for example at the location of our experiment, results in a need of 200,000 m² of areal space, that could possibly be set up as a vertical farming structure to reduce space. One may also see the treatment as a form of reuse and production of valuable resources. When scaling up, we can remove ~300 moles of P each day, that could be reused when harvesting the plants. Furthermore, the plants can be used as fertilizer, or as non-food related products, such as potting

soil for ornamental plants or the extraction of proteins or P from the plants. Both plant-types are also known to be suitable substrates for renewable biofuels (Muradov et al., 2014).

Nutrient removal efficiency of up to 99% is sometimes reached, and more than 75% of the time removal takes place. However, on average this removal efficiency is around 30-40%. Although TP concentrations do not yet meet the standards for receiving waterbodies with good ecological status (STOWA, 2018a, b), average final concentrations of TP (~15 μ mol L⁻¹) and TN (~200 μ mol L⁻¹) are far below limits set by the Water Framework Directive for effluent discharge (EPRS, 2024). Effluent polishing using floating plants may thus be a promising solution to different challenges that we face now: we need to increase water quality and water and nutrient reuse while decreasing GHG emissions. Not only does the treatment sequester GHGs during most of the year, the lower nutrient concentrations in the effluent that is being discharged, will decrease emissions to the receiving waters as well.

Acknowledgements

We thank Tonny Oosterhoff from Hoogheemraadschap de Stichtse Rijnlanden and Harry van Zuijlen from the greenhouse facility at Radboud University for their help in setting up and maintaining the cascades. We would like to thank Teunis Roelofsen and Alexander Kramer from WWTP Rhenen for their help during the experiment and for keeping an eye on the set-up. Furthermore, we thank Sebastian Krosse and Paul van der Ven from the General Instrumentation lab and Germa Verheggen from the Ecology department of Radboud University for performing the sample analyses. Lastly, we greatly appreciate the help of José Paranaíba and Jochem van Beek.

SUPPORTING INFORMATION

S7.1 Model description

The model is set up to assess phosphorus removal efficiency at different hydraulic residence times and different harvesting frequencies. The model is a simplified version of various complex interactions, and we assume PO₄³⁻ to be solely lost due to plant uptake. Growth of both *Azolla* and duckweed was based on maximum growth rate (obtained from our experiments), half-saturation biomass and respiration (Driever et al., 2005), defined as P-dependent, following Monod dynamics (Lüönd, 1980; Temmink et al., 2018). PO₄³⁻ removal was dependent on plant growth, P-content within the plants, plant biomass and water depth (all obtained from our experiments). Furthermore, settling of particulate P was modelled, which was solely based on the settling velocity of particulate P (De Klein, 2008) and the actual water depth (0.12 m).

State variables

Variable	Initial value	Name	
PO ₄ 3-	[0.45] gP m ⁻³	ortho-p concentration	Unit is P
pp	[0.19] gP m ⁻³	particulate p concentration	Unit is P
azolla	[0 - 30] $g_{dw} m^{-2}$	Azolla biomass	In <i>Azolla</i> compartments: 30 g m ⁻² , else 0
duckw	[0 - 30] $g_{dw} m^{-2}$	duckweed biomass	In duckweed compartments: 30 g m ⁻² , else 0

Boundary conditions

Name	Value	
Q inflow	24 L h ⁻¹	range: 12 - 48 L h ⁻¹
PO ₄ ³⁻ in inflow	0.45 gP m ⁻³	experiment setting
pp in inflow	0.19 gP m ⁻³	experiment setting (average from Total-P - PO_4^{3-})
dk_{t}	0.5 hour	calculation timestep

Model parameters

Name	Description	Value	Unit	Source
$f_{ m harv}$	fraction harvesting biomass per calculation timestep	0.25	-	With this harvest fraction 50% of biomass is removed during each harvest event
$f_{\rm res}$	fraction respiration of growth	0.1	-	Driever et al, 2005
hsbm _a	half-saturation biomass azolla	45	$g_{dw}m^{\text{-2}}$	Calibrated of Driever et al, 2005
$hsbm_{\rm d}$	half-saturation biomass duckweed	30	$g_{dw}m^{\text{-2}}$	Driever et al, 2005

Model parameters (continued)

Name	Description	Value	Unit	Source
kp _a	monod constant p azolla growth	0.01	g m ⁻³	Range 0.01 – 0.03; e.g. Temmink et al (2018)
$kp_{\rm d}$	monod constant p duckweed growth	0.01	g m ⁻³	Range 0.01 – 0.05; e.g. Lüönd, (1980)
pdm_a	ratio p in azolla	0.004	g_p/g_{dw}	Measured data, this research
$pdm_{\rm d}$	ratio p in duckweed	0.01	g_p/g_{dw}	Measured data, this research
vgmax _a	maximum growth rate azolla	0.4	1/day	Measured data, this research
vgmax _d	maximum growth rate duckweed	0.35	1/day	Measured data, this research
vs_{pp}	settling velocity particulate p	0.1	m day¹	De Klein, 2008
z	water depth	0.12	m	System setting

Model equations

Variable/function	Unit	Model equation		
Azolla PO ₄ limitation	-	$fp_a = \frac{PO_4^{3-}}{PO_4^{3-} + kp_a}$		
Azolla biomass limitation	-	$biolim_a = \frac{hsbm_a}{azolla + hsbm_a} - f_{res}$		
Azolla growth	g m ⁻²	$growth_a = vgmax_a * fp_a * biolim_a$		
Duckweed PO ₄ ³⁻ limitation	-	$fp_d = \frac{PO_4^{3-}}{PO_4^{3-} + kp_d}$		
Duckweed biomass limitation	-	$biolim_d = \frac{hsbm_d}{duckw + hsbm_d} - f_{res}$		
Duckweed growth	g m ⁻²	$growth_d = vgmax_d * fp_d * biolim_d$		
Harvested azolla	g m ⁻²	$harvest_a = harv * f_{harv} * azolla/dk_t$		
Harvested duckweed	g m ⁻²	$harvest_d = harv * f_{harv} * duckw/dk_t$		
Azolla biomass	g m ⁻²	$\frac{d(azolla)}{dt} = growth_a * (azolla - harvest_a)$		
Duckweed biomass	g m ⁻²	$\frac{d(duckw)}{dt} = growth_d * (duckw - harvest_d)$		
PO ₄ 3 P*	gP m ⁻³	$\frac{d(PO_4^{3-})}{dt} = \frac{-growth_a*azolla*pdm_a}{z} - \frac{growth_a*duckw*pdm_d}{z}$		
Particulate P	gP m ⁻³	$\frac{d(pp)}{dt} = \frac{-pp * vs_{pp}}{z}$		

 $^{^*}$ Example of treatment AD or DA. For treatment AA the equation follows two times *Azolla* uptake, and for treatment DD it follows two times duckweed uptake.

References

- Driever, S. M., van Nes, E. H., Roijackers, R. M. (2005). Growth limitation of Lemna minor due to high plant density. Aquatic Botany, 81 (3), 245-251
- De Klein, J. (2008). From ditch to delta: nutrient retention in running waters. Wageningen University and Research
- Lüönd, A. (1980). Effects of nitrogen and phosphorus upon the growth of some Lemnaceae. Biosystematic investigations in the family of duckweeds (Lemnaceae). Zurich, Veroffentlichungen des Geobotanisches Institut der Edg, 118-141
- Temmink, R. J., Harpenslager, S. F., Smolders, A. J., van Dijk, G., Peters, R. C., Lamers, L. P., van Kempen, M. M. (2018). Azolla along a phosphorus gradient: biphasic growth response linked to diazotroph traits and phosphorus-induced iron chlorosis. Scientific reports, 8 (1), 4451

S7.2 Supplementary figures

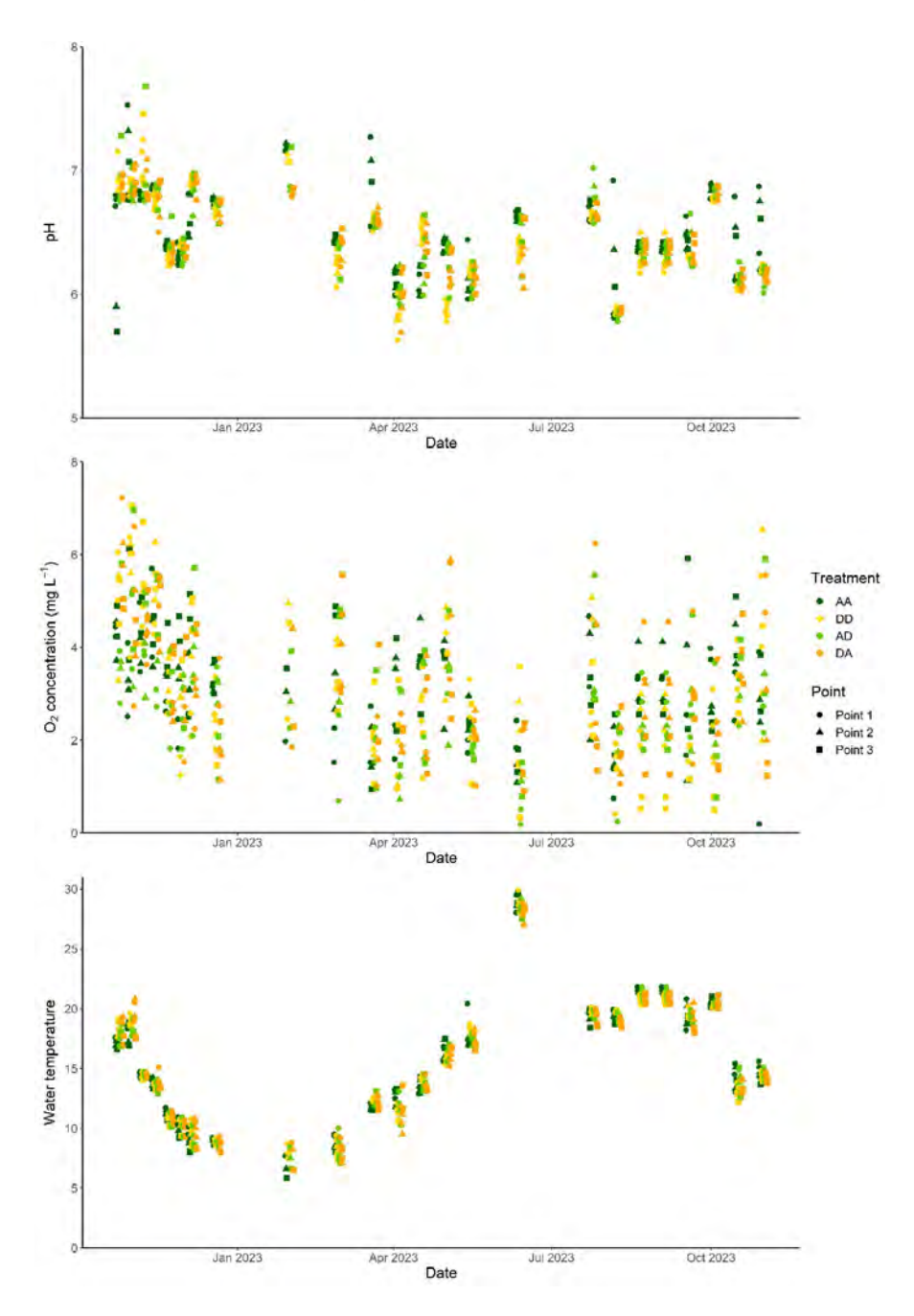


FIGURE S7.1 pH, dissolved oxygen concentration and water temperature for each treatment during the one-year experimental period. Each treatment consisted of duplicates, both are shown in the figures.

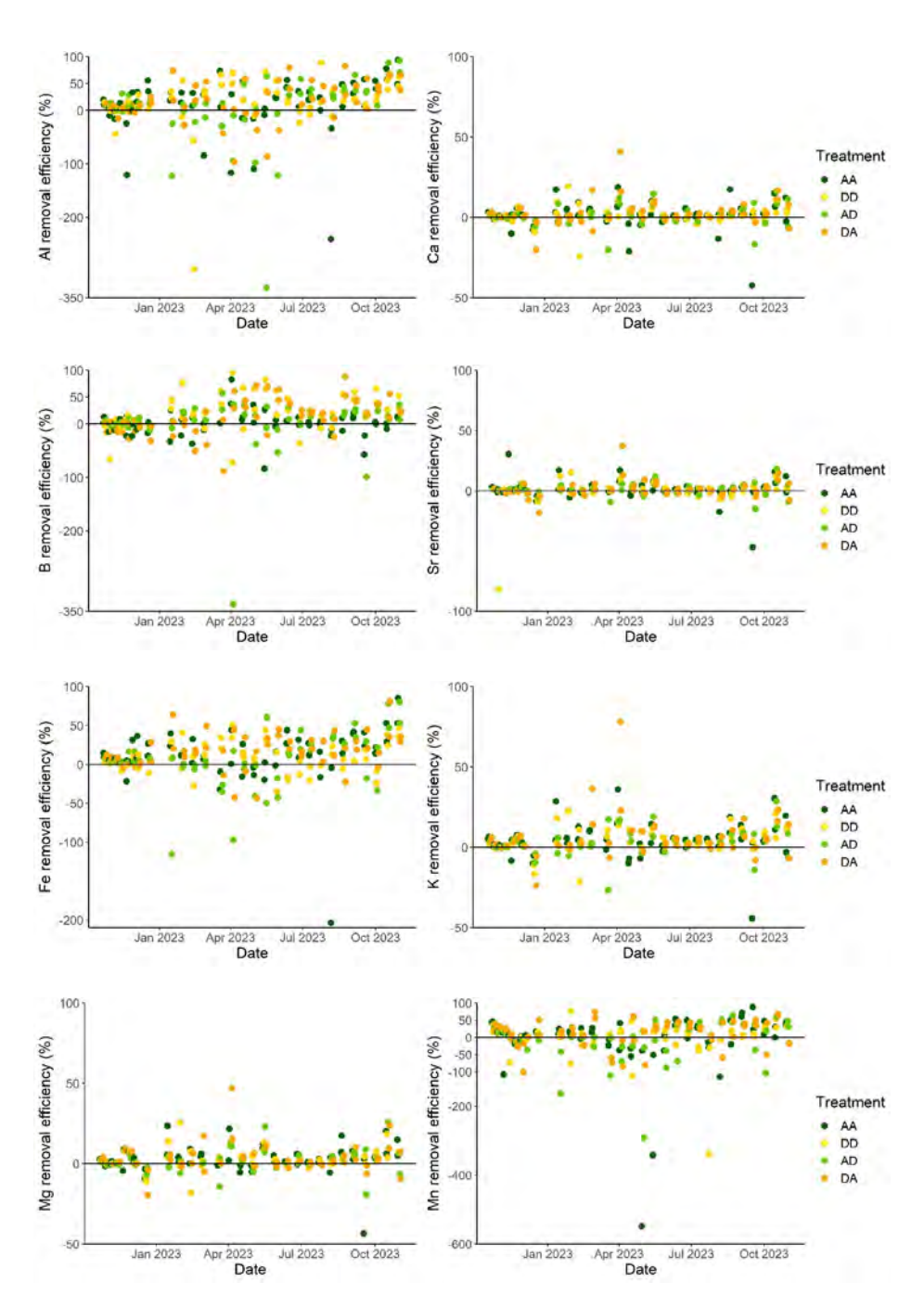


FIGURE 7.2 Removal efficiency of trace elements for each treatment during the one-year experimental period. Each treatment consisted of duplicates, both are shown in the figures. Al = aluminium, Ca = calcium, B = boron, Sr = strontium, Fe = iron, K = potassium, Mg = magnesium, Mn = manganese, Na = sodium, S = sulphur, Si = silicon, Zn = zinc.

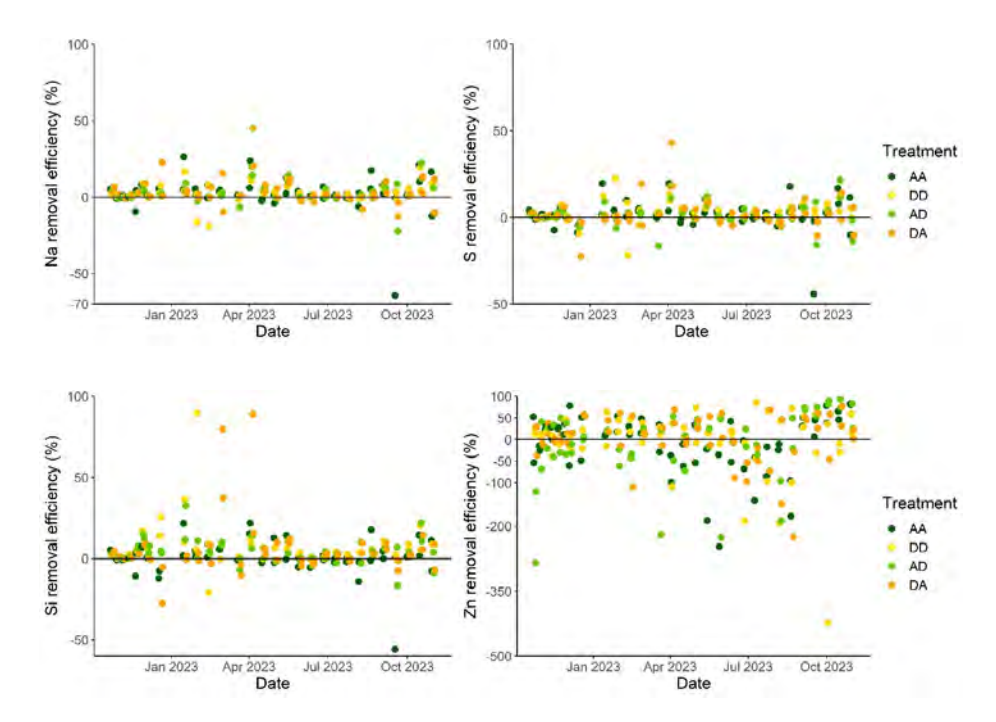


FIGURE S7.2 Continued.

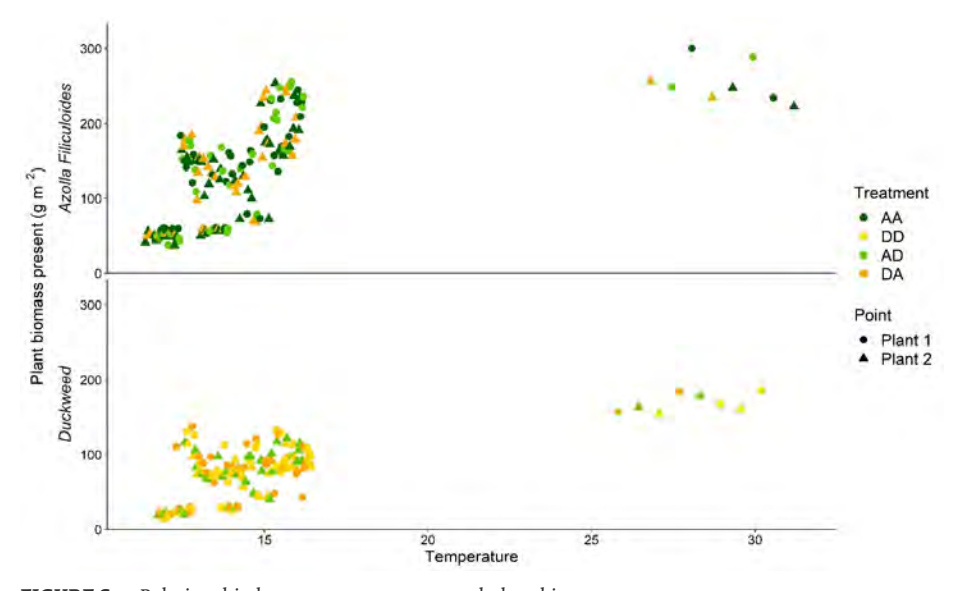


FIGURE S7.3 Relationship between temperature and plant biomass presence.

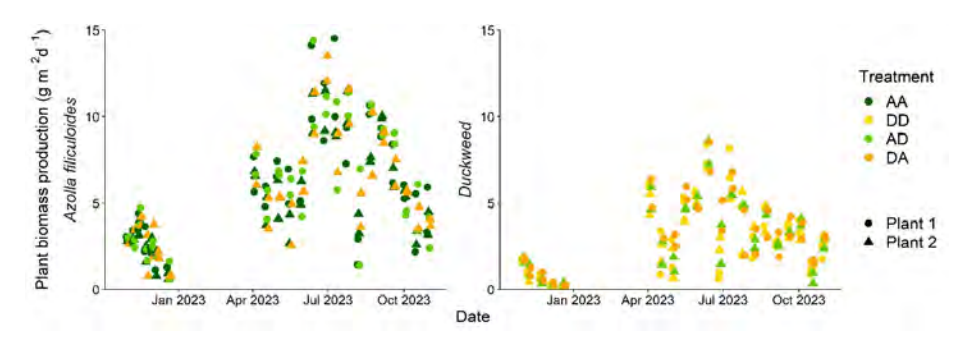


FIGURE S7.4 Production of biomass for *Azolla* and duckweed during the one-year experimental period. Plant 1 is the first plant in the cascade, Plant 2 is second plant in the cascade.

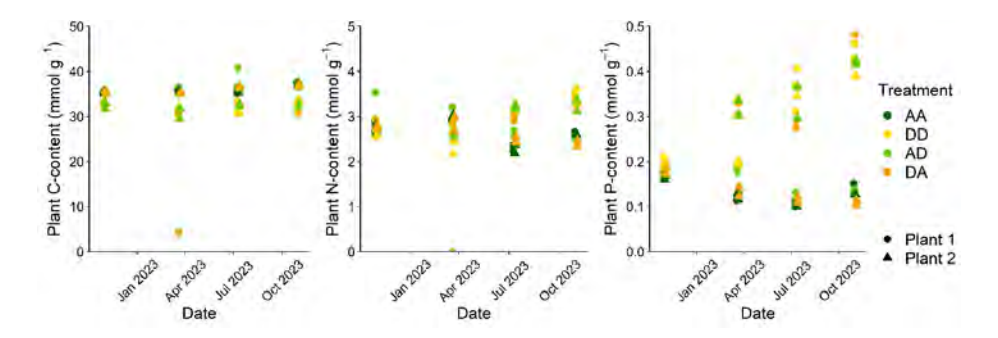


FIGURE S7.5 The amount of carbon (C), nitrogen (N) and phosphorus (P) incorporated per gram plant biomass in each treatment cascade during the one-year experimental period. Plant 1 is the first plant in the cascade, Plant 2 is second plant in the cascade. Note the differences in Y-axes.

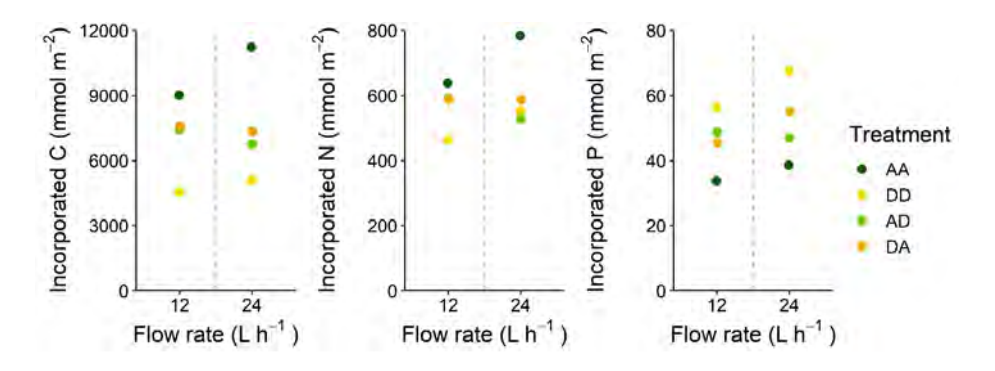


FIGURE S7.6 Difference in the amount of carbon (C), nitrogen (N) and phosphorus (P) incorporated within the total biomass in each treatment cascade between a flow rate of 12 L h-1 (replicate a) and 24 L h-1 (replicate b) in the last month of the one-year experimental period. Note the differences in Y-axes.

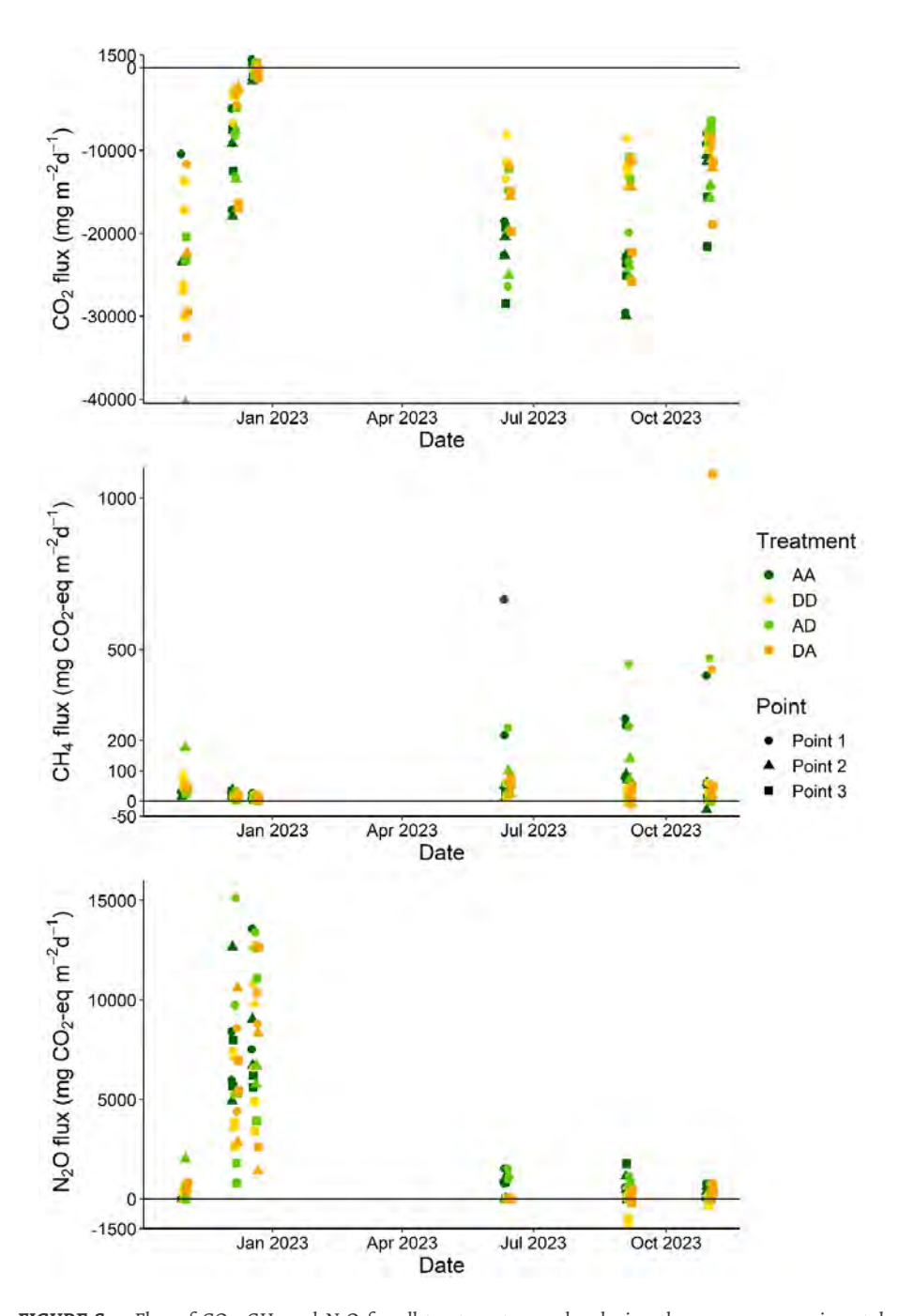


FIGURE S7.7 Flux of CO_2 , CH_4 and N_2O for all treatment cascades during the one-year experimental period. Point 1 and Point 2 are located at the first plant species within the cascade. Point 3 is located at the end of the cascade, with the second plant species. Note the difference in Y-axis.



Chapter 8 General synthesis

8.1 SYNTHESIS

The aim of this thesis was I) to assess how greenhouse gas (GHG) emissions from ditches and rivers are affected by eutrophication, and II) to use aquatic macrophytes and macrofauna in water treatment to ultimately reduce nutrient loading and GHG emission in receiving waterbodies. In my thesis, I showed that eutrophicated water systems show high GHG emissions, as observed in agricultural ditches (chapter 2, see Hendriks et al., 2024a) as well as in rivers polluted by wastewater effluent discharge (chapter 3). At the same time, 60% of European waterbodies exceed N and P thresholds, and national CH₄ emissions continue to rise. This underlines the urgency of counteracting nutrient loading from agriculture and wastewater treatment, to mitigate both eutrophication and GHG emission. In agriculture, while eutrophication may stem from historical nutrient legacies as well, reducing the leaching of nutrients from fertilized soils and the erosion of fertilized soils, and preventing the direct input of manure into drainage ditches, would reduce direct or indirect eutrophication of drainage ditches. Ultimately, this will also reduce GHG emissions from drainage ditches, as well as from the agricultural land, especially from peat soils. Furthermore, it is shown that, although current wastewater treatment in the Netherlands is quite effective, wastewater effluent still seriously affects receiving waterbodies, resulting in higher nutrient concentrations and higher GHG production and emission. Treating wastewater to lower N and P threshold concentrations in WWTP effluent to resemble nutrient concentrations in the receiving waterbodies, would decrease eutrophication and GHG emissions within receiving waters. Ideally, this extra treatment step would be a nature-based one, in order to limit GHG emissions and operational costs at the wastewater treatment plants (chapter 4-7). The desired situation will therefore be to reduce nutrient loading and at the same time reduce GHG emission (Fig. 8.1).

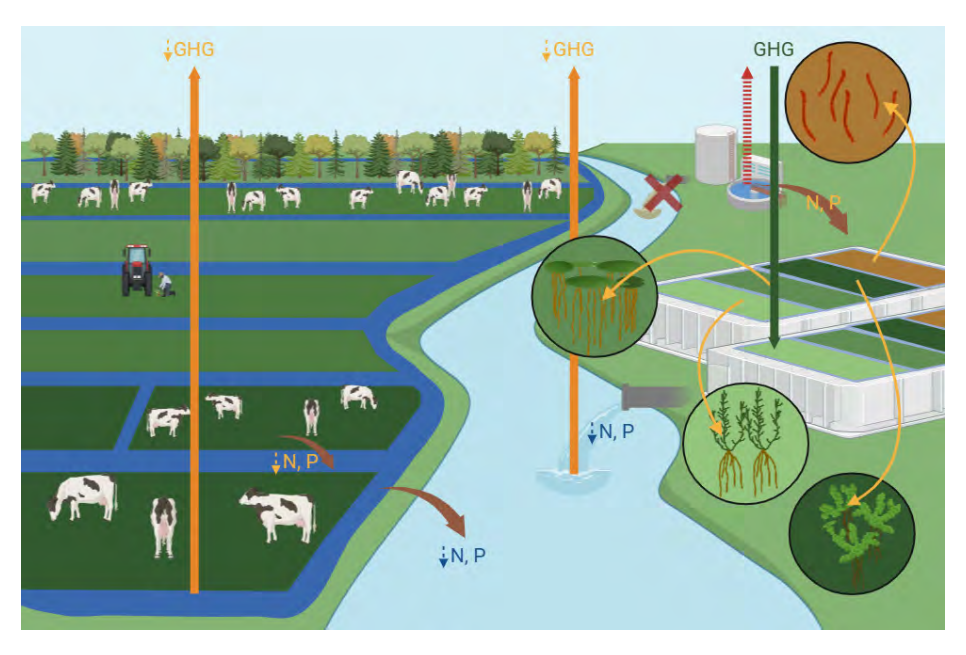


FIGURE 8.1 Desired situation for agricultural land and wastewater treatment. With lower nutrient loading to agricultural fields, there will be less runoff towards the agricultural ditches and other receiving waters. By an extra wastewater treatment step, excess nutrients will be removed, and lower amounts of nutrients will be discharged to receiving waterbodies. Both mitigation processes will lower eutrophication and reduce GHG emission in receiving waters. Dashed lines indicate emission reductions after implementation of mitigation measures.

The use of aquatic plants and animals is a promising nature-based solution in wastewater treatment. For effluent polishing, the most efficient aquatic plant types were shown to be floating species, since they take up high amounts of nutrients from the water layer, sequester high amounts of CO₂ and produce high amounts of biomass (**chapter 4**, see Hendriks et al., 2023). A combination of species, using their specific traits, proves to result in more efficient nutrient removal, on batch scale as well as on a bigger pilot scale (**chapter 5**, 7). Combining plants with animals, in this case bioturbating macroinvertebrates, not only reduces excess sludge, but also decreases nutrient concentrations in the treated effluent (**chapter 6**, see Hendriks et al., 2024b). All these treatment steps show very low CH₄ and N₂O emissions, and high CO₂ sequestration, resulting in a net GHG uptake (~25 g CO₂-eq. m² d⁻¹) of the effluent polishing step.

8.2 HIGH GHG EMISSIONS FROM EUTROPHIC AQUATIC SYSTEMS

GHG emissions from drainage ditches or rivers impacted by wastewater effluent are rarely considered in national GHG inventories. The IPCC shows emission factors for these sources, but they are highly speculative and only based on a few studies (IPCC, 2019). To accurately estimate emissions coming from such systems, more research is needed. Although currently, GHG emissions from drainage ditches are getting more attention (Köhn et al., 2021; Peacock et al., 2021; **chapter 2**), until recently drainage ditches were often omitted when studying emissions coming from drained peatlands. Here, we showed the importance of implementing GHG emissions from drainage ditches in national GHG inventories. Based on our study, CH₄ emissions from these ditches may account for ~10% of total CH₄ emissions in The Netherlands, due to their large surface area of 300,000 km² (**chapter 2**). According to Koschorreck et al. (2020), this contribution may be even higher. Especially CH₄ ebullition, a CH₄ emission pathway that is often omitted and is highly spatially and temporally variable, may contribute for 40% to the total GHG emission coming from these ditches.

Furthermore, in polluted rivers, GHG emissions are substantial (Upadhyay et al., 2023), and wastewater effluent discharge further increases their emissions (Alshboul et al., 2016; Hu et al., 2018). Yet, this effect of WWTP effluent is highly variable, ranging from a 1.1 to a 10.9 times increase in CO₂, CH₄ and N₂O emissions. Therefore, more research is needed for more accurate estimations on the impact of effluent discharge on receiving rivers. The study performed in **chapter 3** contributes to this. By studying six discharge points in two rivers, we show that CH₄ and N₂O emissions increase after effluent discharge, and CO₂ peaks occur at discharge locations. The emissions observed in the studied rivers (up to 70, 5 and 2 g CO₂-equivalents m⁻² d⁻¹ for CO₂, CH₄ and N₂O, respectively) are in the high range compared to other rivers (Alshboul et al., 2016; Upadhyay et al., 2023), and are even higher than agricultural drainage ditches (**chapter 2**). This shows the importance of GHG emissions from effluent-impacted rivers, and solutions to counteract nutrient input towards these systems are therefore crucial in limiting riverine GHG emissions.

8.3 AQUATIC ORGANISMS AND THEIR ROLE IN WATER TREATMENT

8.3.1 Nutrient removal by aquatic plants

Macrophytes take up nutrients for their growth, but also act as substrate for biofilms in which microbial nutrient conversions take place. In our experimental

systems, submerged plants were outcompeted by algae and therefore not able to grow in such a high nutrient environment, while floating plants thrived, showing a high biomass production and high nutrient removal (chapter 4). N was removed by several pathways. In all experiments, nitrification was the dominant NH,+ removal pathway, as demonstrated by a simultaneous decrease of NH₄+ and increase of NO₃-. In all cases, NH, was completely removed from the water column within days (chapter 4-7). Denitrification was most likely limited, due to the high oxygen concentrations present in the water column, which is also reflected by the absence of N, emissions. Removal of NO, is therefore probably caused by plant uptake. Contrary to other studies (Singh et al., 1992; Costa et al., 2009), Azolla did not contribute to NO, removal (except in **chapter 6**), yet it had higher N plant-content than duckweed, which could be explained by N₂ fixation. Even though N was still present in the water column, mostly in the form of NO₃, N₂ fixation by its diazotrophic symbionts was the dominant N source for Azolla, which is also seen in other studies (Okrononkwo, 1989; Costa et al., 2009). Consequently, Azolla may not be a suitable candidate for N removal from wastewater effluent. In contrast, duckweed removed N to concentrations below those of receiving waterbodies (<285 µmol L-1; Carey & Migliaccio, 2009; van Puijenbroek et al., 2010). N removal using duckweed has been thoroughly studied and in all cases duckweed removed N up to 100% from different types of wastewater (Oron et al., 1988; Körner & Vermaat, 1998; Benjawan & Kootatep, 2007; Ozengin & Elmaci, 2007; Alahmady et al., 2012; Zhao et al., 2014). Use of duckweed in effluent polishing may therefore contribute to a reduction of nitrogen loads to receiving waters.

Although in constructed wetlands, precipitation may be the major P removal pathway (Maucieri et al., 2020), P removal in these systems mostly takes place by plant-uptake and harvesting (Keizer-Vlek et al., 2014; Geng et al., 2017; chapter 4, 7). Both duckweed and Azolla were shown to be plant types with great potential to remove P, as also seen in other studies (Vermaat & Hanif, 1998; Kadir et al., 2020; Rezania et al., 2021), leading to 100% P removal in batch experiments (chapter 4). Yet, contrary to growth in constructed wetlands, Azolla grown on wastewater effluent may be limited by low concentrations of for example P or trace elements. Azolla and duckweed are known for their high potential for luxury uptake of P (Peeters et al., 2016). At P concentrations below 10 µmol L-1, which was most often the case in our experiments (**chapter 4, 5, 7**), Azolla growth may be hampered, and additionally iron deficiency may result in chlorosis of the plants (Temmink et al., 2018). Although the plant was growing well in all experiments, P uptake was sometimes lower than in duckweed (chapter 4, 7). In wastewater with higher P concentrations of ~3 mmol L-1, where Tubifex worms enhanced P release during sludge degradation (Schuijt et al., 2021), Azolla was able to produce more biomass (7 compared to 3-4 g dryweight m⁻² d⁻¹ in **chapter 6**),

yet did not differ in P sequestration rates (both 0.3 mmol P g dry weight⁻¹ d⁻¹). Thus, P binding to sludge when *Chironomus* larvae were present, resulted in a lower *Azolla* biomass production, but the same plant P-uptake (**chapter 6**).

Contrary to P, which can only be taken up as PO₄³⁻, and hence becomes limiting through plant uptake and P-binding, *Azolla* can obtain N from both dissolved and atmospheric supplies. As a consequence, even when reactive N is depleted in the water column, *Azolla* can meet its N-demand and continue to grow and absorb P. This does not apply to duckweed species, that need both nutrients in the surface water for growth. When N concentrations are limited, due to for example high coupled nitrification-denitrification, duckweed will not be able to remove P from the water column. N:P stoichiometry is therefore important, and combining species may thus be a solution to combat a potential nutrient imbalance (**chapter 5, 7**).

8.3.2 GHG mitigation by aquatic plants

In wastewater treatment using aquatic plants, focus has thus far been on nutrient removal. Significantly less research has been done on the impact of plant-mediated water treatment in terms of GHG emissions. In many aquatic ecosystems, the presence of floating plant species increases GHG emissions, especially CH, due to decrease in oxygen concentrations and light penetration (Kosten et al., 2016; Oliveira-Junior et al., 2018; Aben et al., 2022). However, their presence can also lead to trapping of CH₄ and consequent CH₄ oxidation in the oxygenated rhizosphere which decreases CH₄ emission (Harpenslager et al., 2022; Wang et al., 2024). In effluent treatment, the floating plants were found to sequester the highest amount of CO, compared to submerged plants, while limiting CH₄ and N₂O emission (chapter 4). Submerged plants were able to further oxygenate the water column, leading to ~2 times lower CH, emission compared to floating plants. However, in all situations CH₄ emission was negligible (chapter 4). Since no sediment was used, there were few anoxic habitats, and thus CH₄ production was hampered in all plant treatments. Yet, this may not always be the case in other hydroponic systems. Although GHG emission from hydroponic systems is poorly studied, CH, emission may still occur under oxic conditions, due to plant-mediated flux (Abdulmajeed et al., 2017) and potentially also by oxic-methane production associated to submerged plants and phytoplankton growth, although this has not yet been studied for waste water treatment systems (Keppler et al., 2009; Hilt et al., 2022). Occasionally, N₂O emissions were substantial, coinciding with N removal and especially when $NH_{_4}^{_+}$ concentrations were low and NO₃ concentrations were highest. This suggests that N₂O emissions were related to coupled nitrification-denitrification where the plants have an indirect effect through their biofilm formation. Yet, high CO uptake due to photosynthesis and growth still

led to net GHG sequestration in almost all cases, even taking into account the higher global warming potentials of $\mathrm{CH_4}$ and $\mathrm{N_2O}$ (**chapter 4-7**). In this way, plant-mediated effluent polishing has a negative carbon footprint - depending on how the harvested biomass is processed - and can add to the target of net zero emissions in 2050.

8.3.3 Macroinvertebrates for sludge degradation and GHG mitigation

Burrowing macroinvertebrates prove to be suitable for the treatment of wastewater sludge (chapter 6). As these organisms live within sediment, they oxygenate the sediment or, in the case of wastewater treatment, sludge. In this way, their bioturbation aids in microbial aerobic degradation of the sludge and coupled nitrification-denitrification, and accelerates these processes (Svensson et al., 2001; Shang et al., 2013; Chakraborty et al., 2022). As organic sludge is removed, inorganic C and N are released to the water column or atmosphere. In contrast, P binds to the metal-oxides present in the sludge and this binding increases with higher oxygen concentrations. Yet, this depends on the macroinvertebrate species, as some species such as Asellus aquaticus increased P concentration in the water column (Van der Meer et al., 2021). Furthermore, macroinvertebrates feed on the sludge for their growth, degrading the sludge even more. They incorporate N, P and C in their biomass and in this way remove these substances from the sludge, but also release these substances through their excretion. Whether N, P, C and other elements are transported from sludge to water column or biomass, or remain bound to the sludge, depends on the traits of the invertebrate species used (Van der Meer, 2023).

The effects of macroinvertebrates on GHG emissions in aquatic systems remains poorly studied and shows contradicting results, where macroinvertebrates either affect GHG emissions positively (Benelli & Bartoli, 2021), or negatively (Figueiredo-Barros et al., 2009), or sometimes have no effect (Serrano et al., 2016). The tubes formed by burrowing macroinvertebrates may be microsites where CH, production and oxidation are tightly coupled, resulting in a net zero effect on CH4 fluxes (Kajan & Frenzel, 1999). Yet, in our wastewater treatment system (chapter 6), CH emission, both through diffusive and ebullitive pathways, was drastically reduced by Chironomus larvae. Additionally, CO2 release from respiration was compensated by increased oxygen penetration and possibly lower CO, release from microbial activity, leading to net zero CO, emissions. This is the first time that this effect on CH₄ emission was observed in wastewater treatment. Another study found no effect of macroinvertebrates on CH₄ emission from activated sludge (Serrano et al., 2016). Bioturbating macroinvertebrates may therefore contribute to nature-based water treatment in the form of sludge degradation, nutrient removal and, depending on the system, GHG mitigation.

8.3.4 Influence of algae on water treatment

Algae grow well on wastewater effluent, and in our study, they outcompeted slower growing submerged plant species (chapter 4). Also in treatments without plants, i.e. in all control treatments in the experiments of this thesis (chapter 4-6), algae thrived. Here, they performed the same roles as the plants in water treatment: they removed nutrients and took up carbon, leading to net GHG sequestration. Furthermore, they are known to remove micropollutants (De Wilt et al., 2016) and may be used in a circular economy (Fernandes et al., 2022). Algae may thus be useful as well in wastewater effluent polishing, as also suggested by other studies (Nie et al., 2020; Kong et al., 2021; Mohsenpour et al., 2021; Rezania et al., 2021). However, the cultivation, harvesting and use of algal biomass remains a challenge, requiring high energy demands and chemicals (Abinandan et al., 2018; Nie et al., 2020; Yin et al., 2020), challenging implementation of algae in wastewater treatment. Yet, natural harvesting techniques are emerging, using mussels that feed on algae (Van der Meer et al., 2023). When using vascular plants in effluent polishing, it is difficult to prevent algal growth. Using UV-C lights only partly limited algal growth (chapter 5), and covering the aquaria with a cloth still was insufficient to keep the water algae-free (chapter 6). Yet, floating plants are found to prevent most algal growth (chapter 4-7) and thus are suitable plants in instances where algae are not desired.

8.3.5 Microbial importance in water treatment

The most important organisms in water treatment may be those invisible to the naked eye: microorganisms. They are widely used in conventional wastewater treatment, for example in the form of activated sludge (Ren et al., 2020; Dai et al., 2022; Feng et al., 2022). Also in the experiments performed in this thesis, nitrification and denitrification, performed by microorganisms, were the most important N removal pathways. This was especially seen by the fact that also in control treatments, at the times where algae were not present yet, these processes removed N at the same rate as the plant treatments (chapter 4-6). It may therefore be suggested that plant N uptake is less important than nitrification and the plants mainly function as substrate for biofilms, although denitrification may be hampered or incomplete due to the restrictively high oxygen concentrations in the water column (Rassamee et al., 2011; chapter 4-7). During these microbial processes, N₂O may be produced and emitted (chapter 4, 5). Thus, ensuring optimal conditions for complete denitrification to N, instead of N,O, or for CH, oxidation, is crucial for optimal wastewater treatment. Furthermore, microorganisms are also influenced by eutrophication in natural waterbodies. In agricultural ditches, decomposition of organic material and methanogenesis was higher when nutrient input was high. This resulted in year-round GHG emissions coming from these ditches (chapter 2).

8

This was also observed in effluent-receiving riverine systems, where $\mathrm{CH_4}$ and $\mathrm{N_2O}$ production increased after effluent discharge (**chapter 3**). Additionally, the rivers' microbial communities were affected by effluent discharge (**chapter 2**), as also seen in other studies (Mansfeldt et al., 2020; Ruprecht et al., 2021; Wang et al., 2022). Optimizing the conditions for nitrification and denitrification has received a lot of attention in wastewater treatment research, but reducing GHG emission by tailoring conditions for microbial conversions has received less attention, and has not yet been translated to management of surface waters.

8.4 IMPLICATIONS AND CHALLENGES FOR WATER TREATMENT

The incentive of the experiments shown in this thesis rooted in the practical question whether it is possible to improve wastewater treatment while at the same time producing high-value biomass. This question is embedded in an initiative: Aquafarm. Making use of natural processes, using vascular plants and invertebrate fauna, in water treatment could be beneficial, since technical solutions are costly and also have their limitations. Using aquatic plants and animals in wastewater treatment reduces nutrient loading to receiving waterbodies, and the treatment in itself has a net GHG sequestration (chapter 4-7). While treating the water, the organisms grow and thereby produce biomass. Harvesting the organisms permanently removes nutrients, carbon and other pollutants that the organisms have taken up from the water. In this way, the effluent contains less nutrients, reducing emissions to freshwater systems and coastal waters. Since P is a finite resource, the recycling of this element will be crucial in the future.

8.4.1 Biomass usage for a circular economy

A big difference with other treatment techniques, is the fact that using aquatic plants and animals produces biomass that can be used for other products and therefore could contribute to a circular economy. Using the biomass produced is therefore essential for this type of water. Furthermore, P is a non-renewable resource (Chowdhury et al., 2017), that will be depleted in the future (Desmidt et al., 2015). Reusing P may therefore be a crucial step to ensure food security. Duckweed and especially *Azolla* are suitable alternatives as feed (Brouwer et al., 2018; Paryanto et al., 2023), for example for fish (Yohana et al., 2023; Minich & Michael, 2024), poultry (Alagawany et al., 2023) or livestock (Korsa et al., 2024). Furthermore, due to their high N and P content, the plant biomass could be used as biofertilizer (Prabakaran et al., 2022; Babatunde et al., 2023; Korsa et al., 2024). *Chironomus* larvae are suitable as feed for fish or other

ornamental aquatic animals (Elissen et al., 2010; Sulistiyarto et al., 2014). However, since the biomass is grown on potentially polluted waters, bringing back the biomass into the food chain will not always be an option, depending on the concentrations of pollutants in the plants and animals used in the treatment process. Although also already present in agricultural soils (Nguyen et al., 2023), chemicals of emerging concern should be considered, as there are indications of uptake of pharmaceuticals and other harmful compounds by plants (Madikizela et al., 2018; Keerthanan et al., 2021; Salah et al., 2023) and aquatic invertebrates (Timmermans et al., 1992; Meredith-Williams et al., 2012). The question rises which pollutants should be considered in deciding whether the organisms could be used as feed or fertilizer. Nevertheless, there are several non-food applications, ranging from low-value to high-value. One could think of fermentation, biofuel or biogas production (Hendrickx, 2009; Arefin et al., 2021; Prabakaran et al., 2022; Korsa et al., 2024). Higher-value applications include amino acids, fatty acids and enzymes. Those substances can individually be extracted and used for applications like coatings, glues, cleaning products, plastics, detergents and packaging film (Elissen et al., 2010; Rani & Venkatachalam, 2022; Babatunde et al., 2023; Namasivayam et al., 2023). When desired, a high-value plant, such as Trapa natans due to its high starch an protein content, could be implemented in the treatment process even though it might not add to the nutrient removal. In that case, such plant type could be placed in the last step of the cascading system, to remove the remaining nutrients and to produce high-value biomass.

8.4.2 Water quality versus biomass production

To make a plant- and animal based treatment system work, a choice between the importance of both water quality and biomass production should be considered. A higher treatment efficiency, and thus higher nutrient removal, requires a longer hydraulic retention time, to ensure enough time for the organisms to remove all pollutants. Yet, this may mean a lower biomass production, since in the end the nutrients will become limited, although this may not be the case when modelling our findings (chapter 7). Starting the application of this nature-based solution earlier in the treatment process, as in the case in chapter 6, would increase P recovery, sludge degradation and production of biomass due to high nutrient concentrations. Yet, in this case nutrient concentrations in the effluent will probably still be too high. One may then choose to return this water to the conventional treatment and only focus on biomass production and nutrient recovery. This trade-off between water quality and biomass production should be taken into account when deciding how to upscale the nature-based treatment step, and different places within a conventional wastewater treatment plant may be considered (Fig. 8.2).

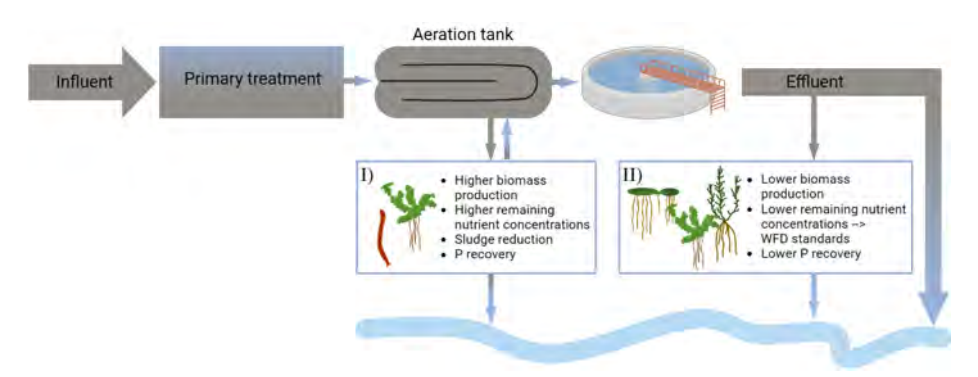


FIGURE 8.2 Schematic overview of two options to place a nature-based solution using higher organisms: I) as biomass production and nutrient recovery process, and II) as effluent polishing-step to achieve nutrient loads in line with the Water Framework Directive standards for surface waters.

8.4.3 Challenges in upscaling

Some challenges need to be considered when scaling-up the experiments from this thesis towards a functioning wastewater treatment using higher organisms. These nature-based solutions are highly space demanding. This is the case for constructed treatment wetlands (Zapater-Pereyra et al., 2015; Ilyas & Masih, 2017), but also for a more controlled system that was studied in this thesis (chapter 4-7). Furthermore, a relatively high retention time of at least 12 hours is needed for sufficient nutrient removal. For treatment of 50 m³ d⁻¹ wastewater effluent, one would already need ~800 m² of aquatic plants to polish this effluent towards nutrient concentrations below concentrations stated in the Water Framework Directive (report Adrie Otte, Sweco, on the instructions of Aquafarm). In a densely populated country like The Netherlands, space is limited and costly, and for this reason scaling up is challenging. Additionally, temperature and light availability are limiting factors for plant growth. In colder winter months, temperature and light availability may be too low to obtain high treatment efficiency and biomass production, even though nutrient removal still takes place and may not differ significantly from warmer months (chapter 7). Furthermore, aquatic animals need oxygen which means that the part of the system where these animals are present needs to be aerated (chapter 6). When making decisions on these aspects, one should consider the trade-off between space and energy demand. Vertical farming may drastically reduce space use, especially since the plants used in the studies of this thesis only need a water column of ~10 cm. Yet, the plants need light for growth, and thus using a vertical farm requires artificial light, which increases energy demand and costs. Combatting low temperature and light availability in winter by heating and artificial light may increase treatment efficiency in these colder months, but at the same time this also increases energy demand and costs. Consequently, the positive carbon footprint of the nature-based water treatment may not apply here.

Furthermore, long-term performance of such nature-based solution should be investigated. Although the plants survived on wastewater effluent for a whole year including cold winter months (**chapter 7**), and macroinvertebrates were able to reproduce during sludge degradation (**chapter 6**), treatment using plants and animals is still prone to some challenges. It remains unclear whether the organisms could survive extremely high pollutant pulses, during WWTP irregularities. Next, the organisms are prone to pests and diseases. Also, the effects of chemicals of emerging concern, such as pharmaceuticals and heavy metals, on survival and thereby treatment performance, should be studied further in order to assess whether wastewater treatment using aquatic plants and animals is robust enough to be further developed.

In order to ensure high treatment efficiency, continuous measurements are required on nutrient concentrations in the water column and GHG emission from the treatment. Knowing the dynamics of the treatment allows development of a flexible system where one could alter water-conditions, such as retention time. It also allows for altering conditions during each season. Additionally, manual harvesting of the plants and animals is very labour-intensive. For example, harvesting of the plants in the relatively small pilot of **chapter 7**, took at least 3 hours. Automated, continuous, harvesting may therefore be necessary, ensuring the plants and animals are always growing at their maximum growth rate while preventing space limitation. Lastly, some of the species used in the experiments in this thesis are considered invasive in The Netherlands, and may form a risk when discharged into receiving waterbodies. The trade-off between high treatment efficiency from invasive species and lower efficiency from native species should be considered. Key is to ensure that the organisms, that may contain pollutants, are not discharged with the effluent, or are escaping from the treatment, as may be the case for, for example, adult Chironomus midges. Possible measures to prevent organism escape are sand filters or mesh nets. Furthermore, there are restrictions for growing and transporting invasive organisms, as well as creating products that are associated with wastewater. Yet, new proposals have been made to increase the reuse of wastewater effluent and sludge, avoiding the loss of valuable resources (European Commission, 2022), which increases the applicability of implementing wastewater treatment using aquatic plants and animals.

8.4.4 Chances for low-income countries

Worldwide, only 50% of the wastewater produced is being treated. In low-income countries, this is only 4% (Jones et al., 2021). Yet, these places offer the opportunities for new nature-based solutions. Generally speaking, these are the locations where

space is less limited, where high-tech solutions are often too costly, and where poor water quality affects societal and ecosystem health. Furthermore, these are the places where such nature-based solution could thrive. Low-income countries are often located in (sub)tropical areas with high temperatures, where light, temperature and space limitation are less of a problem. Furthermore, the produced biomass could stimulate income and job opportunities. Studying and creating nature-based solutions in high-income countries could therefore not only benefit these specific countries, but also large other parts of the world.

8.5 CONCLUSION

Aquatic ecosystems have been under pressure in the current changing world. Extreme events reduce water security, and high nutrient loadings result in eutrophication of waterbodies with all its consequences, including greenhouse gas emissions. The human impact on water quality is substantial, as agriculture and wastewater are the main sources of nitrogen and phosphorus in our surface waters. Drainage ditches receiving large amounts of nutrients from agriculture and rivers receiving wastewater, are prone to eutrophication and emit high amounts of greenhouse gases due to this nutrient loading. Nature-based water treatment may be one of the solutions to counteract the eutrophication of receiving waters. Aquatic plants and animals can treat water through nutrient removal and sludge reduction. In addition, wastewater is full of resources, such as phosphorus, that opens up opportunities for resource reuse, to prevent losses of these valuable resources. Furthermore, treatment using aquatic plants and animals results potentially in net greenhouse gas sequestration, and their biomass can be implemented for further use, contributing to a future-proof, circular economy. The world is facing different problems, and the challenges are piling up: we have to become circular, with net zero emissions, and our ecosystems need to be cleaner. While one is tempted to search for expensive hightech solutions, one must not forget the processes nature is already providing us for free. In a modern world, where we want more and more, maybe sometimes going back to the basics is where the solution lies.



Appendices
References
Data management
Summary
Samenvatting
Dankwoord
About the author
Scientific outreach

REFERENCES

A

- Abdulmajeed, A. M., Derby, S. R., Strickland, S. K., Qaderi, M. M. (2017). Interactive effects of temperature and UVB radiation on methane emissions from different organs of pea plants grown in hydroponic system. *Journal of Photochemistry and Photobiology B: Biology*, 166, 193-201
- Aben, R. C. H., Barros, N., Van Donk, E., Frenken, T., Hilt, S., Kazanjian, G., Lamers, L. P. M., Peeters, E. T. H. M., Roelofs, J. G. M., de Senerpont Domis, L. N., Stephan, S., Velthuis, M., Van de Waal, D. B., Wik, M., Thornton, B. F., Wilkinson, J., DelSontro, T., Kosten, S. (2017). Cross continental increase in methane ebullition under climate change. *Nature Communications*, 8 (1), 1–8
- Aben, R. C. H., Velthuis, M., Kazanjian, G., Frenken, T., Peeters, E. T. H. M., Van de Waal, D. B., Hilt, S., De Senerpont Domis, L. N., Lamers, L. P. M., Kosten, S. (2022). Temperature response of aquatic greenhouse gas emissions differs between dominant plant types. *Water Research*, 226, 119251
- Abinandan, S., Subashchandrabose, S. R., Venkateswarlu, K., Megharaj, M. (2018). Nutrient removal and biomass production: advances in microalgal biotechnology for wastewater treatment. Critical Reviews in Biotechnology, 38 (8), 1244-1260
- Ahn, K.-H., Song, K.-G., Yeom, I.-T., Park, K.-Y. (2001). Performance comparison of direct membrane separation and membrane bioreactor for domestic wastewater treatment and water reuse. Water Supply, 1 (5-6), 315-323
- Aho, K. S., Raymond, P. A. (2019). Differential response of greenhouse gas evasion to storms in forested and wetland streams. *Journal of Geophysical Research: Biogeosciences*, 124 (3), 649-662
- Alagawany, M., Elnesr, S. S., Saleh, A. A., El-Shall, N. A., Azzam, M. M., Dhama, K., Farag, M. R. (2023).

 An updated review of azolla in poultry diets. World's Poultry Science Journal, 80 (1), 155-170
- Alahmady, K. K., Stevens, K., Atkinson, S. (2012). Effects of Hydraulic Detention Time, Water Depth, and Duration of Operation on Nitrogen and Phosphorus Removal in a Flow-Through Duckweed Bioremediation System. *Journal of Environmental Engineering*, 139 (2), 160-166
- Alcamo, J. (2019). Water quality and its interlinkages with the sustainable development goals. Current Opinion in *Environmental Sustainability*, 36, 126-140
- Almeida, R. M., Nóbrega, G. N., Junger, P. C., Figueiredo, A. V., Andrade, A. S., de Moura, C. G. B.,
 Tonetta, D., Oliveira, F., Araújo, E.S., Rust, F., Piñeiro-Guerra, J. M., Mendonça, J. R., Medeiros, L.
 R., Pinheiro, L., Miranda, M., Costa, M. R. A., Melo, M. L., Nobre, R. L. G., Benevides, T., Roland,
 F., de Klein, J., Barros, N. O., Mendonça, R., Becker, V., Huszar, V. L. M., Kosten, S. (2016). High
 primary production contrasts with intense carbon emission in a eutrophic tropical reservoir.
 Frontiers in Microbiology, 7, 1-13
- Alshboul, Z., Encinas-Fernández, J., Hofmann, H., Lorke, A. (2016). Export of dissolved methane and carbon dioxide with effluents from municipal wastewater treatment plants. *Environmental Science & Technology*, 50 (11), 5555-5563
- Arefin, M. A., Rashid, F., Islam, A. (2021). A review of biofuel production from floating aquatic plants: an emerging source of bio-renewable energy. *Biofuels, Bioproducts and Biorefining*, 15 (2), 574-591
- Arets, E. J. M. M., Van der Kolk, J. W. H., Hengeveld, G. M., Lesschen, J. P., Kramer, H., Kuikman, P. J., Schelhaas, M. J. (2019). Greenhouse gas reporting of the LULUCF sector in the Netherlands: Methodological background, update 2019. Wettelijke Onderzoekstaken Natuur & Milieu, WOt-Technical Report 146.
- Atashgahi, S., Aydin, R., Dimitrov, M. R., Sipkema, D., Hamonts, K., Lahti, L., Maphosa, F., Kruse, T., Saccenti, E., Springael, D., Dejonghe, W., Smidt, H. (2015). Impact of a wastewater treatment plant on microbial community composition and function in a hyporheic zone of a eutrophic river. Scientific reports, 5 (1), 17284

- Attermeyer, K., Flury, S., Jayakumar, R., Fiener, P., Steger, K., Arya, V., Wilken, F., van Geldern, R., Premke, K. (2016). Invasive floating macrophytes reduce greenhouse gas emissions from a small tropical lake. *Scientific reports*, 6, 20424
- Attermeyer, K., Casas-Ruiz, J. P., Fuss, T., Pastor, A., Cauvy-Fraunié, S., Sheath, D., Nydahl, A. C., Doretto, A., Portela, A. P., Doyle, B. C., Simov, N., Gutmann Roberts, C., Niedrist, G. H., Timoner, X., Evtimova, V., Barral-Fraga, L., Bašić, T., Audet, J., Deininger, A., Busst, G., Fenoglio, S., Catalán, N., de Eyto, E., Pilotto, F., Mor, J.-R., Monteiro, J., Fletcher, D., Noss, C., Colls, M., Nagler, M., Liu, L., Romero González-Quijano, C., Romero, F., Pansch, N., Ledesma, J. L. J., Pegg, J., Klaus, M., Freixa, A., Herrero Ortega, S., Mendoza-Lera, C., Bednařík, A., Fonvielle, J. A., Gilbert, P. J., Kenderov, L. A., Rulík, M., Bodmer, P. (2021). Carbon dioxide fluxes increase from day to night across European streams. Communications Earth & Environment, 2, 118

В

- Babatunde, E. O., Gurav, R., Hwang, S. (2023). Recent Advances in Invasive Aquatic Plant Biomass Pretreatments for Value Addition. Waste and Biomass Valorization, 14, 3503-3527
- Badiou, P., Page, B., Ross, L. (2019). A comparison of water quality and greenhouse gas emissions in constructed wetlands and conventional retention basins with and without submerged macrophyte management for storm water regulation. *Ecological Engineering*, 127, 292-301
- Baker, J.A., Entsch, B., McKay, D.B. (2003). The cyanobiont in an Azolla fern is neither Anabaena nor Nostoc. FEMS Microbiology Letters, 229 (1), 43-47
- Bartosiewicz, M., Laurion, I., Clayer, F., Maranger, R. (2016). Heat-Wave Effects on Oxygen, Nutrients, and Phytoplankton Can Alter Global Warming Potential of Gases Emitted from a Small Shallow Lake. Environmental Science and Technology, 50 (12), 6267–6275
- Bastviken, D. (2009). Methane. In Encyclopedia of Inland Waters, Academic Press, 783–805. ISBN 9780123706263
- Bastviken, D., Cole, J. J., Pace, M. L., Van de-Bogert, M. C. (2008). Fates of methane from different lake habitats: Connecting whole-lake budgets and CH4 emissions. *Journal of Geophysical Research:*Biogeosciences, 113 (2), 1–13
- Bastviken, D., Cole, J., Pace, M., Tranvik, L. (2004). Methane emissions from lakes: Dependence of lake characteristics, two regional assessments, and a global estimate. *Global Biogeochemical Cycles*, 18(4), 1–12
- Bastviken, D., Tranvik, L. J., Downing, J. A., Crill, P. M., Enrich-Prast, A. (2011). Freshwater methane emissions offset the continental carbon sink. *Science*, 331(6013), 50
- Bates, D., Maechler, M., Bolker, B., Walker, S. (2015). Fitting Linear Mixed-Effects Models Using {lme4}. Journal of Statistical Software, 67 (1), 1-48
- Baulch, H. M., Dillon, P. J., Maranger, R., Schiff, S. L. (2011). Diffusive and ebullitive transport of methane and nitrous oxide from streams: Are bubble-mediated fluxes important? Journal of Geophysical Research: *Biogeosciences*, 116 (4)
- Beaulieu, J. J., DelSontro, T., Downing, J. A. (2019). Eutrophication will increase methane emissions from lakes and impoundments during the 21st century. *Nature Communications*, 10 (1), 3–7
- Benelli, S., & Bartoli, M. (2021). Worms and submersed macrophytes reduce methane release and increase nutrient removal in organic sediments. *Limnology And Oceanography Letters*, 6 (6), 329–338
- Benjawan, L., Koottatep, T. (2007). Nitrogen removal in recirculated duckweed ponds system. Water Science & Technology, 55 (11) 103-110
- Betlach, M. R., Tiedje, J. M. (1981). Kinetic Explanation for Accumulation of Nitrite, Nitric Oxide, and Nitrous Oxide During Bacterial Denitrification. Applied and Environmental Microbiology, 42 (6), 1074-1084

- Birch, H. F. (1961). Phosphorus transformations during plant decomposition. Plant and Soil, 15 (4), 347-366
- Bodelier, P. L. E., Laanbroek, H. J. (2004). Nitrogen as a regulatory factor of methane oxidation in soils and sediments. FEMS Microbiology Ecology, 47 (3), 265-277
- Boström, B., Andersen, J. M., Fleischer, S., & Jansson, M. (1988). Exchange of Phosphorus Across the Sediment-Water Interface. *Phosphorus in Freshwater Ecosystems*, 229–244
- Brouwer, P., Bräutigam, A., Buijs, V. A., Tazelaar, A. O. E., van der Werf, A., Schlüter, U., Reichart, G.-J., Bolger, A., Usadel, B., Weber, A. P. M., Schluepmann, H. (2017). Metabolic adaptation, a specialized leaf organ structure and vascular responses to diurnal N2 fixation by nostoc azollae sustain the astonishing productivity of azolla ferns without nitrogen fertilizer. Frontiers in Plant Science, 8
- Brouwer, P., Schluepmann, H., Nierop, K. G. J., Elderson, J., Bijl, P. K., van der Meer, I. M., de Visser, W., Reichart, G. J., Smeekens, S., van der Werf A. (2018). Growing Azolla to produce sustainable protein feed: the effect of differing species and CO2 concentrations on biomass productivity and chemical composition. Journal of the Science of Food and Agriculture, 98 (12), 4759–4768
- Bunce, J. T., Ndam, E., Ofiteru, I. D., Moore, A., Graham, D. W. (2018). A review of phosphorus removal technologies and their applicability to small-scale domestic wastewater treatment systems. Frontiers in Environmental Science, 6 (FEB), 1–15
- Burdon, F. J., Bai, Y., Reyes, M., Tamminen, M., Staudacher, P., Mangold, S., Singer, H., Räsänen, K., Joss, A., Tiegs, S. D., Jokela, J., Eggen, R. I. L., Stamm, C. (2020). Stream microbial communities and ecosystem functioning show complex responses to multiple stressors in wastewater. *Global Change Biology*, 26 (11), 6363–6382
- Buys, B. R., Klapwijk, A., Elissen, H., Rulkens, W. H. (2008). Development of a test method to assess the sludge reduction potential of aquatic organisms in activated sludge. *Bioresource Technology*, 99 (17), 8360–8366

C

- Callahan, B. J., McMurdie, P. J., Rosen, M. J., Han, A. W., Johnson, A. J. A., Holmes, S. P. (2016). DADA2: High-resolution sample inference from Illumina amplicon data. *Nature methods*, 13 (7), 581-583
- Caporaso, J. G., Lauber, C. L., Walters, W. A., Berg-Lyons, D., Huntley, J., Fierer, N., Owens, S. M., Betley, J., Fraser, L., Bauer, M., Gormley, N., Gilbert, J. A., Smith, G., Knight, R. (2012). Ultra-highthroughput microbial community analysis on the Illumina HiSeq and MiSeq plat-forms. The ISME Journal, 6, 1621–1624
- Carey, R. O., Migliaccio, K. W. (2009). Contribution of Wastewater Treatment Plant Effluents to Nutrient Dynamics in Aquatic Systems: A Review. *Environmental Management*, 44, 205–217
- Casas-Ruiz, J. P., Bodmer, P., Bona, K. A., Butman, D., Couturier, M., Emilson, E. J. S., Finlay, K., Genet, H., Hayes, D., Karlsson, J., Paré, D., Peng, C., Striegl, R., Webb, J., Wei, X., Ziegler, S. E., del Giorgio, P. A. (2023). Integrating terrestrial and aquatic ecosystems to constrain estimates of land-atmosphere carbon exchange. *Nature Communications*, 14, 1571
- CBS (Centraal Bureau voor de Statistiek). (2021). Zuivering van stedelijk afvalwater; per regionale waterkwaliteitsbeheerder (*Urban wastewater treatment; per regional water quality manager*). https://www.cbs.nl/nl-nl/cijfers/detail/71476ned
- CBS, PBL, RIVM, WUR (2024). Oppervlaktewater in Nederland (indicator 1401, versie 01, 21 juni 2021) www.clo.nl. Centraal Bureau voor de Statistiek (CBS), Den Haag; PBL Planbureau voor de Leefomgeving, Den Haag; RIVM Rijksinstituut voor Volksgezondheid en Milieu, Bilthoven; en Wageningen University and Research, Wageningen
- Cébron, A., Coci, M., Garnier, J., Laanbroek, H. J. (2004). Denaturing gradient gel electrophoretic analysis of ammonia-oxidizing bacterial community structure in the lower Seine River: impact of Paris wastewater effluents. *Applied and Environmental Microbiology*, 70 (11), 6726-6737

- Chakraborty, A., Saha, G. K., Aditya, G. (2022). Macroinvertebrates as engineers for bioturbation in freshwater ecosystem. *Environmental Science and Pollution Research*, 29, 64447-64468
- Chen, M., Ding, S., Liu, L., Xu, D., Han, C., Zhang, C. (2015). Iron-coupled inactivation of phosphorus in sediments by macrozoobenthos (chironomid larvae) bioturbation: Evidences from high-resolution dynamic measurements. *Environmental Pollution*, 204, 241–247
- Chen, Y.-C. (2019). Estimation of greenhouse gas emissions from a wastewater treatment plant using membrane bioreactor technology. Water Environment Research, 91 (2), 85-174
- Cherry, K. A., Shepherd, M., Withers, P. J. A., Mooney, S. J. (2008). Assessing the effectiveness of actions to mitigate nutrient loss from agriculture: A review of methods. *Science of the Total Environment*, 406 (1-2), 1-23
- Chingangbam, S. S., Khoiyangbam, R. S. (2023). Submerged macrophytes enhance carbon emission (CO2 and CH4) from the freshwater wetland in Keibul Lamjao National Park, Manipur, India. *Limnologica*, 103, 126125
- Chowdhury, R. B., Moore, G. A., Weatherley, A. J., Arora, M. (2017). Key sustainability challenges for the global phosphorus resource, their implications for global food security, and options for mitigation. *Journal of Cleaner Production*, 140 (2), 945-963
- Christiansen, J. R., Outhwaite, J., Smukler, S. M. (2015). Comparison of CO2, CH4 and N2O soilatmosphere exchange measured in static chambers with cavity ring-down spectroscopy and gas chromatography. *Agricultural and Forest Meteorology*, 2015, 211–212, 48–57
- Christiansen, N. H., Andersen, F. Ø., Jensen, H. S. (2016). Phosphate uptake kinetics for four species of submerged freshwater macrophytes measured by a ³³P phosphate radioisotope technique. *Aquatic Botany*, 128, 58-67
- Coenen, P. W. H. G., van der Maas, C. W. M., Zijlema, P. J., Arests, E. J. M. M., Baas, K., van der Berghe, A. C. W. M., van Huis, E. P., Geilenkirchen, G., Hoogsteen, M., Spijker, J., te Molder, R., Dröge, R., Montfoort, J. A., Peek, C. J., Vonk, J., Oude Voshaar, S., Dellaert, S. (2017). Greenhouse Gas Emissions in the Netherlands 1990-2015: National Inventory Report 2017, 364.
- Connolly, J., Holden, N. M. (2017). Detecting peatland drains with Object Based Image Analysis and Geoeye-1 imagery. Carbon Balance and Management, 12, 7
- Conthe, M., Lycus, P., Arntzen, M. Ø., Ramos da Silva, A., Frostegård, Å., Bakken, L. R., Kleerebezem, R., Van Loosdrecht, M. C. M. (2019). Denitrification as an N2O sink. *Water Research*, 151, 381-387
- Cooper, M. D. A., Evans, C. D., Zielinski, P., Levy, P. E., Gray, A., Peacock, M., Norris, D., Fenner, N., Freeman, C. (2014). Infilled Ditches are Hotspots of Landscape Methane Flux Following Peatland Re-wetting. *Ecosystems*, 17 (7), 1227–1241
- Costa, M. L., Santos, M. C. R., Carrapiço, F., Pereira, A. L. (2009). Azolla-Anabaena's behaviour in urban wastewater and artificial media Influence of combined nitrogen. *Water Research*, 43 (15), 3743–3750
- Couwenberg, J., Dommain, R., Joosten, H. (2010). Greenhouse gas fluxes from tropical peatlands in south-east Asia. *Global Change Biology*, 16 (6), 1715–1732
- Crawford, J. T., Stanley, E. H., Spawn, S. A., Finlay, J. C., Loken, L. C., Striegl, R. G. (2014). Ebullitive methane emissions from oxygenated wetland streams. *Global Change Biology*, 20 (11), 3408–3422

D

- Dai, H., Sun, Y., Wan, D., Abbasi, H. N., Guo, Z., Geng, H., Wang, X., Chen, Y. (2022). Simultaneous denitrification and phosphorus removal: A review on the functional strains and activated sludge processes. *Science of the Total Environment*, 835, 155409
- Daims, H., Lebedeva, E. V., Pjevac, P., Han, P., Herbold, C., Albertsen, M., Jehmlich, N., Palatinszky, M., Vierheilig, J., Bulaev, A., Kirkegaard, R. H., von Bergen, M., Rattei, T., Bendinger, B., Nielsen, P. H., Wagner, M. (2015). Complete nitrification by Nitrospira bacteria. *Nature*, 528 (7583), 504-509

- Danhorn, T., Fuqua, C. (2007) Biofilm formation by plant-associated bacteria. Annual Review of Microbiology, 61 (1), 401-422
- Davidson, T. A., Audet, J., Jeppesen, E., Landkildehus, F., Lauridsen, T. L., Søndergaard, M., Syväranta, J. (2018). Synergy between nutrients and warming enhances methane ebullition from experimental lakes. *Nature Climate Change*, 8 (2), 156–160
- Dean, J. F., Meisel, O. H., Martyn Rosco, M., Belelli Marchesini, L., Garnett, M. H., Lenderink, H., van Logtestijn, R., Borges, A. V., Bouillon, S., Lambert, T., Röckmann, T., Maximov, T., Petrov, R., Karsanaev, S., Aerts, R., van Huissteden, J., Vonk, J. E., Dolman, A. J. (2020). East Siberian Arctic inland waters emit mostly contemporary carbon. *Nature Communications*, 11 (1), 1627
- Deemer, B. R., Holgerson, M.A. (2021). Drivers of Methane Flux Differ Between Lakes and Reservoirs, Complicating Global Upscaling Efforts. *Journal of Geophysical Research*: Biogeosciences, 126 (4)
- DelSontro, T., Beaulieu, J. J., Downing, J. A. (2018). Greenhouse gas emissions from lakes and impoundments: Upscaling in the face of global change. Limnology and Oceanography Letters, 3 (3), 64–75
- Desmidt, E., Ghyselbrecht, K., Zhang, Y., Pinoy, L., Van der Bruggen, B., Verstraete, W., Rabaey, K., Meesschaert, B. (2015). Global Phosphorus Scarcity and Full-Scale P-Recovery Techniques: A Review. Critical Reviews in Environmental Science and Technology, 45 (4), 336-384
- De Wilt, A., Butkovskyi, A., Tuantet, K., Hernandez Leal, L., Fernandes, T. V., Langenhoff, A., Zeeman, G. (2016). Micropollutant removal in an algal treatment system fed with source separated wastewater streams. *Journal of Hazardous Materials*, 304, 84-92
- Diaz, O. A., Reddy, K. R., Moore Jr., P. A. (1995). Solubility of inorganic phosphorus in stream water as influences by pH and calcium concentration. *Water Research*, 28 (8), 1755-1763
- Dickson, A. G., Millero, F. J. (1987). A comparison of the equilibrium constants for the dissociation of carbonic acid in seawater media. *Deep Sea Research Part A, Oceanographic Research Papers*, 34 (10), 1733–1743
- Dinno A. (2017). _dunn.test: Dunn's Test of Multiple Comparisons Using Rank Sums_. R package version 1.3.5 (1.3.5). https://CRAN.R-project.org/package=dunn.test
- Do, T. T., Delaney, S., Walsh, F. (2019). 16S rRNA gene based bacterial community structure of wastewater treatment plant effluents. FEMS microbiology letters, 366 (3)
- Dong, Y., Liu, J., Cheng, X., Fan, F., Lin, W., Zhou, C., Wang, S., Xiao, S., Wang, C., Li, Y., Li, C. (2023). Wastewater-influenced estuaries are characterized by disproportionately high nitrous oxide emissions but overestimated IPCC emission factor. *Communications Earth & Environment*, 4 (1), 395
- Dos Reis Oliveira, P. C., Kraak, M. H. S., Pena-Ortiz, M., Van der Geest, H. G., Verdonschot, P. F. M. (2020). Responses of macroinvertebrate communities to land use specific sediment food and habitat characteristics in lowland streams. *Science of the Total Environment*, 703, 135060
- Drury, B., Rosi-Marshall, E., Kelly, J. J. (2013). Wastewater treatment effluent reduces the abundance and diversity of benthic bacterial communities in urban and suburban rivers. *Applied and environmental microbiology*, 79 (6), 1897-1905
- Duc, N. T., Crill, P., Bastviken, D. (2010). Implications of temperature and sediment characteristics on methane formation and oxidation in lake sediments. *Biogeochemistry*, 100, 185-196

E

- EEA (European Environment Agency). (2018). European Waters Assessment of status and pressures 2018. EEA report 7/2018, ISBN 978-92-9213-947-6
- Emsens, W.-J., Aggenbach, C. J. S., Schoutens, K., Smolders, A. J. P., Zak, D., Van Diggelen, R. (2016). Soil Iron Content as a Predictor of Carbon and Nutrient Mobilization in Rewetted Fens. *PLOS ONE*, 11 (4), e0153166

- EPRS (European Parliamentary Research Service) (2024). Urban wastewater treatment: updating EU rules. Briefing, EU Legislation in Progress. Report no. PE 739.370 April 2024
- Eriksson, P. G., Weisner, S. E. B. (1999). An experimental study on effects of submersed macrophytes on nitrification and denitrification in ammonium-rich aquatic systems. *Limnology and Oceanography*, 44 (8), 1993-1999
- Ettwig, K. F., Butler, M. K., Le Paslier, D., Pelletier, E., Mangenot, S., Kuypers, M. M., Schreiber, F., Dutilh, B. E., Zedelius, J., de Beer, D., Gloerich, J., Wessels, H. J. C. T., van Alen, T., Luesken, F., Wu, M. L., van de Pas-Schoonen, K. T., Op den Kamp, H. J. M., Janssen-Megens, E. M., Francoijs, K.-J., Stunnenberg, H., Weissenbach, J., Jetten, M. S. M., Strous, M. (2010). Nitrite-driven anaerobic methane oxidation by oxygenic bacteria. *Nature*, 464 (7288), 543-548
- European Commission. (2021). 'Fit for 55': delivering the EU's 2030 Climate Target on the way to climate neutrality. Communication from the Commission to the European Parliament, the Council, the European Economic and Social Committee and the Committee of the Regions, COM(2021) 550 final, Brussels
- European Commission. (2022). Press release European Green Deal: Commission proposes rules for cleaner air and water. In IP/22/6278. 2022
- Evans, C. D., Renou-Wilson, F., Strack, M. (2016). The role of waterborne carbon in the greenhouse gas balance of drained and re-wetted peatlands. *Aquatic Sciences*, 78 (3), 573–590
- Evers, C.H.M., van den Broek, A.J.M., Buskens, R., van Leerdam, A., Knoben, R.A.E., van Herpen, F.C.J., Pot, R. (2018). Omschrijving MEP en maatlatten voor sloten en kanalen voor de Kaderrichtlijn Water 2021-2027 (in Dutch). Stichting Toegepast Onderzoek Waterbeheer (STOWA), report 2018-50. ISBN: 978.90.5773.814.2

F

- FAO and UN Water. (2021). Progress on Level of Water Stress. Global status and acceleration needs for SDG Indicator 6.4.2. Rome
- Feng, Y., Luo, S., Zhang, Y., Wang, S., Peng, Y. (2022). Enhanced nutrient removal from mainstream sewage via denitrifying dephosphatation, endogenous denitrification and anammox in a novel continuous flow process. *Bioresource Technology*, 351, 127003
- Fernandes, T. V., Trebuch, L. M., Wijffels, R. H. (2022). Chapter 4 Microalgae-based technologies for circular wastewater treatment. Integrated Wastewater Management and Valorization using Algal Cultures, 81-112
- Figueiredo-Barros, M. P., Caliman, A., Leal, J. J. F., Bozelli, R. L., Farjalla, V. F., Esteves, F. A. (2009).

 Benthic bioturbator enhances CH4 fluxes among aquatic compartments and atmosphere in experimental microcosms. Canadian Journal of Fisheries and Aquatic Sciences, 66 (10), 1649-1657
- Firestone, M. K., Davidson, E. A. (1989). Microbiological Basis of NO and N2O Production and Consumption in Soil. Exchange of Trace Gases between Terrestrial Ecosystems and the Atmosphere, 47, 7-21
- Flury, S., Glud, R. N., Premke, K., McGinnis, D. F. (2015). Effect of Sediment Gas Voids and Ebullition on Benthic Solute Exchange. *Environmental Science and Technology*, 49 (17), 10413–10420
- Foucault, Q., Wieser, A., Waldvogel, A. M., Feldmeyer, B., Pfenninger, M. (2018). Rapid adaptation to high temperatures in Chironomus riparius. *Ecology and Evolution*, 8 (24), 12780–12789
- Fox, J., Weisberg, S. (2019). An {R} Companion to Applied Regression (3rd ed.). Sage. https://socialsciences.mcmaster.ca/jfox/Books/Companion/
- Francis, C. A., Beman, J. M., Kuypers, M. M. M. (2007). New processes and players in the nitrogen cycle: the microbial ecology of anaerobic and archaeal ammonia oxidation. *The ISME Journal*, 1 (1), 19-27

- Friendly, M., Fox, J., Monette, G. (2022). heplots: Visualizing Tests in Multivariate Linear Models. R package version 1.4-2 (1.4-2). https://CRAN.R-project.org/package=heplots
- Fuchs, A., Lyautey, E., Montuelle, B., Casper, P. (2016). Effects of increasing temperatures on methane concentrations and methanogenesis during experimental incubation of sediments from oligotrophic and mesotrophic lakes. *Journal of Geophysical Research: Biogeosciences*, 121 (5), 1394–1406

G

- Gacia, E., Bernal, S., Nikolakopoulou, M., Carreras, E., Morgado, L., Ribot, M., Isnard, M., Sorolla, A., Sabater, F., Martí, E. (2019). The role of helophyte species on nitrogen and phosphorus retention from wastewater treatment plant effluents. *Journal of Environmental Management*, 252, 109585
- Galantini, L., Lapierre, J.-F., Maranger, R. (2021). How Are Greenhouse Gases Coupled Across Seasons in a Large Temperate River with Differential Land Use? *Ecosystems*, 24, 2007-2027
- Garcia Chance, L.M., Majsztrik, J.C., Bridges, W.C., Willis, A., Albano, J.P., White, S.A. (2020).

 Comparative Nutrient Remediation by Monoculture and Mixed Species Plantings within Floating
 Treatment Wetlands. Environmental Science & Technology, 54 (14), 8710-8718
- Gautreau, E., Volatier, L., Nogaro, G., Gouze, E., Mermillod-Blondin, F. (2020). The influence of bioturbation and water column oxygenation on nutrient recycling in reservoir sediments. Hydrobiologia, 847 (4), 1027–1040
- Ge, S., Champagne, P. (2017). Cultivation of the Marine Macroalgae Chaetomorpha linum in Municipal Wastewater for Nutrient Recovery and Biomass Production. Environmental Science and Technology, 51 (6), 3558–3566
- Geng, Y., Han, W., Yu, C., Jiang, Q., Wu, J., Chang, J., Ge, Y. (2017). Effect of plant diversity on phosphorus removal in hydroponic microcosms simulating floating constructed wetlands. *Ecological Engineering*, 107, 110-119
- Ghosh, D., Gopal, B. (2010). Effect of hydraulic retention time on the treatment of secondary effluent in a subsurface flow constructed wetland. *Ecological Engineering*, 36 (8), 1044-1051
- Golterman, H. L. (2004). The chemistry of Phosphate and Nitrogen Compounds in Sediments. Kluwer Academic Publishers. ISBN: 1-4020-1951-3
- Graça, M. A. S. (2001). The role of invertebrates on leaf litter decomposition in streams—a review. *International Review of Hydrobioly*, 86 (4–5), 383–393
- Grasset, C., Mendonça, R., Saucedo, G. V., Bastviken, D., Roland, F., Sobek, S. (2018). Large but variable methane production in anoxic freshwater sediment upon addition of allochthonous and autochthonous organic matter. *Limnology and Oceanography*, 63 (4), 1488-1501
- Graves, S., Piepho, H.-P., Selzer L., with help from Dorai-Raj, S. (2019). multcompView: Visualizations of Paired Comparisons. R package version 0.1-8. https://CRAN.R-project.org/package=multcompView
- Groenendijk, D., Postma, J. F., Kraak, M. H. S., Admiraal, W. (1998). Seasonal dynamics and larval drift of Chironomus riparius (Diptera) in a metal contaminated lowland river. *Aquatic Ecology*, 32 (4), 341–351
- Groenendijk, P., van Boekel, E., Renaud, L., Greijdanus, A., Michels, R., de Koeijer T. (2016). Landbouw en de KRW-opgave voor nutriënten in regionale wateren; Het aandeel van landbouw in de KRW-opgave, de kosten van enkele maatregelen en de effecten ervan op de uit- en afspoeling uit landbouwgronden (Agriculture and the WFD tasking for nutrients in regional waters; The share of agriculture in the WFD tasking, the costs of some measures and their effects on leaching and run-off from agricultural land). Wageningen, Wageningen Environmental Research, Rapport 2749
- Groffman, P. M., Butterbach-Bahl, K., Fulweiler, R. W., Gold, A. J., Morse, J. L., Stander, E. K., Tague, C., Tonitto, C., Vidon, P. (2009). Challenges to incorporating spatially and temporally explicit phenomena (hotspots and hot moments) in denitrification models. *Biogeochemistry*, 93, 49-77

- Günthel, M., Donis, D., Kirillin, G., Ionescu, D., Bizic, M., McGinnis, D. F., Grossart, H.-P., Tang, K. W. (2019). Contribution of oxic methane production to surface methane emission in lakes and its global importance. *Nature Communications*, 10, 5497
- Günther, A., Barthelmes, A., Huth, V., Joosten, H., Jurasinski, G., Koebsch, F., Couwenberg, J. (2020).

 Prompt rewetting of drained peatlands reduces climate warming despite methane emissions.

 Nature Communications, 11 (1), 1–5
- Gutierrez, O., Park, D., Sharma, K. R., Yuan, Z. (2010). Iron salts dosage for sulfide control in sewers induces chemical phosphorus removal during wastewater treatment. *Water Research*, 44 (11), 3467–3475

Н

- Halekoh, U., Højsgaard, S. (2014). A kenward-roger approximation and parametric bootstrap methods for tests in linear mixed models—the R package pbkrtest. *Journal of Statistical Software*, 59 (9), 1-30
- Hama-Aziz, Z. Q., Hiscock, K. M., Cooper, R. J. (2017). Indirect Nitrous Oxide Emission Factors for Agricultural Field Drains and Headwater Streams. Environmental Science and Technology, 51 (1), 301–307
- Hamdan, H. Z., Houri, A. F. (2022). CO2 sequestration by propagation of the fast-growing Azolla spp. Environmental Science and Pollution Research, 29 (12), 16912–16924
- Han, B., Zhang, S., Zhang, L., Liu, K., Yan, L., Wang, P., Wang, C., Pang, S. (2018). Characterization of microbes and denitrifiers attached to two species of floating plants in the wetlands of Lake Taihu. PLOS ONE, 13 (11), e0207443
- Haroon, M. F., Hu, S., Shi, Y., Imelfort, M., Keller, J., Hugenholtz, P., Yuan, Z., Tyson, G. W. (2013). Anaerobic oxidation of methane coupled to nitrate reduction in a novel archaeal lineage. *Nature*, 500 (7464), 567-570
- Harpenslager, S. F., Thiemer, K., Levertz, C., Misteli, B., Sebola, K. M., Schneider, S. C., Hilt, S., Köhler, J. (2022). Short-term effects of macrophyte removal on emission of CO2 and CH4 in shallow lakes. *Aquatic Botany*, 182, 103555
- Harter, R. D. (1969). Phosphorus adsorption sites in soils. Soil Science Society of America Journal, 33, 630-632
- Hartmann, J., Moosdorf, N., Lauerwald, R., Hinderer, M., West, A. J. (2014). Global chemical weathering and associated P-release - The role of lithology, temperature and soil properties. Chemical Geology, 363, 145–1630
- Heiri, O., Lotter, A. F., Lemcke, G. (2001). Loss on ignition as a method for estimating organic and carbonate content in sediments: reproducibility and comparability of results. *Journal of Paleolimnology*, 25, 101–110
- Hendrickx, T. L. G. (2009). Aquatic Worm Reactor for Improved Sludge Processing and Resource Recovery. PhD thesis, Wageningen University, the Netherlands, p. 168
- Hendriks, A. T. W. M., Langeveld, J. G. (2017). Rethinking wastewater treatment plant effluent standards: nutrient reduction or nutrient control? *Environmental Science & Technology*, 51 (9), 4735-4737
- Hendriks, L., Smolders, A. J. P., Van den Brink, T., Lamers, L. P. M., Veraart, A. J. (2023). Polishing wastewater effluent using plants: floating plants perform better than submerged plants in both nutrient removal and reduction of greenhouse gas emission. Water Science & Technology, 88 (1), 23-34
- Hendriks, L., Weideveld, S., Fritz, C., Stepina, T., Aben, R. C. H., Fung, N. E., Kosten, S. (2024a). Drainage ditches are greenhouse gas hotlines in peat landscapes with strong seasonal and spatial variation in diffusive and ebullitive emissions. *Freshwater Biology*, 69 (1), 143-156
- Hendriks, L., Van Der Meer, T. V., Kraak, M. H. S., Verdonschot, P. F. M., Smolders, A. J. P., Lamers, L. P. M., Veraart, A. J. (2024b). Sludge degradation, nutrient removal and reduction of greenhouse gas emission by a Chironomus-Azolla wastewater treatment cascade. *PLOS ONE*, 19 (5), e0301459

- Hendriks, L., Smolders, A. J. P., van Erp, I., Lamers, L. P. M., Veraart, A. J. (subm.). Combining different floating plants for optimal wastewater effluent polishing and carbon-capture
- Hensen, A., Groot, T. T., Van Den Bulk, W. C. M., Vermeulen, A. T., Olesen, J. E., Schelde, K. (2006). Dairy farm CH4 and N2O emissions, from one square metre to the full farm scale. Agriculture, Ecosystems and Environment, 112 (2-3), 146-152
- Herlemann, D. P., Labrenz, M., Jürgens, K., Bertilsson, S., Waniek, J. J., Andersson, A. F. (2011). Transitions in bacterial communities along the 2000 km salinity gradient of the BalticSea. The ISME Journal, 5, 1571-1579
- Hernández, M. E., Galindo-Zetina, M., Hernández-Hernández, J. C. (2018). Greenhouse gas emissions and pollutant removal in treatment wetlands with ornamental plants under subtropical conditions. Ecological Engineering, 114, 88-95
- Hilt, S., Grossart, H.-P., McGinnis, D. F., Keppler, F. (2022). Potential role of submerged macrophytes for oxic methane production in aquatic ecosystems. Limnology and Oceanography, 67 (S2), S76-S88
- Hilton, J., O'Hare, M., Bowes, M. J., Jones, J. I. (2006). How green is my river? A new paradigm of eutrophication in rivers. Science of the Total environment, 365, 66-83
- Holgerson, M. A. (2015). Drivers of carbon dioxide and methane supersaturation in small, temporary ponds. Biogeochemistry, 305-318
- Holomuzki, J. R., Feminella, J. W., Power, M. E. (2010). Biotic interactions in freshwater benthic habitats. Journal of the North American Benthological Society, 29 (1), 220-244
- Hooijer, A., Page, S., Jauhiainen, J., Lee, W. A., Lu, X. X., Idris, A., Anshari, G. (2012). Subsidence and carbon loss in drained tropical peatlands. *Biogeosciences*, 9 (3), 1053-1071
- Hooper, H. L., Sibly, R. M., Hutchinson, T., Maund, S. J. (2003). The influence of larval density, food availability and habitat longevity on the life history and population growth rate of the midge Chironomus riparius. Oikos, 102, 515-524
- Höskuldsson, A. (1988). PLS Regression methods. Journal of Chemometrics, 2, 211-228
- Hotchkiss, E. R., Hall Jr, R. O., Sponseller, R. A., Butman, D., Klaminder, J., Laudon, H., Rosvall, M., Karlsson, J. (2015). Sources of and processes controlling CO2 emissions change with the size of streams and rivers. Nature Geoscience, 8, 696-699
- Hu, B., Wang, D., Zhou, J., Meng, W., Li, C., Sun, Z., Guo, X., Wang, Z. (2018). Greenhouse gases emission from the sewage draining rivers. Science of the Total Environment, 612, 1454-1462
- Hu, Y., Hao, X., van Loosdrecht, M., Chen, H. (2017). Enrichment of highly settleable microalgal consortia in mixed cultures for effluent polishing and low-cost biomass production. Water Research, 125, 11-22
- Hube, S., Eskafi, M., Hrafnkelsdóttir, K.F., Bjarnadóttir, B., Bjarnadóttir, M.A., Axelsdóttir, S., Wu, B. (2020). Direct membrane filtration for wastewater treatment and resource recovery: A review. Science of The Total Environment, 710, 136375

- Ilyas, H., Masih, I. (2017). Intensification of constructed wetlands for land area reduction: a review. Environmental Science and Pollution Research, 24, 12081-12091
- IPCC (2019). 2019 Refinement to the 2006 IPCC Guidelines for National Greenhouse Gas Inventories, Calvo Buendia, E., Tanabe, K., Kranjc, A., Baasansuren, J., Fukuda, M., Ngarize, S., Osako, A., Pyrozhenko, Y., Shermanau, P. and Federici, S. (eds). Published: IPCC, Switzerland. ISBN 978-4-88788-232-4

- IPCC (2021). Summary for Policymakers. In: Climate Change 2021: The Physical Science Basis. Contribution of Working Group I to the Sixth Assessment Report of the Intergovernmental Panel on Climate Change [Masson-Delmotte, V., P. Zhai, A. Pirani, S. L. Connors, C. Péan, S. Berger, N. Caud, Y. Chen, L. Goldfarb, M. I. Gomis, M. Huang, K. Leitzell, E. Lonnoy, J.B.R. Matthews, T. K. Maycock, T. Waterfield, O. Yelekçi, R. Yu and B. Zhou (eds.)]. Cambridge University Press, Cambridge, United Kingdom and New York, NY, USA, pp. 3–32
- IPCC (2023). Summary for Policymakers. In: Climate Change 2023: Synthesis Report. Contribution of Working Groups I, II and III to the Sixth Assessment Report of the Intergovernmental Panel on Climate Change [Core Writing Team, H. Lee and J. Romero (eds.)]. IPCC, Geneva, Switzerland, pp. 1-34
- Ito, O., Watanabe, I. (1983). The relationship between combined nitrogen uptakes and nitrogen fixation in Azolla-Anabaena symbiosis. *The New Phytologist*, 95, 647-654
- Iwata, H., Hirata, R., Takahashi, Y., Miyabara, Y., Itoh, M., Iizuka, K. (2018). Partitioning Eddy-Covariance Methane Fluxes from a Shallow Lake into Diffusive and Ebullitive Fluxes. Boundary-Layer Meteorology, 169 (3), 413-428

J

- Janes, R. (1998). Growth and survival of Azolla filiculoides in Britain: I. Vegetative reproduction. New Phytologist, 138 (2), 367-375
- Jarek, S. (2012). _mvnormtest: Normality test for multivariate variables_. R package version 0.1-9 (0.1-9). https://CRAN.R-project.org/package=mvnormtest
- Ji, Q., Babbin, A. R., Jayakumar, A., Oleynik, S., Ward, B. B. (2015). Nitrous oxide production by nitrification and denitrification in the Eastern Tropical South Pacific oxygen minimum zone. Geophysical Research Letters, 42 (24), 10755-10764
- Johnson, M. S., Matthews, E., Du, J., Genovese, V., Bastviken, D. (2022). Methane Emission From Global Lakes: New Spatiotemporal Data and Observation-Driven Modeling of Methane Dynamics Indicates Lower Emissions. *Journal of Geophysical Research: Biogeosciences*, 127 (7), e2022JG006793
- Johnston, J., LaPara, T., Behrens, S. (2019). Composition and dynamics of the activated sludge microbiome during seasonal nitrification failure. Scientific reports, 9 (1), 4565
- Johnston, J., Du, Z., Behrens, S. (2023). Ammonia-Oxidizing Bacteria Maintain Abundance but Lower amoA-Gene Expression during Cold Temperature Nitrification Failure in a Full-Scale Municipal Wastewater Treatment Plant. Microbiology Spectrum, 11 (2), e02571-22
- Jones, E.R., van Vliet, M. T. H., Qadir, M., Bierkens, M. F. P. (2021). Country-level and gridded estimates of wastewater production, collection, treatment and reuse. Earth System Science Data, 13 (2), 237–254
- Joosten, H. (2010). The Global Peatland Carbon dioxide Picture. Quaternary Science Reviews, 1–10
- Joosten, H., Clarke, D. (2002). Wise use of mires and peatlands: background and principles including a framework for decision-making. ISBN 951-97744-8-3
- Ju, F., Guo, F., Ye, L., Xia, Y., Zhang, T. (2014). Metagenomic analysis on seasonal microbial variations of activated sludge from a full-scale wastewater treatment plant over 4 years. Environmental microbiology reports, 6 (1), 80-89

ĸ

- Kadir, A. A., Abdullah, S. R. S., Othman, B. A., Hasan, H. A., Othman, A. R., Imron, M. F., Ismail, N. 'I., Kurniawan, S. B. (2020). Dual function of Lemna minor and Azolla pinnata as phytoremediator for Palm Oil Mill Effluent and as feedstock. *Chemosphere*, 259, 127468
- Kajan, R., Frenzel, P. (1999). The effect of chironomid larvae on production, oxidation and fluxes of methane in a flooded rice soil. FEMS Microbiology Ecology, 28 (2), 121-129

- Kankanamge, C. E., Kodithuwakku, H. (2017). Effect of interspecific competition on the growth and nutrient uptake of three macrophytes in nutrient-rich water. *Aquatic Ecology*, 51, 625-634
- Kartal, B., Kuypers, M. M. M., Lavik, G., Schalk, J., Op den Camp, H. J. M., Jetten, M. S. M., Strous, M. (2007). Anammox bacteria disguised as denitrifiers: nitrate reduction to dinitrogen gas via nitrite and ammonium. *Environmental Microbiology*, 9 (3), 635-642
- Kassambara, A. (2020). _ggpubr: "ggplot2" Based Publication Ready Plots_. R package version 0.4.0 (0.4.0). https://CRAN.R-project.org/package=ggpubr
- Kawan, J.A., Suja, F., Pramanik, S.K., Yusof, A., Rahman, R.A., Hasan, H.A. (2022). Effect of Hydraulic Retention Time on the Performance of a Compact Moving Bed Biofilm Reactor for Effluent Polishing of Treated Sewage. *Water*, 14 (1), 81
- Keerthanan, S., Jayasinghe, C., Biswas, J. K., Vithanage, M. (2021). Pharmaceutical and Personal Care Products (PPCPs) in the environment: Plant uptake, translocation, bioaccumulation, and human health risks. Critical Reviews in Environmental Science and Technology, 51 (12), 1221-1258
- Keizer-Vlek, H. E., Verdonschot, P. F. M., Verdonschot, R. C. M., Dekkers, D. (2014). The contribution of plant uptake to nutrient removal by floating treatment wetlands. *Ecological Engineering*, 73, 684-690
- Kelly, D. J., Hughes, N. J., Poole, R. K. (2001). Microaerobic Physiology: Aerobic Respiration, Anaerobic Respiration, and Carbon Dioxide Metabolism. In Helicobacter pylori (eds H.L.T. Mobley, G.L. Mendz and S.L. Hazell)
- Kenward, M.G., Roger, J.H. (1997). Small Sample Inference for Fixed Effects from Restricted Maximum Likelihood. *Biometrics*, 53 (3), 983-997
- Keppler, F., Boros, M., Frankenberg, C., Lelieveld, J., Mcleod, A. R., Pirttilä, A. M., Röckmann, T., Schnitzler, J. P. (2009). Methane formation in aerobic environments. *Environmental Chemistry*, 6, 459-465
- Khomami, A. M., Padasht, M. N., Lahiji, A. A., Mahtab, F. (2019). Reuse of peanut shells and Azolla mixes as a peat alternative in growth medium of Dieffenbachia amoena 'tropic snow'. *International Journal of Recycling of Organic Waste in Agriculture*, 8, 151-157
- Kim, D., Begum, M., Choi, J., Jin, H., Chea, E., Park, J. (2019). Comparing effects of untreated and treated wastewater on riverine greenhouse gas emissions. APN Science Bulletin, 9 (1)
- Köhn, D., Welpelo, C., Günther, A., Jurasinski, G. (2021). Drainage Ditches Contribute Considerably to the CH4 Budget of a Drained and a Rewetted Temperate Fen. Wetlands, 41 (6)
- Körner, S., Vermaat, J.E. (1998). The relative importance of Lemna gibba L., bacteria and algae for the nitrogen and phosphorus removal in duckweed-covered domestic wastewater. *Water Research*, 32 (12), 3651-3661
- Körner, S., Vermaat, J.E., Veenstra, S. (2003). The Capacity of Duckweed to Treat Wastewater: Ecological Considerations for a Sound Design. *Journal of Environmental Quality*, 32 (5), 1583-1590
- Kong, W., Shen, B., Lyu, H., Kong, J., Ma, J., Wang, Z., Feng, S. (2021). Review on carbon dioxide fixation coupled with nutrients removal from wastewater by microalgae. *Journal of Cleaner Production*, 292, 125975
- Kooijman, A. M., Cusell, C., Mettrop, I. S., Lamers, L. P. M. (2016). Recovery of target bryophytes in floating rich fens after 25 yr of inundation by base-rich surface water with lower nutrient contents. *Applied Vegetation Science*, 19 (1), 53–65
- Körner, S., Vermaat, J. E. (1998). The relative importance of Lemna gibba L., bacteria and algae for the nitrogen and phosphorus removal in duckweed-covered domestic wastewater. *Water Research*, 32 (12), 3651–3661
- Korsa, G., Alemu, D., Ayele, A. (2024). Azolla Plant Production and Their Potential Applications. International Journal of Agronomy, 1716440

- Koschorreck, M., Downing, A. S., Hejzlar, J., Marcé, R., Laas, A., Arndt, W. G., Keller, P. S., Smolders, A. J. P., van Dijk, G., Kosten, S. (2020). Hidden treasures: Human-made aquatic ecosystems harbour unexplored opportunities. *Ambio*, 49 (2), 531–540
- Kosten, S., Piñeiro, M., de Goede, E., de Klein, J., Lamers, L. P. M., Ettwig, K. (2016). Fate of methane in aquatic systems dominated by free-floating plants. *Water Research*, 104, 200–207
- Kreiling, R. M., Richardson, W. B., Bartsch, L. A., Thoms, M. C., Christensen, V. G. (2019). Denitrification in the river network of a mixed land use watershed: unpacking the complexities. *Biogeochemistry*, 143 (3), 327-346
- Kuznetsova, A., Brockhoff, P.B., Christensen, R.H.B. (2017). ImerTest Package: Tests in Linear Mixed Effects Models. *Journal of Statistical Software*, 82 (13)
- Kuzyakov, Y., Gavrichkova, O. (2010). REVIEW: Time lag between photosynthesis and carbon dioxide efflux from soil: a review of mechanisms and controls. *Global Change Biology*, 16 (12), 3386–3406

L

- Langenegger, T., Vachon, D., Donis, D., McGinnis, D. F. (2019). What the bubble knows: Lake methane dynamics revealed by sediment gas bubble composition. *Limnology and Oceanography*, 64 (4), 1526–1544
- Law, Y., Ye, L., Pan, Y., Yuan, Z. (2012). Nitrous oxide emissions from wastewater treatment processes. Philosophical Transactions of the Roal Society B, 367, 1265-1277
- Leifeld, J., Menichetti, L. (2018). The underappreciated potential of peatlands in global climate change mitigation strategies. *Nature Communications*, 9 (1)
- Lemoine, D. G., Mermillod-Blondin, F., Barrat-Segretain, M.-H., Massé, C., Malet, E. (2012). The ability of aquatic macrophytes to increase root porosity and radial oxygen loss determines their resistance to sediment anoxia. *Aquatic Ecology*, 46, 191-200
- Lenth R. (2022). _emmeans: Estimated Marginal Means, aka Least-Squares Means_. R package version 1.8.0 (1.8.0). https://CRAN.R-project.org/package=emmeans
- Li, L., Yang, Y., Tam, N.F.Y., Yang, L., Mei, X-Q., Yang, F-J. (2013). Growth characteristics of six wetland plants and their influences on domestic wastewater treatment efficiency. *Ecological Engineering*, 60, 382-392
- Li, Y., Shang, J., Zhang, C., Zhang, W., Niu, L., Wang, L., Zhang, H. (2021). The role of freshwater eutrophication in greenhouse gas emissions: A review. Science of the Total Environment, 768
- Liland, K. H., Mevik, B.-H., Wehrens, R. (2021). pls: Partial Least Squares and Principal Component Regression. R package version 2.8-o. https://CRAN.R-project.org/package=pls
- Little, C. J., Altermatt, F. (2018). Species turnover and invasion of dominant freshwater invertebrates alter biodiversity—ecosystem-function relationship. *Ecological Monographs*, 88 (3), 461-480
- Liu, L., Sotiri, K., Dück, Y., Hilgert, S., Ostrovsky, I., Uzhansky, E., Katsman, R., Katsnelson, B., Bookman, R., Wilkinson, J., Lorke, A. (2020). The control of sediment gas accumulation on spatial distribution of ebullition in Lake Kinneret. Geo-Marine Letters, 40 (4), 453–466
- Liu, W., Fritz, C., Weideveld, S. T. J., Aben, R. C. H., Van den Berg, M., Velthuis, M. (2022). Annual CO2 Budget Estimation From Chamber-Based Flux Measurements on Intensively Drained Peat Meadows: Effect of Gap-Filling Strategies. Frontiers in Environmental Science, 10, 803746
- Liu, Y., Xu, H., Yu, C., Zhou, G. (2021). Multifaceted roles of duckweed in aquatic phytoremediation and bioproducts synthesis. *GCB Bioenergy*, 13 (1), 70–82
- Lofton, D. D., Whalen, S. C., Hershey, A. E. (2014). Effect of temperature on methane dynamics and evaluation of methane oxidation kinetics in shallow Arctic Alaskan lakes. *Hydrobiologia*, 721, 209-222
- Lordkipanidze, M., Lulofs, K., Bressers, H. (2019). Towards a new model for the governance of the Weerribben-Wieden National Park. Science of the total environment, 648, 56–65

- Lovelock, C. E., Evans, C., Barros, N., Prairie, Y., Alm, J., Bastviken, D., Beaulieu, J. J., Garneau, M., Harby, A., Harrison, J., Pare, D., Lerche Raadal, H., Sherman, B., Zhang, C., Ogle, S. M. (2019). 2019 Refinement to the 2006 IPCC Guidelines for National Greenhouse Gas Inventories, Chapter 7: Wetlands
- Lozing van afvalwater uit -rioolwaterzuiveringsinstallaties (paragraaf 4.49 Bal). (2024, May 15). In Informatiepunt Leefomgeving. https://iplo.nl/thema/water/afvalwater-activiteiten/biologisch-afbreekbaar-afvalwater/behandeling-stedelijk-afvalwater/lozen-rwzi/
- Lu, B., Xu, Z., Li, J., Chai, X. (2018). Removal of water nutrients by different aquatic plant species: An alternative way to remediate polluted rural rivers. *Ecological engineering*, 110, 18-26
- Lu, X. M., Lu, P. Z. (2014). Characterization of bacterial communities in sediments receiving various wastewater effluents with high-throughput sequencing analysis. *Microbial ecology*, 67, 612-623
- Luan, J., Wu, J. (2015). Long-term agricultural drainage stimulates CH4 emissions from ditches through increased substrate availability in a boreal peatland. Agriculture, Ecosystems & Environment, 214, 68-77
- Luo, P., Tong, X., Liu, F., Huang, M., Xu, J., Xiao, R., Wu, J. (2020). Nutrients release and greenhouse gas emission during decomposition of Myriophyllum aquaticum in a sediment-water system. Environmental Pollution, 260, 114015

M

- Madigan, M. T., Bender, K. S., Buckley, D. H., Sattley, M., Stahl, D. A. (2018). Brock Biology of Microorganisms. 15th edition. Pearson, Essex, England
- Madikizela, L. M., Ncube, S., Chimuka, L. (2018). Uptake of pharmaceuticals by plants grown under hydroponic conditions and natural occurring plant species: A review. *Science of The Total Environment*, 636, 477-486
- Maeck, A., Hofmann, H., Lorke, A. (2014). Pumping methane out of aquatic sediments ebullition forcing mechanisms in an impounded river. *Biogeosciences*, 11, 2925–2938
- Magwaza, S. T., Magwaza, L. S., Odindo, A. O., Mditshwa, A. (2020). Hydroponic technology as decentralised system for domestic wastewater treatment and vegetable production in urban agriculture: A review. *Science of the Total Environment*, 698, 134-154
- Mander, Ü., Dotro, G., Ebie, Y., Towprayoon, S., Chiemchaisri, C., Furlan Nogueira, S., Jamsranjav, B., Kasak, K., Truu, J., Tournebize, J., Mitsch, W.J. (2014). Greenhouse gas emission in constructed wetlands for wastewater treatment: A review. *Ecological Engineering*, 66, 19-35
- Mansfeldt, C., Deiner, K., Mächler, E., Fenner, K., Eggen, R. I. L., Stamm, C., Schönenberger, U., Walser, J.-C., Altermatt, F. (2020). Microbial community shifts in streams receiving treated wastewater effluent. Science of the Total Environment, 709, 135727
- Marcon, L., Sotiri, K., Bleninger, T., Lorke, A., Männich, M., Hilgert, S. (2022). Acoustic Mapping of Gas Stored in Sediments of Shallow Aquatic Systems Linked to Methane Production and Ebullition Patterns. Frontiers in Environmental Science, 10, 876540
- Marotta, H., Pinho, L., Gudasz, C., Bastviken, D., Tranvik, L. J., Enrich-Prast, A. (2014). Greenhouse gas production in low-latitude lake sediments responds strongly to warming. *Nature Climate Change*, 4 (6), 467–470
- Martinez-Cruz, K., Sepulveda-Jauregui, A., Casper, P., Anthony, K. W., Smemo, K. A., Thalasso, F. (2018). Ubiquitous and significant anaerobic oxidation of methane in freshwater lake sediments. *Water Research*, 144, 332-340
- Maucieri, C., Salvato, M., Borin, M. (2020). Vegetation contribution on phosphorus removal in constructed wetlands. *Ecological Engineering*, 152, 105853

- McClure, R. P., Lofton, M. E., Chen, S., Krueger, K. M., Little, J. C., Carey, C. C. (2020). The Magnitude and Drivers of Methane Ebullition and Diffusion Vary on a Longitudinal Gradient in a Small Freshwater Reservoir. *Journal of Geophysical Research: Biogeosciences*, 125 (3), 1–19
- McMurdie, P. J., Holmes, S. (2013). phyloseq: an R package for reproducible interactive analysis and graphics of microbiome census data. *PloS one*, 8 (4), e61217
- Mekonnen, M. M., Hoekstra, A. Y. (2015). Global Gray Water Footprint and Water Pollution Levels Related to Anthropogenic Nitrogen Loads to Fresh Water. Environmental Science & Technology, 49 (21), 12860-12868
- Mekonnen, M. M., Hoekstra, A. Y. (2017). Global Anthropogenic Phosphorus Loads to Freshwater and Associated Grey Water Footprints and Water Pollution Levels: A High-Resolution Global Study. Water Resources Research, 54 (1), 345-358
- Meng, F., Huang, G., Yang, X., Li, Z., Li, J., Cao, J., Wang, Z., Sun, L. (2013). Identifying the sources and fate of anthropogenically impacted dissolved organic matter (DOM) in urbanized rivers. *Water Research*, 47 (14), 5027-5039
- Meng, X., Zhu, Z., Xue, J., Wang, C., Sun, X. (2023). Methane and Nitrous Oxide Emissions from a Temperate Peatland under Simulated Enhanced Nitrogen Deposition. *Sustainability*, 15 (2), 1010
- Menon, R., Holland, M. M. (2014). Phosphorus Release due to Decomposition of Wetland Plants. Wetlands, 34, 1191-1196
- Mevik, B.-H., Wehrens, R. (2007). The pls Package: Principal Component and Partial Least Squares Regression in R. Journal of Statistical Software, 18 (2)
- Minich, J. J., Michael, T. P. (2024). A review of using duckweed (Lemnaceae) in fish feeds. Reviews in Aquaculture
- Mohsenpour, S. F., Hennige, S., Willoughby, N., Adeloye, A., Gutierrez, T. (2021). Integrating micro-algae into wastewater treatment: A review. Science of the Total Environment, 752, 142168
- Moorhead, K. K., Reddy, K. R. (1988). Oxygen Transport through Selected Aquatic Macrophytes. *Journal of Environmental Quality*, 17 (1), 138-142
- Mor, J. R., Dolédec, S., Acuña, V., Sabater, S., Muñoz, I. (2019). Invertebrate community responses to urban wastewater effluent pollution under different hydro-morphological conditions. *Environmental Pollution*, 252, 483–492

N

- Namasivayam, S. K. R., Prakash, P., Babu, V., Paul, E. J., Bharani, R. S. A., Kumar, J. A., Kavisri, M., Moovendhan, M. (2023). Aquatic biomass cellulose fabrication into cellulose nanocomposite and its application in water purification. *Journal of Cleaner Production*, 396, 136386
- Newman, E. I. (1995). Phosphorus inputs to terrestrial ecosystems. Journal of Ecology, 83, 713-726
- Ng, Y.S., Chan, D.J.C. (2018). Phytoremediation capabilities of Spirodela polyrhiza, Salvinia molesta and Lemna sp. in synthetic wastewater: A comparative study. *International Journal of Phytoremediation*, 20 (12), 1179-1186
- Nguyen, M.-K., Lin, C., Nguyen, H.-L., Hung, N. T. Q., La, D. D., Nguyen, X. H., Chang, S. W., Chung, W. J., Nguyen, D. D. (2023). Occurrence, fate, and potential risk of pharmaceutical pollutants in agriculture: Challenges and environmentally friendly solutions. *Science of The Total Environment*, 899, 165323
- Nickerson, N. (2016). Evaluating gas emission measurements using Minimum-Detectable Flux (MDF). Eosense Inc.
- Nie, X., Mubashar, M., Zhang, S., Qin, Y., Zhang, X. (2020). Current progress, challenges and perspectives in microalgae-based nutrient removal for aquaculture waste: A comprehensive review. *Journal of Cleaner Production*, 277, 124209

- Nieminen, M., Palviainen, M., Sarkkola, S., Laurén, A., Marttila, H., Finér, L. (2018). A synthesis of the impacts of ditch network maintenance on the quantity and quality of runoff from drained boreal peatland forests. *Ambio*, 47 (5), 523–534
- Nijman, T. P. A. (2023). Methane cycling in shallow lakes. PhD thesis, Radboud University Nijmegen, the Netherlands
- Nijman, T. P. A., Davidson, T. A., Weideveld, S. T. J., Audet, J., Esposito, C., Levi, E. E. Ho, A., Lamers, L. P. M., Jeppesen, E., Veraart, A. J. (2021). Warming and eutrophication interactively drive changes in the methane oxidizing community of shallow lakes. ISME Communications, 1, 32
- Norström, A., Larsdotter, K., Gumaelius, L., la Cour Jansen, J., Dalhammer, G. (2004). A small scale hydroponics wastewater treatment system under Swedish conditions. *Water Science & Technology*, 48 (11-12), 161-167

0

- Ojanen, P., Minkkinen, K., Alm, J., Penttilä, T. (2010). Soil-atmosphere CO2, CH4 and N2O fluxes in boreal forestry-drained peatlands. Forest Ecology and Management, 260 (3), 411–421
- Okoronkwo, N., Van Hove, C., Eskew, D. L. (1989). Evaluation of nitrogen fixation by different strains of the Azolla-Anabaena symbiosis in the presence of a high level of ammonium. *Biology and Fertility of* Soils, 7, 275–278
- Oliveira-Junior, E. S., Tang, Y., Van den Berg, S. J. P., Cardoso, S. J., Lamers, L. P. M., Kosten, S. (2018). The impact of water hyacinth (Eichhornia crassipes) on greenhouse gas emission and nutrient mobilization depends on rooting and plant coverage. *Aquatic Botany*, 145, 1-9
- Østgaard, K., Christensson, M., Lie, E., Jönsson, K., Welander, T. (1997). Anoxic biological phosphorus removal in a full-scale UCT process. *Water Research*, 31 (11), 2719-2726
- Oron, G., De-Vegt, A., Porath, D. (1988). Nitrogen removal and conversion by duckweed grown on wastewater. Water Research, 22 (2), 179-184
- Outram, F. N., Hiscock, K. M. (2012). Indirect Nitrous Oxide Emissions from Surface Water Bodies in a Lowland Arable Catchment: A Significant Contribution to Agricultural Greenhouse Gas Budgets? Environmental Science and Technology, 46 (15), 8156–8163
- Ozengin, N., Elmaci, A. (2007). Performance of Duckweed (Lemna minor L.) on different types of wastewater treatment. *Journal of Environmental Biology*, 28 (2), 307-314

P

- Paerl, H. W., Huisman, J. (2009). Climate change: a catalyst for global expansion of harmful cyanobacterial blooms. *Environmental Microbiology Reports*, 1 (1), 27-37
- Pärn, J., Pinay, G., Mander, Ü. (2012). Indicators of nutrients transport from agricultural catchments under temperate climate: A review. *Ecological Indicators*, 22, 4-15
- Parravicini, V., Svardal, K., Krampe, J. (2016). Greenhouse Gas Emissions from Wastewater Treatment Plants. Energy Procedia, 97, 246–253
- Paryanto, P., Faizin, M., Rusnaldy, R. (2023). Azolla processing technologies for an alternative feed raw material. *Results in Engineering*, 19, 101313
- Patrick Jr, W. H., Khalid, R. A. (1974). Phosphate Release and Sorption by Soils and Sediments: Effect of Aerobic and Anaerobic Conditions. *Science*, 186 (4158), 53-55
- Peacock, M., Audet, J., Bastviken, D., Futter, M. N., Gauci, V., Grinham, A., Harrison, J. A., Kent, M. S., Kosten, S., Lovelock, C. E., Veraart, A. J., Evans, C. D. (2021). Global importance of methane emissions from drainage ditches and canals. *Environmental Research Letters*, 16 (4), 044010

- Peacock, M., Ridley, L. M., Evans, C. D., Gauci, V. (2017). Management effects on greenhouse gas dynamics in fen ditches. Science of the Total Environment, 578, 601–612
- Peeters, E. T. H. M., Neefjes, R. E. M., Van Zuidam, B. G. (2016). Competition between Free-Floating Plants Is Strongly Driven by Previously Experienced Phosphorus Concentrations in the Water Column. PLOS ONE, 11 (9), e0162780
- Pereda, O., Solagaistua, L., Atristain, M., de Guzmán, I., Larrañaga, A., von Schiller, D., Elosegi, A. (2020). Impact of wastewater effluent pollution on stream functioning: A whole-ecosystem manipulation experiment. *Environmental Pollution*, 258, 113719
- Peterse, I. F., Hendriks, L., Weideveld, S. T. J., Smolders, A. J. P., Lamers, L. P. M., Lücker, S., Veraart, A. J. (2024). Wastewater-effluent discharge and incomplete denitrification drive riverine CO2, CH4 and N2O emissions. *Science of The Total Environment*, 951, 175797
- Prabakaran, S., Mohanraj, T., Arumugam, A., Sudalai, S. (2022). A state-of-the-art review on the environmental benefits and prospects of Azolla in biofuel, bioremediation and biofertilizer applications. *Industrial Crops and Products*, 183
- Prajapati, M., van Bruggen, J. J. A., Dalu, T., Malla, R. (2017). Assessing the effectiveness of pollutant removal by macrophytes in a floating wetland for wastewater treatment. *Applied Water Science*, 7, 4801-4809
- Preisner, M., Neverova-Dziopak, E., Kowalewski, Z. (2020). Analysis of eutrophication potential of municipal wastewater. *Water Science and Technology*, 81 (9), 1994-2003
- Price, J. R., Ledford, S. H., Ryan, M. O., Toran, L., Sales, C. M. (2018). Wastewater treatment plant effluent introduces recoverable shifts in microbial community composition in receiving streams. *Science of the Total Environment*, 613, 1104-1116

0

- Qadir, M., Drechsel, P., Jiménez Cisneros, B., Kim, Y., Pramanik, A., Mehta, P., Olaniyan, O. (2020). Global and regional potential of wastewater as a water, nutrient and energy source. *Natural Resources Forum*, 44, 40–51
- Quast, C., Pruesse, E., Yilmaz, P., Gerken, J., Schweer, T., Yarza, P., Peplies, J., Glöckner, F. O. (2012). The SILVA ribosomal RNA gene database project: improved data processing and web-based tools. Nucleic acids research, 41 (D1), D590-D596
- Quick, A. M., Reeder, W. J., Farrell, T. B., Tonina, D., Feris, K. P., Benner, S. G. (2019). Nitrous oxide from streams and rivers: A review of primary biogeochemical pathways and environmental variables. *Earth-science reviews*, 191, 224-262

R

- R Core Team. (2021). R: A language and environment for statistical computing. R Foundation for Statistical Computing, Vienna, Austria. URL https://www.R-project.org/
- R Core Team. (2022). R: A language and environment for statistical computing (4.2.1). R Foundation for Statistical Computing. URL https://www.R-project.org/
- R Core Team (2024). _R: A Language and Environment for Statistical Computing_. R Foundation for Statistical Computing, Vienna, Austria. URL https://www.R-project.org/
- Ramirez, J. A., Baird, A. J., Coulthard, T. J., Waddington, J. M. (2015). Ebullition of methane from peatlands: Does peat act as a signal shredder? *Geophysical Research Letters*, 42, 3371–3379
- Rani, B. S. J., Venkatachalam, S. (2022). A neoteric approach for the complete valorization of Typha angustifolia leaf biomass: A drive towards environmental sustainability. *Journal of Environmental Managament*, 318, 115579

- Rassamee, V., Sattayatewa, C., Pagilla, K., Chandran, K. (2011). Effect of oxic and anoxic conditions on nitrous oxide emissions from nitrification and denitrification processes. *Biotechnology and Bioengineering*, 108 (9), 2036–2045
- Reddy, K. R., DeBusk, W. F. (1985a). Growth characteristics of aquatic macrophytes cultured in nutrientenriched water: II. Azolla, Duckweed, and Salvinia. *Economic Botany*, 39, 200–208
- Reddy, K. R., DeBusk, W. F. (1985b). Nutrient Removal Potential of Selected Aquatic Macrophytes. *Journal of Environmental Quality*, 14 (4), 459-462
- Ren, Y., Ngo, H. H., Guo, W., Wang, D., Peng, L., Ni, B.-J., Wei, W., Liu, Y. (2020). New perspectives on microbial communities and biological nitrogen removal processes in wastewater treatment systems. *Bioresource Technology*, 297, 122491
- Rezania, S., Kamyab, H., Rupani, P. F., Park, J., Nawrot, N., Wojciechowska, E., Yadav, K. K., Ghahroud, M. L., Mohammadi, A. A. Thirugnana, S. T., Cehlliapan, S., Cabral-Pinto, M. M. S. (2021). Recent advances on the removal of phosphorus in aquatic plant-based systems. *Environmental Technology & Innovation*, 24, 101933
- Richardson, A. E., Simpson, R. J. (2011). Soil Microorganisms Mediating Phosphorus Availability Update on Microbial Phosphorus. *Plant Physiology*, 156 (3), 989-996
- Riis, T., Tank, J. L., Reisinger, A. J., Aubenau, A., Roche, K. R., Levi, P. S., Baattrup-Pedersen, A., Alnoee, A. B., Bolster, D. (2020). Riverine macrophytes control seasonal nutrient uptake via both physical and biological pathways. *Freshwater Biology*, 65 (2), 178-192
- Rissanen, A. J., Karvinen, A., Nykänen, H., Peura, S., Tiirola, M., Mäki, a., Kankaala, P. (2017). Effects of alternative electron acceptors on the activity and community structure of methane-producing and consuming microbes in the sediments of two shallow boreal lakes. FEMS Microbiology Ecology, 93 (7), fixo78
- Rodriguez, M., Gonsiorczyk, T., Casper, P. (2018). Methane Production increases With warming and carbon additions to incubated sediments from a semiarid reservoir. *Inland Waters*, 8, 109-121
- Rosentreter, J. A., Borges, A. V., Deemer, B. R., Holgerson, M. A., Liu, S., Song, C., Melack, J., Raymond, P. A., Duarte, C. M., Allen, G. H., Olefeldt, D., Poulter, B., Battin, T. I., Eyre, B. D. (2021). Half of global methane emissions come from highly variable aquatic ecosystem sources. *Nature Geoscience*, 14, 225–230
- Roulet, N. T., Moore, T. R. (1995). The effect of forestry drainage practices on the emission of methane from northern peatlands. *Canadian Journal of Forest Research*, 25(3), 491–499
- Ruprecht, J. E., Birrer, S. C., Dafforn, K. A., Mitrovic, S. M., Crane, S. L., Johnston, E. L., Wemheuer, F., Navarro, A., Harrison, A. J., Turner, I. L., Glamore, W. C. (2021). Wastewater effluents cause microbial community shifts and change trophic status. *Water Research*, 200, 117206

S

- Sabba, F., Picioreanu, C., Boltz, J. P., Nerenberg, R. (2017). Predicting N2O emissions from nitrifying and denitrifying biofilms: a modeling study. *Water Science & Technology*, 75 (3), 530–538
- Sakai, S., Ehara, M., Tseng, I. C., Yamaguchi, T., Bräuer, S. L., Cadillo-Quiroz, H., Zinder, S. H., Imachi, H. (2012). Methanolinea mesophila sp. nov., a hydrogenotrophic methanogen isolated from rice field soil, and proposal of the archaeal family Methanoregulaceae fam. nov. within the order Methanomicrobiales. *International journal of systematic and evolutionary microbiology*, 62 (Pt 6), 1389-1395
- Salah, M., Zheng, Y., Wang, Q., Li, C., Li, Y., Li, F. (2023). Insight into pharmaceutical and personal care products removal using constructed wetlands: A comprehensive review. Science of The Total Environment, 885, 163721

- Sander, R. (2015). Compilation of Henry's law constants (version 4.0) for water as solvent. *Atmospheric Chemistry and Physics*, 15 (8), 4399–4981
- Sarmento, A.P., Borges, A.C., Teixeira de Matos, A. (2013). Effect of cultivated species and retention time on the performance of constructed wetlands. *Environmental Technology*, 34 (8), 961-965
- Scheffer, M., Hosper, S. H., Meijer, M.-L., Moss, B., Jeppesen, E. (1993). Alternative equilibria in shallow lakes. *Trends in Ecology and Evolution*, 8 (8), 275-279
- Schindler, D. W. (2006). Recent advances in the understanding and management of eutrophication. Limnology and Oceanography, 51 (1part2), 356-363
- Schrier-Uijl, A. P., Kroon, P. S., Leffelaar, P. A., van Huissteden, J. C., Berendse, F., Veenendaal, E. M. (2010). Methane emissions in two drained peat agro-ecosystems with high and low agricultural intensity. *Plant and Soil*, 329 (1), 509–520
- Schrier-Uijl, A. P., Veraart, A. J., Leffelaar, P. A., Berendse, F., Veenendaal, E. M. (2011). Release of CO 2 and CH 4 from lakes and drainage ditches in temperate wetlands. *Biogeochemistry*, 102, 265–279
- Schuijt, L. M., Van Bergen, T. J. H. M., Lamers, L. P. M., Smolders, A. J. P., Verdonschot, P. F. M. (2021). Aquatic worms (Tubificidae) facilitate productivity of macrophyte Azolla filiculoides in a wastewater biocascade system. Science of the Total Environment, 787
- Seitzinger, S., Harrison, J. A., Böhlke, J. K., Bouwman, A. F., Lowrance, R., Peterson, B., Tobias, C., Drecht, G. V. (2006). Denitrification across landscapes and waterscapes: a synthesis. *Ecological applications*, 16 (6), 2064-2090
- Selvaraj, D., Velvizhi, G. (2021). Sustainable ecological engineering systems for the treatment of domestic wastewater using emerging, floating and submerged macrophytes. *Journal of Environmental Management*, 286
- Serrano, A., Hendrickx, T. L. G., Elissen, H. H. J., Laarhoven, B., Buisman, C. J. N., Temmink, H. (2016). Can aquatic worms enhance methane production from waste activated sludge? *Bioresource Technology*, 211, 51-57
- Servais, P., Garnier, J., Demarteau, N., Brion, N., Billen, G. (1999). Supply of organic matter and bacteria to aquatic ecosystems through waste water effluents. *Water Research*, 33 (16), 3521-3531
- Shah, M., Hashmi, H. N., Ali, A., Ghumman, A.R. (2014). Performance assessment of aquatic macrophytes for treatment of municipal wastewater. *Journal of Environmental Health Science & Engineering*, 12, 106
- Shang, J., Zhang, L., Shi, C., Fan, C. (2013). Influence of Chironomid Larvae on oxygen and nitrogen fluxes across the sediment-water interface (Lake Taihu, China). *Journal of Environmental Sciences*, 25 (5), 978-985
- Sheng, A.L.K., Bilad, M.R., Osman, N.B., Arahman, N. (2017). Sequencing batch membrane photobioreactor for real secondary effluent polishing using native microalgae: Process performance and full-scale projection. *Journal of Cleaner Production*, 168, 708-715
- Shilton, A.N., Powell, N., Guieysse, B. (2012). Plant based phosphorus recovery from wastewater via algae and macrophytes. *Current Opinion in Biotechnology*, 23 (6), 884-889
- Shingala, M. C., Rajyaguru, A. (2015). Comparison of Post Hoc Tests for Unequal Variance. *International Journal of New Technologies in Science and Engineering*, 2 (5), 22-33
- Si, C., Zhang, L. M., Yu, F. H. (2019). Effects of physical space and nutrients on the growth and intraspecific competition of a floating fern. *Aquatic Ecology*, 53, 295-302
- Singh, P. K., Singh, D. P., Singh R. P. (1992). Growth, Acetylene Reduction Activity, Nitrate Uptake and Nitrate Reductase Activity of Azolla caroliniana and Azolla pinnata at Varying Nitrate Levels. Biochemie und Physiologie der Pflanzen, 188 (2), 121-127
- Smith, M. S. (1982). Dissimilatory Reduction of NO2- to NH4+ and N2O by a Soil Citrobacter sp. *Applied* and Environmental Microbiology, 43, 854-860

- Smolders, A. J. P., Lamers, L. P. M., Moonen, M., Zwaga, K., Roelofs, J. G. M. (2001). Controlling phosphate release from phosphate-enriched sediments by adding various iron compounds. *Biogeochemistry*, 54 (2), 219-228
- Smolders, A. J. P., Moonen, M., Zwaga, K., Lucassen, E. C. H. E. T., Lamers, L. P. M., Roelofs, J. G. M. (2006). Changes in pore water chemistry of desiccating freshwater sediments with different sulphur contents. *Geoderma*, 132 (3-4), 372-383
- Sobek, S., Delsontro, T., Wongfun, N., Wehrli, B. (2012). Extreme organic carbon burial fuels intense methane bubbling in a temperate reservoir. *Geophysical Research Letters*, 39 (1), 2–5
- Sooknah, R.D., Wilkie, A.C. (2004). Nutrient removal by floating aquatic macrophytes cultured in anaerobically digested flushed dairy manure wastewater. *Ecological Engineering*, 22 (1), 27-42
- STOWA / MX-systems (2004). Duflow Manual, version 3.7. pp. 118. Delft, The Netherlands: STOWA / MX-systems
- STOWA (2012). Emissie Broeikasgassen vanuit RWZI's. STOWA, report no. 2012-20. Emissions of greenhouse gases from WWTPs
- STOWA (2018a). Referenties en maatlatten voor natuurlijke watertypen voor de kaderrichtlijn water 2021-2027. STOWA, report no. 2018-49. References and standards for natural water types for the water framework directive 2021-2027
- STOWA (2018b). Omschrijving MEP en maatlatten voor sloten en kanalen voor de kaderrichtlijn water 2021-2027. STOWA, report no. 2018-50. Description of MEP (maximum ecological potential) and standards for ditches and canals for the water framework directive 2021-2027
- Strous, M., Fuerst, J. A., Kramer, E. H. M., Logemann, S., Muyzer, G., Van de Pas-Schoonen, K. T., Webb, R., Kuenen, J. G., Jetten, M. S. M. (1999). Missing lithotroph identified as new planctomycete. Nature, 400, 446-449
- Strous, M., Jetten, M. S. M. (2004). Anaerobic oxidation of methane and ammonium. *Annual Review of Microbiology*, 58, 99-117
- Stumm, W., Morgan, J. J. (1995). Aquatic chemistry: chemical equilibria and rates in natural waters. Wiley-Interscience
- Sudiarto, S.I.A., Renggaman, A., Choi, H.L. (2019). Floating aquatic plants for total nitrogen and phosphorus removal from treated swine wastewater and their biomass characteristics. *Journal of Environmental Management*, 231, 753-769
- Sulistiyarto, B., Christiana, I., Yulintine, Y. (2014). Developing production technique of bloodworm (Chironomidae larvae) in floodplain waters for fish feed. *International Journal of Fisheries and Aquaculture*, 6 (4), 39-45
- Sun, H., Xu, S., Wu, S., Wang, R., Zhuang, G., Bai, Z., Deng, Y., Zhuang, X. (2019). Enhancement of facultative anaerobic denitrifying communities by oxygen release from roots of the macrophyte in constructed wetlands. *Journal of Environmental Management*, 246, 157-163
- Svensson, J. M., Enrich-Prast, A., Leonardson, L. (2001). Nitrification and denitrification in a eutrophic lake sediment bioturbated by oligochaetes. *Aquatic Microbial Ecology*, 23 (2), 177-186

1

- Takai, K. E. N., Horikoshi, K. (2000). Rapid detection and quantification of members of the archaeal community by quantitative PCR using fluorogenic probes. *Applied and environmental microbiology*, 66 (11), 5066-5072
- Tammeorg, O., Nürnberg, G., Horppila, J., Haldna, M., Niemistö, J. (2020). Redox-related release of phosphorus from sediments in large and shallow Lake Peipsi: Evidence from sediment studies and long-term monitoring data. Journal of Great Lakes Research, 46 (6), 1595-1603

- Tang, Y., Harpenslager, S. F., van Kempen, M. M. L., Verbaarschot, E. J. H., Loeffen, L. M. J. M., Roelofs, J. G. M., Smolders, A. J. P., Lamers, L. P. M. (2017). Aquatic macrophytes can be used for wastewater polishing but not for purification in constructed wetlands. *Biogeosciences*, 14, 755–766
- Teh, Y. A., Silver, W. L., Sonnentag, O., Detto, M., Kelly, M., Baldocchi, D. D. (2011). Large Greenhouse Gas Emissions from a Temperate Peatland Pasture. *Ecosystems*, 14 (2), 311–325
- Tel-Or, E., Forni, C. (2011). Phytoremediation of hazardous toxic metals and organics by photosynthetic aquatic systems. *Plant Biosystems*, 145 (1), 224-235
- Temmink, R.J.M., Harpenslager, S.F., Smolders, A.J.P., van Dijk, G., Peters, R.C.J.H., Lamers, L.P.M., van Kempen, M.M.L. (2018). Azolla along a phosphorus gradient: biphasic growth response linked to diazotroph traits and phosphorus-induced iron chlorosis. *Scientific Reports*, 8, 4451
- Thottathil, S.D., Reis, P. C. J., del Giorgio, P. A., Prairie, Y. T. (2018). The extent and regulation of summer methane oxidation in Northern lakes. *Journal of Geophysical Research: Biogeosciences*, 123 (10), 3216–3230
- Thottathil, S. D., Reis, P. C. J., Prairie, Y. T. (2022). Magnitude and Drivers of Oxic Methane Production in Small Temperate Lakes. *Environmental Science & Technology*, 56, 11041-11050
- Tian, C., Wang, C., Tian, Y., Wu, X., Xiao, B. (2015). Root Radial Oxygen Loss and the Effects on Rhizosphere Microarea of Two Submerged Plants. *Polish Journal of Environmental Studies*, 24 (4),1795-1802
- Tian, H., Xu., R., Canadell, J. G., Thompson, R. L., Winiwarter, W., Suntharalingam, P., Davidson, E. A., Ciais, P., Jackson, R. B., Janssens-Maenhout, G., Prather, M. J., Regnier, P., Pan, N., Pan, S., Peters, G. P., Shi, H., Tubiello, F. N., Zaehle, S., Zhou, F., Arneth, A., Battaglia, G., Berthet, S., Bopp, L., Bouwman, A. F., Buitenhuis, E. T., Chang, J., Chipperfield, M. P., Dangal, S. R. S., Dlugokencky, E., Elkins, J. W., Eyre, B. D., Fu, B., Hall, B., Ito, A., Joos, F., Krummel, P. B., Landolfi, A., Laruelle, G. G., Lauerwald, R., Li, W., Lienert, S., Maavara, T., MacLeod, M., Millet, D. B., Olin, S., Patra, P. K., Prinn, R. G., Raymond, P. A., Ruiz, D. J., van der Werf, G. R., Vuichard, N., Wang, J., Weiss, R. F., Wells, K. C., Wilson, C., Yang, J., Yao, Y. (2020). A comprehensive quantification of global nitrous oxide sources and sinks. Nature, 586, 248–256
- Tiemeyer, B., Albiac Borraz, E., Augustin, J., Bechtold, M., Beetz, S., Beyer, C., Drösler, M., Ebli, M., Eickenscheidt, T., Fiedler, S., Förster, C., Freibauer, A., Giebels, M., Glatzel, S., Heinichen, J., Hoffmann, M., Höper, H., Jurasinski, G., Leiber-Sauheitl, K., Peichl-Brak, M., Rosskopf, N., Sommer, M., Zeitz, J. (2016). High emissions of greenhouse gases from grasslands on peat and other organic soils. *Global Change Biology*, 22 (12), 4134–4149
- Timmermans, K. R., Peeters, W., Tonkers, M. (1992). Cadmium, zinc, lead and copper inChironomus riparius (Meigen) larvae (Diptera, Chironomidae): uptake and effects. *Hydrobiologia*, 241, 119-134
- Toet, S., Huibers, L. H. F. A., Van Logtestijn, R. S. P., Verhoeven, J. T. A. (2003). Denitrification in the periphyton associated with plant shoots and in the sediment of a wetland system supplied with sewage treatment plant effluent. *Hydrobiologia*, 501, 29-44
- Tokida, T., Miyazaki, T., Mizoguchi, M., Nagata, O., Takakai, F., Kagemoto, A., Hatano, R. (2007). Falling atmospheric pressure as a trigger for methane ebullition from peatland. *Global Biogeochemical Cycles*, 21 (2)
- Tong, Y., Wang, M., Peñuelas, J., Liu, X., Paerl, H. W., Elser, J. J., Sardans, J., Couture, R.-M., Larssen, T., Hu, H., Dong, X., He, W., Zhang, W., Wang, X., Zhang, Y., Liu, Y., Zeng, S., Kong, X., Janssen, A. B. G., Lin, Y. (2020). Improvement in municipal wastewater treatment alters lake nitrogen to phosphorus ratios in populated regions. PNAS, 117 (21), 11566-11572
- Tripathi, B.D., Upadhyay, A.R. (2003). Dairy Effluent Polishing by Aquatic Macrophytes. Water, Air, & Soil Pollution, 143, 377–385
- Trolle, D., Staehr, P. A., Davidson, T. A., Bjerring, R., Lauridsen, T. L., Søndergaard, M., Jeppesen, E. (2012). Seasonal Dynamics of CO 2 Flux Across the Surface of Shallow Temperate Lakes. *Ecosystems*, 15, 336–347

- Trotsenko, Y. A., Murrell, J. C. (2008). Metabolic Aspects of Aerobic Obligate Methanotrophy. *Advances in Applied Microbiology*, 63, 183-229
- Tubiello, F. N., Biancalani, R., Salvatore, M., Rossi, S., Conchedda, G. (2016). A worldwide assessment of greenhouse gas emissions from drained organic soils. *Sustainability (Switzerland)*, 8 (4), 1–13
- Tumendelger. A., Alshboul. Z., Lorke. A. (2019). Methane and nitrous oxide emission from different treatment units of municipal wastewater treatment plants in Southwest Germany. *PLoS ONE*, 14 (1), e0209763
- Turner, P. A., Griffis, T. J., Lee, X., Baker, J. M., Venterea, R. T., Wood, J. D. (2015). Indirect nitrous oxide emissions from streams within the US Corn Belt scale with stream order. *Proceedings of the National Acadamy of Sciences*, 112 (32), 9839–9843

U

Upadhyay, P., Prajapati, S. K., Kumar, A. (2023). Impacts of riverine pollution on greenhouse gas emissions: A comprehensive review. *Ecological Indicators*, 154, 110649

V

- Vaillant, N., Monnet, F., Sallanon, H., Coudret, A., Hitmi, A. (2003). Treatment of domestic wastewater by an hydroponic NFT system. *Chemosphere*, 50 (1), 121-129
- Van Bergen, T. J. H. M., Barros, N., Mendonça, R., Aben, R. C. H., Althuizen, I. H. J., Huszar, V., Lamers, L. P. M., Lürling, M., Roland, F., Kosten, S. (2019). Seasonal and diel variation in greenhouse gas emissions from an urban pond and its major drivers. *Limnology and Oceanography*, 64 (5), 2129-2139
- Van de Leemput, I. A., Veraart, A. J., Dakos, V., de Klein, J. J., Strous, M., Scheffer, M. (2011). Predicting microbial nitrogen pathways from basic principles. *Environmental microbiology*, 13 (6), 1477-1487
- Van den Berg, M., van den Elzen, E., Ingwersen, J., Kosten, S., Lamers, L. P. M., Streck, T. (2020). Contribution of plant-induced pressurized flow to CH4 emission from a Phragmites fen. *Scientific Reports*, 10, 12304.
- Van der Grift, B., Broers, H. P., Berendrecht, W., Rozemeijer, J., Osté, L., Griffioen, J. (2016). High-frequency monitoring reveals nutrient sources and transport processes in an agriculture-dominated lowland water system. Hydrology and Earth System Sciences, 20, 1851–1868
- Van der Meer, T. V., Van der Lee, G. H., Verdonschot, R. C. M., Verdonschot, P. F. M. (2021).

 Macroinvertebrate interactions stimulate decomposition in WWTP effluent-impacted aquatic ecosystems. *Aquatic Sciences*, 83 (4)
- Van der Meer, T. V., Verdonschot, P. F. M., Dokter, L., Absalah, S., Kraak, M. H. S. (2022a). Organic matter degradation and redistribution of sediment associated contaminants by benthic invertebrate activities. *Environmental Pollution*, 306
- Van der Meer, T. V., Verdonschot, P. F. M., Van Eck, L., Narain-Ford, D. M., Kraak, M. H. S. (2022b). Wastewater treatment plant contaminant profiles affect macroinvertebrate sludge degradation. Water Research, 222
- Van der Meer, T. V. (2023). Macroinvertebrate redistribution of environmental pollution. PhD thesis. University of Amsterdam
- Van der Meer, T. V., Davey, C. J. E., Verdonschot, P. F. M., Kraak, M. H. S. (2023). Removal of nutrients from WWTP effluent by an algae-mussel trophic cascade. *Ecological Engineering*, 190
- Van Geest, G. J., Verdonschot, P. F. M., Schipper, P. N. M., Veraart, A. J., Roelofs, J. G. M., Tomassen, H. B. M. (2021). Factsheet: Ecologische effecten van stikstof op Nederlandse oppervlaktewateren. Notitie Kennisimpuls Waterkwaliteit. Factsheet: ecological effects of nitrogen on Dutch surfacewaters
- Van Kessel, M. A., Speth, D. R., Albertsen, M., Nielsen, P. H., Op den Camp, H. J., Kartal, B., Jetten, M.S.M., Lücker, S. (2015). Complete nitrification by a single microorganism. *Nature*, 528 (7583), 555-559

- Van Puijenbroek, P. J. T. M., Cleij, P., Visser H. (2010). Nutriënten in het Nederlandse zoete oppervlaktewater: toestand en trends (Nutrients in the Dutch fresh surface water: status and trends)
- Veraart, A. J., de Bruijne, W. J. J., de Klein, J. J. M., Peeters, E. T. H. M., Scheffer, M. (2011). Effects of aquatic vegetation type on denitrification. *Biogeochemistry*, 104, 267-274
- Veraart, A. J., Dimitrov, M. R., Schrier-Uijl, A. P., Smidt, H., de Klein, J. J. M. (2017). Abundance, activity and community structure of denitrifiers in drainage ditches in relation to sediment characteristics, vegetation and land-use. *Ecosystems*, 20, 928-943
- Vermaat, J. E., Hanif, M. K. (1998). Performance of common duckweed species (Lemnaceae) and the waterfern Azolla filiculoides on different types of waste water. Water Research, 32 (9), 2569-2576
- Vermaat, J. E., Hellmann, F. (2010). Covariance in water- and nutrient budgets of Dutch peat polders: what governs nutrient retention? Biogeochemistry, 99, 109–126
- Vermaat, J. E., Hellmann, F., Dias, A. T. C., Hoorens, B., Van Logtestijn, R. S. P., Aerts, R. (2011). Greenhouse gas fluxes from dutch peatland water bodies: Importance of the surrounding landscape. Wetlands, 31 (3), 493–498
- Vos, J. H., Peeters, E. T. H. M., Gylstra, R., Kraak, M. H. S., Admiraal, W. (2004). Nutritional value of sediments for macroinvertebrate communities in shallow eutrophic waters. Archiv für Hydrobiologie, 161 (4), 469-487
- Vroom, R. J. E., Xie, F., Geurts, J. J. M., Chojnowska, A., Smolders, A. J. P., Lamers, L. P. M., Fritz, C. (2018). Typha latifolia paludiculture effectively improves water quality and reduces greenhouse gas emissions in rewetted peatlands. *Ecological Engineering*, 124, 88–98
- Vroom, R. J. E., Van den Berg, M., Pangala, S. R. Van der Scheer, O. E., Sorrell, B. K. (2022). Physiological processes affecting methane transport by wetland vegetation A review. *Aquatic Botany*, 182, 103547
- Vymazal, J. (2013). Emergent plants used in free water surface constructed wetlands: a review. *Ecological Engineering*, 61(Part A), 582-592
- Vymazal, J., Zhao, Y., Mander, Ü. (2021). Recent research challenges in constructed wetlands for wastewater treatment: A review. *Ecological Engineering*, 169, 106318

TX

- Wagner, G.M. (1997). Azolla: A review of its biology and utilization. The Botanical Review, 63, 1-26
- Wakelin, S. A., Colloff, M. J., Kookana, R. S. (2008). Effect of wastewater treatment plant effluent on microbial function and community structure in the sediment of a freshwater stream with variable seasonal flow. *Applied and environmental microbiology*, 74 (9), 2659-2668
- Wang, B. (1987). The development of ecological wastewater treatment and utilization systems (EWTUS) in China. Water Science & Technology, 19 (1-2), 51-63
- Wang, C., Li, S., Lai, D.Y.F., Wang, W., Ma, Y. (2015). The effect of floating vegetation on CH4 and N2O emissions from subtropical paddy fields in China. *Paddy and Water Environment*, 13, 425-431
- Wang, F., Zhang, S., Hu, X., Lv, X., Liu, M., Ma, Y., Manirakiza, B. (2024). Floating plants reduced methane fluxes from wetlands by creating a habitat conducive to methane oxidation. *Journal of Environmental Sciences*, 135, 149-160
- Wang, J., Chen, Y., Cai, P., Gao, Q., Zhong, H., Sun, W., Chen, Q. (2022). Impacts of municipal wastewater treatment plant discharge on microbial community structure and function of the receiving river in Northwest Tibetan Plateau. *Journal of Hazardous Materials*, 423 (B), 127170
- Ward, N. D., Bianchi, T. S., Medeiros, P. M., Seidel, M., Richey, J. E., Keil, R. G., Sawakuchi, H. O. (2017).
 Where Carbon Goes When Water Flows: Carbon Cycling across the Aquatic Continuum. Frontiers in Marine Science, 4, 7

- Wehrens, R., Mevik, B.-H. (2007). The pls package: principal component and partial least squares regression in R. *Journal of Statistical Software*, 18 (2)
- Weideveld, S. T. J., Liu, W., Van den Berg, M., Lamers, L. P. M., Fritz, C. (2021). Conventional subsoil irrigation techniques do not lower carbon emissions from drained peat meadows. *Biogeosciences*, 18,3881–3902
- Weinstein, M. M., Prem, A., Jin, M., Tang, S., Bhasin, J. M. (2019). FIGARO: An efficient and objective tool for optimizing microbiome rRNA gene trimming parameters. bioRxiv, 610394
- Welch, B. L. (1951). On the Comparison of Several Mean Values: An Alternative Approach. *Biometrika*, 38 (3/4), 330-336
- Wickham, H. (2009). ggplot2. Springer New York
- Wik, M., Thornton, B. F., Bastviken, D., Uhlbäck, J., Crill, P. M. (2016). Biased sampling of methane release from northern lakes: A problem for extrapolation. *Geophysical Research Letters*, 1256–1262
- Wilcock, R. J., Sorrell, B. K. (2008). Emissions of greenhouse gases CH4 and N2O from low-gradient streams in agriculturally developed catchments. *Water, Air, and Soil Pollution*, 188 (1–4), 155–170
- Wilson, L., Wilson, J., Holden, J., Johnstone, I., Armstrong, A., Morris, M. (2011). Ditch blocking, water chemistry and organic carbon flux: Evidence that blanket bog restoration reduces erosion and fluvial carbon loss. *Science of the Total Environment*, 409 (11), 2010–2018
- Wrage-Mönnig, N., Horn, M. A., Well, R., Müller, C., Velthof, G., Oenema, O. (2018). The role of nitrifier denitrification in the production of nitrous oxide revisited. *Soil Biology and Biochemistry*, 123, A3-A16
- Wu, H., Zhang, J., Ngo, H.H., Guo, W., Liang, S. (2017). Evaluating the sustainability of free water surface flow constructed wetlands: Methane and nitrous oxide emissions. *Journal of Cleaner Production*, 147, 152-156
- Wu, W., Niu, X., Yan, Z., Li, S., Comer-Warner, S. A., Tian, H., Li, S.-L., Zou, J., Yu, G., Liu, C.-Q. (2023).

 Agricultural ditches are hotspots of greenhouse gas emissions controlled by nutrient input. Water
 Research, 242, 120271
- WWAP (United Nations World Water Assessment Programme) (2017). The United Nations World Water Development Report 2017. Wastewater: The Untapped Resource. Paris, UNESCO

X

- Xiao, Q., Xu, X., Zhang, M., Duan, H., Hu, Z., Wang, W., Xiao, W., Lee, X. (2019). Coregulation of nitrous oxide emissions by nitrogen and temperature in China's third largest freshwater lake (Lake Taihu). Limnology and Oceanography, 64, 1070–1086
- Xu, M., Li, P., Tang, T., Hu, Z. (2015). Roles of SRT and HRT of an algal membrane bioreactor system with a tanks-in-series configuration for secondary wastewater effluent polishing. *Ecological Engineering*, 85, 257-264

Y

- Yao, Y., Tian, H., Shi, H., Pan, S., Xu, R., Pan, N., Canadell, J. G. (2019). Increased global nitrous oxide emissions from streams and rivers in the Anthropocene. *Nature Climate Change*, 10, 138–142
- Yin, Z., Zhu, L., Li, S., Hu, T., Chu, R., Mo, F., Hu, D., Liu, C., Li, B. (2020). A comprehensive review on cultivation and harvesting of microalgae for biodiesel production: Environmental pollution control and future directions. Bioresource Technology, 301, 122804
- Yohana, M. A., Ray, G. W., Yang, Q., Tan, B., Chi, S., Asase, A., Shiyu, K., Derrick, A. (2023). A Review on the Use of Azolla Meal as a Feed Ingredient in Aquatic Animals' Diets. *Aquaculture Research*, 2633412
- Yoshinari, T. (1985). Nitrite and nitrous oxide production by Methylosinus trichosporium. *Canadian Journal of Microbiology*, 31, 139-144

- Zapater-Pereyra, M., Ilyas, H., Lavrnić, Van Bruggen, J. J. A., Lens, P. N. L. (2015). Evaluation of the performance and space requirement by three different hybrid constructed wetlands in a stack arrangement. *Ecological Engineering*, 82, 290-300
- Zehr, J. P., Jenkins, B. D., Short, S. M., Steward, G. F. (2003). Nitrogenase gene diversity and microbial community structure: a cross-system comparison. *Environmental Microbiology*, 5 (7), 539-554
- Zhang, S., Liu, F., Luo, P., Xiao, R., Zhu, H., Wu, J. (2019). Nitrous oxide emissions from pilot scale threestage constructed wetlands with variable nitrogen loading. *Bioresource Technology*, 289, 121687
- Zhang, X., Yu, H., Yu, H., Liu, C., Fan, S., Yu, D. (2021). Highly competitive native aquatic species could suppress the growth of invasive aquatic species with similar traits. *Biological Invasions*, 23, 267-280
- Zhao, Y., Fang, Y., Jin, Y., Huang, J., Bao, S., He, Z., Wang, F., Zhao, H. (2014). Effects of operation parameters on nutrient removal from wastewater and high-protein biomass production in a duckweed-based (Lemma aequinoctialis) pilot-scale system. Water Science & Technology, 70 (7), 1195-1204
- Zhou, A., Tang, H., Wang, D. (2005). Phosphorus adsorption on natural sediments: Modeling and effects of pH and sediment composition. *Water Research*, 39 (7), 1245-1254
- Zhou, Z., Pan, J., Wang, F., Gu, J.-D., Li, M. (2018). Bathyarchaeota: globally distributed metabolic generalists in anoxic environments. FEMS microbiology reviews, 42 (5), 639-655
- Zietzschmann, F., Altmann, J., Ruhl, A. S., Dünnbier, U., Dommisch, I., Sperlich, A., Meinel, F., Jekel, M. (2014). Estimating organic micro-pollutant removal potential of activated carbons using UV absorption and carbon characteristics. Water Research, 56, 48-55



DATA MANAGEMENT

The research in this thesis has been carried out under the RDM policy of the Radboud Institute for Biological and Environmental Sciences, version 1-Dec-2022 accessed at www.ru.nl/ribes. Data generated or used in this thesis can be found in the following way:

Chapter 1 No data were produced. All figures are created in https://BioRender.com Chapter 2 Data available in the DANS Data Station Life Sciences repository at doi: 10.17026/dans-25a-4xsy Chapter 3 Data available in the DANS Data Station Life Sciences repository at doi: 10.17026/LS/9TPAJN Chapter 4 Data available in the DANS Data Station Life Sciences repository at doi: 10.17026/LS/AHK4GQ Data available in the DANS Data Station Physical and Technical Sciences Chapter 5 repository at doi: 10.17026/dans-zs6-53v5 Data available in the DANS Data Station Life Sciences repository at Chapter 6 doi: 10.17026/LS/AoCPDD

Chapter 7 Data available in the DANS Data Station Life Sciences repository at

doi: 10.17026/LS/HXXJAO

Chapter 8 No data were produced. All figures are created in https://BioRender.com



SUMMARY

Due to an increase in global human activity since the industrial revolution, concentrations of greenhouse gases (GHGs) in the atmosphere as well as emissions towards the atmosphere have risen and have continued to increase ever since. Increase in extreme events, such as heatwaves, heavy precipitation or extreme droughts, reduces water security and affects freshwater quality. Poor quality of catchment soils and underwater sediments, and high input of carbon, pathogens, pesticides and especially nutrients impacts human health, ecosystems, and water system reliability. Excess of nutrients, especially of nitrogen (N), phosphorus (P) and carbon (C), in freshwater systems, called eutrophication, additionally enhances GHG production and emission.

Nitrogen, phosphorus and carbon cycle differently through the water system. Nitrogen in the water column is mostly present as ammonium (NH $_{\!\scriptscriptstyle 4}^{\scriptscriptstyle +}$) and nitrate (NO₃-), but also atmospheric N can enter the water column through N-fixation. N is used in numerous processes including nitrification, denitrification, mineralisation, assimilation, dissimilatory nitrate reduction and anammox. Within the N cycle, nitrous oxide (N,O) can be formed, which is a very potent greenhouse gas that contributes 273 times more to global warming than carbon dioxide (CO₂) on a 100year timescale. Phosphorus is released by weathering from rocks or deposited from the atmosphere. The inorganic form of P, PO₄ 3-, is incorporated in the biomass of plants and algae, and the organic form can be made available through bacterial mineralisation. The mobilization and availability of P is regulated by the availability of metals such as iron, aluminium and calcium, as well as by pH and organic matter content and quality. Carbon enters the water column through diffusion from the atmosphere (inorganic C) or through lateral inflow from the land (organic C). Inorganic carbon is used by primary producers for photosynthesis, incorporating in their biomass as organic C. The organic C can be stored in the sediment, but can also, through respiration, be converted to inorganic C and emitted to the atmosphere as CO₂. Organic C within the sediment can be converted to methane (CH₂) as the last step of decomposition of organic matter, which contributes 27 times more to global warming than CO, and is strongly related to temperature. CH, can enter the atmosphere through diffusion or via bubbles that are directly released, called ebullition. Yet, it can also be converted back to CO₂ through oxidation, a process also influenced by temperature and substrate availability.

Agriculture is not only the worldwide main water user, it is also the main contributor of N and P into surface waters as a non-point source. It therefore contributes to

eutrophication of these waters. Next to agriculture, wastewater is an important (point) source of nutrients and harmful compounds. Worldwide, only half of produced wastewater is being treated and the untreated wastewater discharges high amounts of nutrients to receiving water bodies such as rivers, streams and lakes. However, also when being treated, which is the case in for example the Netherlands, nutrient concentrations of the treated wastewater, called effluent, exceed the concentrations present in the receiving waters leading to eutrophication of (natural) waterbodies. It is expected that also carbon enters the aquatic systems mostly through agriculture and wastewater, yet quantitative data are lacking. Although the total input of N and P has lowered since the 1990s, its decrease is stagnating since 2005 and still too high. Due to this high input of N, P and C, many ditches and other freshwater systems, such as rivers, are (highly) eutrophic and are facing a bad water quality. In order to manage, protect and improve the quality of water resources across the European Union, the Water Framework Directive (WFD) came into force in 2000. It requires Member States to achieve good status in all waterbodies by 2027. Yet, in 2018, 60% of the waterbodies in Europe still failed to meet the objectives of the WFD and the question rises whether it is possible to achieve the goal in 2027. Furthermore, eutrophication in aquatic systems can be expected to also result in higher GHG emissions. Yet, the emissions coming from these systems have been poorly quantified and are, for example in the case of ditches, not always taken into account in national GHG inventories. Omitting emissions from such systems may therefore underestimate GHG budgets.

The aquatic systems themselves may to some extent mitigate N, P and C input and emissions through several processes, and the question rises how high this mitigation may be. Aquatic organisms, such as plants, macroinvertebrates, algae and microorganisms, are found to remove nutrients, organic matter and toxic compounds from the surface water in nature. In eutrophic waters, highly competitive organisms outcompete slower growing species and the system transitions from a biodiverse system to a system dominated by only a few species. Yet, the nutrient and carbon cycling through these different groups of organisms could help combatting the high nutrient and carbon loading and GHG production within the waterbodies, both in natural waters and in constructed wetlands using different groups of plants, macroinvertebrates, algae and microorganisms.

Aquatic plants have already been used in water treatment, for example in constructed wetlands. Constructed wetlands have emerged as a sustainable and effective approach for water treatment, removing various pollutants through natural processes. They mimic the functions of natural wetlands, making use of

the interactions between plants, microorganisms, and environmental conditions to treat water and aquatic plants play an important role in this. Despite the numerous benefits offered by constructed wetlands, several challenges remain, such as fluctuations in environmental conditions. Additionally, plants in constructed wetlands are mostly indirectly involved in nutrient removal and it remains unclear which part of the removed nutrients can be released to the water column, for example by plant decomposition. Furthermore, constructed wetlands can emit substantial amounts of GHGs, especially N₂O, and may thereby offset their contribution to sustainable water treatment. That is why recently, hydroponic water treatment has gained interest. Aquatic plants are grown directly on to-be treated water without a sediment layer, and thus nutrient removal is also directly influenced by plantuptake. By harvesting the biomass, nutrients that have been taken up by the plants are permanently removed from the water column. Until now, focus has been on water treatment through nutrient removal, but not GHG flux mitigation, and the question remains whether hydroponic water treatment can aid in reducing GHG emissions from these waters.

The present thesis had two general aims: I) to quantify links between eutrophication and GHG emission in aquatic systems, and II) to find novel ways to reduce nutrient and GHG emission in wastewater treatment using natural mechanisms. The main objectives within these aims were I) to quantify GHG emissions coming from two water types facing the highest nutrient loading from either agriculture or wastewater discharge: agricultural drainage ditches and wastewater effluent receiving rivers, and II) to develop a natural and low-emission technique to enhance nutrient removal from municipal wastewater, using aquatic organisms, that counteracts eutrophication and GHG emission.

In quantifying GHG emissions from eutrophic waterbodies, the aim of **chapter 2** was to assess the role of drainage ditches in the GHG budget of agricultural landscapes, since GHG inventories strongly lack this information. Year-round diffusive emissions of $\rm CO_2$, $\rm CH_4$ and $\rm N_2O$, and $\rm CH_4$ ebullition were quantified in 10 drainage ditches located between heavily fertilized, peaty agricultural fields. Seasonal variations were assessed, as well as differences between ditches. The mean annual emissions from the studied ditches were 2 times higher than the emission factor, the estimate of average emissions per unit area (EF), reported by the IPCC. $\rm CO_2$ fluxes contributed on average 43% and diffusive $\rm CH_4$ fluxes contributed 16% to this total GHG emission. Ebullition of $\rm CH_4$ made up nearly half of the total GHG emission, whereas $\rm N_2O$ emissions were mostly low. Possibly, $\rm N_2O$ emissions were underestimated as $\rm N_2O$ tends to be emitted in hot-spots and hot-moments and is therefore difficult to measure. $\rm CO_2$ emissions

were higher in winter months, while CH₄ ebullition was higher during spring and summer. Ditch emissions were also higher than the EF used for the surrounding drained peatlands, indicating that ditch emissions can be important on the landscape scale and should be considered to be included in national greenhouse gas reporting.

Next, in chapter 3, GHG emissions from another important source of eutrophication were assessed: the discharge of wastewater treatment effluent in rivers. GHG emissions were measured in rivers affected by wastewater effluent discharge. It is known that effluent discharge can increase emissions over the whole river, but the direct effect of this effluent remained understudied. Two rivers were sampled: one river with 5 effluent discharge locations and one river with one location. GHG flux was measured upstream, downstream and right at the effluent discharge points. Additionally, sediment and water samples were taken to test if microbial community composition changes after effluent discharge. Measured GHG emissions from the two rivers were comparable to eutrophic rivers in urban and agricultural environments. CO emissions peaked at most discharge locations, whereas CH emission was highest 2 km downstream. Dissolved N₂O concentrations were strongly related to NO, content of the water column which points towards incomplete riverine denitrification. Methanogenic archaea were more abundant downstream of effluent discharge locations. However, overall microbial community composition remained relatively unaffected in both rivers. In conclusion, we demonstrate a clear link between wastewater effluent discharge and enhanced downstream GHG emission of the two rivers. Mitigating the impact of wastewater effluent on receiving rivers will be crucial to reduce riverine GHG contributions.

Next, different studies were performed on developing a natural water treatment technique using aquatic organisms, focussing especially on aquatic plants and wastewater effluent polishing. First, we assessed which plant growth form would be most efficient in wastewater effluent polishing. In **chapter 4**, two floating plant species were compared to two submerged species in nutrient removal efficiency, GHG reduction (CO₂ uptake, and CH₄ and N₂O emission reduction) and biomass production when grown on wastewater effluent for two weeks. The floating plants produced most biomass, whereas submerged plants were rapidly overgrown by filamentous algae. Floating plants removed nutrients most efficiently, up to 100% N and P removal, as opposed to a removal of 41-64% in submerged plant with algae treatments. Moreover, aquaria covered by floating plants had roughly three times higher GHG uptake than the treatments with submerged plants or controls without plants. Thus, effluent polishing by floating plants can be a promising avenue for climate-smart wastewater polishing.

Using the results of chapter 4 as a starting point, in **chapter 5** different floating plant species (Azolla filiculoides, Azolla pinnata, Lemna minuta and Trapa natans) were compared to quantify the most efficient species for effluent polishing, focussing on nutrient removal, GHG balance and biomass production. All species completely removed ammonium via nitrification. Lemna minuta and Trapa natans efficiently removed nitrate. Both Azolla species showed highest P uptake. All systems hardly emitted methane or nitrous oxide, and captured CO₂, with both Azolla species having the highest CO₂ uptake. Furthermore, it was studied whether a combination of the two most efficient floating plant species is removing nutrients more efficiently compared to a single cultivation of those species, and whether the sequence in which these species are placed matters. We sequentially cultivated Azolla filiculoides and Lemna minor using the same effluent, and compared this to single species cultivation. Although the single cultivation of Lemna minor removed all nutrients most efficiently, we argue that - because of the high carbon sequestration of Azolla filiculoides - combining both species works best as a low-emission effluent polishing technique.

Combinations of organisms are not limited to plant-plant combinations. Wastewater treatment plants are facing, next to excess nutrients and carbon, the problem of sludge production and processing. This sludge is a sediment-like substance consisting of organic material, microorganisms and pollutants attached to organic particles. Sludge processing is a costly process. Since aquatic animals, especially bioturbating macroinvertebrates, are feeding on sediment in natural waterbodies, a combination of these macroinvertebrates and floating plants was used in chapter 6 to assess how well a cascading system of both organisms is able to degrade sludge, remove nutrients and decrease GHG emissions. The presence of macroinvertebrates led to an increased sludge degradation, a decreased transport of P from the sludge and an increased transport of N out of the sludge. Furthermore, macroinvertebrate activity decreased methane emissions by 92%. The presence of plants resulted in a lower P concentration in the effluent, and a high CO, uptake. These additive effects of macroinvertebrates and plants resulted in an almost two times higher sludge degradation, and an almost two times lower P concentration in the effluent. This is the first study that showed that a bio-based cascade can strongly reduce GHG and P emissions simultaneously during the combined polishing of wastewater sludge and effluent, benefitting from the additive effects of the presence of both macrophytes and invertebrates. Applying macroinvertebrate-plant cascades may therefore be a promising tool to tackle the present and future challenges of WWTPs.

The above-mentioned water-treatment experiments were performed in batch systems, under controlled circumstances. To test whether effluent polishing using

plants would also work on a larger scale, an experiment that lasted for a whole year was designed at a wastewater treatment plant, where the system was continuously fed with effluent coming directly from the plant (chapter 7). Here, it was assessed whether a combination of species results in higher effluent polishing efficiency on a bigger scale, and whether seasonal changes or effluent flow rate affects the efficiency of the system. To test the nutrient uptake efficiency and CO₂ uptake of two functional groups of floating plants, we grew the water fern Azolla filiculoides and duckweed on wastewater effluent in a year-round experiment at a wastewater treatment plant. The floating plants were grown in cascading tanks, containing either one single planttype or both plant-types in different sequences. All four treatments were run in duplicate. We assessed nutrient removal efficiency for a full seasonal cycle and with two different flow rates. Furthermore, we constructed a model to assess the effect of hydraulic residence time and harvesting frequency on P removal efficiency. Plant growth and nutrient removal took place throughout the experiment, including colder winter months. Plant growth was higher in summer, but this did not increase nutrient removal efficiency. A lower flow rate increased N removal, while it did not increase P removal. Yet, modelled P removal did increase at a longer hydraulic residence time. Azolla showed highest C sequestration, especially in summer. In winter, however, peak emissions of N₂O were observed, leading to a net emission of GHGs. The cascades in which duckweed was placed before Azolla had highest mean nutrient removal rates, showing that dual-plant cascades perform better than single-plant cultivation, and that the plant sequence matters. Thus, effluent polishing combining floating plant species may be a promising low-cost, low-emission, effluent polishing solution.

Within this thesis, I concluded that nature-based water treatment may be one of the solutions to counteract the eutrophication of receiving waters. Aquatic plants and animals can treat water through nutrient removal and sludge reduction. In addition, wastewater is full of resources, such as phosphorus, that opens up opportunities for resource reuse. Furthermore, treatment using aquatic plants and animals potentially results in net GHG sequestration, and their biomass can be implemented for further use, contributing to a future-proof, circular economy. The world is facing different problems, and the challenges are piling up. While one is tempted to search for expensive high-tech solutions, one must not forget the processes nature is already providing us for free. In a modern world, where we want more and more, maybe sometimes going back to the basics is where the solution lies.

SAMENVATTING

Door een toename aan menselijke activiteiten sinds the industriële revolutie, zijn concentraties van broeikasgassen (BKGs) in the atmosfeer toegenomen, en emissies naar de lucht zijn nog steeds substantieel. Tegelijkertijd heeft een toename van extreme events, zoals hittegolven, extreme neerslag of droogte, effecten op waterzekerheid en zoetwaterkwaliteit. De slechte kwaliteit van de bodems en onderwatersedimenten, en de hoge toevoer van koolstof, ziekteverwekkers, pesticiden en vooral nutriënten, hebben gevolgen voor de menselijke gezondheid, ecosystemen en de betrouwbaarheid van het watersysteem. Een teveel aan nutriënten, vooral stikstof (N), fosfor (P) en koolstof (C), in zoetwatersystemen, ook wel eutrofiëring genoemd, verhoogt bovendien de productie en uitstoot van BKGs.

Stikstof, fosfor en koolstof circuleren verschillend door het watersysteem. Stikstof is in de waterkolom vooral aanwezig als ammonium (NH +) en nitraat (NO , maar ook atmosferische N kan via N-fixatie in de waterkolom terechtkomen. N wordt gebruikt verschillende processen waaronder nitrificatie, denitrificatie, mineralisatie, assimilatie, dissimilerende nitraatreductie en anammox. Binnen de N-cyclus kan lachgas (N₂O) worden gevormd, een zeer krachtig broeikasgas dat 273 keer meer bijdraagt aan de opwarming van de aarde dan kooldioxide (CO2) op een tijdschaal van 100 jaar. Fosfor komt vrij door verwering uit rotsen of wordt afgezet vanuit de atmosfeer. De anorganische vorm van P, PO 3-, wordt opgenomen in de biomassa van planten en algen, en de organische vorm kan beschikbaar worden gemaakt door bacteriële mineralisatie. De mobilisatie en beschikbaarheid van P wordt gereguleerd door de beschikbaarheid van metalen zoals ijzer, aluminium en calcium, maar ook door de pH en door het gehalte en de kwaliteit van organische stof. Koolstof komt de waterkolom binnen door diffusie vanuit de atmosfeer (anorganisch C) of door zijdelingse instroom vanuit het land (organisch C). Anorganisch C wordt door primaire producenten gebruikt voor fotosynthese, en opgenomen in hun biomassa als organisch C. De organische C kan worden opgeslagen in het sediment, maar kan ook door respiratie worden omgezet in anorganisch C en als CO, in de atmosfeer worden uitgestoten. Organisch C in het sediment kan worden omgezet in methaan (CH₂) in de laatste stap in de afbraak van organisch materiaal, dat 27 keer meer bijdraagt aan de opwarming van de aarde dan CO, en gereguleerd wordt door temperatuur. CH, kan de atmosfeer binnendringen door diffusie of via bellen die direct vrijkomen, oftewel ebullitie. Toch kan het ook via oxidatie weer worden omgezet in CO2, een proces dat ook wordt beïnvloed door de temperatuur en substraat beschikbaarheid.

Landbouw is niet alleen wereldwijd de belangrijkste watergebruiker, maar levert ook de grootste bijdrage aan N en P in oppervlaktewateren als 'niet-puntbron'. Het draagt daarom bij aan de eutrofiëring van deze wateren. Naast landbouw is afvalwater een belangrijke (punt)bron van nutriënten en schadelijke stoffen. Wereldwijd wordt slechts de helft van het geproduceerde afvalwater gezuiverd, en het onbehandelde afvalwater loost grote hoeveelheden nutriënten naar ontvangende waterlichamen zoals rivieren, beken en meren. Maar ook bij zuivering, bijvoorbeeld het geval in Nederland, zijn de nutriëntenconcentraties van het behandelde afvalwater, effluent genoemd, hoger dan de concentraties in de ontvangende wateren, wat leidt tot eutrofiëring van (natuurlijke) waterlichamen. Er wordt verwacht dat koolstof ook voornamelijk via landbouw en afvalwater in de aquatische systemen terechtkomt, maar kwantitatieve gegevens ontbreken. Hoewel de totale input van N en P sinds de jaren negentig is afgenomen, stagneert de afname sinds 2005 en is deze nog steeds te hoog. Door deze hoge aanvoer van N, P en C zijn veel sloten en andere zoetwatersystemen, zoals rivieren, (sterk) eutroof en kampen ze met een slechte waterkwaliteit. Om de kwaliteit van de watervoorraden in de hele Europese Unie te beheren, beschermen en verbeteren, is in 2000 de Kaderrichtlijn Water (KRW) van kracht geworden. Deze verplicht de lidstaten om tegen 2027 een goede toestand van alle waterlichamen te bereiken. Toch voldeed 60% van de waterlichamen in Europa in 2018 nog steeds niet aan de doelstellingen van de KRW en de vraag rijst of het mogelijk is om het doel in 2027 te bereiken. Bovendien kan worden verwacht dat eutrofiëring in aquatische systemen ook zal resulteren in hogere BKG emissies. Toch zijn de emissies afkomstig van deze systemen slecht gekwantificeerd en worden ze, bijvoorbeeld in het geval van sloten, niet altijd in aanmerking genomen in de nationale BKG inventarisaties. Het weglaten van emissies uit dergelijke systemen kan daarom de BKG budgetten onderschatten.

De aquatische systemen zelf kunnen de N-, P- en C-input en -emissies tot op zekere hoogte verminderen via verschillende processen, en de vraag rijst hoe hoog deze mitigatie kan zijn. Waterorganismen, zoals planten, macro-invertebraten, algen en micro-organismen, blijken in de natuur nutriënten, organische stoffen en toxische stoffen uit het oppervlaktewater te verwijderen. In eutrofe wateren concurreren zeer competitieve organismen met langzamere groeiers en het systeem verandert van een biodivers systeem naar een systeem dat wordt gedomineerd door slechts een paar soorten. Toch zou de nutriënten- en koolstofcyclus door deze verschillende groepen organismen kunnen helpen bij het bestrijden van de hoge nutriënten- en koolstofbelasting en de productie van BKGs in de waterlichamen, zowel in natuurlijke wateren als in zogenoemde 'constructed wetlands', waarbij verschillende groepen planten, macro-invertebraten, algen en micro-organismen worden gebruikt.

Waterplanten worden al gebruikt bij de waterzuivering, bijvoorbeeld in constructed wetlands. Constructed wetlands zijn naar voren gekomen als een duurzame en effectieve aanpak voor waterzuivering, waarbij verschillende verontreinigende stoffen via natuurlijke processen worden verwijderd. Ze bootsen de functies van natuurlijke wetlands na en maken gebruik van de interacties tussen planten, microorganismen en omgevingsomstandigheden om water te behandelen. Waterplanten spelen hierbij een belangrijke rol. Ondanks de talrijke voordelen die constructed wetlands bieden, blijven er verschillende uitdagingen bestaan, zoals schommelingen in de omgevingsomstandigheden. Bovendien zijn planten in constructed wetlands meestal indirect betrokken bij de verwijdering van nutriënten en blijft het onduidelijk welk deel van de verwijderde nutriënten in de waterkolom terecht kan komen, bijvoorbeeld door afbraak van planten. Bovendien kunnen constructed wetlands aanzienlijke hoeveelheden BKGs uitstoten, vooral NO, en daarmee hun bijdrage aan duurzame waterzuivering compenseren. Dat is de reden dat hydrocultuurwaterbehandeling de laatste tijd steeds meer in de belangstelling staat. Waterplanten worden direct op te behandelen water gekweekt zonder sedimentlaag, waardoor de verwijdering van nutriënten ook direct wordt beïnvloed door de opname van planten. Door de biomassa te oogsten worden nutriënten die door de planten zijn opgenomen permanent uit de waterkolom verwijderd. Tot nu toe lag de nadruk op waterbehandeling door het verwijderen van nutriënten, maar niet op het beperken van BKG uitstoot, en de vraag blijft of hydrocultuur-waterbehandeling kan helpen bij het verminderen van de uitstoot van BKGs uit deze wateren.

Het huidige proefschrift had twee algemene doelstellingen: I) het kwantificeren van de verbanden tussen eutrofiëring en de uitstoot van BKGs in aquatische systemen, en II) het vinden van nieuwe manieren om de uitstoot van nutriënten en BKGs bij de behandeling van afvalwater te verminderen met behulp van natuurlijke mechanismen. De belangrijkste doelen binnen deze doelstellingen waren I) het kwantificeren van de BKG emissies die afkomstig zijn van twee watertypen die te maken hebben met de hoogste nutriëntenbelasting door landbouw of door afvalwaterlozingen: landbouw afwateringssloten en rivieren die gezuiverd afvalwater ontvangen, en II) het ontwikkelen van een natuurlijke en emissiearme techniek om de verwijdering van nutriënten uit gemeentelijk afvalwater te verbeteren die, met behulp van waterorganismen, eutrofiëring en de uitstoot van BKGs tegengaat.

Om de broeikasgasemissies uit eutrofe waterlichamen te kwantificeren, was het doel van **hoofdstuk 2** om de rol van afwateringssloten in het BKG budget van landbouwlandschappen te beoordelen, aangezien in BKG inventarissen deze informatie sterk ontbreekt. Het hele jaar door werden de diffuse emissies van CO₂,

CH₄ en N₂O en de CH₄-ebullitie gekwantificeerd in 10 afwateringssloten gelegen tussen zwaar bemeste, veenachtige landbouwvelden. Seizoensvariaties werden beoordeeld, evenals verschillen tussen sloten. De gemiddelde jaarlijkse emissies uit de onderzochte sloten waren 2 keer hoger dan de emissiefactor, de schatting van de gemiddelde emissies per oppervlakte-eenheid (EF), gerapporteerd door het IPCC. CO₂ uitstoot droeg gemiddeld 43% bij en diffuse CH₄ uitstoot droeg 16% bij aan deze totale broeikasgasemissie. CH₄-ebullitie vertegenwoordigde bijna de helft van de totale uitstoot van BKGs, terwijl de uitstoot van N₂O grotendeels laag was. Mogelijk wordt N₂O uitstoot onderschat, omdat N₂O met name wordt uitgestoten op 'hotspots' en 'hot-moments' en daarom moeilijk te meten is. De CO₂-uitstoot was hoger in de wintermaanden, terwijl de CH₄-ebullitie hoger was in de lente en de zomer. De slootemissies waren ook hoger dan de EF die werd gebruikt voor de omliggende gedraineerde veengebieden, wat aangeeft dat slootemissies belangrijk kunnen zijn op landschapsschaal en moeten worden opgenomen in nationale BKG rapportages.

Vervolgens werd in hoofdstuk 3 de BKG emissie van een andere belangrijke bron van eutrofiëring beoordeeld: de lozing van gezuiverd afvalwater, oftwel effluent, in rivieren. De uitstoot van BKGs werd gemeten in rivieren die getroffen waren door de lozing van gezuiverd afvalwater. Het is bekend dat de lozing van effluent de emissies over de hele rivier kan verhogen, maar het directe effect van dit effluent bleef tot nu toe onderbelicht. Er zijn twee rivieren bemonsterd: één rivier met 5 effluentlozingslocaties en één rivier met één locatie. De BKG flux werd stroomopwaarts, stroomafwaarts en direct bij de lozingspunten van het effluent gemeten. Daarnaast werden sediment- en watermonsters genomen om te testen of de samenstelling van de microbiële gemeenschap verandert na lozing van effluent. De gemeten BKG emissies van de twee rivieren waren vergelijkbaar met eutrofische rivieren in stedelijke en agrarische omgevingen. De CO₂-uitstoot piekte op de meeste lozingslocaties, terwijl de CH₄-uitstoot het hoogst was 2 km stroomafwaarts. De concentraties opgeloste N2O waren sterk gerelateerd aan het NO3-gehalte van de waterkolom, wat wijst op onvolledige denitrificatie in de rivieren. Methanogene archaea waren overvloediger stroomafwaarts van effluent-lozingslocaties. De algehele samenstelling van de microbiële gemeenschap bleef in beide rivieren echter relatief onaangetast. Concluderend tonen we een duidelijk verband aan tussen de lozing van afvalwater en de verhoogde stroomafwaartse BKG emissies van de twee rivieren. Het mitigeren van de impact van effluent op de ontvangende rivieren zal van cruciaal belang zijn om de BKG bijdrage van de rivieren te verminderen.

Vervolgens werden verschillende onderzoeken uitgevoerd naar de ontwikkeling van een natuurlijke waterbehandelingstechniek met behulp van aquatische organismen, waarbij de nadruk vooral lag op waterplanten en het nazuiveren van afvalwater. Eerst hebben we beoordeeld welke plantengroeivorm het meest efficiënt zou zijn bij het nazuiveren van afvalwatereffluent. In **hoofdstuk 4** werden twee drijvende plantensoorten vergeleken met twee ondergedompelde soorten wat betreft de efficiëntie van nutriëntenverwijdering, reductie van BKGs (CO2-opname en reductie van CH4- en N2O-emissies) en biomassaproductie wanneer ze gedurende twee weken op afvalwatereffluent werden gekweekt. De drijvende planten produceerden de meeste biomassa, terwijl ondergedompelde planten snel overwoekerd werden door draadalgen. Drijvende planten verwijderden nutriënten het meest efficiënt, tot 100% N- en P-verwijdering, in tegenstelling tot een verwijdering van 41-64% bij ondergedompelde planten met algen. Bovendien hadden aquaria bedekt met drijvende planten een ruwweg drie keer hogere BKG opname dan de behandelingen met ondergedompelde planten of controles zonder planten. Het nazuiveren van effluent door drijvende planten kan dus een veelbelovende weg zijn voor een klimaatslimme afvalwaterzuivering.

Gebruikmakend van de resultaten uit hoofdstuk 4 als uitgangspunt, werden in hoofdstuk 5 verschillende drijvende plantensoorten (Azolla filiculoides, Azolla pinnata, Lemna minuta en Trapa natans) vergeleken om de meest efficiënte soorten voor het nazuiveren van afvalwater te kwantificeren, waarbij de nadruk lag op de verwijdering van nutriënten, de BKG balans en biomassaproductie. Alle soorten verwijderden ammonium volledig via nitrificatie. Lemna minuta en Trapa natans verwijderden op efficiënte wijze nitraat. Beide Azolla-soorten vertoonden de hoogste P-opname. Alle systemen stootten nauwelijks methaan of lachgas uit en namen CO, op, waarbij beide Azolla-soorten de hoogste CO₂-opname hadden. Verder is onderzocht of een combinatie van de twee meest efficiënte drijvende plantensoorten nutriënten efficiënter verwijdert dan een enkele teelt van die soorten, en of de volgorde waarin deze soorten worden geplaatst van belang is. We kweekten achtereenvolgens Azolla filiculoides en Lemna minor met hetzelfde effluent en vergeleken dit met de teelt van één soort. Hoewel de enkele teelt van Lemna minor alle nutriënten op de meest efficiënte manier verwijderde, stellen we dat - vanwege de hoge koolstofvastlegging van Azolla filiculoides - het combineren van beide soorten het beste werkt als een emissie-arme effluent nazuiveringstechniek.

Combinaties van organismen zijn niet beperkt tot plant-plantcombinaties. Afvalwaterzuiveringsinstallaties (RWZI's) worden, naast overtollige nutriënten en koolstof, geconfronteerd met het probleem van slibproductie en -verwerking. Dit slib is een sedimentachtige substantie bestaande uit organisch materiaal, micro-organismen en verontreinigende stoffen die aan organische deeltjes vastzitten. Slibverwerking is

een kostbaar proces. Omdat waterdieren, vooral bioturberende macro-invertebraten, zich voeden met sediment in natuurlijke waterlichamen, werd in hoofdstuk 6 een combinatie van deze macro-invertebraten en drijvende planten gebruikt om te beoordelen hoe goed een cascadesysteem van beide organismen in staat is slib af te breken, nutriënten te verwijderen en de uitstoot van BKGs te verminderen. De aanwezigheid van macro-invertebraten leidde tot een verhoogde slibafbraak, een verminderd transport van P uit het slib en een verhoogd transport van N uit het slib. Bovendien verminderde de activiteit van macro-invertebraten de methaanemissies met 92%. De aanwezigheid van planten zorgde voor een lagere P-concentratie in het effluent en een hoge CO₂-opname. Deze additieve effecten van macro-invertebraten en planten resulteerden in een bijna twee keer hogere slibafbraak en een bijna twee keer lagere P-concentratie in het effluent. Dit is de eerste studie die aantoont dat een biogebaseerde cascade de uitstoot van BKGs en P tegelijkertijd sterk kan verminderen tijdens het gecombineerd nazuiveren van afvalwaterslib en effluent, waarbij wordt geprofiteerd van de additieve effecten van de aanwezigheid van zowel macrofyten als ongewervelde dieren. Het toepassen van cascades tussen macro-invertebraten en planten kan daarom een veelbelovend instrument zijn om de huidige en toekomstige uitdagingen van RWZI's aan te pakken.

De bovengenoemde waterbehandelingsexperimenten zijn uitgevoerd in batchsystemen, onder gecontroleerde omstandigheden. Om te testen of het nazuiveren van effluent met planten ook op grotere schaal zou werken, werd een experiment ontworpen dat een heel jaar duurde op een RWZI, waar het systeem continu werd gevoed met effluent dat rechtstreeks uit de installatie kwam (hoofdstuk 7). Hier werd beoordeeld of een combinatie van soorten resulteert in een hogere efficiëntie van het nazuiveren van effluent op grotere schaal, en of seizoensveranderingen of de effluentstroomsnelheid de efficiëntie van het systeem beïnvloeden. Om de efficiëntie van de nutriëntenopname en de CO₂-opname van twee functionele groepen drijvende planten te testen, hebben we het hele jaar door de watervaren Azolla filiculoides en eendenkroos gekweekt op afvalwatereffluent bij een RWZI. De drijvende planten werden gekweekt in gecascadeerde tanks, die één enkel planttype of beide planttypen in verschillende volgorden bevatten. Alle vier de behandelingen werden in tweevoud uitgevoerd. We hebben de efficiëntie van de nutriëntenverwijdering beoordeeld voor een volledige seizoenscyclus en met twee verschillende stroomsnelheden. Verder hebben we een model geconstrueerd om het effect van de hydraulische verblijftijd en de oogstfrequentie op de P-verwijderingsefficiëntie te beoordelen. Plantengroei en verwijdering van nutriënten vonden gedurende het hele experiment plaats, inclusief de koudere wintermaanden. In de zomer was de plantengroei hoger, maar dit verhoogde de efficiëntie van de nutriëntenverwijdering niet. Een lagere stroomsnelheid verhoogde de N-verwijdering, terwijl dit niet de P-verwijdering verhoogde. Toch nam de gemodelleerde P-verwijdering toe bij een langere hydraulische verblijftijd. Azolla vertoonde de hoogste C-vastlegging, vooral in de zomer. In de winter werden echter piekemissies van N_.O waargenomen, wat leidde tot een netto-uitstoot van BKGs. De cascades waarin kroos vóór Azolla werd geplaatst, hadden de hoogste gemiddelde verwijderingssnelheid van nutriënten, wat aantoont dat cascades met twee planten beter presteren dan de teelt met één plantensoort, en dat de plantvolgorde ertoe doet. Het nazuiveren van afvalwater waarbij drijvende plantensoorten worden gecombineerd, kan dus een veelbelovende, goedkope en emissie-arme oplossing voor het nazuiveren van afvalwater zijn.

Binnen dit proefschrift concludeer ik dat natuurgebaseerde waterzuivering één van de oplossingen kan zijn om de eutrofiëring van ontvangende wateren tegen te gaan. Waterplanten en -dieren kunnen water behandelen door het verwijderen van nutriënten en het verminderen van slib. Bovendien zit afvalwater boordevol bronnen, zoals fosfor, wat mogelijkheden biedt voor hergebruik van deze bronnen. Bovendien kan de behandeling met behulp van waterplanten en -dieren potentieel leiden tot netto-opname van BKGs, en kan hun biomassa worden ingezet voor verder gebruik, wat bijdraagt aan een toekomstbestendige, circulaire economie. De wereld wordt geconfronteerd met verschillende problemen en de uitdagingen stapelen zich op. Hoewel men in de verleiding kan komen om te zoeken naar dure hightechoplossingen, mogen we de processen die de natuur ons al gratis ter beschikking stelt niet vergeten. In een moderne wereld, waar we steeds meer willen, ligt misschien wel de oplossing in de basis.

DANKWOORD

Na ruim vier jaar bloed, zweet en ook wel tranen, is het dan zover: mijn proefschrift is klaar. Ondanks het feit dat een groot deel van mijn PhD helaas plaatsvond tijdens de pandemie, heb ik vier mooie jaren gehad waarbij ik ontzettend veel heb geleerd. Niet alleen over het doen van onderzoek, het voeren van overleggen, het geven van presentaties, etc. Maar vooral ook veel geleerd over mezelf. En in al deze processen heb ik heel veel gehad aan heel veel mensen, die ik hier graag wil bedanken.

Natuurlijk om te beginnen met jou, **Annelies**, mijn dagelijks begeleider. We hebben altijd heel fijn contact gehad en ik heb heel veel gehad aan jouw suggesties. Met name de tekstuele aanpassingen aan mijn manuscripten verbaasden me elke keer en ik wist niet hoe snel ik op "accept change" moest drukken. Naast onze prettige wekelijkse overleggen stond jij altijd klaar met een kop thee als het me even zwaar werd. We staan behoorlijk hetzelfde in het leven, wat maakte dat jij altijd heel snel begreep waar ik doorheen ging, en kon dat mooi met voorbeelden van jouw eigen PhD onderbouwen. Heel veel dank dat je zo goed op me hebt gepast de afgelopen jaren. Ook grote dank aan **Leon** en **Fons**. Jullie waren één van de initiatiefnemers van het Aquafarm project, dus zonder jullie was deze PhD überhaupt niet mogelijk geweest. Maar ook enorm bedankt voor de fijne feedback op mijn onderzoeksplannen en manuscripten. Jullie frisse, enthousiaste en ervaren blik hierop hebben flink bijgedragen aan de kwaliteit hiervan.

I would like to thank all members of the promotion committee for dedicating their precious time to read and judge my thesis: Mark Huijbregts, Tânia Vasconcelos Fernandes, Paul Bodelier, Nikki Dijkstra and Gabrielle Rabelo Quadra.

Tom, mijn Aquafarm buddy, we hadden veel eerder moeten gaan samenwerken. Want wat waren die gezamelijke experimenten een feestje met jou. De rode draad van elke proef was wel dat ongeveer alles wat mis kon gaan, ook daadwerkelijk mis ging. Van planten die doodgingen omdat Covid ons beiden te pakken had, tot muggenlarven die doodgingen omdat het transport vanuit Oost Europa toch wat te heftig was. Maar, waar ik de orde in de proeven had en jij de wetenschappelijke kennis, leverde een mooie samenwerking toch hele goede resultaten. Bedankt voor al het monnikenwerk dat je me hebt gegeven (ik heb vaak in mijn dromen muggenlarven uit slib gepulkt) en ik zal altijd moeten gniffelen als ik denk aan de zin "ik ga weer even mijn gezicht wassen". Dank ook aan jouw begeleiders, **Piet** en **Michiel** voor jullie enthousiasme en fijne feedback.

Het Aquafarm project was niet mogelijk geweest zonder de financiële steun van Hoogheemraadschap Hollands Noorderkwartier, Hoogheemraadschap de Stichtse Rijnlanden en Waterschap Rivierenland. Grote dank voor jullie vertrouwen in de wetenschap. Dank aan de (oud)leden van de stuurgroep: Eric, Elvin, Giovanni, Judith, Noor, Ed, Wim, Constantijn, Piet. Grote dank ook aan de (oud)leden van het kernteam van Aquafarm. We konden het super goed met elkaar vinden en dat maakte de samenwerking ook zo leuk. Niet alleen onze maandelijkse overleggen waren prettig en leerzaam, ook heb ik enorm veel lol gehad tijdens onze borrels en etentjes. Dank aan Nikki, Floor, Wobke, Lotte, Floris, Judith en in het bijzonder Hugo. Bedankt Hugo, dat je zo enthousiast hebt geholpen in Rhenen, dat heeft mij heel wat grijze haren gescheeld. Grote dank ook aan Teunis[†], Tonny en Alexander voor de hulp tijdens voorbereidingen en voor het in de gaten houden van de proeven op RWZI Rhenen. Tonny, wat hebben we geklooid met die pompjes, maar wat ben ik je dankbaar voor jouw tijd en geduld. En Teunis, dank dat jij elke dag even controleerde of die verdraaide pompjes het nog wel deden. Het is een enorm gemis dat je er niet meer bent.

Ook wil ik Roy, Germa, Sebastian en Paul enorm bedanken voor alle analyses en hulp bij de verwerking van mijn samples. Wat een bergen hebben we samen verzet, en het was heel fijn dat er zo veel mogelijk was bij jullie, ook op zeer korte termijn. Ook dank aan de mensen van het Technisch Centrum, en dan met name Arjan. Bedankt dat je zo enorm mee gedacht hebt. In het bijzonder nog dank voor de medewerkers van het Kassencomplex: Koos, Harry en Walter. Niets was te gek en jullie dachten altijd enthousiast mee over mogelijkheden en oplossingen. Enorme dank aan Harry voor het helpen opbouwen van experimenten, de vele ritjes naar Rhenen met honderden liters afvalwater in de achterbak, en voor het zijn van onze reddende engel door een ritje naar Groningen voor één enkel pompje. Peter, bedankt voor het meedenken bij technische uitdagingen, en de gezelligheid in Ierland. Ook dank aan Jiry voor je advies en levering van de planten.

I would like to thank all students that I have supervised over the last years: **Maarten**, **Thom**, **Fleur**, **Inez**, **Willemijn**, **Luke**, **Adam**, **Martine**. You have helped making this thesis possible and I learned a lot from all of you. Also thanks to the students from the HAS and to the students that I supervised during courses and coaching sessions.

Furthermore, I thank all (former) members of the (Aquatic) Ecology department for the nice coffeebreaks, lunches, drinks, pokernights, theme parties, and just pleasant conversations. It is a great pleasure to have worked in such enthousiastic environment. Thank you to all my former colleagues for making the last few years so enjoyable. Also thanks to the many students that performed their internships at

the department during the last years. **Ida**, bedankt voor de leuke samenwerking. Het was een feestje om in de laatste maanden van mijn PhD nog heerlijk wat dagen op de rivier door te brengen en het heeft tot een super mooie publicatie geleid. En **Stefan**, bedankt voor je enorme hulp tijdens die dagen (en in Rhenen).

I also thank the following members of other departments and universities for some very fruitful collaborations and nice conversations: Amir, Ana, Anne, Ake, Ellen, Erbil, Fiona[†], Guus, Jeroen, Jessica, Lara, Lieneke, Martien, Nicole, Roderik, Sebastian, Simona, Steef, Tamara, Thomas.

Rens en Aniek, grote dank dat jullie mijn paranimfen willen zijn. Rens, dank voor het vele thuiswerken samen tijdens de pandemie, en ook voor de etentjes en lunchwandelingen daarna. Fijn ook dat je mij een beetje algemene kennis hebt gegeven over de oudheid en oorlogen. Binnenkort weer eens schilderen? Aniek, als mijn beste vriendinnetje was de keuze snel gemaakt om jou te vragen ook mijn paranimf te zijn. Jij kent mij door en door en hebt me enorm gesteund afgelopen jaren. Sorry voor de 18 minuten durende spraakmemo's, en bedankt voor het vele lachen en de goede gesprekken. Ik hoop zo erg dat je al je dromen waar kunt maken en ik zit op de eerste rij om je aan te moedigen.

Ook heel veel dank aan mijn andere lieve vrienden. Caitlin, Ingeborg, Janneke, Milet en Nicole (en natuurlijk ook Caecilia, Charlotte en Marike), bedankt voor alle woensdagavonden, borrelavondjes, weekendjes weg, feestjes, festivalletjes, vakanties, maar ook voor de steun en goede gesprekken. Luuk, het was altijd heerlijk om met jou in de TKB te staan en ik hoop dat we dat snel weer voortzetten. Maar ik geniet ook zeker van onze lange wandelingen en biertjes op het terras. Noortje, Sanne (en Soha), de studietijd was al een enorm feest met jullie, en het is zo fijn dat we elkaar nog regelmatig spreken. Jullie zijn schatten. Eline, als oud-roomie zat jij altijd eerste rang om mijn verhalen aan te horen, en ik bij jou. Hoe fijn was het om samen de lockdown door te maken in ons fijne huisje, nadat we hele avonturen hadden beleefd in Brazilië. En hoe fijn is het om nu heerlijk bij te kletsen en lekker de diepte in te gaan. Ook dank aan alle andere oud-roomies van de GBW. Annika, Bianca, Monica, Simon en Tommy, jullie waren mijn maatjes bij de NLP en wat heb ik veel aan jullie gehad tijdens en na dat traject. Zo leuk dat we af en toe nog bijpraten. Anita, Carlos, David, Francisco, Frank, Isabel, Jelena, Megan and Saskia, thanks for being my friends at the Camino. It was the most amazing experience we had together.

Lieve pap, mam, Timmo en Maxime, bedankt dat jullie er altijd voor me zijn. Het is heel fijn om te voelen dat ik bij jullie terecht kan en dat jullie trots op me zijn.

Bedankt voor de goede gesprekken en de oprechte interesse. Pap en mam, super dat jullie vanuit Spanje over zijn gekomen voor deze bijzondere dag. We zijn een heel fijn gezin, en ik hou van jullie. En natuurlijk ook dank aan alle ooms, tantes, neven, nichten en oma voor de interesse in mijn werk de afgelopen jaren.

Lieve **Wester**, wat heerlijk dat we elkaar een jaar geleden gevonden hebben. Ik kon natuurlijk ook niet anders dan voor die man in rode skibroek vallen. Bedankt dat je alles zo goed kunt relativeren en mij met beide benen op de grond houdt. Jij brengt de ideëen en ik het geheugen. Bedankt voor je enorme steun in de laatste maanden van mijn PhD, zonder jou was het afmaken van mijn "werkstuk" een stukje pittiger geweest. Love you baby.

Thank you all for being a part of my journey and for making it possible to defend my thesis today!

Lisanne



ABOUT THE AUTHOR

Lisanne Hendriks was born on June 24, 1995, in Haarlem, The Netherlands. She spent her youth in Heemstede after which she moved to the countryside of Hoenderloo when she was 10 years old. She loved being in nature, while riding her horses in the forests. The appreciation of nature did not end in the Veluwe's forests, but reached far around the world. On holidays with her family in Vietnam, Norway and the mountains of Austria. But also as a volunteer in Argentina. After graduation in 2013 from high school Het Christelijk Lyceum in Apeldoorn, Lisanne began her Bachelor's degree in Medical Biology at Radboud



University. However, after a few months, she decided to change this to 'green' Biology after joining an ecology course to Terschelling. In-between Bachelor and Master, Lisanne spent 6 months enjoying the beautiful nature of Australia and Fiji, enjoying a huge adventure. After this, she started to become more serious about her studies. During her first internship she conducted research in drainage ditches in the Dutch peatlands, which turned into chapter 2 of this thesis. Her Masters finished with an internship in Juiz de Fora, Brazil, an amazing experience that was concluded with a holiday through all the beauties Brazil has to offer. During that holiday, Lisanne also applied for her PhD, which she began in April, 2020, during complete Covid lockdown. Her PhD, part of the Aquafarm project, was initiated by Radboud University together with three water authorities and Wageningen Environmental Research, with which Lisanne worked closely. The main goal of the project was to investigate a form of wastewater treatment, by using aquatic plants and animals. Lisanne's work involved several laboratory studies on macrophytes, and concluded with a bigger-scale experiment at a wastewater treatment plant. The findings from these studies have been published in scientific peer-reviewed international journals and presented at various conferences and webinars both in the Netherlands and abroad. Furthermore, Lisanne presented her research during two radio-performances: Vroege Vogels Radio and BNR Nieuwsradio. Over the course of her PhD, she supervised eight students and was involved in several courses. After submitting her PhD thesis, Lisanne took some time off to pursuit her dream: walking the Camino to Santiago de Compostella. In 30 days she walked 800 km to, among other things, contemplate on her PhD adventure. After this break, she started working as a consultant at Arcadis, focusing on water quality of the Netherlands.

SCIENTIFIC OUTREACH

Publications

Hendriks, L., Smolders, A. J. P., Van den Brink, T., Lamers, L. P. M., Veraart, A. J. (2023). Polishing wastewater effluent using plants: floating plants perform better than submerged plants in both nutrient removal and reduction of greenhouse gas emission. *Water Science & Technology*, 88 (1), 23-34

Hendriks, L., Weideveld, S., Fritz, C., Stepina, T., Aben, R. C. H., Fung, N. E., Kosten, S. (2024a). Drainage ditches are greenhouse gas hotlines in peat landscapes with strong seasonal and spatial variation in diffusive and ebullitive emissions. *Freshwater Biology*, 69 (1), 143-156

Hendriks, L., Van Der Meer, T. V., Kraak, M. H. S., Verdonschot, P. F. M., Smolders, A. J. P., Lamers, L. P. M., Veraart, A. J. (2024b). Sludge degradation, nutrient removal and reduction of greenhouse gas emission by a Chironomus-Azolla wastewater treatment cascade. *PLOS ONE*, 19 (5), e0301459

Hendriks, L., Smolders, A. J. P., van Erp, I., Lamers, L. P. M., Veraart, A. J. (in revision). Combining different floating plants for optimal wastewater effluent polishing and carbon-capture

Peterse, I. F., Hendriks, L., Weideveld, S. T. J., Smolders, A. J. P., Lamers, L. P. M., Lücker, S., Veraart, A. J. (2024). Wastewater-effluent discharge and incomplete denitrification drive riverine CO2, CH4 and N2O emissions. *Science of The Total Environment*, 951, 175797

Presentations

- Invited lecture ManuResource conference (2024), Antwerpen, Belgium
- Invited lecture RIBES annual day (2022), Nijmegen, the Netherlands
- Invited lecture Aquafarm networking day (2022), Utrecht, the Netherlands
- Invited lecture webinar for CWE (Commissie Waterketens en Emissies) (2022), online
- Scientific talk NAEM conference (2022), Lunteren, the Netherlans
- Invited lecture CWE (Commissie Waterketens en Emissies) (2021), Nijmegen, the Netherlands
- Scientific talk NAEM conference (2021), online

Media

- Radio appearance (2023), Vroege Vogels radio
- Radio appearance (2023), BNR nieuwsradio

